JAERI-M
87-044

BWR LOCA INTEGRAL TEST SIMULATING A 100% MAIN STEAM LINE BREAK OUTSIDE REACTOR CONTAINMENT VESSEL IN ROSA-III PROGRAM, RUN 955

—ANALOGY OF STEAM LINE BREAK AND RECIRCULATION LINE SMALL BREAK—

March 1987

Mitsuhiro SUZUKI, Taisuke YONOMOTO,
Yoshinari ANODA, Hiroshige KUMAMARU
Hideo NAKAMURA and Kanji TASAKA

日本原子力研究所
Japan Atomic Energy Research Institute

JAERI-Mレポートは，日本原子力研究所が不定期に公刊している研究報告書です。

入手の問合わせは，日本原子力研究所技術情報部情報資料課（〒319－11茨城県那珂郡東海村）あて，お申しこしください。なお，このほかに財団法人原子力弘済会資料センター（〒319-11茨城県那珂郡東海村日本原子力研究所内）で複写による実費頒布をおこなっております。

JAERI-M reports are issued irregularly.

Inquiries about availability of the reports should be addressed to Information Division, Department of Technical Information, Japan Atomic Energy Research Institute, Tokai-mura, Naka-gun, Ibaraki-ken 319-11, Japan.

編集兼発行　日本原子力研究所
印　　刷　日立高速印刷株式会社

JAERI-M 87-044

BWR LOCA INTEGRAL TEST SIMULATING A 100% MAIN STEAM LINE BREAK OUTSIDE REACTOR CONTAINMENT VESSEL IN ROSA-III PROGRAM, RUN 955 - ANALOGY OF STEAM LINE BREAK AND RECIRCULATION LINE SMALL BREAK -

Mitsuhiro SUZUKI, Taisuke YONOMOTO, Yoshinari ANODA
Hiroshige KUMAMARU, Hideo NAKAMURA and Kanji TASAKA

Department of Nuclear Safety Research,
Tokai Research Establishment,
Japan Atomic Energy Research Institute
Tokai-mura, Naka-gun, Ibaraki-ken

(Received February 17, 1987)

This report presents the ROSA-III experimental results of RUN 955, which simulates a 100% steam line break (SLB) LOCA outside the BWR reactor containment vessel (RCV) with an assumption of high pressure core spray (HPCS) system failure. The ROSA-III test facility simulates a BWR system with volumetric scale of 1/424 and has the principal systems, i.e., four half-length electrically heated fuel bundles, two active recirculation loops, four types of ECCSs, and steam and feedwater systems.

The report clarifies that the 100% SLB LOCA outside the RCV becomes similar to a small SLB LOCA with the safety/relief valve (SRV) operation after the main steam isolation valve (MSIV) closure and that it is analogous to a small recirculation line break (RLB) LOCA with break area less than 2% of the scaled pipe flow area.

Keywords: BWR, LOCA, Integral Test, ROSA-III Program
Steam Line Break, Reactor Containment Vessel
Recirculation Line Break, Analogy, Data Report

ＲＯＳＡ－Ⅲ計画におけるＢＷＲ格納容器外100％主蒸気管破断ＬＯＣＡ総合実験，ＲＵＮ955 ―蒸気配管破断と再循環配管小破断の類似性―

日本原子力研究所東海研究所原子炉安全工学部
鈴木　光弘・与能本泰介・安濃田良成・熊丸　博滋
中村　秀夫・田坂　完二

（１９８７年２月17日受理）

本報告は，ＲＯＳＡ－Ⅲにおいて実施された，ＢＷＲ格納容器外100％主蒸気管破断LOCAを模擬した実験，ＲＵＮ955の実験結果をまとめたものである。実験では高圧炉心スプレイ系統の不作動を仮定した。ＲＯＳＡ－Ⅲ試験装置は，ＢＷＲを1／424の容積比で模擬する次の主要なシステムを有する。それらは，１／２実長の電気加熱燃料集合体４体，再循環ループ２系統，ＥＣＣＳ４系統，主蒸気系及び給水系である。

本報では，格納容器外100％主蒸気管破断ＬＯＣＡが，主蒸気隔離弁閉鎖後に逃し安全弁作動に基づく蒸気配管小破断ＬＯＣＡと同じになること，そしてその事象は破断面積２％以下の再循環配管小破断ＬＯＣＡ事象と類似していることを明らかにしている。

東海研究所：〒319-11 茨城県那珂郡東海村白方字白根２－４

Contents

目　　次

List of Tables for RUN 955

List of Figures

List of Figures of Experiment Data for RUN 955

List of Figures for Section 6

1. Introduction

The rig of safety assessment (ROSA)-III program[1][2] was initiated in 1976 to study the thermal hydraulic behavior of a boiling water reactor[3] (BWR) during a postulated loss-of-coolant accident (LOCA) with the emergency core cooling system (ECCS) actuation and to provide the data base to evaluate the predictability of computer codes developed for reactor safety analysis. To meet these objectives various kinds of ROSA-III tests have been performed and those results have been published.[4]-[34] The ROSA-III test facility consists of a volumetrically scaled (1/424) primary system of a 3800 MW BWR/6(251-848) with the electrically heated core, the break simulator, steam and feedwater systems, instrumentations including water level measurements and the scaled ECCS.

Up to the present time, similar experimental studies on the BWR LOCA phenomena have been performed with respect to some test parameters in the integral test programs of TLTA[35], FIST[36] and TBL.[37] Thus, the characteristic features of BWR LOCA caused by a recirculation line break (RLB) have been clarified both experimentally and analytically. However, the steam line break (SLB) LOCA phenomena in a BWR system have been studied little in the integral test programs,[38][39] especially for a large SLB LOCA in the reactor containment vessel (RCV).

In the ROSA-III program, six SLB LOCA tests have been performed with test objectives to study (1) the characteristic features of the BWR SLB LOCA, (2) the effects of ECCSs on core cooling capability, (3) the effects of steam line break area, (4) the effects of break location at upstream-side and downstream-side of MSIV (inside and outside of the RCV) and (5) the effects of ADS and relief valve actuation on the small SLB LOCA. The results of five SLB LOCA tests with break location in the RCV are already published.[40]-[42] Moreover, the effects of system inherent features on a large SLB LOCA phenomena have been clarified experimentally[43] and analytically.[44] It was also clarified in these studies that a large SLB LOCA was apparently distinguished from a large RLB LOCA by the pressure and and water level respopnses.

The report presents the experimental results of RUN 955, which simulates a 100% SLB LOCA outside the RCV (downstream-side of MSIV) with an assumption of high pressure core spray (HPCS) system failure. By closing the MSIV in the case of this SLB LOCA, the core decay heat should be released by dis-

charging the generated steam through the safety/relief valves (SRVs) in the main steam line (MSL) and thereafter, the 100% SLB LOCA becomes a small SLB LOCA followed by the steam discharge through the SRV and actuation of the automatic depressurization system (ADS).

The primary objectives of this report are to clarify (1) the characteristic features of the 100% SLB LOCA outside the RCV and (2) an analogy of small break LOCA phenomena between the SLB and RLB in the BWR system. The water mass inventory in the pressure vessel (PV) is estimated in two different methods (remaining PV mass and net discharged steam mass subtracted from the initial mass) and is related with transient core thermal responses. Two small RLB LOCA tests with similar initial test conditions are compared with RUN 955 to clarify an analogy between their transient phenomena. They are 2% and 0% RLB LOCA tests, RUN 920 and RUN 923, respectively. The 0% RLB LOCA test simulates an extreme condition of small LOCA and is the same as a loss-of-feedwater transient test with scram and pump trip at the same time of feedwater loss initiation.

Details of the ROSA-III test facility and instrumentations are described in Sections 2 and 3, respectively. Test conditions and test procedures are described in Section 4. Section 5 shows experiment data of RUN 955. The characteristic features of the 100% SLB LOCA outside the RCV and the analogy of small break LOCA phenomena between the SLB and RLB are shown in Section 6.

2. ROSA-III Test Facility

The ROSA-III test facility is a volumetrically scaled (1/424) BWR system with an electrically heated core designed to study the response of the primary system, the core and the ECCS during the postulated LOCA. The test facility is instrumented such that various thermal-hydraulic parameters are measured and recorded during the test. Details of the test facility can be refered to the reference (2).

The test facility consists of four subsystems. These subsystems are : (a) the pressure vessel, (b) the steam line and the feedwater line, (c) the recirculation loops and (d) the ECCS. Figures 2.1, 2.2 and 2.3 illustrate configuration of the test facility, the pressure vessel internals and the piping schematics, respectively. Table 2.1 compares the major dimensions of the ROSA-III test facility to the corresponding dimensions of the reference BWR system.

The ROSA-III pressure vessel includes various components in it simulating the internal structures of the reactor vessel in the BWR system as shown in Fig. 2.4. The interior of the vessel is divided into the core, the lower plenum, the upper plenum, the downcomer annulus, the steam separator, the steam dome and the steam dryer. The core consists of four simulated fuel assemblies of half length and a control rod simulator. Each fuel assembly contains 62 heater rods (Fig. 2.5) and 2 water rods spaced in a 8 x 8 square array and supported by spacers and upper and lower tie plates. The heater rod is heated electrically with chopped cosine power distribution along the axis as shown in Fig. 2.6. The effective heated length is 1880 mm, one half of the active length of a BWR fuel rod. The high power with radial peaking factor of 1.4 was supplied to the fuel assembly "A" and average power was supplied to the other three bundles "B", "C" and "D" with radial peaking factor of 1.0. The heater rods in each assembly are divided into three groups with respect to heat generation rate as shown in Fig. 2.7. The total electric power is limitted as 4.24 MW by limitation of the power supply system. The relative power generation rate of a heater rod in each group is 1.1, 1.0 and 0.875 respectively. The orifice plate with 44 mm I.D. in one assembly is inserted at each core inlet to control the core inlet flow.

The steam line is connected to the steam dome of the pressure vessel. A control valve is installed in the steam line to control the steam dome

pressure in steady state before the initiation of the tests. The steam line has a branch in which the automatic depressurization system (ADS) is installed. The operation of valves in the steam line including the MSIV is described in Section 4. The feedwater is supplied from the feedwater tank (FWT) through the feedwater line (Fig. 2.8) and the feedwater sparger (Fig.2.9) below the steam separator.

The break unit in the steam line and the recirculation loop are described below. Figure 2.10 shows the main steam line and the two equal recirculation loops. The break is initiated by quickly opening the break valve (break unit B) and the air valve AV-165 in the transient steam line (see Fig. 2.3). The steam break flow is lead to the break unit B (break orifice I.D. = 31.0 mm) and discharged outside the system. The break unit A is isolated both from the steam line and the recirculation loop.

The ROSA-III test facility is furnished with all kinds of the ECCS's available in the BWR system, i.e., the high pressure core spray (HPCS), the low pressure core spray (LPCS), the low pressure coolant injection (LPCI), and the ADS. The HPCS and the LPCS spray the cooling water on the top of the core. The LPCI injects the cooling water into the core bypass. Each ECCS consists of a pump, a tank, piping, and a control system. In RUN 955, a single failure of HPCS diesel generator is assumed.

The water level in the upper downcomer was measured by a differential pressure transducer and used for the actuations of ECCS's. The LPCS and LPCI are designed to actuate by the low downcomer level signal (L1) and to inject the water at their design pressure, P=2.16 MPa and 1.57 MPa, respectively.

The downcomer related trip logics in the present tests are summarized below. The MSIV closure was assumed to actuated at 3 seconds after the break. The ADS trip signal of the low downcomer water level (L2) is different from the BWR/6 trip level of L1. The earlier ADS actuation in the test RUN 955 is discussed in Section 6.

MSIV Closure = 3 s
LPCS Actuation = (L1 + 40 s) + (P less than 2.16 MPa)
LPCI Actuation = (L1 + 40 s) + (P less than 1.57 MPa)
ADS Actuation = L2 + 120 s

3. Instrumentation

The instrumentation of the ROSA-III is designed to obtain thermal-hydraulic data during the simulated BWR LOCA. The data obtained from the experiments will contribute to assess the analytical computer codes for LOCA analyses and to investigate the transient fluid and fuel responses during the simulated LOCA. Table 3.1 summarizes the No.4 instrumentation list used in the steam line break test RUN 955. Tables 3.2 and 3.3 show the measurement list and the core instrumentation list, respectively. The figure numbers in Table 3.2 are described in the section 5. Instrumentation locations are shown in Fig. 3.1 through Fig. 3.6.

Typical measured parameters in the ROSA-III are pressure, differential pressure, flow rate, electric power, pump speed, fluid and metal temperatures, collapsed liquid level, two-phase mixture level, fluid density, trip signals and so on.

Pressure and differential pressure transducers are two-wire, direct-current type which convert diaphragm displacement to electric capacitance. The pressure lead pipes are either the standard single, cylindrical pipes used in conjunction with condensate pots, or dual concentric cylinders capable of the circulation of cooling water to prevent flashing of the fluid.

The flow rate is measured by four types of instrumentations, i.e., turbine flow meter, orifice type flow meter, Venturi type flow meter and momentum flux measurement equipment depending on the fluid condition and measuring location. The turbine flow meter is used for subcooled water flow such as ECCS injection flow and feedwater flow. The orifice type flow meter is used for both flows, one is steam line flow including ADS flow and another one is jet pump discharge flow in the blowdown loop. The Venturi flow meters used for recirculation flows in both loops and jet pump discharge flow in the intact loop. The momentum flux measurement using drag-disk is shown later.

The temperatures of the fluid, structural material and fuel rod cladding are measured with chromel-alumel thermocouples (CA T/C) of 1.6 or 1.0 mmφ. The thermocouples for fuel rod cladding temperatures are imbedded at the surface of the cladding as shown in Fig. 2.5. There are seven (maximum) thermocouples for one fuel rod along the axial direction.

Liquid levels are measured by either differential pressure transducers,

described above or needle type electrical conductivity probes (CP) developed in the ROSA-III program. The probes are distributed along the vessel height to detect the existence of water or vapor at different levels.

The electric power supplied to the simulated fuel rods is controlled to follow the predetermined power curve with function of time and measured by a fast response electric power meter.

Pump speed is measured by a pulse generator integral of the pump. Trip signals such as selected valve positions and pump coastdown simulation initiations and so on are detected in order to record the exact actuation times of trip signals.

Fluid density in the pipe is measured by means of gamma densitometers. Preliminary studies indicate that two-beam and three-beam densitometers should be used to determine the flow regime. Figures 3.7 and 3.8 show the beam directions of the three-beam and two-beam gamma densitometers. The gamma-ray source is ^{137}Cs and the detector is a water cooled NaI(Tl) scintillation counter.

Momentum flux is measured by a drag disk as shown in Fig. 3.9. The combination of signals from a drag disk and a gamma densitometer is used to determine the two-phase flow rate as shown in Fig. 3.10.

The data acquisition system (DATAC 2000B, Iwasaki Tsushinki Co.) scans all of signals with the frequency up to 30 Hz. The data recorded on magnetic tape are processed by the FACOM M200 system computer at JAERI by off-line control. After evaluation, for example by comparing the initial and final pressure values with standard values, the data is reprocessed using the correct conversion factors as determined from the consistency examination. More detailed information on the data processing procedure are available in reference (45).

4. Test Conditions and Procedure

The test RUN 955 is a 100% main steam line break LOCA test with an assumption of HPCS failure. The break location simulates the steam line outside the BWR RCV so that the steam discharge can be terminated by the actuation of MSIV closure. The test conditions are shown in Table 4.1. The break area was simulated by an orifice with 31.0 mm I.D. (OR-5) in the first steam line branch. The measured initial test conditions were; steam dome pressure of 7.35 MPa, total core power of 3.982 MW, core inlet mass flow of 16.8 kg/s, core inlet subcooling of 10.7 K, main steam flow and feedwater flow of 2.06 kg/s, and pressure vessel water level of 5.04 m. The initial average fluid quality in the upper plenum was estimated as 12.6%. The initial enthalpy distribution of the primary fluid system simulated that of the BWR rated conditions.

RUN 955 was performed by the following procedures as shown in Table 4.2. Break was initiated by quickly opening the break valve (QOBV) and the air valve AV-165 in the first steam line. At the same time, the power supply to both recirculation pumps was terminated and the pump speed coasted down rapidly. After the break, the steady state core power was maintained for 9.0 seconds and then decreased along the power curve shown in Fig. 4.2, which simulated the heat transfer rate to coolant during a hypothetical BWR/LOCA.[46] The steam flow to heat up the feedwater from the third steam line was manually stopped immediately after the break by closing the valves CV-1 and CV-2. The feedwater line was closed at 2 s after the break.

The MSIV was assumed to close at 3 seconds by quickly closing the air valve AV-165 and thereafter the steam discharged through the pressure control valve CV-130, which simulated the SRV operation. The ADS was actuated by L2 trip level with time delay of 120 s. The ECCS actuation signal was tripped by L1 level (4.25 m from PV bottom) signal with a time delay of 40 seconds. The LPCS was actuated at 516 s after the break (at 2.2 MPa of the system pressure) and LPCI was actuated at 591 s after the break (at 1.7 MPa of the system pressure). Most of the instruments functioned successfully.

5. Data Processing for RUN 955

In RUN 955, the data acquisition frequency was 5 Hz. The test data was processed and reduced to 1000 data points in a time period of 1000 s for computer plotting. The test data of RUN 955 are shown in Figs. 5.1 through 5.108. In these figures, the measured quantity is identified by the channel number and the alphabetic characters (ref. Table 3.2).

Figure 5.1 shows the representative pressure data in the pressure vessel (PV) and main steam line (MSL). Figures 5.2 through 5.25 show differential pressure data between various positions in the pressure vessel and the recirculation loop. Figures 5.26 and 5.27 show the liquid levels in the ECCS tanks and downcomer. Figures 5.28 and 5.29 show injection flow rates of LPCS and LPCI, and feedwater flow rate, respectively. Figures 5.30 through 5.33 show the flow rates through the jet pumps and main recirculation line. Figure 5.34 shows the electric power supplied to the core with the maximum capacities of 2100 and 3150 kW. The pump speed of the main recirculation pump is shown in Fig. 5.35. The trip signals such as the break initiation signal and the valve positioning signals are shown in Figs. 5.36 through 5.38. Figures 5.39 through 5.44 show the fluid densities measured by the gamma densitometer. Figures 5.45 and 5.46 show momentum fluxes measured by the drag disks.

Figures 5.47 through 5.51 show the fluid temperatures at various positions in the system. The fuel rod cladding temperature and the surface temperatures of the water rods and the channel boxes measured at positions 1 through 7 are given in Figs. 5.52 through 5.59. Metal temperatures on the outer surface of channel box A are shown in Fig. 5.60. Figures 5.61 through 5.74 show the fuel rod cladding temperatures in a different manner. Figures 5.75 through 5.78 show the fluid temperatures at the inlet and outlet of the channel boxes. The liquid level signals in the core, the upper and lower plena, the guide tube and the downcomer are shown in Figs. 5.79 through 5.90. The peak cladding temperature (PCT) distribution in RUN 955 is given in Table 5.1.

Quantities obtained from reduction of above test data are shown in Figs. 5.91 through 5.108 as follows.

Figures 5.91 and 5.92 show the average fluid density calculated from the data shown in Figs. 5.39 through 5.44. The average density is calculated as an arithmetic mean of the densities in multi-directions with the weight of each cord length.

For the three-beam densitometer at the jet pump outlet spool,

$$\rho_{av} = 0.3221\rho_A + 0.43\rho_B + 0.2479\rho_C \tag{5.1}$$

where,

ρ_{av}: average density obtained from the three-beam gamma densitometer,
ρ_A : density measured by beam A (bottom),
ρ_B : density measured by beam B (middle),
ρ_C : density measured by beam C (top).

Figures 5.93 through 5.99 show the fluid flow rates at the steam line, the channel inlet orifices, the bypass hole and the total core inlet flow rate. The fluid flow rates are calculated from the test data which are the pressure drop across the orifices and the liquid density obtained from the temperature and the pressure condition. The equation used for the calculation is as follows :

$$G = C_D \cdot A \cdot \sqrt{2g \cdot \rho_l \cdot \Delta P} \tag{5.2}$$

where,

G : flow rate,
ΔP : pressure drop across the orifice,
C_D : discharge coefficient,
= 0.6552 (the orifice to measure the steam discharge flow rate)
= 0.4761 (the channel inlet orifice)
= 0.8032 (the bypass hole)

A : flow area (m^2)
= 2.875×10^{-3} (the orifice to measure the steam discharge flow rate)
= 1.521×10^{-3} (the channel inlet orifice)
= 1.758×10^{-4} (the bypass hole)

g : gravitational acceleration (= 9.807 m/s^2),

ρ_l : density of the single-phase liquid (kg/m^3),

This calculation method is not applicable for two-phase flow condition after the LPF initiation at the channel inlet orifices and the bypass hole. The calculated value shows only a trend in two-phase flow condition. Total channel inlet flow rate presents the sum of four channel inlet flow rates.

Figures 5.100 and 5.101 show the collapsed water levels in downcomer and inside the core-shroud, respectively. Each level is obtained from corresponding differential pressure data. The differential pressure may include the flow resistance effect, however, the flow resistance becomes negligible after completion of the recirculation pump coastdown.

Figure 5.102 shows the fluid mass inventory in downcomer. The fluid mass inventory is determined from the density and configurational data inside and outside the core shroud,

$$M = \rho_l \cdot Q \tag{5.3}$$

where,

M : fluid inventory,

ρ_l : liquid density estimated from the satulation temperature and/or pressure,

Q : liquid volume calculated from the liquid level.

The volume Q (m^3) inside the shroud is also given as a function of collapsed water level in downcomer (L),

$$\begin{aligned}
Q &= 0.0 && (\quad L \leqq 0.494) \\
Q &= 0.0225L - 0.0111 && (0.494 < L \leqq 1.384) \\
Q &= 0.0697L - 0.0769 && (1.384 < L \leqq 1.519) \\
Q &= 0.0225L - 0.0048 && (1.519 < L \leqq 3.355) \\
Q &= 0.0801L - 0.1980 && (3.355 < L \leqq 4.250) \\
Q &= 0.2443L - 0.8959 && (4.250 < L \leqq 4.413) \\
Q &= 0.2611L - 0.9700 && (4.413 < L \leqq 4.578) \\
Q &= 0.2504L - 0.9211 && (4.578 < L \leqq 4.654) \\
Q &= 0.2375L - 0.8610 && (4.654 < L \leqq 4.815) \\
Q &= 0.2866L - 1.0974 && (4.815 < L \leqq 4.915) \\
Q &= 0.3396L - 1.3580 && (4.915 < L \leqq 5.143)
\end{aligned} \tag{5.4}$$

$$
\begin{aligned}
Q &= 0.3607L - 1.4665 \quad (5.143 < L \leqq 5.365) \\
Q &= 0.3848L - 1.5960 \quad (5.365 < L \leqq 5.995) \\
Q &= 0.7111 \quad (5.995 < L)
\end{aligned}
$$

Figure 5.103 shows the fluid mass inventory inside core shroud. The fluid mass inventory is determined from the density and configurational data inside and outside the core shroud,

$$M = \rho_l \cdot Q \tag{5.5}$$

where,

M : fluid inventory,

ρ_l : liquid density estimated from the satulation temperature and/or pressure,

Q : liquid volume calculated from the liquid level.

The volume Q (m^3) inside the shroud is also given as a function of collapsed water level inside core shroud (L),

$$
\begin{aligned}
Q &= 0.0 \quad (L \leqq 0.0) \\
Q &= 0.2350L \quad (0.0 < L \leqq 0.497) \\
Q &= 0.1245L + 0.0549 \quad (0.497 < L \leqq 1.354) \\
Q &= 0.0698L + 0.1290 \quad (1.354 < L \leqq 3.589) \\
Q &= 0.1648L - 0.2120 \quad (3.589 < L \leqq 3.744) \\
Q &= 0.1963L - 0.3299 \quad (3.744 < L \leqq 4.243) \\
Q &= 0.0196L + 0.4199 \quad (4.243 < L \leqq 4.578) \\
Q &= 0.0186L + 0.4244 \quad (4.578 < L \leqq 4.654) \\
Q &= 0.0410L + 0.3201 \quad (4.654 < L \leqq 5.099) \\
Q &= 0.0196L + 0.4292 \quad (5.099 < L \leqq 5.365) \\
Q &= 0.5344 \quad (5.365 < L)
\end{aligned}
\tag{5.6}
$$

Figures 5.105 and 5.106 compare the collapsed water levels in PV and the mixture levels, which are obtained by reducing the conductivity prove signals previously shown in Figs. 5.79 through 5.90. Figures 5.107 and 5.108 show the dryout and quench times of fuel rods in the high-power bundle (channel A) and among the four bundles.

6. Test Results

The test results of RUN 955 are shown in Section 6.1. The 100% SLB LOCA outside the reactor containment vessel (RCV) becomes a small SLB LOCA due to the safety/relief valve (SRV) operation after the MSIV closure and therefore, it is very different from a 100% SLB LOCA[40],[41] inside the RCV, in which a rapid depressurization continues in spite of the MSIV closure after the break. An analogy of small break LOCA phenomena between the SLB and the main recirculation line break (RLB) is presented in Section 6.2.

6.1 Major Events of 100% SLB outside RCV, RUN 955

(1) Pressure Response and Major Events

The break was initiated by quickly opening both the break valve (QOBV) in the break unit B and the air valve AV-165 in the transient steam line (see Figs. 2.10 and 4.1). The system pressure began to decrease rapidly after the break as shown in Fig. 5.1. Three seconds after the break, the MSIV closure was simulated by quickly closing the AV-165 and thereafter the system pressure turned to increase rapidly. After the system pressure reached the SRV trip point of 8.0 MPa, it was automatically controlled to keep constantly at the pressure of 8.0 MPa by operating the pressure control valve CV-130 in the steady steam line. Thus, the 100% SLB LOCA outside the RCV changed into a small SLB LOCA after the MSIV closure.

As the MSIV closure is tripped on the pressure of 6.6 MPa, which was higher than the saturation pressure of the lower plenum fluid (6.4 MPa), no flashing occurred in the water regions before the ADS actuation.

On the other hand, the core flow began to decrease by the pump trip at the break time (see Figs. 5.94 through 5.99) and thereafter the core flow became nearly stagnant. The feedwater supply was stopped during 1.6 and 4.0 s after the break. The fluid density data shown in Figs. 5.39 through 5.44 indicate that phase separation was observed in the horizontal line at the jet pump outlet after the initiation of lower plenum flashing. The density data of beam C, which passes through the top part of the horizontal pipe (see Fig. 3.7), shows steam density after the flashing initiation, whereas that of beam A, which passes through the bottom part of the pipe, shows

water density at the same time.

The ADS was tripped at 150 s after the break by the low downcomer water level (L2) signal with a time delay of 120 s and it caused rapid depressurization in the system. The effect of different ADS actuation trip level (L1) compared with the ADS actuation by L2 trip level is shown in the next section. The LPCS and LPCI were actuated at 516 s (2.2 MPa) and 591 s (1.6 MPa), respectively (see Fig. 5.28).

The flashing of fluid initiated 28 s after the ADS actuation and resulted in rapid void formation in the water regions such as lower plenum and downcomer. The void formation was observed in the decrease of water head (differential pressure data in Figs. 5.2 through 5.25). The water level swell was observed in the downcomer after the fluid flashing initiation as in the similar SLB LOCA tests.[42]

The core dryout initiated at 330 s after the break (180 s after the ADS actuation) due to the water level decrease inside the core shroud. The upper half core was dried out above the mixture level and quenched finally at 546 s after the break by the water level recovery caused by the LPCS actuation. It should be noted that the core was completely quenched only by the LPCS actuation in RUN 955.

(2) Steam Discharge Flow Rate and Mass Inventory

In RUN 955, the steam mass discharged through the MSL can be directly related with the PV remaining mass inventory since there is no fluid discharge path except for the MSL.

Figure 5.93 shows steam discharge flow rate, which were measured by the orifice-type flow meter located at the main steam line. The orifice-type flow meter can correctly measure a single-phase steam flow but has large umbiguity on the accuracy for the two-phase flow, which may be observed after the lower plenum flashing initiation.

After the break, the total steam flow area was increased from the steady state flow area of CV-130 (estimated as 29.3%)[42] to a sum of the transient (100%) and steady steam flow areas, i.e.,129.3%. And the steam discharge flow rate increased from the steady steam flow rate of 2.06 kg/s to a maximum flow rate of 6.2 kg/s after the break. By the MSIV closure at 3 s after the break, the large steam discharge was terminated. Thereafter steam

discharged through the SRV (CV-130). By actuation of ADS at 150 s after the break, the steam discharge flow increased rapidly. The total steam flow area after the ADS opening became a sum of the SRV area (estimated nearly as 7% of the 1/424 scaled BWR MSL flow area) and the ADS flow area of 35%, i.e., 42%.

The transient fluid mass remaining in the system was estimated by different two ways. One is obtained by the collapsed water levels in PV as shown in Section 5 (see Figs. 5.100, through 5.104). Another one is calculated by using an initial fluid mass (M_0) and a net discharged fluid mass from the system, as follows,

$$M = M_0 + M_F - M_D + M_I$$

where M_F : Injected feedwater mass 6 kg in the first 4 s and inflow after the feedwater flashing.

M_D : Discharged steam mass through the break (OR-5), relief valve (CV-130) and ADS line (OR-4).

M_I : Injected water mass by LPCS and LPCI.

The discharged steam mass was obtained as shown in Table 6.1. The steam mass is correct except for a short time period after the ADS actuation, when some content of water entrainment may not be negligible as shown in Section 5 (see Fig. 5.93). The ECC water flow is correctly measured by the turbine flow meters under the water single phase condition (see Fig. 5.28).

In order to compare the remaining fluid mass in PV, the fluid mass remaining in the jet pumps (JPs) and the main recirculation lines (MRLs) was obtained by estimating an average void fraction (α) in the regions (see Table 6.2) and was subtracted from the total system mass inventory. The initial fluid mass in JPs and MRLs (M_{L0}) was estimated as 129 kg by using the fluid volume of 0.172 m^3. The transient fluid mass in JPs and MRPs (M_L) was calculated by using the following relation,

$$M_L = M_{L0} \times (\rho/\rho_0) \times (1 - \alpha),$$

where ρ and ρ_0 are the saturation water density and the initial water density, respectively.

Table 6.3 compares the PV mass inventories estimated by the two ways. It

is shown that both inventories agreed well within a discrepancy of 13% before the LPCS actuation. The comparatively large discrepancy of 8% in the initial state may be a result of over-estimation of fluid mass in the two phase regions.

The ADS actuation enlarged the discrepancy by the following reason. The water mass in the upper downcomer above 4.25 m was under-estimated or neglected in the fluid mass calculation by using the PV collapsed water levels. Namely the calculated collapsed water level in the whole downcomer became lower than the level of 4.25 m after the ADS actuation time, whereas the collapsed water level in the upper downcomer was higher than the level of 4.25 m as shown in Fig. 6.1. As the upper downcomer above 4.25 m has flow area more than three times wider than that of lower downcomer, location of the collapsed water level in the whole downcomer affects significantly the mass estimation in relation to the boundary elevation of 4.25 m.

By a rough correction, water mass above 4.25 m was estimated from the upper downcomer colappsed water level as shown by the braketted value in Table 6.3, which showed good agreement between the two fluid mass calculations. It is shown that the discrepancy between the two PVfluid mass calculations can be reduced within 5% by correcting the upper downcomer water mass in a time period after the break until the LPCS actuation time. The agreement of the two mass inventories means that these estimations are consistent and reliable.

The water mass in PV decreased to the lowest value of 46% of the initial water mass before the LPCS actuation. The discrepancy between the two mass inventories became larger after the LPCS actuation due to the transient local mass distribution along the ECCS flow paths.

(3) Core Thermal Responses Related with Mixture Levels

The fuel rods in the core showed a temporary temperature increase due to dryout above the mixture levels and a quench caused by water level rcovery after the LPCS actuation at 516 s. The dryout and quench phenomena was strongly related with the core mixture level responses as shown in Figs. 5.105 through 5.108.

The core dryout initiated at 330 s after the break (180 s after the ADS actuation) at a total system mass inventory of 60% of the initial mass (see Table 6.3). The lowest mixture level was observed at the middle height of

the core (at a total mass inventory of 46%). After actuation of LPCS, the water levels in PV recovered rapidly and the fuel rods were quenched. Distributions of dryout and quench times in one bundle and among the four bundles were observed as shown in Figs. 5.107 and 5.108. The distribution depended mainly on the location of fuel rod in the bundle. And there was minor difference of core thermal responses between the four bundles in comparison with the distribution in one bundle.

The highest fuel surface temperature (PCT) was observed at 540 s after the break as 646 K at position 2 of the A88 rod in the high-power bundle. It was observed 24 s after the LPCS actuation. The final core quench was completed 30 s after the LPCS actuation.

6.2 Analogy of LOCA Phenomena between RUN 955 and Two Small RLB Tests, RUNs 920 and 923

In this section, major test results of RUN 955 are compared with those of small RLB LOCA tests with break areas of 2% and 0% of the 1/424 scaled BWR MRL flow area in order to clarify an analogy between them.

(1) Test Conditions of RUNs 955, 920 and 923

Table 6.4 compares the test conditions of the three tests. In RUNs 955 and 923, the primary fluid was discharged only through the main steam line (MSL) whereas the primary fluid in RUN 920 discharged through two lines, i.e., the MSL and the main recirculation line (MRL).

The initial test conditions of the three tests were the same. Their transient conditions were the same except for the MSIV closure and ADS opening logics. In RUN 955, a larger steam flow rate in the MSL after the break could sent an MSIV closure signal with a time delay of 3 s. On the other hand, the MSIV was tripped by the low downcomer water level of L2 with time delay of 120 s in RUNs 920 and 923 at 29 s and 35 s, respectively.

The LPCS and LPCI were actuated by the same trip logics among the three tests. However, the ADS actuation trip level of RUN 955 was different from the two RLB tests. Namely, the ADS actuation in RUN 955 was tripped by the low downcomer water level of L2 with time delay of 120 s, whereas those in

RUNs 920 and 923 were tripped at 188 s and 355 s after the break by the low-low downcomer trip level of L1 with time delay of 120 s, which simulated the BWR/6 trip logic. Thus, the ADS in RUN 955 was actuated earlier than a reference BWR LOCA condition.

However, the ADS actuation time of RUN 920 was close to that time of RUN 955 because of faster mass discharge from the downcomer in the former. On the other hand, as the mass discharge conditions of RUNs 955 and 923 were the same, the effects of ADS actuation trip level on the transient system responses can be shown by comparing the test results of RUNs 955 and 923. Therefore, the effect of ADS actuation time on the small SLB LOCA or the 100% SLB LOCA outside the RCV can be estimated by comparing the test results of RUN 955 with those of RUNs 920 and 923.

(2) Comparison of RUN 955 with 2% RLB Test, RUN 920

Major events of RUNs 920 and 955 are compared in Table 6.5. Figures 6.2 through 6.15 compare the major results of the two tests. Figure 6.16 shows the collapsed water levels in the whole downcomer, upper downcomer and inside core-shroud of RUN 920 and is compared with those of RUN 955 (see Fig. 6.1). Followings are reduced through these comparisons.

(A) The pressure response of RUN 955 became close to that of RUN 920 due to the similar ADS actuation times between them (see Fig. 6.2). Actually, the time differences of the major events between the two tests were 26 s of MSIV closure, 63 s of SRV initiation, 38 s of ADS actuation and 81 s of LPCS actuation (see Table 6.4). As there was larger remaining water mass in RUN 955 than in RUN 920, the depressurization rate after the ADS actuation became slower in the former.

(B) The water levels in downcomer and inside core-shroud of RUN 955 were higher than those of RUN 920 because of no mass discharge from the downcomer in the former (see Figs. 6.1 and 6.16). The PV mass inventory in RUN 955 was approximately 100 kg larger than that of RUN 920 before the LPCS actuation time as shown in Fig. 6.15.

(C) A common relation between the collapsed water levels in downcomer and inside core-shroud was observed in the transient phase of the two tests (Figs. 6.1 and 6.16). Namely, the collapsed water level inside the core-shroud was 0.5 - 0.6 m higher than that in the whole downcomer

before the ADS actuation in both tests. On the contrary, the water level in the whole downcomer became higher by 0.5 m in RUN 920 and by 0.5 - 1.0 m in RUN 955 than the collapsed water level inside the core-shroud after the ADS actuation because the pressure balance in PV was changed clearly by the ADS actuation. As a large pressure loss of the uprizing two phase flow shown in Fig. 5.3 was induced at the steam separator after the ADS actuation, the water head inside core-shroud was lowered corresponding to increase of the pressure loss through the steam separator. The collapsed water levels inside core-shroud of RUNs 955 and 920 were lower than each downcomer water level by less than 2m and 1m, respectively, before the LPCS actuation time. Thus, a reversal of the relation between the collapsed water levels across the core-shroud was commonly observed in both tests after the ADS actuation.

(D) The core dryout initiation time was 50 s earlier and the final core quench time was 8 s later in RUN 920 than in RUN 955 (Table 6.4). As the core dryout time period of RUN 920 was 58 s longer than RUN 955, the PCT of the former became 155 K higher than the latter. This is a result of smaller PV mass inventory in RUN 920. The dryout and quench behaviors of fuel rods were strongly related with the mixture level responses in the core in both tests.

(E) It was concluded that 100% SLB outside the RCV became a small SLB LOCA after the MSIV closure and that it was similar to a 2% RLB LOCA test, RUN 920, by a similar pressure transient. However, the core cooling conditions in RUN 955 was better than RUN 920 because of larger PV mass inventory and lower PCT.

(3) Comparison of RUN 955 with 0% RLB Test, RUN 923

Major events of RUNs 923 and 955 are compared in Table 6.5. Figures 6.17 through 6.32 compare the major results of the two tests as in the previous section. Figures 6.18 through 6.25 compare the test results of RUN 955 with those of RUN 923 by assuming the same ADS actuation time as in RUN 955 (150 s after the break). The effects of ADS actuation in RUN 955 by the L1 trip level instead of the L2 trip level can be estimated by comparing these test results. Followings are reduced through these comparisons.

(A) Figures 6.18 through 6.25 show that the principal phenomena in RUN 955

after the ADS actuation were quite analogous to those of RUN 923 with slight differences between them. The time difference of ADS actuations between RUNs 955 and 923 was 205 s caused by their different ADS trip levels.

(B) The pressure response of RUN 955 after the ADS actuation was nearly equal to that of RUN 923 because of the same ADS flow area and the similar PV mass inventories at the ADS actuation time in both tests. The ADS actuations of RUNs 955 and 923 were 150 s and 355 s after the break, respectively, which were tripped by the L2 (4.76 m) and L1 (4.25 m) levels, respectively. It is shown from this comparison that if the ADS were actuated by the L1 level in RUN 955, the pressure response would be the same as that of RUN 923 because of the same mass inventory at the ADS actuation time between them.

(C) A small difference of PV mass inventories at the actual ADS actuation times of RUNs 955 and 923 were estimated as follows. The collapsed water levels in PV were 4.43 m in RUN 955 and 4.02 m in RUN 923 at each ADS actuation time (see Fig. 6.23). As there was no void in the downcomer region at that time, the level difference of 0.41 m corresponds to 47 kg of water mass. On the other hand, the difference of differential pressure in PV (see Fig. 6.24) corresponds to 0.07 m in water head and 2 to 3 kg of water mass in the steam separator region. By summing these masses, the PV mass at the ADS actuation time in RUN 955 was 45 kg larger than that of RUN 923. However, this difference of water mass was so small that the pressure response of RUN 955 after the ADS actuation became slightly higher than that of RUN 923 (see Fig. 6.18).

(D) The core thermal responses of the two tests were quite similar in spite of the difference of ADS actuation times between the two tests. The PCT of RUN 955 was observed as 646 K at position 2 of A88 rod and was 9 K higher and 157 s earlier than in RUN 923.

(E) It was concluded that 100% SLB outside the RCV was quite analogous to 0% RLB in spite of the difference of ADS actuation time of 205 s.

7. Conclusions

A 100% steam line break (SLB) LOCA outside the reactor containment vessel (RCV) was experimentally studied in the ROSA-III program. Characteristic features of the LOCA test and an analogy of LOCA phenomena between the SLB and recirculation line break (RLB) were clarified as follows by comparing the test results with those of two small RLB tests, RUNs 920 and 923 with break areas of 2% and 0%, respectively. The 0% RLB means a loss of feedwater transient with scram and pump trip at the time of break signal and is considered as an extremely small RLB LOCA.

(1) A 100% SLB LOCA outside the RCV (downstream-side of MSIV) becomes a small SLB LOCA with the safety/relief valve (SRV) operation after the MSIV closure. And the 100% SLB LOCA outside the RCV is quite analogous to a small RLB LOCA with break area less than 2% because of the similar actuations of MSIV trip, SRV operation, and ADS opening.

(A) The pressure response of RUN 955 was close to that of 2% RLB (RUN 920) by the similar ADS actuation time. The principal phenomena after the ADS actuation time of RUN 955 was quite analogous to those of 0% RLB (RUN 923) because of the similar PV mass inventories at the initiation of ADS opening and the same ADS flow area.

(B) The effects of ADS actuation on the water level responses are commonly observed in RUN 955 and small RLB LOCA tests. In a high pressure phase during the SRV operation, the collapsed water level inside core-shroud was rather higher than the upper downcomer water level. However, the water level inside core-shroud becomes lower than the downcomer water level after the ADS actuation. This reversal of water levels relation across the core-shroud is a result of large pressure loss across the steam separator, which is induced by the uprising two-phase flow across after the ADS actuation. In RUNs 955 and 920, the collapsed water levels inside the core-shroud were 1.0 to 2.0 m lower than each upper downcomer water level after the ADS actuation.

(C) The ADS actuation times of RUNs 955 and 923 were 150 s (L2 + 120s)

and 355 s (L1 + 120s), respectively. The L2 level trip of RUN 955 does not simulate the BWR ADS trip level. By considering the analogy of transient system responses shown above, the test results of RUN 923 can be considered approximately the same as test results of 100% SLB LOCA outside the RCV with ADS trip level of L1 as in the BWR system.

(2) The core dryout initiated by the water level decrease inside core-shroud 180 s after the ADS actuation in RUN 955. The PV mass inventory at the core dryout initiation was estimated as 60% of the initial PV mass. The lowest PV mass inventory was estimated as 46% at the LPCS actuation time. The core water level recovered soon after the LPCS actuation and quenched completely within 30 s only by the LPCS. The peak cladding temperature (PCT) was observed as 646 K at position 2 (upper core region) of A88 rod in the high-power bundle. It was found that the LPCS has sufficient capability of core cooling in the case of 100% SLB LOCA outside the RCV.

Acknowledgment

The authors are grateful to Mr. H. MURATA of Reactor Safety Laboratory I for his large contribution of the experiment conduction, H. ASAHI, T. ODAIRA, T. TAKAYASU, Y. KITANO and T. NUMATA of Nuclear Engineering Corporation for their assistance in conducting the experiment, K. HIYAMA and K. HAKUTA of Information System Laboratory Corpolation for preparing the data plots and M. KIKUCHI of Nihon Computer Bureau for type writing the manuscripts.

References

(1) K.TASAKA, et al., "Study on the Similarity between ROSA-III Experiment and BWR LOCA", JAERI-M 6703 (1976) (in Japanese).
(2) Y.ANODA, et al.,"ROSA-III System Description for Fuel Assembly No. 4", JAERI-M 9363 (1981) (in Japanese).
(3) General Electric Company, "General Electric Standard Safety Analysis Report, BWR/6", DOCKET-STN-50477 (1978).
(4) K.TASAKA, et al.,"ROSA-III Base Test Series for a Large Break Loss of Coolant Accident in a Boiling Water Reactor", Nucl. Technol. 57, 179-191 (1982).
(5) K.SODA, et al.,"Boiling Water Reactor Loss of Coolant Test (Single Failure Test with ROSA-III)", J. Nucl. Sci. Technol. 20, 537-558 (1983).
(6) K.TASAKA, et al.,"Simulation Experiment of Five Percent Small Break LOCA of BWR", J. Nucl. Sci. Technol. 20, 89-104 (1983).
(7) K.TASAKA, et al.,"ROSA-III Double-Ended Break Test Series for a Loss-of-Coolant Accident in a Boiling Water Reactor", Nucl. Technol. 68, 77-93 (1985).
(8) M.SUZUKI, et al.,"Recirculation Pump Discharge Line Break Tests at ROSA-III for a Boiling Water Reactor", Nucl. Technol. 70, 189-203 (1985).
(9) Y.KOIZUMI, et al., "Experiment Analysis of Power Curve Sensitivity Test Series at ROSA-III", Nucl. Eng. and Design 86, 267-287 (1985)
(10) H.KUMAMARU, et al.,"Five Percent Break BWR LOCA/ECC Test at ROSA-III without HPCS Actuation---Two Dimensional Core Thermal Hydraulic Phenomena", Nucl. Eng. and Design 86, 219-239 (1985).

Acknowledgment

The authors are grateful to Mr. H. MURATA of Reactor Safety Laboratory I for his large contribution of the experiment conduction, H. ASAHI, T. ODAIRA, T. TAKAYASU, Y. KITANO and T. NUMATA of Nuclear Engineering Corporation for their assistance in conducting the experiment, K. HIYAMA and K. HAKUTA of Information System Laboratory Corpolation for preparing the data plots and M. KIKUCHI of Nihon Computer Bureau for type writing the manuscripts.

References

(1) K.TASAKA, et al., "Study on the Similarity between ROSA-III Experiment and BWR LOCA", JAERI-M 6703 (1976) (in Japanese).

(2) Y.ANODA, et al.,"ROSA-III System Description for Fuel Assembly No. 4", JAERI-M 9363 (1981) (in Japanese).

(3) General Electric Company, "General Electric Standard Safety Analysis Report, BWR/6", DOCKET-STN-50477 (1978).

(4) K.TASAKA, et al.,"ROSA-III Base Test Series for a Large Break Loss of Coolant Accident in a Boiling Water Reactor", Nucl. Technol. 57, 179-191 (1982).

(5) K.SODA, et al.,"Boiling Water Reactor Loss of Coolant Test (Single Failure Test with ROSA-III)", J. Nucl. Sci. Technol. 20, 537-558 (1983).

(6) K.TASAKA, et al.,"Simulation Experiment of Five Percent Small Break LOCA of BWR", J. Nucl. Sci. Technol. 20, 89-104 (1983).

(7) K.TASAKA, et al.,"ROSA-III Double-Ended Break Test Series for a Loss-of-Coolant Accident in a Boiling Water Reactor", Nucl. Technol. 68, 77-93 (1985).

(8) M.SUZUKI, et al.,"Recirculation Pump Discharge Line Break Tests at ROSA-III for a Boiling Water Reactor", Nucl. Technol. 70, 189-203 (1985).

(9) Y.KOIZUMI, et al., "Experiment Analysis of Power Curve Sensitivity Test Series at ROSA-III", Nucl. Eng. and Design 86, 267-287 (1985)

(10) H.KUMAMARU, et al.,"Five Percent Break BWR LOCA/ECC Test at ROSA-III without HPCS Actuation---Two Dimensional Core Thermal Hydraulic Phenomena", Nucl. Eng. and Design 86, 219-239 (1985).

(11) K.TASAKA, et al.,"Analysis of ROSA-III Break Area Spectrum Experiments on BWR Loss-of-Coolant Accident", Nucl. Technol. 71, 3, 628-643 (1985).

(12) T.YONOMOTO, et al.,"Investigation of BWR/LOCA at ROSA-III---Effect of Break Configuration on System Transient---", Nucl. Eng. and Design 92, 195-205 (1986).

(13) M.SOBAJIMA, et al.,"Experiment Test Data of ROSA-III Test RUN 701 (Decay Heat Simulation Test with ECCS Actuation)", JAERI-M 8604 (1979).

(14) Y.ANODA et al.,"Experiment Data of ROSA-III Test RUN 703 (Split Break Simulation Test with ECCS Actuation)", JAERI-M 8967 (1980).

(15) Y.ANODA et al.,"Experiment Data of ROSA-III Test RUN 704 (Standard Test with ECCS Actuation)", JAERI-M 8968 (1980).

(16) M.OKAZAKI et al.,"Experimet Test Data of ROSA-III Integral Test RUN 705 (Isothermal Blowdown Test without ECCS Actuation)", JAERI-M 8723 (1980).

(17) M.SUZUKI et al.,"Experiment Data of ROSA-III Integral Test, RUN 706", JAERI-M 8737 (1980).

(18) M.OKAZAKI et al.,"Experiment Data of ROSA-III Integral Test RUN 708 (Standard Test without ECCS Actuation)", JAERI-M 8738 (1980).

(19) Y.KOIZUMI et al.,"Experiment Data of ROSA-III Integral Test, RUN 710", JAERI-M 9249 (1981).

(20) Y.ANODA et al.,"Experimet Data of ROSA-III Integral Test RUN912 (5% Split Break Test without HPCS Actuation)", JAERI-M 82-010.

(21) H.NAKAMURA et al.,"Experiment Data of ROSA-III Integral Test RUN 901 (200% Double-Ended Break with Full ECCS Actuation)", JAERI-M 84-007.

(22) H.NAKAMURA et al.,"Experiment Data of ROSA-III Integral Test RUN 926 (200% Double-Ended Break with HPCS Failure)", JAERI-M 84-008.

(23) M.SUZUKI et al.,"Experiment Data of 200% Recirculation Pump Discharge Line Break Integral Test RUN 961 with HPCS Failure at ROSA-III and Comparison with Results of Suction Line Break Tests", JAERI-M 84-045, (1984).

(24) M.SUZUKI, et al.,"Recirculation Pump Suction Line 2.8% Break Integral Test at ROSA-III with HPCS Failure, RUN 984", JAERI-M 84-100, (1984).

(25) M.SUZUKI, et al.,"Recirculation Pump Suction Line 200% Break Integral Test at ROSA-III with Two LPCI Failures, RUN 983", JAERI-M 84-135, (1984).

(26) M.SUZUKI, et al.,"BWR Recirculation Loop Discharge Line Break LOCA Tests with Break Areas of 50 and 100% Assuming HPCS Failure at ROSA-III Facility", JAERI-M 85-037, (1985).

(27) T.YONOMOTO, et al.,"ROSA-III 50% Break Integral Test RUN 916 (Break Area Parameter Test)", JAERI-M 85-109, (1985).

(28) H.NAKAMURA, et al.,"Recirculation Pump Suction Line 5% Split Break Test of ROSA-III (RUNs 922 and 932 with HPCS Failure)", JAERI-M 85-128, (1985).

(29) T.YONOMOTO, et al.,"ROSA-III 50% Break Integral Test RUN 928 (Break Configuration Sensitivity Test)", JAERI-M 85-151 (1985).

(30) H.NAKAMURA et al.,"Recirculation Pump Suction Line 1% Split Break LOCA Test of ROSA-III (RUNs 921 and 931 with HPCS Failure)", JAERI-M 85-209 (1986).

(31) M.SUZUKI, et al.,"BWR 200% Recirculation Pump Suction Line Break LOCA Tests, RUNs 942 and 943 at ROSA-III without HPCS (Effects of Initial Fluid Conditions on LOCA)", JAERI-M 86-038 (1986).

(32) M.SUZUKI, et al.,"Heat Loss and Fluid Leakage Tests of the ROSA-III Facility", JAERI-M 9834 (1981).

(33) M.SUZUKI, et al.,"Characteristics of the ROSA-III Test Facility (Characteristics Test of the Jet Pumps in Normal and Reverse Flow)", JAERI-M 8670, (1980) (in Japanese).

(34) M.SUZUKI, et al.,"Evaluation of a Jet Pump Model for RELAP5 Code", JAERI-M 84-245, (1985) (in Japanese).

(35) W. J. Letzring, et al.,"BWR Blowdown/ECC Program Preliminary Facility Description Report for the BD/ECC1a Test Phase", GEAP-23592.

(36) GE, EPRI and NRC,"Full Integral Simulation Test (FIST) Program Test Plan", EPRI NP-2313, GEAP 22053, (1981).

(37) M.MURASE et al., "BWR Loss-of-Coolant Integral Test -- Parallel Channel Effect", NUREG/CP-0027-Vol.3, (1982).

(38) W.S. HWANG, M.D. ALAMGIR and W.A. SUTHERLAND, "BWR Full Integral Simulation Test (FIST) Phase 1 Test Results", NUREG/CR-3711, General Electric Company (1983).

(39) S. ITOYA and N. ABE, "Analysis of TBL Main Steam Line Break Test by SAFER03 and TRAC-BD1", NUREG/CP-0072, Proceedings of the 13th WRSR Information Meeting, (Oct. 1985).

(40) M.KAWAJI, et al.,"A Main Steam Line Break Experiment at ROSA-III RUN 952 (Standard Run with Full ECCS)", JAERI-M 84-229, (1984).

(41) M.KAWAJI, et al.,"A Main Steam Line Break Experiment at ROSA-III, RUN 953 (100% Break with an HPCS Failure)", JAERI-M 85-029 (1985).

(42) M.SUZUKI, et al.,"BWR Main Steam Line Break LOCA Tests RUNs 951, 954 and 956 at ROSA-III (Beak Area Effects with HPCS Failure)", JAERI-M

85-202 (1985).

(43) K.TASAKA, et al.,"Comparison of ROSA-III and FIST BWR Loss of Coolant Accident Simulation Tests", JAERI-M 85-158 (1985).

(44) M.SUZUKI, et al.,"Similarity Study of Large Steam Line Break LOCAs in ROSA-III, FIST and BWR/6", Nucl. Eng. and Design 98,1, 39-56 (1986).

(45) M.SOBAJIMA et al.,"Instrumentation and Data Processing Method of the ROSA-III Test", JAERI-M 8499 (1979) (in Japanese).

(46) N.ABE et al.,"Electric Power Tansient Curve for ROSA-III Tests", JAERI-M 8728 (1980).

Table 2.1 Primary chracteristics of ROSA-III and BWR/6

	BWR-6	ROSA-III	BWR/ROSA
No. of Recirc. Loops	2	2	1
No. of Jet Pumps	24	4	6
No. of Separators	251	1	251
No. of Fuel Assemblies	848	4	212
Active Fuel Length (m)	3.76	1.88	2
Total Volume (m^3)	621	1.42	437
Power (MW)	3800	4.40	864
Pressure (MPa)	7.23	7.23	1
Core Flow (kg/s)	1.54×10^4	36.4	424
Recirculation Flow (l/s)	2970	7.01	424
Feedwater Flow (kg/s)	2060	4.86	424
Feedwater Temp (K)	489	489	1

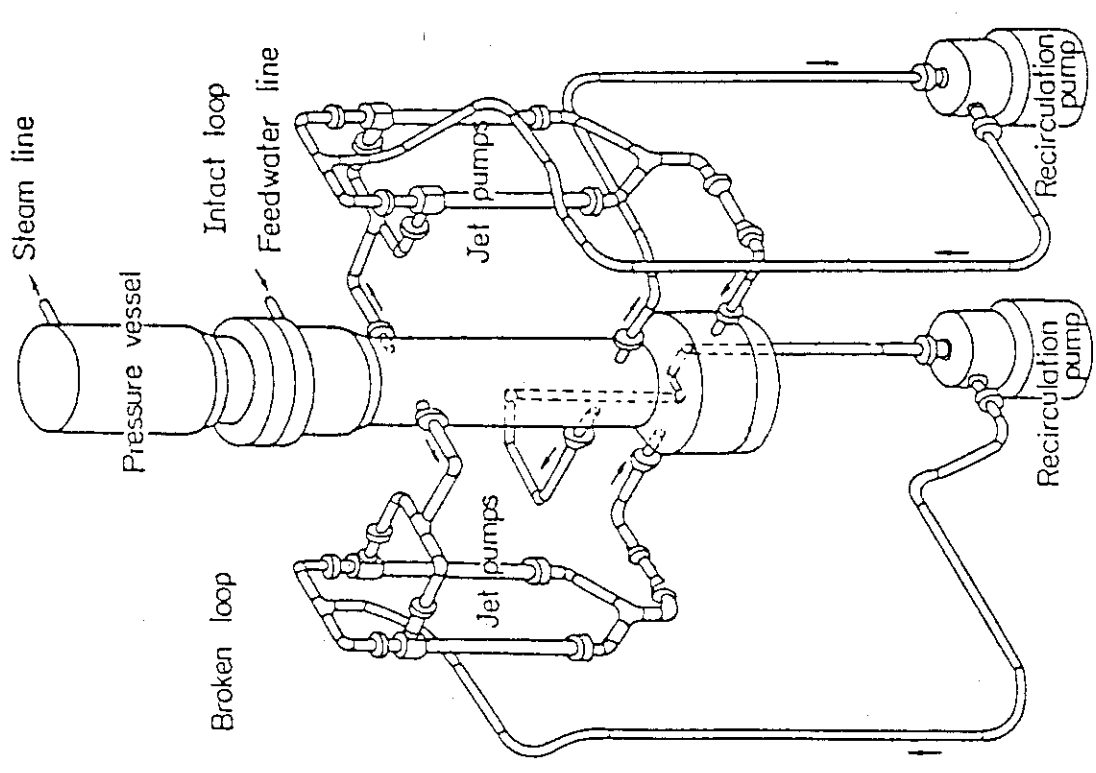

Fig. 2.1 Schematic diagram of ROSA-III test facility

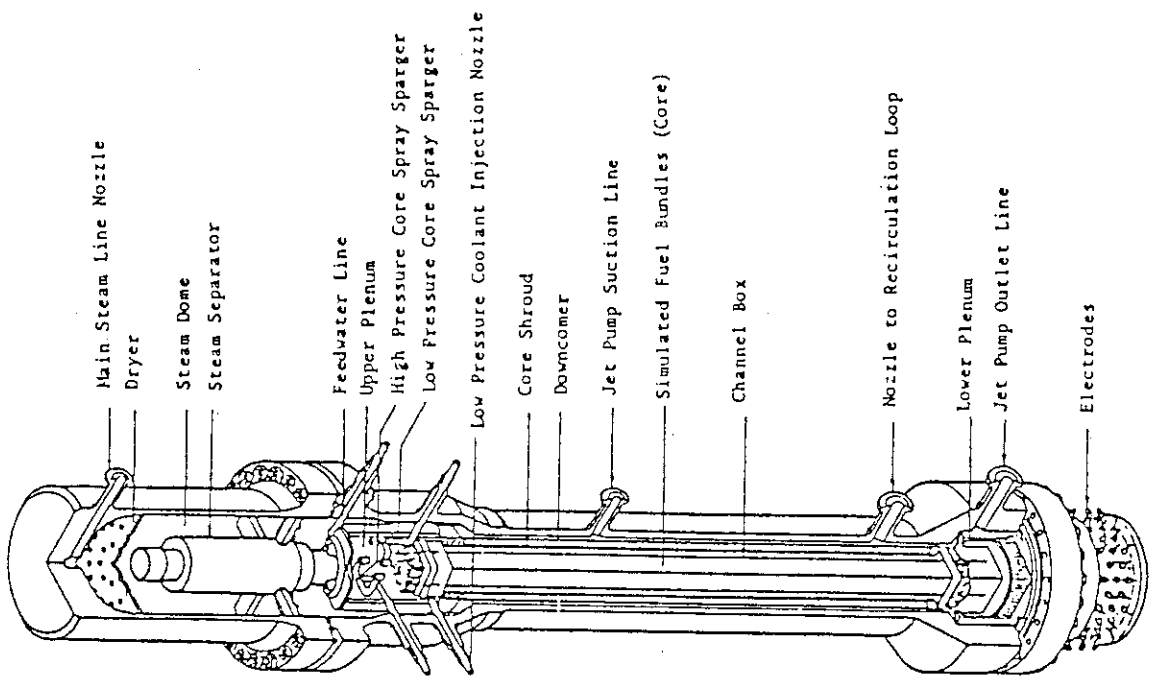

Fig. 2.2 Internal structure of pressure vessel of ROSA-III

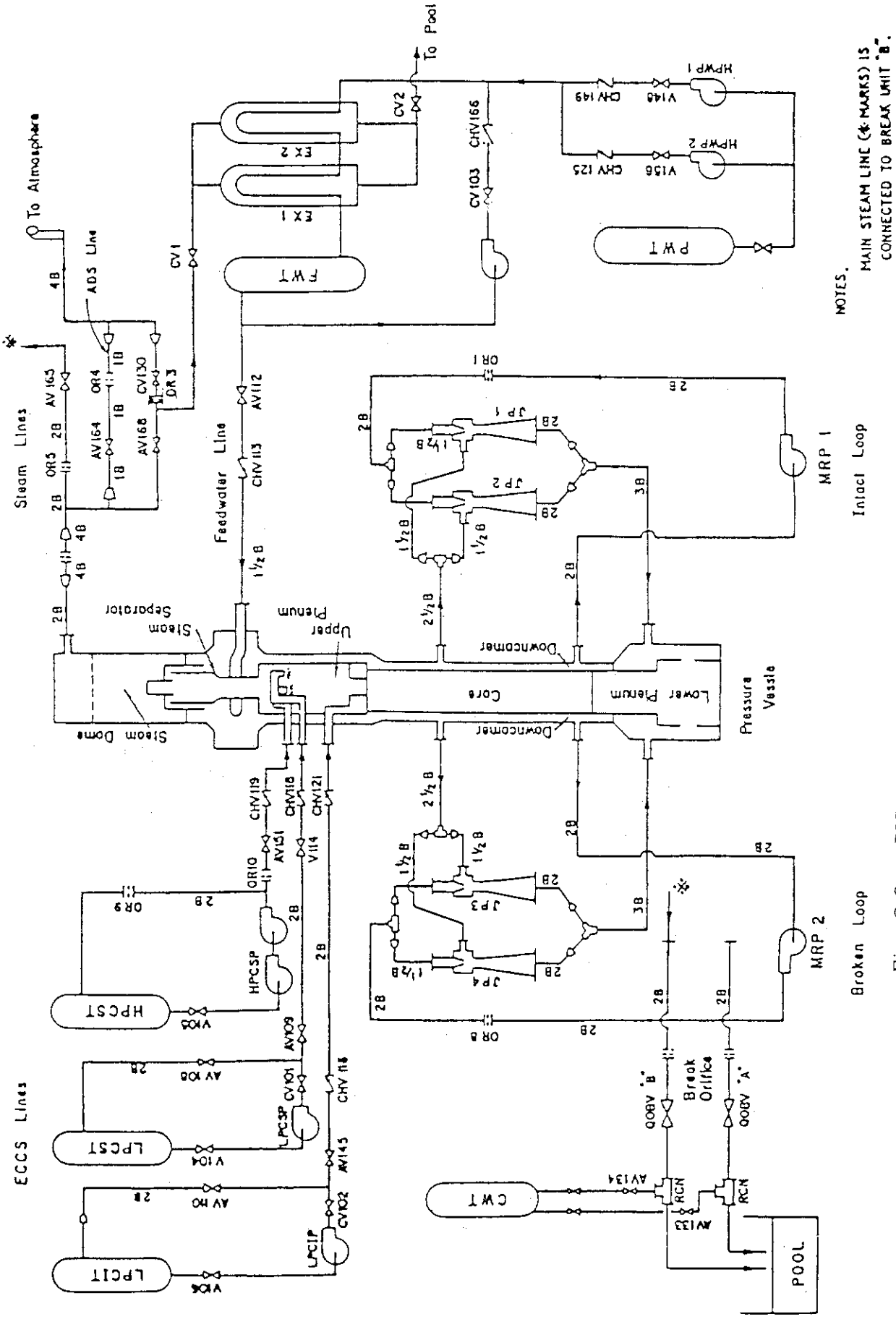

Fig. 2.3 ROSA-III piping schematic

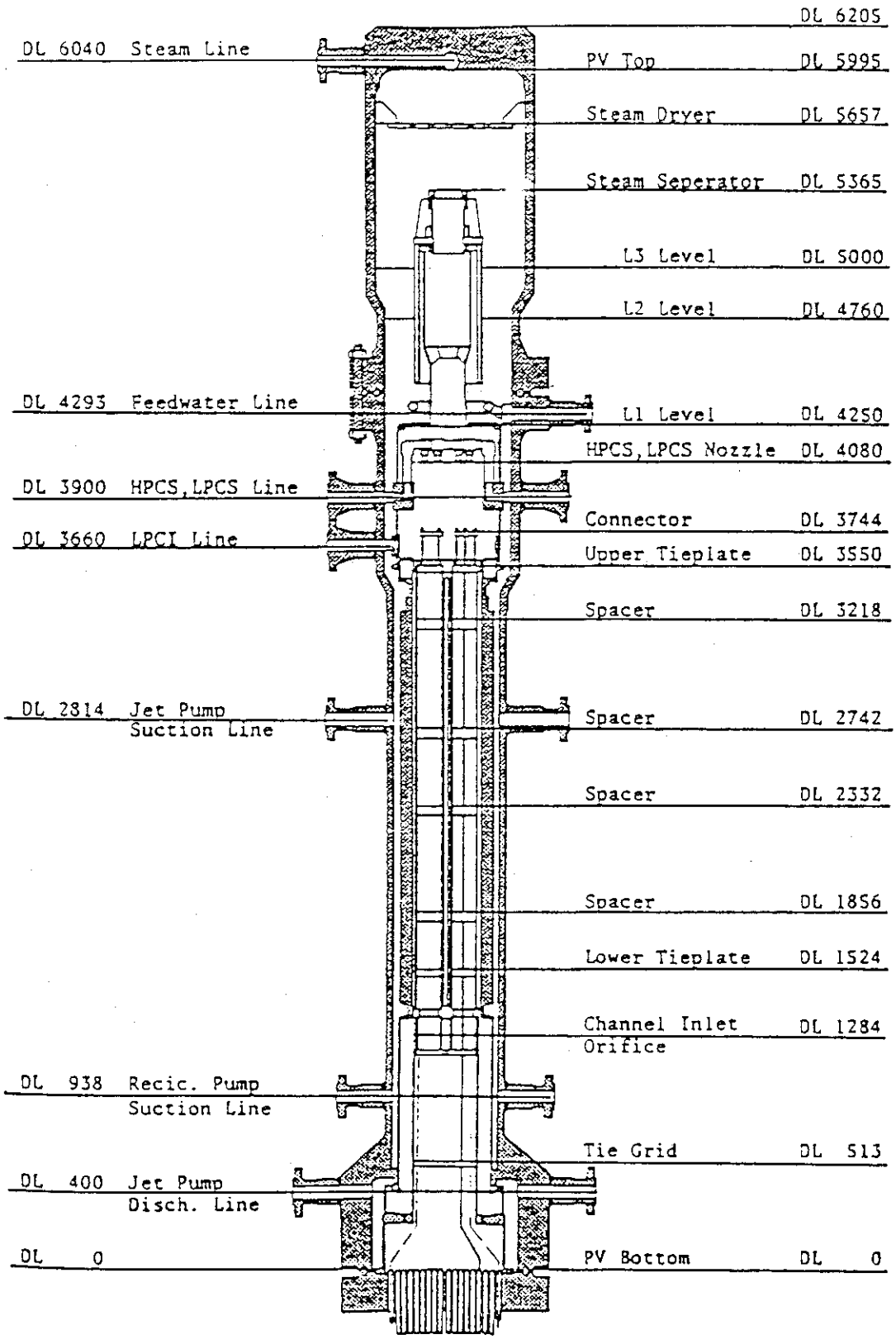

Fig. 2.4 Pressure vessel internals arrangement

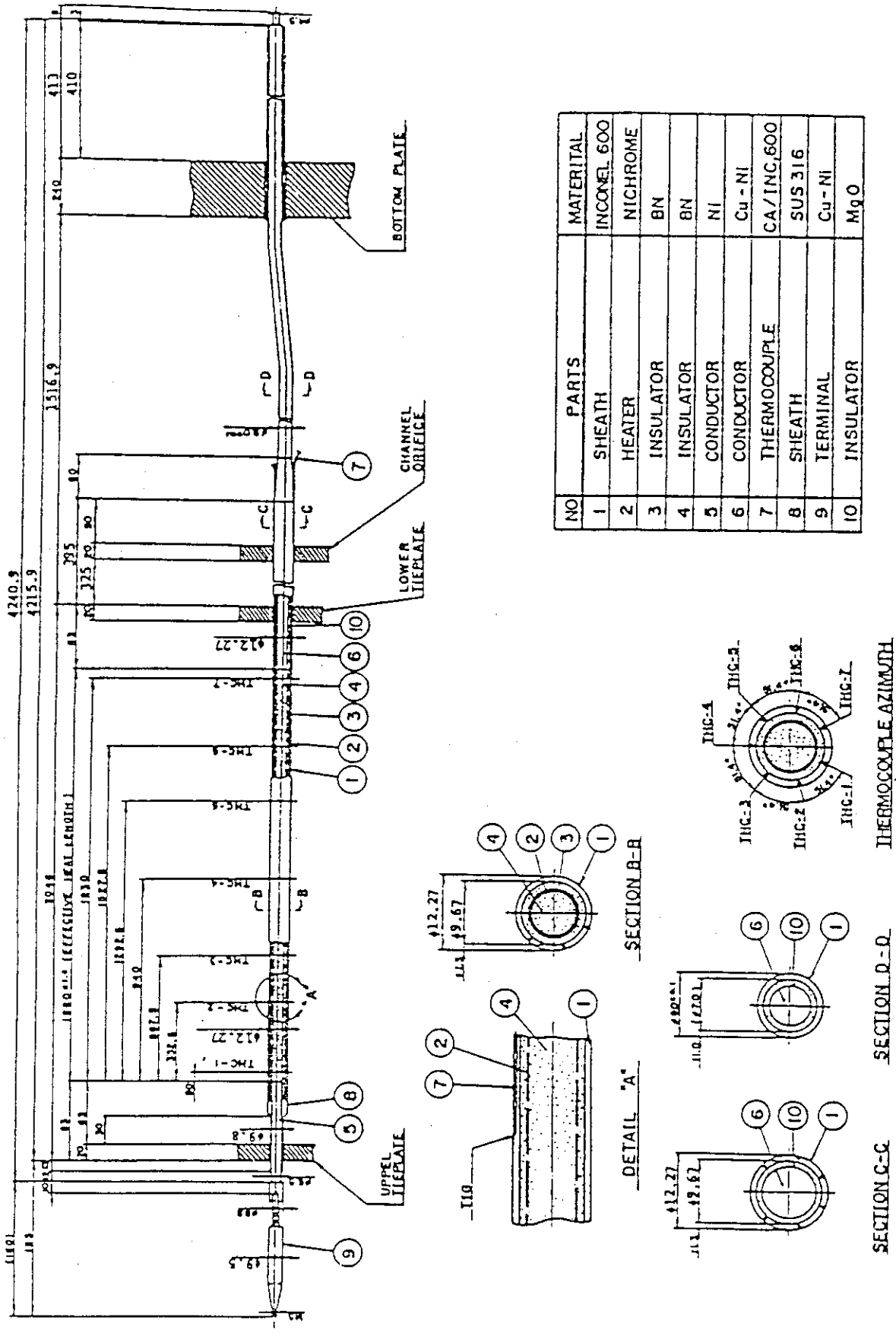

NO	PARTS	MATERITAL
1	SHEATH	INCONEL 600
2	HEATER	NICHROME
3	INSULATOR	BN
4	INSULATOR	BN
5	CONDUCTOR	NI
6	CONDUCTOR	Cu - NI
7	THERMOCOUPLE	CA/INC.600
8	SHEATH	SUS 316
9	TERMINAL	Cu - NI
10	INSULATOR	MgO

Fig. 2.5 Simulated fuel rod of ROSA-III

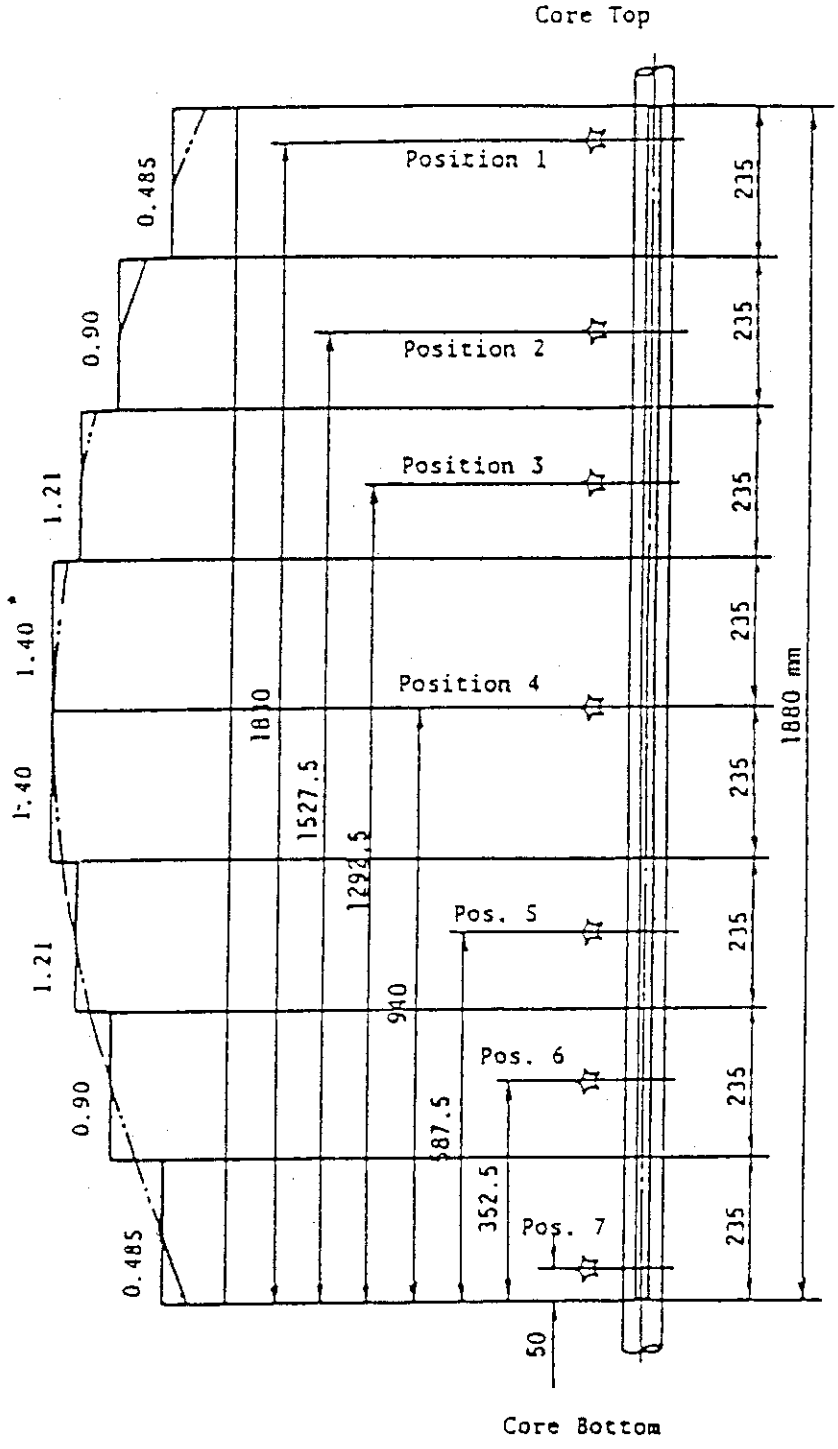

Fig. 2.6 Axial power distribution of heater rod

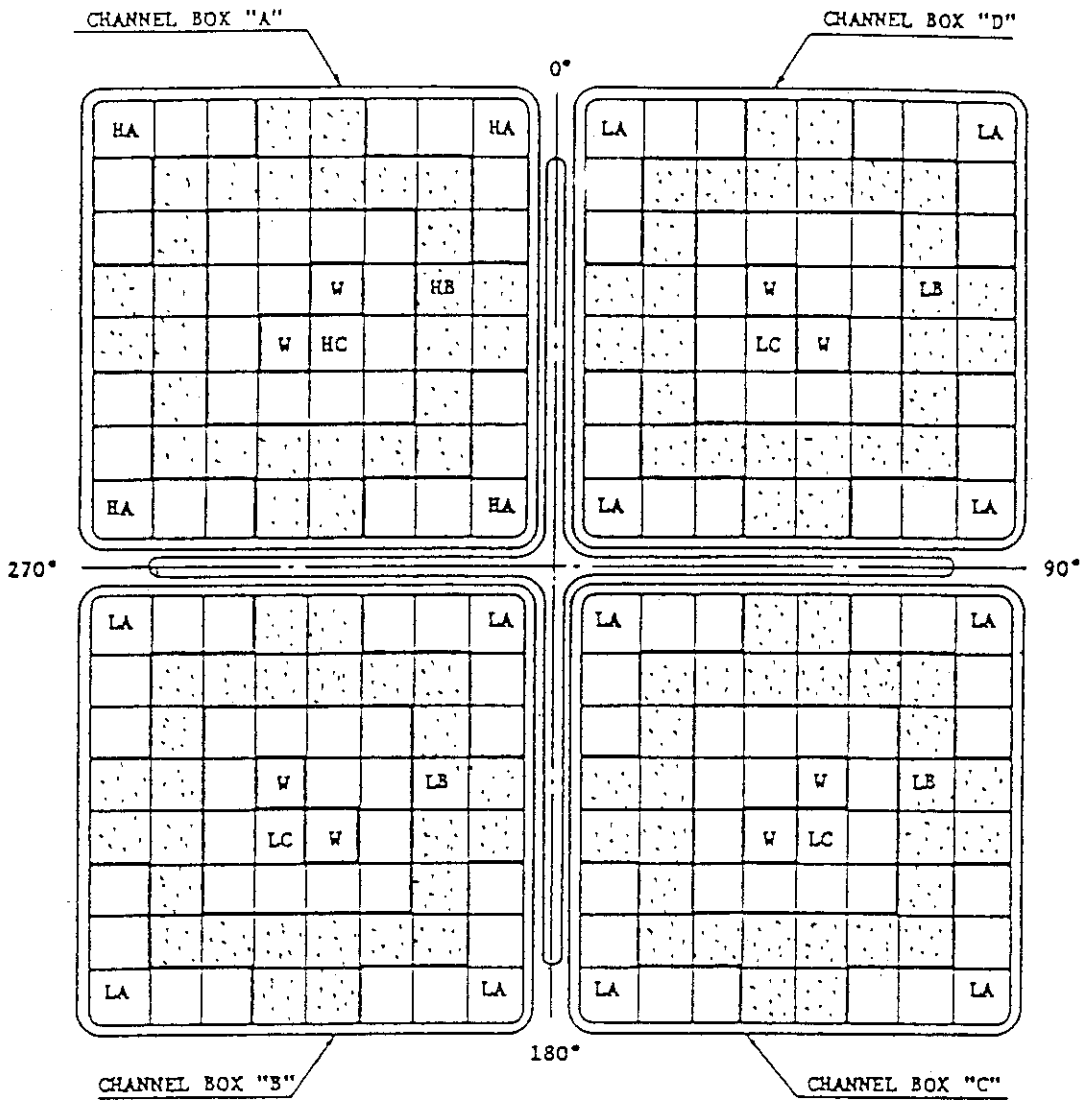

Region	HA	HB	HC	LA	LB	LC	W
Lenear Heat Rate (kW/m)	18.5	16.81	14.41	13.21	12.01	10.29	0.0
Local peaking factor	1.1	1.0	0.875	1.1	1.0	0.875	0.0
No. of Rods	20	28	14	60	84	42	8

* note : Radial peaking factor is 1.4

Fig. 2.7 Radial power distribution of core

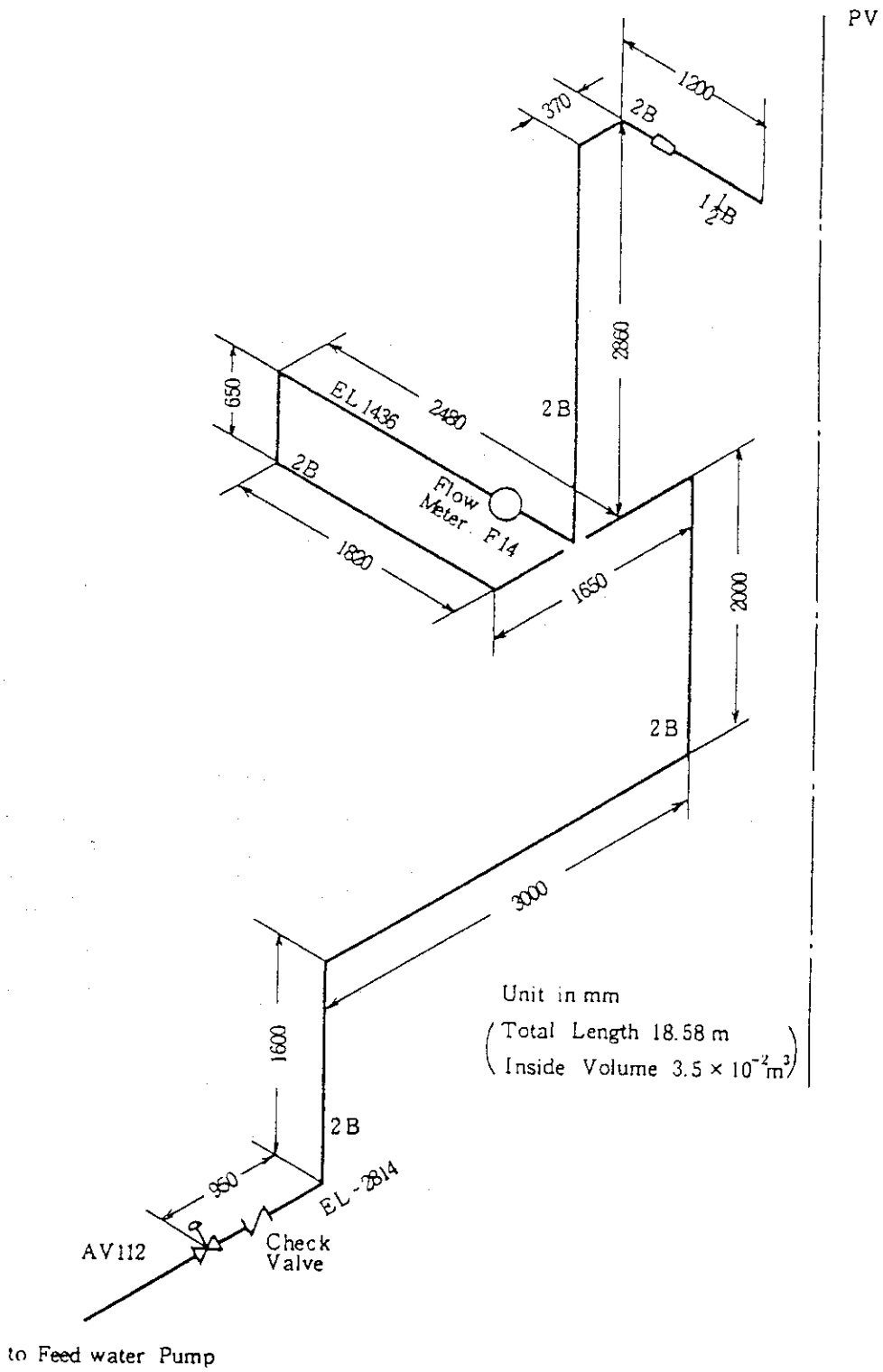

Fig. 2.8 Feedwater line between PV and AV-112

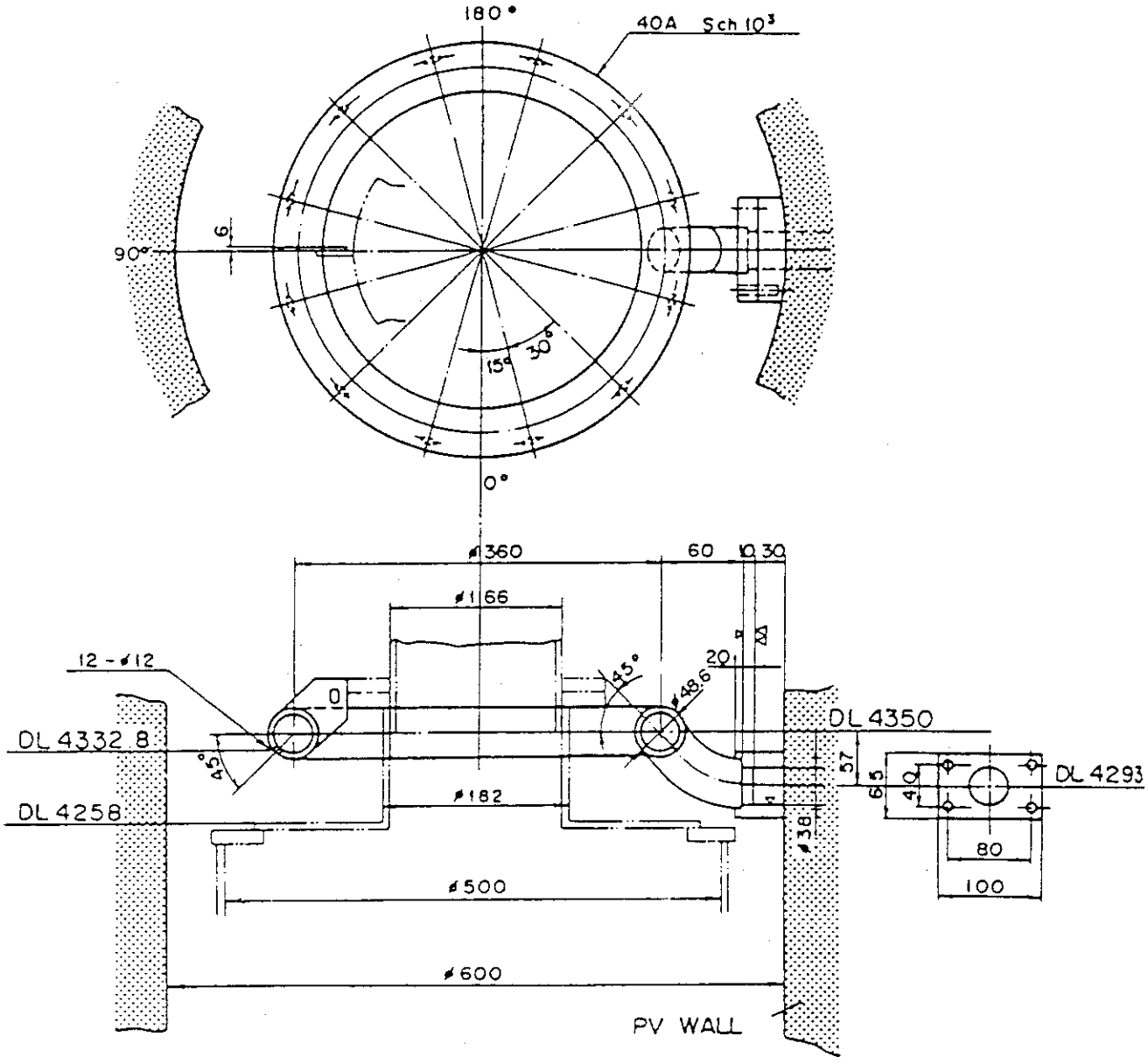

Fig. 2.9 Feedwater sparger configuration

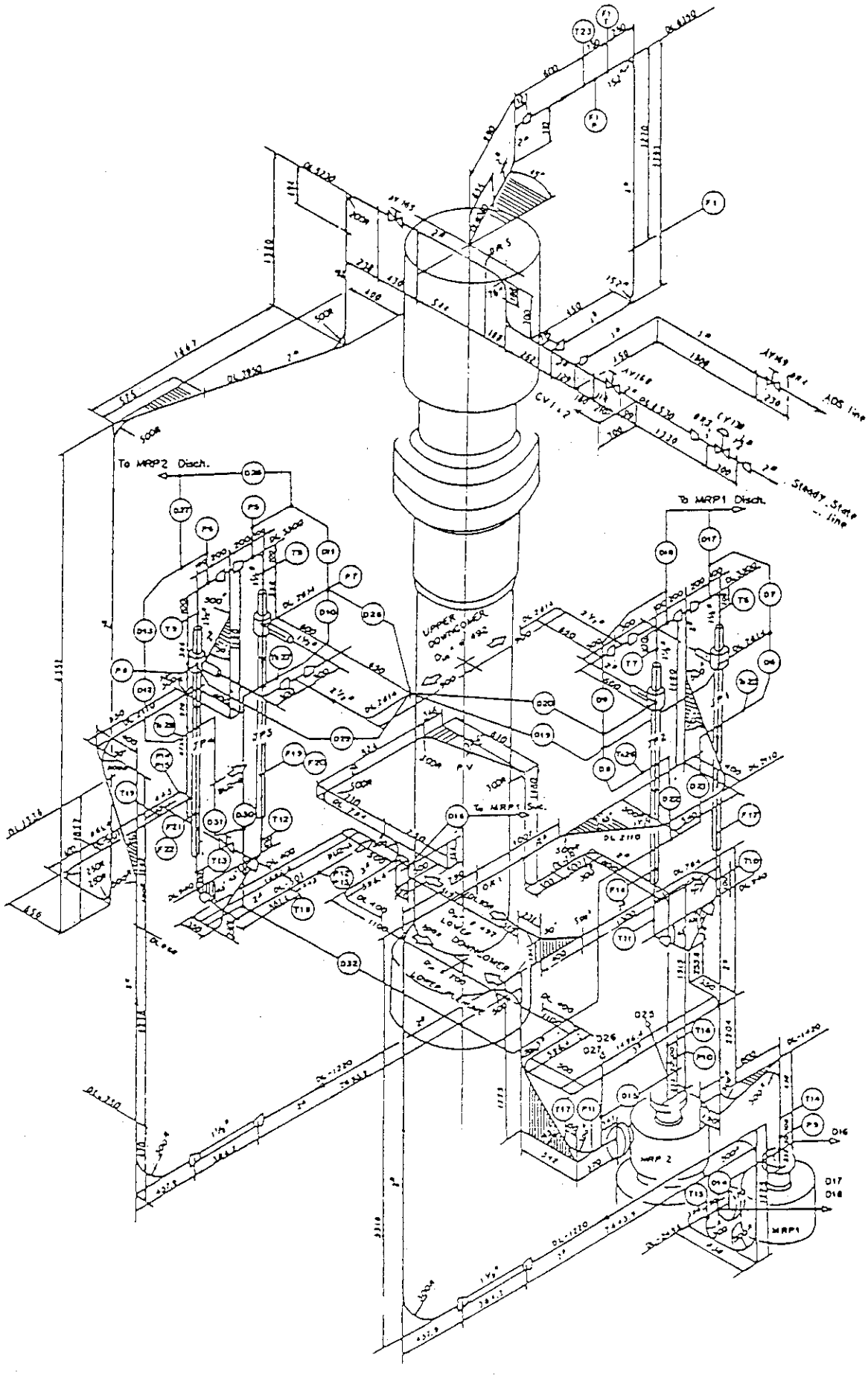

Fig. 2.10 Details of ROSA-III system piping

Table 3.1 ROSA-III instrumentation summary list

TYPE	SENSOR	NUMBER	NOTE	
PRESSURE	PRESSURE TRANSDUCER	20		
DIFFERENTIAL PRESSURE	DP CELL	60	PV AND LOOP	44
			LEVEL MEASUREMENT	5
			FLOW METER	11
FLUID TEMPERATURE	CA THERMOCOUPLE	129	PRIMARY LOOP	23
			DTT	4
			TIE ROD	28
			UPPER PLENUM	10
			LOWER PLENUM	10
			TIE PLATE	40
			BY PASS	14
FUEL ROD TEMPERATURE	CA THERMOCOUPLE	213		
SLAB SURFACE TEMPERATURE	CA THERMOCOUPLE	70	CORE BARREL	24
			PRESSURE VESSEL	3
			CHANNEL BOX	35
			SHROUD SUPPORT	8
SLAB INNER TEMPERATURE	CA THERMOCOUPLE	9	JP DIFFUSER	4
			PV WALL	5
VOLUMETRIC FLOW RATE	TURBINE METER	3	ECCS LOOP	3
	VENTURI METER	4	PRIMARY LOOP	10
	ORIFICE METER	6		
MASS FLOW RATE	TURBINE METER	4	RECIC. LOOP	4
	ORIFICE METER	3	STEAM LINE	3
LIQUID LEVEL	CONDUCTIVITY PROBE	138		
	CAPACITANCE PROBE	2		
DENSITY	GAMMA DENSITOMETER	10	2 BEAM GD	2
			3 BEAM GD	2
MOMENTUMR FLUX	DRAG DISK	7		
SIGNAL	ON/OFF SWITCH	14		
PUMP SPEED	REVOLUTION COUNTER	2		
ELECTRIC POWER	VA METER	2		
TOTAL		696		

Table 3.2 Measurement List for RUN 955

1Ch.- 50Ch.

Ch.	Item	Symbol	ID.		Location	Fig.No.	Range			Unit	Accuracy
1	Press.	P- 1	PA	1	Lower Plenum	Fig.5. 1	0.100	-	10.0	MPa	1.08%FS
2	Press.	P- 2	PA	2	Upper Plenum	Fig.5. 1	0.100	-	10.0	MPa	1.08%FS
3	Press.	P- 3	PA	3	Steam Dome	Fig.5. 1	0.100	-	10.0	MPa	1.08%FS
4	Press.	P- 4	PA	4	Downcomer Bottom	Fig.5. 1	0.100	-	10.0	MPa	1.08%FS
5	Press.	P- 5	PA	5	JP-3 Drive		0.100	-	10.0	MPa	1.08%FS
6	Press.	P- 6	PA	6	JP-4 Drive		0.100	-	10.0	MPa	1.08%FS
7	Press.	P- 7	PA	7	JP-3 Suction		0.100	-	10.0	MPa	1.08%FS
8	Press.	P- 8	PA	8	JP-4 Suction		0.100	-	10.0	MPa	1.08%FS
9	Press.	P- 9	PA	9	MRP-1 Suction		0.100	-	10.0	MPa	1.08%FS
10	Press.	P-10	PA	10	MRP-2 Suction		0.100	-	10.0	MPa	1.08%FS
11	Press.	P-11	PA	11	MRP-2 Delivery		0.100	-	10.0	MPa	1.08%FS
12	Press.	P-12	PA	12	Break A Upstream	Not Measured	0.100	-	10.0	MPa	1.08%FS
13	Press.	P-13	PA	13	Break A Downstream	Not Measured	0.100	-	10.0	MPa	1.08%FS
14	Press.	P-14	PA	14	Break B Upstream		0.100	-	10.0	MPa	1.08%FS
15	Press.	P-15	PA	15	Break B Downstream		0.100	-	10.0	MPa	1.08%FS
16	Press.	P-16	PA	16	Steam Line		0.100	-	10.0	MPa	1.08%FS
17	Press.	P-17	PA	17	JP-1,2 Outlet Spool		0.100	-	10.0	MPa	1.08%FS
18	Press.	P-18	PA	18	JP-3,4 Outlet Spool		0.100	-	10.0	MPa	1.08%FS
19	Press.	P-19	PA	19	Break A Spool Piece	Not Measured	0.100	-	10.0	MPa	1.08%FS
20	Press.	P-30	PA	20	Break B Spool Piece		0.100	-	10.0	MPa	1.08%FS
21	Diff.P.	D- 1	PD	21	Lower Pl.-Upper Pl.	FIG.5. 2	-50.0	-	350.	kPa	0.63%FS
22	Diff.P.	D- 2	PD	22	Upper Pl.-Steam Dome	FIG.5. 3	-10.0	-	90.0	kPa	0.63%FS
23	Diff.P.	D- 3	PD	23	Lower Plenum Head	Not Measured					
24	Diff.P.	D- 4	PD	24	Downcomer Head		0.0	-	100.	kPa	0.63%FS
25	Diff.P.	D- 5	PD	25	PV Bottom-Top	FIG.5. 4	-100.	-	900.	kPa	0.63%FS
26	Diff.P.	D- 6	PD	26	JP-1 Disch.-Suction	FIG.5. 5	-100.	-	300.	kPa	0.63%FS
27	Diff.P.	D- 7	PD	27	JP-1 Drive -Suction	FIG.5. 6	0.0	-	2.50	MPa	0.63%FS
28	Diff.P.	D- 8	PD	28	JP-2 Disch.-Suction	FIG.5. 5	-100.	-	300.	kPa	0.63%FS
29	Diff.P.	D- 9	PD	29	JP-2 Drive -Suction	FIG.5. 6	0.0	-	2.50	MPa	0.63%FS
30	Diff.P.	D-10	PD	30	JP-3 Disch.-Suction	FIG.5. 7	-100.	-	300.	kPa	0.63%FS
31	Diff.P.	D-11	PD	31	JP-3 Drive -Suction	FIG.5. 8	-4.00	-	2.00	MPa	0.63%FS
32	Diff.P.	D-12	PD	32	JP-4 Disch.-Suction	FIG.5. 7	-100.	-	300.	kPa	0.63%FS
33	Diff.P.	D-13	PD	33	JP-4 Drive -Suction	FIG.5. 8	-4.00	-	2.00	MPa	0.63%FS
34	Diff.P.	D-14	PD	34	MRP-1 Deliv.-Suction	FIG.5. 9	-0.100	-	2.50	MPa	0.63%FS
35	Diff.P.	D-15	PD	35	MRP-2 Deliv.-Suction	FIG.5. 9	-0.100	-	2.50	MPa	0.63%FS
36	Diff.P.	D-16	PD	36	DC Bottom- MRP-1 Suc.	FIG.5.10	-50.0	-	50.0	kPa	0.63%FS
37	Diff.P.	D-17	PD	37	MRP1 Deliv.-JP1 Drive	FIG.5.11	0.0	-	250.	kPa	0.63%FS
38	Diff.P.	D-18	PD	38	MRP1 Deliv.-JP2 Drive	FIG.5.11	0.0	-	250.	kPa	0.63%FS
39	Diff.P.	D-19	PD	39	DC Middle-JP1 Suction	FIG.5.12	0.0	-	250.	kPa	0.63%FS
40	Diff.P.	D-20	PD	40	DC Middle-JP2 Suction	FIG.5.12	0.0	-	250.	kPa	0.63%FS
41	Diff.P.	D-21	PD	41	JP1 Disch.-Lower Pl.	FIG.5.13	-100.	-	100.	kPa	0.63%FS
42	Diff.P.	D-22	PD	42	JP2 Disch.-Lower Pl.	FIG.5.13	-100.	-	100.	kPa	0.63%FS
43	Diff.P.	D-23	PD	43	DC Bottom- Break B		-60.0	-	540.	kPa	0.63%FS
44	Diff.P.	D-24	PD	44	Break B- Break A	Not Measured	0.0	-	100.	kPa	0.63%FS
45	Diff.P.	D-25	PD	45	Break A- MRP2 Suction	Not Measured	-500.	-	100.	kPa	0.63%FS
46	Diff.P.	D-26	PD	46	MRP2 Deliv.-JP3 Drive	FIG.5.14	-500.	-	500.	kPa	0.63%FS
47	Diff.P.	D-27	PD	47	MRP2 Deliv.-JP4 Drive	FIG.5.14	-500.	-	500.	kPa	0.63%FS
48	Diff.P.	D-28	PD	48	DC Middle-JP3 Suction	FIG.5.15	-250.	-	250.	kPa	0.63%FS
49	Diff.P.	D-29	PD	49	DC Middle-JP4 Suction	FIG.5.15	-250.	-	250.	kPa	0.63%FS
50	Diff.P.	D-30	PD	50	JP3 Disch.-Confluence	FIG.5.16	-100.	-	100.	kPa	0.63%FS

Table 3.2 Measurement List for RUN 955 (Continued)

51Ch.- 100Ch.

Ch.	Item	Symbol	ID.		Location	Fig.No.	Range			Unit	Accuracy
51	Diff.P.	D-31	PD	51	JP4 Disch.-Confluence	FIG.5.16	-100.	-	100.	kPa	0.63%FS
52	Diff.P.	D-32	PD	52	Confluence -Lower Pl.	FIG.5.17	-50.0	-	50.0	kPa	0.63%FS
53	Diff.P.	D-33	PD	53	Lower Pl.-DC Middle		-250.	-	250.	kPa	0.63%FS
54	Diff.P.	D-34	PD	54	Lower Pl.-DC Bottom		-250.	-	250.	kPa	0.63%FS
55	Diff.P.	D-35	PD	55	DC Bottom-DC Middle	FIG.5.18	-50.0	-	50.0	kPa	0.63%FS
56	Diff.P.	D-36	PD	56	DC Middle-Steam Dome	FIG.5.19	-50.0	-	50.0	kPa	0.63%FS
57	Diff.P.	D-37	PD	57	Lower Pl.Mid-Upper PL	Not Measured					
58	Diff.P.	D-38	PD	58	Lower Pl.Bottom-Mid.	FIG.5.20	0.0	-	50.0	kPa	0.63%FS
59	Diff.P.	D-39	PD	59	Upper Pl.-DC High	Not Used	-20.0	-	100.	kPa	0.63%FS
60	Diff.P.	D-40	PD	60	Channel Orifice A	FIG.5.21	-50.0	-	50.0	kPa	0.63%FS
61	Diff.P.	D-41	PD	61	Channel Orifice B	FIG.5.22	-50.0	-	50.0	kPa	0.63%FS
62	Diff.P.	D-42	PD	62	Channel Orifice C	FIG.5.23	-25.0	-	75.0	kPa	0.63%FS
63	Diff.P.	D-43	PD	63	Channel Orifice D	FIG.5.24	-50.0	-	50.0	kPa	0.63%FS
64	Diff.P.	D-44	PD	64	Bypass Hole	FIG.5.25	-100.	-	100.	KPA	0.63%FS
65	Level	WL- 1	LM	65	HPCS Tank	Not Used	0.0	-	2.30	m	1.00%FS
66	Level	WL- 2	LM	66	LPCS Tank	FIG.5.26	0.0	-	2.30	m	1.00%FS
67	Level	WL- 3	LM	67	LPCI Tank	FIG.5.26	0.0	-	4.25	m	1.00%FS
68	Level	WL- 4	LM	68	Upper Downcomer	FIG.5.27	3.90	-	6.04	m	1.00%FS
69	Level	WL- 5	LM	69	Lower Downcomer	FIG.5.27	0.938	-	3.90	m	1.00%FS
70	Mass.F.	F- 1	FM	70	Steam Line (Low Range)		0.0	-	1.13	kg/s	0.92%FS
71	Mass.F.	F- 2	FM	71	Steam Line(High Range)		0.0	-	3.00	kg/s	0.92%FS
72	Mass.F.	F- 3	FM	72	Steam Line (Mid Range)		0.0	-	1.94	kg/s	1.40%FS
73	Vol.F.	F- 7	FV	73	HPCS (Upper Plenum)	Not Used	0.0	-	0.250E-02	m3/s	0.79%FS
74	Vol.F.	F- 9	FV	74	LPCS (Upper Plenum)	FIG.5.28	0.0	-	0.250E-02	m3/s	0.79%FS
75	Vol.F.	F-11	FV	75	LPCI (Core Bypass)	FIG.5.28	0.0	-	0.830E-02	m3/s	0.79%FS
76	Vol.F.	F-15	FV	76	Feedwater	FIG.5.29	0.0	-	0.100E-01	m3/s	0.79%FS
77	Vol.F.	F-16	FV	77	PWT Flow	Not Measured	0.0	-	0.420E-02	m3/s	0.79%FS
78	Vol.F.	F-17	FV	78	JP1 Discharge	FIG.5.30	0.0	-	0.170E-01	m3/s	0.88%FS
79	Vol.F.	F-18	FV	79	JP2 Discharge	FIG.5.30	0.0	-	0.170E-01	m3/s	0.88%FS
80	Vol.F.	F-19	FV	80	JP3 Disch. Positive	FIG.5.31	0.0	-	0.170E-01	m3/s	0.92%FS
81	Vol.F.	F-20	FV	81	JP3 Disch. Negative	FIG.5.32	0.0	-	0.500E-02	m3/s	0.92%FS
82	Vol.F.	F-21	FV	82	JP4 Disch. Positive	FIG.5.31	0.0	-	0.170E-01	m3/s	0.92%FS
83	Vol.F.	F-22	FV	83	JP4 Disch. Negative	FIG.5.32	0.0	-	0.500E-02	m3/s	0.92%FS
84	Mass.F.	F-23	FM	84	JP1,2 Outlet Spool	Not Measured	0.0	-	30.0	kg/s	1.40%FS
85	Mass.F.	F-24	FM	85	JP3,4 Outlet Spool	Not Measured	0.0	-	30.0	kg/s	1.40%FS
86	Mass.F.	F-25	FM	86	Break A Spool Piece	Not Measured	0.0	-	30.0	kg/s	1.40%FS
87	Mass.F.	F-26	FM	87	Break B Spool Piece	Not Measured	0.0	-	30.0	kg/s	1.40%FS
88	Vol.F.	F-27	FV	88	MRP-1	Failure	0.0	-	0.120E-01	m3/s	0.88%FS
89	Vol.F.	F-28	FV	89	MRP-2	FIG.5.33	0.0	-	0.120E-01	m3/s	0.63%FS
90	Diff.P.	D-F1	PD	90	F1 Orifice		0.0	-	4.90	kPa	0.63%FS
91	Diff.P.	D-F2	PD	91	F2 Orifice		0.0	-	34.9	kPa	0.63%FS
92	Diff.P.	D-F3	PD	92	F3 Orifice		0.0	-	14.6	kPa	0.63%FS
93	Diff.P.	D-F17	PD	93	F17 Venturi		0.0	-	98.1	kPa	0.63%FS
94	Diff.P.	D-F18	PD	94	F18 Venturi		0.0	-	98.1	kPa	0.63%FS
95	Diff.P.	D-F19	PD	95	F19 Orifice		0.0	-	147.	kPa	0.63%FS
96	Diff.P.	D-F20	PD	96	F20 Orifice		0.0	-	13.2	kPa	0.63%FS
97	Diff.P.	D-F21	PD	97	F21 Orifice		0.0	-	147.	kPa	0.63%FS
98	Diff.P.	D-F22	PD	98	F22 Orifice		0.0	-	13.2	kPa	0.63%FS
99	Diff.P.	D-F27	PD	99	F27 Venturi		0.0	-	200.	kPa	0.63%FS
100	Diff.P.	D-F28	PD	100	F28 Venturi		0.0	-	200.	kPa	0.63%FS

Table 3.2 Measurement List for RUN 955 (Continued)

101Ch.- 150Ch.

Ch.	Item	Symbol	ID.		Location	Fig.No.	Range			Unit	Accuracy
101	Power	W- 1	WE	101	2100 kW Power Supplier	FIG.5.34	0.0	-	0.210E+04	kW	1.00%FS
102	Power	W- 2	WE	102	3150 kW Power Supplier	FIG.5.34	0.0	-	0.315E+04	kW	1.00%FS
103											
104	Rev.	N- 1	SR	104	MRP-1 Revolution		0.0	-	0.500E+04	RPM	1.08%FS
105	Rev.	N- 2	SR	105	MRP-2 Revolution	FIG.5.35	0.0	-	0.500E+04	RPM	1.08%FS
106	Signal	S- 1	EV	106	Break Signal A	Not Measured					
107	Signal	S- 2	EV	107	Break Signal B	FIG.5.36					
108	Signal	S- 3	EV	108	QSV Signal	FIG.5.36					
109	Signal	S- 6	EV	109	HPCS Valve	FIG.5.37					
110	Signal	S- 7	EV	110	LPCS Valve	FIG.5.37					
111	Signal	S- 8	EV	111	LPCI Valve	FIG.5.37					
112	Signal	S- 9	EV	112	Feedwater Control	FIG.5.36					
113	Signal	S-10	EV	113	MSIV Signal	FIG.5.36					
114	Signal	S-11	EV	114	Steam Line Valve	FIG.5.36					
115	Signal	S-12	EV	115	ADS Valve	FIG.5.37					
116	Signal	S-13	EV	116	MRP-1 Power OFF	FIG.5.38					
117	Signal	S-14	EV	117	MRP-2 Power OFF	FIG.5.38					
118	Signal	RD- 1	EV	118	MRP-1 Rev. Direction	Failure					
119	Signal	RD- 2	EV	119	MRP-2 Rev. Direction	Failure					
120	Density	DF- 1	DE	120	JP1,2 Outlet Beam A	FIG.5.39	0.0	-	0.100E+04	kg/m3	1.00%FS
121	Density	DF- 2	DE	121	JP1,2 Outlet Beam B	FIG.5.40	0.0	-	0.100E+04	kg/m3	1.00%FS
122	Density	DF- 3	DE	122	JP1,2 Outlet Beam C	FIG.5.41	0.0	-	0.100E+04	kg/m3	1.00%FS
123	Density	DF- 4	DE	123	JP3,4 Outlet Beam A	FIG.5.42	0.0	-	0.100E+04	kg/m3	1.00%FS
124	Density	DF- 5	DE	124	JP3,4 Outlet Beam B	FIG.5.43	0.0	-	0.100E+04	kg/m3	1.00%FS
125	Density	DF- 6	DE	125	JP3,4 Outlet Beam C	FIG.5.44	0.0	-	0.100E+04	kg/m3	1.00%FS
126	Density	DF- 7	DE	126	Break A Beam A	Not Measured	0.0	-	0.100E+04	kg/m3	1.00%FS
127	Density	DF- 8	DE	127	Break A Beam B	Not Measured	0.0	-	0.100E+04	kg/m3	1.00%FS
128	Density	DF- 9	DE	128	Break B Beam A		0.0	-	0.100E+04	kg/m3	1.00%FS
129	Density	DF-10	DE	129	Break B Beam B		0.0	-	0.100E+04	kg/m3	1.00%FS
130	Mo.Flux	M- 1	MF	130	JP1,2 Outlet Spool	FIG.5.45	0.0	-	0.220E+05	kg/ms2	1.00%FS
131	Mo.Flux	M- 2	MF	131	JP3,4 Outlet Spool	FIG.5.46	0.0	-	0.220E+05	kg/ms2	1.00%FS
132	Mo.Flux	M- 3	MF	132	Break A (Low Range)	Not Measured	0.0	-	0.220E+05	kg/ms2	1.00%FS
133	Mo.Flux	M- 4	MF	133	Break B (Low Range)		0.0	-	0.220E+05	kg/ms2	1.00%FS
134	Mo.Flux	M- 5	MF	134	Break A (High Range)	Not Measured	0.0	-	0.220E+06	kg/ms2	1.00%FS
135	Mo.Flux	M- 6	MF	135	Break B (High Range)		0.0	-	0.220E+06	kg/ms2	1.00%FS
136	Mo.Flux	M- 7	MF	136	Break Orifice	Not Measured	0.0	-	0.220E+05	kg/ms2	1.00%FS
137											
138	Fluid T.	T- 1	TE	138	Lower Plenum	FIG.5.47	273.	-	673.	K	0.64%FS
139	Fluid T.	T- 2	TE	139	Upper Plenum	FIG.5.47	273.	-	673.	K	0.64%FS
140	Fluid T.	T- 3	TE	140	Steam Dome	FIG.5.47	273.	-	673.	K	0.64%FS
141	Fluid T.	T- 4	TE	141	Upper Downcomer	FIG.5.48	273.	-	673.	K	0.64%FS
142	Fluid T.	T- 5	TE	142	Lower Downcomer	FIG.5.48	273.	-	673.	K	0.64%FS
143	Fluid T.	T- 6	TE	143	JP-1 Drive	FIG.5.49	273.	-	673.	K	0.64%FS
144	Fluid T.	T- 7	TE	144	JP-2 Drive	FIG.5.49	273.	-	673.	K	0.64%FS
145	Fluid T.	T- 8	TE	145	JP-3 Drive	FIG.5.50	273.	-	673.	K	0.64%FS
146	Fluid T.	T- 9	TE	146	JP-4 Drive	FIG.5.50	273.	-	673.	K	0.64%FS
147	Fluid T.	T-10	TE	147	JP-1 Discharge		273.	-	673.	K	0.64%FS
148	Fluid T.	T-11	TE	148	JP-2 Discharge		273.	-	673.	K	0.64%FS
149	Fluid T.	T-12	TE	149	JP-3 Discharge		273.	-	673.	K	0.64%FS
150	Fluid T.	T-13	TE	150	JP-4 Discharge		273.	-	673.	K	0.64%FS

Table 3.2 Measurement List for RUN 955 (Continued)

151Ch.- 200Ch.

Ch.	Item	Symbol	ID.		Location	Fig.No.	Range			Unit	Accuracy
151	Fluid T.	T-14	TE	151	MRP-1 Suction	FIG.5.49	273.	-	673.	K	0.64%FS
152	Fluid T.	T-15	TE	152	MRP-1 Delivery	FIG.5.49	273.	-	673.	K	0.64%FS
153	Fluid T.	T-16	TE	153	MRP-2 Suction	FIG.5.50	273.	-	673.	K	0.64%FS
154	Fluid T.	T-17	TE	154	MRP-2 Delivery	FIG.5.50	273.	-	673.	K	0.64%FS
155	Fluid T.	T-18	TE	155	Break A Upstream	Not Measured	273.	-	673.	K	0.64%FS
156	Fluid T.	T-19	TE	156	Break B Upstream	FIG.5.51	273.	-	673.	K	0.64%FS
157	Fluid T.	T-20	TE	157	RCN A Condenced Water	Not Used	273.	-	698.	K	0.64%FS
158	Fluid T.	T-21	TE	158	RCN B Condenced Water	Not Used	273.	-	698.	K	0.64%FS
159	Fluid T.	T-22	TE	159	Discharged Steam	FIG.5.47	273.	-	673.	K	0.64%FS
160	Fluid T.	T-24	TE	160	JP-1,2 Outlet Spool		273.	-	763.	K	0.64%FS
161	Fluid T.	T-25	TE	161	JP-3,4 Outlet Spool		273.	-	763.	K	0.64%FS
162	Fluid T.	T-26	TE	162	Break A Spool Piece		273.	-	763.	K	0.64%FS
163	Fluid T.	T-27	TE	163	Break B Spool Piece		273.	-	763.	K	0.64%FS
164	Fluid T.	T-28	TE	164	Feedwater		273.	-	673.	K	0.64%FS
165	Fluid T.	T-29	TE	165	Break Orifice 1		273.	-	673.	K	0.64%FS
166	Fluid T.	T-30	TE	166	Break Orifice 2		273.	-	673.	K	0.64%FS
167	Fluid T.	T-31	TE	167	Break A Down DD(Low)	Not Measured	273.	-	673.	K	0.64%FS
168	Fluid T.	T-32	TE	168	Break B Down DD(Low)	Not Measured	273.	-	673.	K	0.64%FS
169	Fluid T.	T-33	TE	169	Break A Up. DD(High)	Not Measured	273.	-	673.	K	0.64%FS
170	Fluid T.	T-34	TE	170	Break B Up. DD(High)		273.	-	673.	K	0.64%FS
171	Fluid T.	T-F17	TE	171	JP1 Fluid D. Correc.		273.	-	673.	K	0.64%FS
172	Fluid T.	T-F18	TE	172	JP2 Fluid D. Correc.		273.	-	673.	K	0.64%FS
173	Fluid T.	T-F19	TE	173	JP3 Fluid D. Correc.		273.	-	673.	K	0.64%FS
174	Fluid T.	T-F21	TE	174	JP4 Fluid D. Correc.		273.	-	673.	K	0.64%FS
175	Slab T.	TS-11	TE	175	Core Barrel A Pos.5	Not Measured	273.	-	673.	K	0.64%FS
176	Slab T.	TS-12	TE	176	Core Barrel A Pos.6	Not Measured	273.	-	673.	K	0.64%FS
177	Slab T.	TS-13	TE	177	Filler Block C Pos.1	Not Measured	273.	-	673.	K	0.64%FS
178	Slab T.	TS-14	TE	178	Filler Block C Pos.2	Not Measured	273.	-	673.	K	0.64%FS
179	Slab T.	TS-15	TE	179	Filler Block C Pos.3	Not Measured	273.	-	673.	K	0.64%FS
180	Slab T.	TS-16	TE	180	Filler Block C Pos.4	Not Measured	273.	-	673.	K	0.64%FS
181	Slab T.	TS-17	TE	181	Filler Block C Pos.5	Not Measured	273.	-	673.	K	0.64%FS
182	Slab T.	TS-18	TE	182	Filler Block C Pos.6	Not Measured	273.	-	673.	K	0.64%FS
183	Slab T.	TS-19	TE	183	Filler Block A Pos.1	Not Measured	273.	-	673.	K	0.64%FS
184	Slab T.	TS-20	TE	184	Filler Block A Pos.2	Not Measured	273.	-	673.	K	0.64%FS
185	Slab T.	TS-21	TE	185	Filler Block A Pos.3	Not Measured	273.	-	673.	K	0.64%FS
186	Slab T.	TS-22	TE	186	Filler Block A Pos.4	Not Measured	273.	-	673.	K	0.64%FS
187	Slab T.	TS-23	TE	187	Filler Block A Pos.5	Not Measured	273.	-	673.	K	0.64%FS
188	Slab T.	TS-24	TE	188	Filler Block A Pos.6	Not Measured	273.	-	673.	K	0.64%FS
189	Slab T.	TS-25	TE	189	JP-1 Diffuser Wall	Not Measured	273.	-	673.	K	0.64%FS
190	Slab T.	TS-26	TE	190	JP-2 Diffuser Wall	Not Measured	273.	-	673.	K	0.64%FS
191	Slab T.	TS-27	TE	191	JP-3 Diffuser Wall	Not Measured	273.	-	673.	K	0.64%FS
192	Slab T.	TS-28	TE	192	JP-4 Diffuser Wall	Not Measured	273.	-	673.	K	0.64%FS
193	Slab T.	TS-29	TE	193	PV Wall Inside 1-1	Not Measured	273.	-	673.	K	0.64%FS
194	Slab T.	TS-30	TE	194	PV Inner Surface 1-2	Not Measured	273.	-	673.	K	0.64%FS
195	Slab T.	TS-31	TE	195	PV Inner Surface 1-3	Not Measured	273.	-	673.	K	0.64%FS
196	Slab T.	TS-32	TE	196	PV Wall Inside 2	Not Measured	273.	-	673.	K	0.64%FS
197	Slab T.	TS-33	TE	197	PV Wall Inside 3	Not Measured	273.	-	673.	K	0.64%FS
198	Slab T.	TS-34	TE	198	PV Wall Inside 4	Not Measured	273.	-	673.	K	0.64%FS
199	Slab T.	TS-35	TE	199	L.P. Inner Surface	Not Measured	273.	-	673.	K	0.64%FS
200	Slab T.	TS-36	TE	200	L.P. Wall Inside	Not Measured	273.	-	673.	K	0.64%FS

Table 3.2 Measurement List for RUN 955 (Continued)

201Ch.- 250Ch.

Ch.	Item	Symbol	ID.	Location	Fig.No.	Range	Unit	Accuracy
201	Temp.	TF- 1	TE 201	A11 Fuel Rod Pos.1	FIG.5.52	273. - 0.147E+04	K	0.64%FS
202	Temp.	TF- 2	TE 202	A11 Fuel Rod Pos.2	FIG.5.52	273. - 0.147E+04	K	0.64%FS
203	Temp.	TF- 3	TE 203	A11 Fuel Rod Pos.3	FIG.5.52	273. - 0.147E+04	K	0.64%FS
204	Temp.	TF- 4	TE 204	A11 Fuel Rod Pos.4	FIG.5.52	273. - 0.147E+04	K	0.64%FS
205	Temp.	TF- 5	TE 205	A11 Fuel Rod Pos.5	FIG.5.52	273. - 0.147E+04	K	0.64%FS
206	Temp.	TF- 6	TE 206	A11 Fuel Rod Pos.6	FIG.5.52	273. - 0.147E+04	K	0.64%FS
207	Temp.	TF- 7	TE 207	A11 Fuel Rod Pos.7	FIG.5.52	273. - 0.147E+04	K	0.64%FS
208	Temp.	TF- 8	TE 208	A12 Fuel Rod Pos.1		273. - 0.147E+04	K	0.64%FS
209	Temp.	TF- 9	TE 209	A12 Fuel Rod Pos.2		273. - 0.147E+04	K	0.64%FS
210	Temp.	TF- 10	TE 210	A12 Fuel Rod Pos.3		273. - 0.147E+04	K	0.64%FS
211	Temp.	TF- 11	TE 211	A12 Fuel Rod Pos.4		273. - 0.147E+04	K	0.64%FS
212	Temp.	TF- 12	TE 212	A12 Fuel Rod Pos.5		273. - 0.147E+04	K	0.64%FS
213	Temp.	TF- 13	TE 213	A12 Fuel Rod Pos.6		273. - 0.147E+04	K	0.64%FS
214	Temp.	TF- 14	TE 214	A12 Fuel Rod Pos.7		273. - 0.147E+04	K	0.64%FS
215	Temp.	TF- 15	TE 215	A13 Fuel Rod Pos.1		273. - 0.147E+04	K	0.64%FS
216	Temp.	TF- 16	TE 216	A13 Fuel Rod Pos.2		273. - 0.147E+04	K	0.64%FS
217	Temp.	TF- 17	TE 217	A13 Fuel Rod Pos.3		273. - 0.147E+04	K	0.64%FS
218	Temp.	TF- 18	TE 218	A13 Fuel Rod Pos.4		273. - 0.147E+04	K	0.64%FS
219	Temp.	TF- 19	TE 219	A13 Fuel Rod Pos.5		273. - 0.147E+04	K	0.64%FS
220	Temp.	TF- 20	TE 220	A13 Fuel Rod Pos.6		273. - 0.147E+04	K	0.64%FS
221	Temp.	TF- 21	TE 221	A13 Fuel Rod Pos.7		273. - 0.147E+04	K	0.64%FS
222	Temp.	TF- 22	TE 222	A14 Fuel Rod Pos.1		273. - 0.147E+04	K	0.64%FS
223	Temp.	TF- 23	TE 223	A14 Fuel Rod Pos.2		273. - 0.147E+04	K	0.64%FS
224	Temp.	TF- 24	TE 224	A14 Fuel Rod Pos.3		273. - 0.147E+04	K	0.64%FS
225	Temp.	TF- 25	TE 225	A14 Fuel Rod Pos.4		273. - 0.147E+04	K	0.64%FS
226	Temp.	TF- 26	TE 226	A14 Fuel Rod Pos.5		273. - 0.147E+04	K	0.64%FS
227	Temp.	TF- 27	TE 227	A14 Fuel Rod Pos.6		273. - 0.147E+04	K	0.64%FS
228	Temp.	TF- 28	TE 228	A14 Fuel Rod Pos.7		273. - 0.147E+04	K	0.64%FS
229	Temp.	TF- 29	TE 229	A15 Fuel Rod Pos.1		273. - 0.147E+04	K	0.64%FS
230	Temp.	TF- 30	TE 230	A15 Fuel Rod Pos.4		273. - 0.147E+04	K	0.64%FS
231	Temp.	TF- 31	TE 231	A17 Fuel Rod Pos.1		273. - 0.147E+04	K	0.64%FS
232	Temp.	TF- 32	TE 232	A17 Fuel Rod Pos.4		273. - 0.147E+04	K	0.64%FS
233	Temp.	TF- 33	TE 233	A22 Fuel Rod Pos.1	FIG.5.53,61	273. - 0.147E+04	K	0.64%FS
234	Temp.	TF- 34	TE 234	A22 Fuel Rod Pos.2	FIG.5.53,62	273. - 0.147E+04	K	0.64%FS
235	Temp.	TF- 35	TE 235	A22 Fuel Rod Pos.3	FIG.5.53,63	273. - 0.147E+04	K	0.64%FS
236	Temp.	TF- 36	TE 236	A22 Fuel Rod Pos.4	FIG.5.53,64	273. - 0.125E+04	K	0.64%FS
237	Temp.	TF- 37	TE 237	A22 Fuel Rod Pos.5	FIG.5.53,65	273. - 0.125E+04	K	0.64%FS
238	Temp.	TF- 38	TE 238	A22 Fuel Rod Pos.6	FIG.5.53,66	273. - 0.125E+04	K	0.64%FS
239	Temp.	TF- 39	TE 239	A22 Fuel Rod Pos.7	FIG.5.53,67	273. - 0.125E+04	K	0.64%FS
240	Temp.	TF- 40	TE 240	A24 Fuel Rod Pos.1		273. - 0.125E+04	K	0.64%FS
241	Temp.	TF- 41	TE 241	A24 Fuel Rod Pos.2		273. - 0.125E+04	K	0.64%FS
242	Temp.	TF- 42	TE 242	A24 Fuel Rod Pos.3		273. - 0.125E+04	K	0.64%FS
243	Temp.	TF- 43	TE 243	A24 Fuel Rod Pos.4		273. - 0.125E+04	K	0.64%FS
244	Temp.	TF- 44	TE 244	A24 Fuel Rod Pos.5		273. - 0.125E+04	K	0.64%FS
245	Temp.	TF- 45	TE 245	A24 Fuel Rod Pos.6		273. - 0.125E+04	K	0.64%FS
246	Temp.	TF- 46	TE 246	A24 Fuel Rod Pos.7		273. - 0.125E+04	K	0.64%FS
247	Temp.	TF- 47	TE 247	A26 Fuel Rod Pos.1		273. - 0.125E+04	K	0.64%FS
248	Temp.	TF- 48	TE 248	A26 Fuel Rod Pos.2		273. - 0.125E+04	K	0.64%FS
249	Temp.	TF- 49	TE 249	A28 Fuel Rod Pos.1		273. - 0.125E+04	K	0.64%FS
250	Temp.	TF- 50	TE 250	A28 Fuel Rod Pos.4		273. - 0.125E+04	K	0.64%FS

Table 3.2 Measurement List for RUN 955 (Continued)

251Ch.- 300Ch.

Ch.	Item	Symbol	ID.	Location	Fig.No.	Range	Unit	Accuracy
251	Temp.	TF- 51	TE 251	A31 Fuel Rod Pos.1		273. - 0.125E+04	K	0.64%FS
252	Temp.	TF- 52	TE 252	A31 Fuel Rod Pos.4		273. - 0.125E+04	K	0.64%FS
253	Temp.	TF- 53	TE 253	A33 Fuel Rod Pos.1	FIG.5.54	273. - 0.125E+04	K	0.64%FS
254	Temp.	TF- 54	TE 254	A33 Fuel Rod Pos.2	FIG.5.54	273. - 0.125E+04	K	0.64%FS
255	Temp.	TF- 55	TE 255	A33 Fuel Rod Pos.3	FIG.5.54	273. - 0.125E+04	K	0.64%FS
256	Temp.	TF- 56	TE 256	A33 Fuel Rod Pos.4	FIG.5.54	273. - 0.125E+04	K	0.64%FS
257	Temp.	TF- 57	TE 257	A33 Fuel Rod Pos.5	FIG.5.54	273. - 0.125E+04	K	0.64%FS
258	Temp.	TF- 58	TE 258	A33 Fuel Rod Pos.6	FIG.5.54	273. - 0.125E+04	K	0.64%FS
259	Temp.	TF- 59	TE 259	A33 Fuel Rod Pos.7	FIG.5.54	273. - 0.125E+04	K	0.64%FS
260	Temp.	TF- 60	TE 260	A34 Fuel Rod Pos.1		273. - 0.125E+04	K	0.64%FS
261	Temp.	TF- 61	TE 261	A34 Fuel Rod Pos.2		273. - 0.125E+04	K	0.64%FS
262	Temp.	TF- 62	TE 262	A34 Fuel Rod Pos.3		273. - 0.125E+04	K	0.64%FS
263	Temp.	TF- 63	TE 263	A34 Fuel Rod Pos.4		273. - 0.125E+04	K	0.64%FS
264	Temp.	TF- 64	TE 264	A34 Fuel Rod Pos.5		273. - 0.125E+04	K	0.64%FS
265	Temp.	TF- 65	TE 265	A34 Fuel Rod Pos.6		273. - 0.125E+04	K	0.64%FS
266	Temp.	TF- 66	TE 266	A34 Fuel Rod Pos.7		273. - 0.125E+04	K	0.64%FS
267	Temp.	TF- 67	TE 267	A37 Fuel Rod Pos.1		273. - 0.125E+04	K	0.64%FS
268	Temp.	TF- 68	TE 268	A37 Fuel Rod Pos.4		273. - 0.125E+04	K	0.64%FS
269	Temp.	TF- 69	TE 269	A42 Fuel Rod Pos.1		273. - 0.125E+04	K	0.64%FS
270	Temp.	TF- 70	TE 270	A42 Fuel Rod Pos.4		273. - 0.125E+04	K	0.64%FS
271	Temp.	TF- 71	TE 271	A44 Fuel Rod Pos.1		273. - 0.125E+04	K	0.64%FS
272	Temp.	TF- 72	TE 272	A44 Fuel Rod Pos.2		273. - 0.125E+04	K	0.64%FS
273	Temp.	TF- 73	TE 273	A44 Fuel Rod Pos.3		273. - 0.125E+04	K	0.64%FS
274	Temp.	TF- 74	TE 274	A44 Fuel Rod Pos.4		273. - 0.125E+04	K	0.64%FS
275	Temp.	TF- 75	TE 275	A44 Fuel Rod Pos.5		273. - 0.125E+04	K	0.64%FS
276	Temp.	TF- 76	TE 276	A44 Fuel Rod Pos.6		273. - 0.125E+04	K	0.64%FS
277	Temp.	TF- 77	TE 277	A44 Fuel Rod Pos.7		273. - 0.125E+04	K	0.64%FS
278	Temp.	TF- 78	TE 278	A48 Fuel Rod Pos.1		273. - 0.125E+04	K	0.64%FS
279	Temp.	TF- 79	TE 279	A48 Fuel Rod Pos.4		273. - 0.125E+04	K	0.64%FS
280	Temp.	TF- 80	TE 280	A51 Fuel Rod Pos.1		273. - 0.125E+04	K	0.64%FS
281	Temp.	TF- 81	TE 281	A51 Fuel Rod Pos.4		273. - 0.125E+04	K	0.64%FS
282	Temp.	TF- 82	TE 282	A53 Fuel Rod Pos.1		273. - 0.125E+04	K	0.64%FS
283	Temp.	TF- 83	TE 283	A53 Fuel Rod Pos.4		273. - 0.125E+04	K	0.64%FS
284	Temp.	TF- 84	TE 284	A57 Fuel Rod Pos.1		273. - 0.125E+04	K	0.64%FS
285	Temp.	TF- 85	TE 285	A57 Fuel Rod Pos.4		273. - 0.125E+04	K	0.64%FS
286	Temp.	TF- 86	TE 286	A62 Fuel Rod Pos.1		273. - 0.125E+04	K	0.64%FS
287	Temp.	TF- 87	TE 287	A62 Fuel Rod Pos.4		273. - 0.125E+04	K	0.64%FS
288	Temp.	TF- 88	TE 288	A66 Fuel Rod Pos.1		273. - 0.125E+04	K	0.64%FS
289	Temp.	TF- 89	TE 289	A66 Fuel Rod Pos.4		273. - 0.125E+04	K	0.64%FS
290	Temp.	TF- 90	TE 290	A68 Fuel Rod Pos.1		273. - 0.125E+04	K	0.64%FS
291	Temp.	TF- 91	TE 291	A68 Fuel Rod Pos.4		273. - 0.125E+04	K	0.64%FS
292	Temp.	TF- 92	TE 292	A71 Fuel Rod Pos.1		273. - 0.125E+04	K	0.64%FS
293	Temp.	TF- 93	TE 293	A71 Fuel Rod Pos.4		273. - 0.125E+04	K	0.64%FS
294	Temp.	TF- 94	TE 294	A73 Fuel Rod Pos.1		273. - 0.125E+04	K	0.64%FS
295	Temp.	TF- 95	TE 295	A73 Fuel Rod Pos.4		273. - 0.125E+04	K	0.64%FS
296	Temp.	TF- 96	TE 296	A75 Fuel Rod Pos.1		273. - 0.125E+04	K	0.64%FS
297	Temp.	TF- 97	TE 297	A75 Fuel Rod Pos.4		273. - 0.125E+04	K	0.64%FS
298	Temp.	TF- 98	TE 298	A77 Fuel Rod Pos.1	FIG.5.55, 68	273. - 0.125E+04	K	0.64%FS
299	Temp.	TF- 99	TE 299	A77 Fuel Rod Pos.2	FIG.5.55, 69	273. - 0.125E+04	K	0.64%FS
300	Temp.	TF-100	TE 300	A77 Fuel Rod Pos.3	FIG.5.55, 70	273. - 0.125E+04	K	0.64%FS

Table 3.2 Measurement List for RUN 955 (Continued)

301Ch.- 350Ch.

Ch.	Item	Symbol	ID.	Location	Fig.No.	Range	Unit	Accuracy
301	Temp.	TF-101	TE 301	A77 Fuel Rod Pos.4	FIG.5.55, 71	273. - 0.125E+04	K	0.64%FS
302	Temp.	TF-102	TE 302	A77 Fuel Rod Pos.5	FIG.5.55, 72	273. - 0.125E+04	K	0.64%FS
303	Temp.	TF-103	TE 303	A77 Fuel Rod Pos.6	FIG.5.55, 73	273. - 0.125E+04	K	0.64%FS
304	Temp.	TF-104	TE 304	A77 Fuel Rod Pos.7	Failure	273. - 0.125E+04	K	0.64%FS
305	Temp.	TF-105	TE 305	A82 Fuel Rod Pos.1		273. - 0.125E+04	K	0.64%FS
306	Temp.	TF-106	TE 306	A82 Fuel Rod Pos.4	Not Used	273. - 0.125E+04	K	0.64%FS
307	Temp.	TF-107	TE 307	A84 Fuel Rod Pos.1		273. - 0.125E+04	K	0.64%FS
308	Temp.	TF-108	TE 308	A84 Fuel Rod Pos.4		273. - 0.125E+04	K	0.64%FS
309	Temp.	TF-109	TE 309	A85 Fuel Rod Pos.1		273. - 0.125E+04	K	0.64%FS
310	Temp.	TF-110	TE 310	A85 Fuel Rod Pos.2		273. - 0.125E+04	K	0.64%FS
311	Temp.	TF-111	TE 311	A85 Fuel Rod Pos.3		273. - 0.125E+04	K	0.64%FS
312	Temp.	TF-112	TE 312	A85 Fuel Rod Pos.4		273. - 0.125E+04	K	0.64%FS
313	Temp.	TF-113	TE 313	A85 Fuel Rod Pos.5		273. - 0.125E+04	K	0.64%FS
314	Temp.	TF-114	TE 314	A85 Fuel Rod Pos.6		273. - 0.125E+04	K	0.64%FS
315	Temp.	TF-115	TE 315	A85 Fuel Rod Pos.7		273. - 0.125E+04	K	0.64%FS
316	Temp.	TF-116	TE 316	A87 Fuel Rod Pos.1		273. - 0.125E+04	K	0.64%FS
317	Temp.	TF-117	TE 317	A87 Fuel Rod Pos.2		273. - 0.125E+04	K	0.64%FS
318	Temp.	TF-118	TE 318	A87 Fuel Rod Pos.3		273. - 0.125E+04	K	0.64%FS
319	Temp.	TF-119	TE 319	A87 Fuel Rod Pos.4		273. - 0.125E+04	K	0.64%FS
320	Temp.	TF-120	TE 320	A87 Fuel Rod Pos.5		273. - 0.125E+04	K	0.64%FS
321	Temp.	TF-121	TE 321	A87 Fuel Rod Pos.6		273. - 0.125E+04	K	0.64%FS
322	Temp.	TF-122	TE 322	A87 Fuel Rod Pos.7		273. - 0.125E+04	K	0.64%FS
323	Temp.	TF-123	TE 323	A88 Fuel Rod Pos.1	FIG.5.56	273. - 0.125E+04	K	0.64%FS
324	Temp.	TF-124	TE 324	A88 Fuel Rod Pos.2	FIG.5.56	273. - 0.125E+04	K	0.64%FS
325	Temp.	TF-125	TE 325	A88 Fuel Rod Pos.3	FIG.5.56	273. - 0.125E+04	K	0.64%FS
326	Temp.	TF-126	TE 326	A88 Fuel Rod Pos.4	FIG.5.56	273. - 0.125E+04	K	0.64%FS
327	Temp.	TF-127	TE 327	A88 Fuel Rod Pos.5	FIG.5.56	273. - 0.125E+04	K	0.64%FS
328	Temp.	TF-128	TE 328	A88 Fuel Rod Pos.6	FIG.5.56	273. - 0.125E+04	K	0.64%FS
329	Temp.	TF-129	TE 329	A88 Fuel Rod Pos.7	FIG.5.56	273. - 0.125E+04	K	0.64%FS
330	Temp.	TF-130	TE 330	B11 Fuel Rod Pos.1		273. - 0.125E+04	K	0.64%FS
331	Temp.	TF-131	TE 331	B11 Fuel Rod Pos.2		273. - 0.125E+04	K	0.64%FS
332	Temp.	TF-132	TE 332	B11 Fuel Rod Pos.3		273. - 0.125E+04	K	0.64%FS
333	Temp.	TF-133	TE 333	B11 Fuel Rod Pos.4		273. - 0.125E+04	K	0.64%FS
334	Temp.	TF-134	TE 334	B11 Fuel Rod Pos.5		273. - 0.125E+04	K	0.64%FS
335	Temp.	TF-135	TE 335	B11 Fuel Rod Pos.6		273. - 0.125E+04	K	0.64%FS
336	Temp.	TF-136	TE 336	B11 Fuel Rod Pos.7	Not Measured	273. - 0.125E+04	K	0.64%FS
337	Temp.	TF-137	TE 337	B13 Fuel Rod Pos.4		273. - 0.125E+04	K	0.64%FS
338	Temp.	TF-138	TE 338	B22 Fuel Rod Pos.1	FIG.5.57, 61	273. - 0.125E+04	K	0.64%FS
339	Temp.	TF-139	TE 339	B22 Fuel Rod Pos.2	FIG.5.57, 62	273. - 0.125E+04	K	0.64%FS
340	Temp.	TF-140	TE 340	B22 Fuel Rod Pos.3	FIG.5.57, 63	273. - 0.125E+04	K	0.64%FS
341	Temp.	TF-141	TE 341	B22 Fuel Rod Pos.4	Failure	273. - 0.125E+04	K	0.64%FS
342	Temp.	TF-142	TE 342	B22 Fuel Rod Pos.5	FIG.5.15, 65	273. - 0.125E+04	K	0.64%FS
343	Temp.	TF-143	TE 343	B22 Fuel Rod Pos.6	FIG.5.57, 66	273. - 0.125E+04	K	0.64%FS
344	Temp.	TF-144	TE 344	B22 Fuel Rod Pos.7	Not Measured	273. - 0.125E+04	K	0.64%FS
345	Temp.	TF-145	TE 345	B31 Fuel Rod Pos.4		273. - 0.125E+04	K	0.64%FS
346	Temp.	TF-146	TE 346	B33 Fuel Rod Pos.4		273. - 0.125E+04	K	0.64%FS
347	Temp.	TF-147	TE 347	B51 Fuel Rod Pos.4		273. - 0.125E+04	K	0.64%FS
348	Temp.	TF-148	TE 348	B53 Fuel Rod Pos.4		273. - 0.125E+04	K	0.64%FS
349	Temp.	TF-149	TE 349	B66 Fuel Rod Pos.4		273. - 0.125E+04	K	0.64%FS
350	Temp.	TF-150	TE 350	B77 Fuel Rod Pos.1	FIG.5.68	273. - 0.125E+04	K	0.64%FS

Table 3.2 Measurement List for RUN 955 (Continued)

351Ch.- 400Ch.

Ch.	Item	Symbol	ID.	Location	Fig.No.	Range	Unit	Accuracy
351	Temp.	TF-151	TE 351	B77 Fuel Rod Pos.2	FIG.5.69	273. - 0.125E+04	K	0.64%FS
352	Temp.	TF-152	TE 352	B77 Fuel Rod Pos.3	FIG.5.70	273. - 0.125E+04	K	0.64%FS
353	Temp.	TF-153	TE 353	B77 Fuel Rod Pos.4	FIG.5.71	273. - 0.125E+04	K	0.64%FS
354	Temp.	TF-154	TE 354	B77 Fuel Rod Pos.5	FIG.5.72	273. - 0.125E+04	K	0.64%FS
355	Temp.	TF-155	TE 355	B77 Fuel Rod Pos.6	FIG.5.73	273. - 0.125E+04	K	0.64%FS
356	Temp.	TF-156	TE 356	B77 Fuel Rod Pos.7	FIG.5.74	273. - 0.125E+04	K	0.64%FS
357	Temp.	TF-157	TE 357	B86 Fuel Rod Pos.4		273. - 0.125E+04	K	0.64%FS
358	Temp.	TF-158	TE 358	C11 Fuel Rod Pos.1		273. - 0.125E+04	K	0.64%FS
359	Temp.	TF-159	TE 359	C11 Fuel Rod Pos.2		273. - 0.125E+04	K	0.64%FS
360	Temp.	TF-160	TE 360	C11 Fuel Rod Pos.3		273. - 0.125E+04	K	0.64%FS
361	Temp.	TF-161	TE 361	C11 Fuel Rod Pos.4		273. - 0.125E+04	K	0.64%FS
362	Temp.	TF-162	TE 362	C11 Fuel Rod Pos.5		273. - 0.125E+04	K	0.64%FS
363	Temp.	TF-163	TE 363	C11 Fuel Rod Pos.6		273. - 0.125E+04	K	0.64%FS
364	Temp.	TF-164	TE 364	C11 Fuel Rod Pos.7		273. - 0.125E+04	K	0.64%FS
365	Temp.	TF-165	TE 365	C13 Fuel Rod Pos.1		273. - 0.125E+04	K	0.64%FS
366	Temp.	TF-166	TE 366	C13 Fuel Rod Pos.2		273. - 0.125E+04	K	0.64%FS
367	Temp.	TF-167	TE 367	C13 Fuel Rod Pos.3		273. - 0.125E+04	K	0.64%FS
368	Temp.	TF-168	TE 368	C13 Fuel Rod Pos.4		273. - 0.125E+04	K	0.64%FS
369	Temp.	TF-169	TE 369	C13 Fuel Rod Pos.5		273. - 0.125E+04	K	0.64%FS
370	Temp.	TF-170	TE 370	C13 Fuel Rod Pos.6		273. - 0.125E+04	K	0.64%FS
371	Temp.	TF-171	TE 371	C13 Fuel Rod Pos.7		273. - 0.125E+04	K	0.64%FS
372	Temp.	TF-172	TE 372	C15 Fuel Rod Pos.4		273. - 0.125E+04	K	0.64%FS
373	Temp.	TF-173	TE 373	C22 Fuel Rod Pos.1	FIG.5.61	273. - 0.125E+04	K	0.64%FS
374	Temp.	TF-174	TE 374	C22 Fuel Rod Pos.2	FIG.5.62	273. - 0.125E+04	K	0.64%FS
375	Temp.	TF-175	TE 375	C22 Fuel Rod Pos.3	FIG.5.63	273. - 0.125E+04	K	0.64%FS
376	Temp.	TF-176	TE 376	C22 Fuel Rod Pos.4	FIG.5.64	273. - 0.125E+04	K	0.64%FS
377	Temp.	TF-177	TE 377	C22 Fuel Rod Pos.5	FIG.5.65	273. - 0.125E+04	K	0.64%FS
378	Temp.	TF-178	TE 378	C22 Fuel Rod Pos.6	FIG.5.66	273. - 0.125E+04	K	0.64%FS
379	Temp.	TF-179	TE 379	C22 Fuel Rod Pos.7	FIG.5.67	273. - 0.125E+04	K	0.64%FS
380	Temp.	TF-180	TE 380	C31 Fuel Rod Pos.4		273. - 0.125E+04	K	0.64%FS
381	Temp.	TF-181	TE 381	C33 Fuel Rod Pos.1		273. - 0.125E+04	K	0.64%FS
382	Temp.	TF-182	TE 382	C33 Fuel Rod Pos.2		273. - 0.125E+04	K	0.64%FS
383	Temp.	TF-183	TE 383	C33 Fuel Rod Pos.3		273. - 0.125E+04	K	0.64%FS
384	Temp.	TF-184	TE 384	C33 Fuel Rod Pos.4		273. - 0.125E+04	K	0.64%FS
385	Temp.	TF-185	TE 385	C33 Fuel Rod Pos.5		273. - 0.125E+04	K	0.64%FS
386	Temp.	TF-186	TE 386	C33 Fuel Rod Pos.6		273. - 0.125E+04	K	0.64%FS
387	Temp.	TF-187	TE 387	C33 Fuel Rod Pos.7		273. - 0.125E+04	K	0.64%FS
388	Temp.	TF-188	TE 388	C35 Fuel Rod Pos.4		273. - 0.125E+04	K	0.64%FS
389	Temp.	TF-189	TE 389	C66 Fuel Rod Pos.4		273. - 0.125E+04	K	0.64%FS
390	Temp.	TF-190	TE 390	C68 Fuel Rod Pos.4		273. - 0.125E+04	K	0.64%FS
391	Temp.	TF-191	TE 391	C77 Fuel Rod Pos.1	FIG.5.68	273. - 0.125E+04	K	0.64%FS
392	Temp.	TF-192	TE 392	C77 Fuel Rod Pos.2	FIG.5.69	273. - 0.125E+04	K	0.64%FS
393	Temp.	TF-193	TE 393	C77 Fuel Rod Pos.3	FIG.5.70	273. - 0.125E+04	K	0.64%FS
394	Temp.	TF-194	TE 394	C77 Fuel Rod Pos.4	FIG.5.71	273. - 0.125E+04	K	0.64%FS
395	Temp.	TF-195	TE 395	C77 Fuel Rod Pos.5	FIG.5.72	273. - 0.125E+04	K	0.64%FS
396	Temp.	TF-196	TE 396	C77 Fuel Rod Pos.6	FIG.5.73	273. - 0.125E+04	K	0.64%FS
397	Temp.	TF-197	TE 397	C77 Fuel Rod Pos.7	FIG.5.74	273. - 0.125E+04	K	0.64%FS
398	Temp.	TF-198	TE 398	D11 Fuel Rod Pos.4		273. - 0.125E+04	K	0.64%FS
399	Temp.	TF-199	TE 399	D13 Fuel Rod Pos.4		273. - 0.125E+04	K	0.64%FS
400	Temp.	TF-200	TE 400	D22 Fuel Rod Pos.1	FIG.5.59, 61	273. - 0.125E+04	K	0.64%FS

Table 3.2 Measurement List for RUN 955 (Continued)

401Ch.- 450Ch.

Ch.	Item	Symbol	ID.	Location	Fig.No.	Range	Unit	Accuracy
401	Temp.	TF-201	TE 401	D22 Fuel Rod Pos.2	FIG.5.59, 62	273. - 0.125E+04	K	0.64%FS
402	Temp.	TF-202	TE 402	D22 Fuel Rod Pos.3	FIG.5.59, 63	273. - 0.125E+04	K	0.64%FS
403	Temp.	TF-203	TE 403	D22 Fuel Rod Pos.4	FIG.5.59, 64	273. - 0.125E+04	K	0.64%FS
404	Temp.	TF-204	TE 404	D22 Fuel Rod Pos.5	FIG.5.59, 65	273. - 0.125E+04	K	0.64%FS
405	Temp.	TF-205	TE 405	D22 Fuel Rod Pos.6	FIG.5.59, 66	273. - 0.125E+04	K	0.64%FS
406	Temp.	TF-206	TE 406	D22 Fuel Rod Pos.7	FIG.5.59, 67	273. - 0.125E+04	K	0.64%FS
407	Temp.	TF-207	TE 407	D31 Fuel Rod Pos.4		273. - 0.125E+04	K	0.64%FS
408	Temp.	TF-208	TE 408	D33 Fuel Rod Pos.4		273. - 0.125E+04	K	0.64%FS
409	Temp.	TF-209	TE 409	D51 Fuel Rod Pos.4		273. - 0.125E+04	K	0.64%FS
410	Temp.	TF-210	TE 410	D53 Fuel Rod Pos.4		273. - 0.125E+04	K	0.64%FS
411	Temp.	TF-211	TE 411	D66 Fuel Rod Pos.4		273. - 0.125E+04	K	0.64%FS
412	Temp.	TF-212	TE 412	D77 Fuel Rod Pos.4		273. - 0.125E+04	K	0.64%FS
413	Temp.	TF-213	TE 413	D86 Fuel Rod Pos.4		273. - 0.125E+04	K	0.64%FS
414	Fluid T.	TW- 1	TE 414	A45 Tie Rod Pos.1		273. - 0.125E+04	K	0.64%FS
415	Fluid T.	TW- 2	TE 415	A45 Tie Rod Pos.2		273. - 0.125E+04	K	0.64%FS
416	Fluid T.	TW- 3	TE 416	A45 Tie Rod Pos.3		273. - 0.125E+04	K	0.64%FS
417	Fluid T.	TW- 4	TE 417	A45 Tie Rod Pos.4		273. - 0.125E+04	K	0.64%FS
418	Fluid T.	TW- 5	TE 418	A45 Tie Rod Pos.5		273. - 0.125E+04	K	0.64%FS
419	Fluid T.	TW- 6	TE 419	A45 Tie Rod Pos.6		273. - 0.125E+04	K	0.64%FS
420	Fluid T.	TW- 7	TE 420	A45 Tie Rod Pos.7		273. - 0.125E+04	K	0.64%FS
421	Fluid T.	TW- 8	TE 421	B45 Tie Rod Pos.1		273. - 0.125E+04	K	0.64%FS
422	Fluid T.	TW- 9	TE 422	B45 Tie Rod Pos.2		273. - 0.125E+04	K	0.64%FS
423	Fluid T.	TW-10	TE 423	B45 Tie Rod Pos.3		273. - 0.125E+04	K	0.64%FS
424	Fluid T.	TW-11	TE 424	B45 Tie Rod Pos.4		273. - 0.125E+04	K	0.64%FS
425	Fluid T.	TW-12	TE 425	B45 Tie Rod Pos.5		273. - 0.125E+04	K	0.64%FS
426	Fluid T.	TW-13	TE 426	B45 Tie Rod Pos.6		273. - 0.125E+04	K	0.64%FS
427	Fluid T.	TW-14	TE 427	B45 Tie Rod Pos.7		273. - 0.125E+04	K	0.64%FS
428	Fluid T.	TW-15	TE 428	C45 Tie Rod Pos.1		273. - 0.125E+04	K	0.64%FS
429	Fluid T.	TW-16	TE 429	C45 Tie Rod Pos.2		273. - 0.125E+04	K	0.64%FS
430	Fluid T.	TW-17	TE 430	C45 Tie Rod Pos.3	Not Measured	273. - 0.125E+04	K	0.64%FS
431	Fluid T.	TW-18	TE 431	C45 Tie Rod Pos.4		273. - 0.125E+04	K	0.64%FS
432	Fluid T.	TW-19	TE 432	C45 Tie Rod Pos.5		273. - 0.125E+04	K	0.64%FS
433	Fluid T.	TW-20	TE 433	C45 Tie Rod Pos.6		273. - 0.125E+04	K	0.64%FS
434	Fluid T.	TW-21	TE 434	C45 Tie Rod Pos.7		273. - 0.125E+04	K	0.64%FS
435	Fluid T.	TW-22	TE 435	D45 Tie Rod Pos.1		273. - 0.125E+04	K	0.64%FS
436	Fluid T.	TW-23	TE 436	D45 Tie Rod Pos.2		273. - 0.125E+04	K	0.64%FS
437	Fluid T.	TW-24	TE 437	D45 Tie Rod Pos.3		273. - 0.125E+04	K	0.64%FS
438	Fluid T.	TW-25	TE 438	D45 Tie Rod Pos.4		273. - 0.125E+04	K	0.64%FS
439	Fluid T.	TW-26	TE 439	D45 Tie Rod Pos.5		273. - 0.125E+04	K	0.64%FS
440	Fluid T.	TW-27	TE 440	D45 Tie Rod Pos.6		273. - 0.125E+04	K	0.64%FS
441	Fluid T.	TW-28	TE 441	D45 Tie Rod Pos.7		273. - 0.125E+04	K	0.64%FS
442	Fluid T.	TC- 1	TE 442	Channel Box A Inlet	FIG.5.75	273. - 0.125E+04	K	0.64%FS
443	Fluid T.	TC- 2	TE 443	Channel Box B Inlet	FIG.5.75	273. - 0.125E+04	K	0.64%FS
444	Fluid T.	TC- 3	TE 444	Channel Box C Inlet	FIG.5.75	273. - 0.125E+04	K	0.64%FS
445	Fluid T.	TC- 4	TE 445	Channel Box D Inlet	FIG.5.75	273. - 0.125E+04	K	0.64%FS
446	Fluid T.	TC- 5	TE 446	Channel Box Outlet A-1		273. - 0.125E+04	K	0.64%FS
447	Fluid T.	TC- 6	TE 447	Channel Box Outlet A-2		273. - 0.125E+04	K	0.64%FS
448	Fluid T.	TC- 7	TE 448	Channel Box Outlet A-3		273. - 0.125E+04	K	0.64%FS
449	Fluid T.	TC- 8	TE 449	Channel Box Outlet A-4		273. - 0.125E+04	K	0.64%FS
450	Fluid T.	TC- 9	TE 450	Channel Box Outlet A-6		273. - 0.125E+04	K	0.64%FS

Table 3.2 Measurement List for RUN 955 (Continued)

451Ch.- 500Ch.

Ch.	Item	Symbol	ID.		Location	Fig.No.	Range			Unit	Accuracy
451	Fluid T.	TC-10	TE	451	Channel Box Outlet C-1		273.	-	0.125E+04	K	0.64%FS
452	Fluid T.	TC-11	TE	452	Channel Box Outlet C-2		273.	-	0.125E+04	K	0.64%FS
453	Fluid T.	TC-12	TE	453	Channel Box Outlet C-3		273.	-	0.125E+04	K	0.64%FS
454	Fluid T.	TC-13	TE	454	Channel Box Outlet C-4		273.	-	0.125E+04	K	0.64%FS
455	Fluid T.	TC-14	TE	455	Channel Box Outlet C-6		273.	-	0.125E+04	K	0.64%FS
456	Fluid T.	TG- 1	TE	456	Upper Tieplate A Up.1	FIG.5.76	273.	-	0.125E+04	K	0.64%FS
457	Fluid T.	TG- 2	TE	457	Upper Tieplate A Up.2		273.	-	0.125E+04	K	0.64%FS
458	Fluid T.	TG- 3	TE	458	Upper Tieplate A Up.3		273.	-	0.125E+04	K	0.64%FS
459	Fluid T.	TG- 4	TE	459	Upper Tieplate A Up.4	FIG.5.77	273.	-	0.125E+04	K	0.64%FS
460	Fluid T.	TG- 5	TE	460	Upper Tieplate A Up.5		273.	-	0.125E+04	K	0.64%FS
461	Fluid T.	TG- 6	TE	461	Upper Tieplate A Up.6		273.	-	0.125E+04	K	0.64%FS
462	Fluid T.	TG- 7	TE	462	Upper Tieplate A Up.7		273.	-	0.125E+04	K	0.64%FS
463	Fluid T.	TG- 8	TE	463	Upper Tieplate A Up.8		273.	-	0.125E+04	K	0.64%FS
464	Fluid T.	TG- 9	TE	464	Upper Tieplate A Up.9		273.	-	0.125E+04	K	0.64%FS
465	Fluid T.	TG-10	TE	465	Upper Tieplate A Up.10	FIG.5.78	273.	-	0.125E+04	K	0.64%FS
466	Fluid T.	TG-11	TE	466	Upper Tieplate A Lo.1	FIG.5.76	273.	-	0.125E+04	K	0.64%FS
467	Fluid T.	TG-12	TE	467	Upper Tieplate A Lo.2		273.	-	0.125E+04	K	0.64%FS
468	Fluid T.	TG-13	TE	468	Upper Tieplate A Lo.3		273.	-	0.125E+04	K	0.64%FS
469	Fluid T.	TG-14	TE	469	Upper Tieplate A Lo.4	FIG.5.77	273.	-	0.125E+04	K	0.64%FS
470	Fluid T.	TG-15	TE	470	Upper Tieplate A Lo.5		273.	-	0.125E+04	K	0.64%FS
471	Fluid T.	TG-16	TE	471	Upper Tieplate A Lo.6		273.	-	0.125E+04	K	0.64%FS
472	Fluid T.	TG-17	TE	472	Upper Tieplate A Lo.7		273.	-	0.125E+04	K	0.64%FS
473	Fluid T.	TG-18	TE	473	Upper Tieplate A Lo.8		273.	-	0.125E+04	K	0.64%FS
474	Fluid T.	TG-19	TE	474	Upper Tieplate A Lo.9		273.	-	0.125E+04	K	0.64%FS
475	Fluid T.	TG-20	TE	475	Upper Tieplate A Lo.10	FIG.5.78	273.	-	0.125E+04	K	0.64%FS
476	Fluid T.	TG-21	TE	476	Upper Tieplate C Up.1		273.	-	0.125E+04	K	0.64%FS
477	Fluid T.	TG-22	TE	477	Upper Tieplate C Up.2		273.	-	0.125E+04	K	0.64%FS
478	Fluid T.	TG-23	TE	478	Upper Tieplate C Up.3		273.	-	0.125E+04	K	0.64%FS
479	Fluid T.	TG-24	TE	479	Upper Tieplate C Up.4		273.	-	0.125E+04	K	0.64%FS
480	Fluid T.	TG-25	TE	480	Upper Tieplate C Up.5		273.	-	0.125E+04	K	0.64%FS
481	Fluid T.	TG-26	TE	481	Upper Tieplate C Up.6		273.	-	0.125E+04	K	0.64%FS
482	Fluid T.	TG-27	TE	482	Upper Tieplate C Up.7		273.	-	0.125E+04	K	0.64%FS
483	Fluid T.	TG-28	TE	483	Upper Tieplate C Up.8		273.	-	0.125E+04	K	0.64%FS
484	Fluid T.	TG-29	TE	484	Upper Tieplate C Up.9		273.	-	0.125E+04	K	0.64%FS
485	Fluid T.	TG-30	TE	485	Upper Tieplate C Up.10		273.	-	0.125E+04	K	0.64%FS
486	Fluid T.	TG-31	TE	486	Upper Tieplate C Lo.1		273.	-	0.125E+04	K	0.64%FS
487	Fluid T.	TG-32	TE	487	Upper Tieplate C Lo.2		273.	-	0.125E+04	K	0.64%FS
488	Fluid T.	TG-33	TE	488	Upper Tieplate C Lo.3		273.	-	0.125E+04	K	0.64%FS
489	Fluid T.	TG-34	TE	489	Upper Tieplate C Lo.4		273.	-	0.125E+04	K	0.64%FS
490	Fluid T.	TG-35	TE	490	Upper Tieplate C Lo.5		273.	-	0.125E+04	K	0.64%FS
491	Fluid T.	TG-36	TE	491	Upper Tieplate C Lo.6		273.	-	0.125E+04	K	0.64%FS
492	Fluid T.	TG-37	TE	492	Upper Tieplate C Lo.7		273.	-	0.125E+04	K	0.64%FS
493	Fluid T.	TG-38	TE	493	Upper Tieplate C Lo.8		273.	-	0.125E+04	K	0.64%FS
494	Fluid T.	TG-39	TE	494	Upper Tieplate C Lo.9		273.	-	0.125E+04	K	0.64%FS
495	Fluid T.	TG-40	TE	495	Upper Tieplate C Lo.10		273.	-	0.125E+04	K	0.64%FS
496	Slab T.	TB- 1	TE	496	C.B. A1 Inner ,Pos.1		273.	-	0.125E+04	K	0.64%FS
497	Slab T.	TB- 2	TE	497	C.B. A1 Inner ,Pos.2		273.	-	0.125E+04	K	0.64%FS
498	Slab T.	TB- 3	TE	498	C.B. A1 Inner ,Pos.3		273.	-	0.125E+04	K	0.64%FS
499	Slab T.	TB- 4	TE	499	C.B. A1 Inner ,Pos.4		273.	-	0.125E+04	K	0.64%FS
500	Slab T.	TB- 5	TE	500	C.B. A1 Inner ,Pos.5		273.	-	0.125E+04	K	0.64%FS

Table 3.2 Measurement List for RUN 955 (Continued)

501Ch.- 550Ch.

Ch.	Item	Symbol	ID.	Location	Fig.No.	Range	Unit	Accuracy
501	Slab T.	TB- 6	TE 501	C.B. A1 Inner ,Pos.6		273. - 0.125E+04	K	0.64%FS
502	Slab T.	TB- 7	TE 502	C.B. A1 Inner ,Pos.7		273. - 0.125E+04	K	0.64%FS
503	Slab T.	TB- 8	TE 503	C.B. A2 Inner ,Pos.1		273. - 0.125E+04	K	0.64%FS
504	Slab T.	TB- 9	TE 504	C.B. A2 Inner ,Pos.2		273. - 0.125E+04	K	0.64%FS
505	Slab T.	TB-10	TE 505	C.B. A2 Inner ,Pos.3		273. - 0.125E+04	K	0.64%FS
506	Slab T.	TB-11	TE 506	C.B. A2 Inner ,Pos.4		273. - 0.125E+04	K	0.64%FS
507	Slab T.	TB-12	TE 507	C.B. A2 Inner ,Pos.5		273. - 0.125E+04	K	0.64%FS
508	Slab T.	TB-13	TE 508	C.B. A2 Inner ,Pos.6		273. - 0.125E+04	K	0.64%FS
509	Slab T.	TB-14	TE 509	C.B. A2 Inner ,Pos.7		273. - 0.125E+04	K	0.64%FS
510	Slab T.	TB-15	TE 510	C.B. B Inner ,Pos.1		273. - 0.125E+04	K	0.64%FS
511	Slab T.	TB-16	TE 511	C.B. B Inner ,Pos.2		273. - 0.125E+04	K	0.64%FS
512	Slab T.	TB-17	TE 512	C.B. B Inner ,Pos.3		273. - 0.125E+04	K	0.64%FS
513	Slab T.	TB-18	TE 513	C.B. B Inner ,Pos.4		273. - 0.125E+04	K	0.64%FS
514	Slab T.	TB-19	TE 514	C.B. B Inner ,Pos.5		273. - 0.125E+04	K	0.64%FS
515	Slab T.	TB-20	TE 515	C.B. B Inner ,Pos.6		273. - 0.125E+04	K	0.64%FS
516	Slab T.	TB-21	TE 516	C.B. B Inner ,Pos.7		273. - 0.125E+04	K	0.64%FS
517	Slab T.	TB-22	TE 517	C.B. C Inner ,Pos.1		273. - 0.125E+04	K	0.64%FS
518	Slab T.	TB-23	TE 518	C.B. C Inner ,Pos.2		273. - 0.125E+04	K	0.64%FS
519	Slab T.	TB-24	TE 519	C.B. C Inner ,Pos.3		273. - 0.125E+04	K	0.64%FS
520	Slab T.	TB-25	TE 520	C.B. C Inner ,Pos.4		273. - 0.125E+04	K	0.64%FS
521	Slab T.	TB-26	TE 521	C.B. C Inner ,Pos.5		273. - 0.125E+04	K	0.64%FS
522	Slab T.	TB-27	TE 522	C.B. C Inner ,Pos.6		273. - 0.125E+04	K	0.64%FS
523	Slab T.	TB-28	TE 523	C.B. C Inner ,Pos.7		273. - 0.125E+04	K	0.64%FS
524	Slab T.	TB-29	TE 524	C.B. D Inner ,Pos.1		273. - 0.125E+04	K	0.64%FS
525	Slab T.	TB-30	TE 525	C.B. D Inner ,Pos.2		273. - 0.125E+04	K	0.64%FS
526	Slab T.	TB-31	TE 526	C.B. D Inner ,Pos.3		273. - 0.125E+04	K	0.64%FS
527	Slab T.	TB-32	TE 527	C.B. D Inner ,Pos.4		273. - 0.125E+04	K	0.64%FS
528	Slab T.	TB-33	TE 528	C.B. D Inner ,Pos.5		273. - 0.125E+04	K	0.64%FS
529	Slab T.	TB-34	TE 529	C.B. D Inner ,Pos.6		273. - 0.125E+04	K	0.64%FS
530	Slab T.	TB-35	TE 530	C.B. D Inner ,Pos.7		273. - 0.125E+04	K	0.64%FS
531	Fluid T.	TB-36	TE 531	C.B. A Outer ,Pos.1	FIG.5.60	273. - 0.125E+04	K	0.64%FS
532	Fluid T.	TB-37	TE 532	C.B. A Outer ,Pos.2	FIG.5.60	273. - 0.125E+04	K	0.64%FS
533	Fluid T.	TB-38	TE 533	C.B. A Outer ,Pos.3	FIG.5.60	273. - 0.125E+04	K	0.64%FS
534	Fluid T.	TB-39	TE 534	C.B. A Outer ,Pos.4	FIG.5.60	273. - 0.125E+04	K	0.64%FS
535	Fluid T.	TB-40	TE 535	C.B. A Outer ,Pos.5	FIG.5.60	273. - 0.125E+04	K	0.64%FS
536	Fluid T.	TB-41	TE 536	C.B. A Outer ,Pos.6	FIG.5.60	273. - 0.125E+04	K	0.64%FS
537	Fluid T.	TB-42	TE 537	C.B. A Outer ,Pos.7	FIG.5.60	273. - 0.125E+04	K	0.64%FS
538	Fluid T.	TB-43	TE 538	C.B. C Outer ,Pos.1		273. - 0.125E+04	K	0.64%FS
539	Fluid T.	TB-44	TE 539	C.B. C Outer ,Pos.2		273. - 0.125E+04	K	0.64%FS
540	Fluid T.	TB-45	TE 540	C.B. C Outer ,Pos.3		273. - 0.125E+04	K	0.64%FS
541	Fluid T.	TB-46	TE 541	C.B. C Outer ,Pos.4		273. - 0.125E+04	K	0.64%FS
542	Fluid T.	TB-47	TE 542	C.B. C Outer ,Pos.5		273. - 0.125E+04	K	0.64%FS
543	Fluid T.	TB-48	TE 543	C.B. C Outer ,Pos.6		273. - 0.125E+04	K	0.64%FS
544	Fluid T.	TB-49	TE 544	C.B. C Outer ,Pos.7		273. - 0.125E+04	K	0.64%FS
545	Fluid T.	TP- 1	TE 545	Lower Pl. Center 1		273. - 0.125E+04	K	0.64%FS
546	Fluid T.	TP- 2	TE 546	Lower Pl. Center 2		273. - 0.125E+04	K	0.64%FS
547	Fluid T.	TP- 3	TE 547	Lower Pl. Center 3		273. - 0.125E+04	K	0.64%FS
548	Fluid T.	TP- 4	TE 548	Lower Pl. Center 4		273. - 0.125E+04	K	0.64%FS
549	Fluid T.	TP- 5	TE 549	Lower Pl. Center 5		273. - 0.125E+04	K	0.64%FS
550	Fluid T.	TP- 6	TE 550	Lower Pl. Center 7		273. - 0.125E+04	K	0.64%FS

Table 3.2 Measurement List for RUN 955 (Continued)

551Ch.- 600Ch.

Ch.	Item	Symbol	ID.	Location	Fig.No.	Range	Unit	Accuracy
551	Slab T.	TP- 7	TE 551	Lower Pl. North 1		273. - 0.125E+04	K	0.64%FS
552	Slab T.	TP- 8	TE 552	Lower Pl. North 2		273. - 673.	K	0.64%FS
553	Slab T..	TP- 9	TE 553	Lower Pl. North 4		273. - 673.	K	0.64%FS
554	Slab T.	TP-10	TE 554	Lower Pl. North 6		273. - 673.	K	0.64%FS
555	Slab T.	TP-11	TE 555	Lower Pl. South 1		273. - 673.	K	0.64%FS
556	Slab T.	TP-12	TE 556	Lower Pl. South 2		273. - 673.	K	0.64%FS
557	Slab T.	TP-13	TE 557	Lower Pl. South 4		273. - 673.	K	0.64%FS
558	Slab T.	TP-14	TE 558	Lower Pl. South 6		273. - 673.	K	0.64%FS
559	Level	LB- 1	LM 559	C.B.Liquid Level A1-1				
560	Level	LB- 2	LM 560	C.B.Liquid Level A1-2	Failure			
561	Level	LB- 3	LM 561	C.B.Liquid Level A1-3				
562	Level	LB- 4	LM 562	C.B.Liquid Level A1-4				
563	Level	LB- 5	LM 563	C.B.Liquid Level A1-5				
564	Level	LB- 6	LM 564	C.B.Liquid Level A1-6				
565	Level	LB- 7	LM 565	C.B.Liquid Level A1-7				
566	Level	LB- 8	LM 566	C.B.Liquid Level A2-1	FIG.5.79			
567	Level	LB- 9	LM 567	C.B.Liquid Level A2-2	FIG.5.79			
568	Level	LB-10	LM 568	C.B.Liquid Level A2-3	FIG.5.79			
569	Level	LB-11	LM 569	C.B.Liquid Level A2-4	FIG.5.79			
570	Level	LB-12	LM 570	C.B.Liquid Level A2-5	FIG.5.79			
571	Level	LB-13	LM 571	C.B.Liquid Level A2-6	FIG.5.79			
572	Level	LB-14	LM 572	C.B.Liquid Level A2-7	FIG.5.79			
573	Level	LB-15	LM 573	C.B.Liquid Level B-1	FIG.5.79			
574	Level	LB-16	LM 574	C.B.Liquid Level B-2	FIG.5.80			
575	Level	LB-17	LM 575	C.B.Liquid Level B-3	FIG.5.80			
576	Level	LB-18	LM 576	C.B.Liquid Level B-4	FIG.5.80			
577	Level	LB-19	LM 577	C.B.Liquid Level B-5	FIG.5.80			
578	Level	LB-20	LM 578	C.B.Liquid Level B-6	FIG.5.80			
579	Level	LB-21	LM 579	C.B.Liquid Level B-7	FIG.5.80			
580	Level	LB-22	LM 580	C.B.Liquid Level C-1	FIG.5.81			
581	Level	LB-23	LM 581	C.B.Liquid Level C-2	FIG.5.81			
582	Level	LB-24	LM 582	C.B.Liquid Level C-3	FIG.5.81			
583	Level	LB-25	LM 583	C.B.Liquid Level C-4	FIG.5.81			
584	Level	LB-26	LM 584	C.B.Liquid Level C-5	FIG.5.81			
585	Level	LB-27	LM 585	C.B.Liquid Level C-6	FIG.5.81			
586	Level	LB-28	LM 586	C.B.Liquid Level C-7	FIG.5.81			
587	Level	LB-29	LM 587	C.B.Liquid Level D-1				
588	Level	LB-30	LM 588	C.B.Liquid Level D-2				
589	Level	LB-31	LM 589	C.B.Liquid Level D-3				
590	Level	LB-32	LM 590	C.B.Liquid Level D-4				
591	Level	LB-33	LM 591	C.B.Liquid Level D-5				
592	Level	LB-34	LM 592	C.B.Liquid Level D-6				
593	Level	LB-35	LM 593	C.B.Liquid Level D-7				
594	Level	LL- 1	LM 594	Ch.Box Outlet A1-5				
595	Level	LL- 2	LM 595	Ch.Box Outlet A1-6				
596	Level	LL- 3	LM 596	Ch.Box Outlet A1-7	Failure			
597	Level	LL- 4	LM 597	Ch.Box Outlet A2-5	Failure			
598	Level	LL- 5	LM 598	Ch.Box Outlet A2-6	FIG.5.82			
599	Level	LL- 6	LM 599	Ch.Box Outlet A2-7	FIG.5.82			
600	Level	LL- 7	LM 600	Ch.Box Outlet A-1	FIG.5.83			

Table 3.2 Measurement List for RUN 955 (Continued)

Ch.	Item	Symbol	ID.	Location	Fig.No.	Range	Unit	Accuracy
						601Ch.- 650Ch.		
601	Level	LL- 8	LM 601	Ch.Box Outlet A-2	Failure			
602	Level	LL- 9	LM 602	Ch.Box Outlet A-3	FIG.5.83			
603	Level	LL-10	LM 603	Ch.Box Outlet A-4	FIG.5.83			
604	Level	LL-11	LM 604	Ch.Box Outlet A-6	Failure			
605	Level	LL-12	LM 605	Ch.Box Outlet C1-5	FIG.5.84			
606	Level	LL-13	LM 606	Ch.Box Outlet C1-6	FIG.5.84			
607	Level	LL-14	LM 607	Ch.Box Outlet C1-7	FIG.5.84			
608	Level	LL-15	LM 608	Ch.Box Outlet C2-5				
609	Level	LL-16	LM 609	Ch.Box Outlet C2-6				
610	Level	LL-17	LM 610	Ch.Box Outlet C2-7				
611	Level	LL-18	LM 611	Ch.Box Outlet C-1	FIG.5.85			
612	Level	LL-19	LM 612	Ch.Box Outlet C-2	Failure			
613	Level	LL-20	LM 613	Ch.Box Outlet C-3	FIG.5.85			
614	Level	LL-21	LM 614	Ch.Box Outlet C-4	FIG.5.85			
615	Level	LL-22	LM 615	Ch.Box Outlet C-6	FIG.5.85			
616	Level	LL-23	LM 616	Ch.Box Inlet A-1	FIG.5.86			
617	Level	LL-24	LM 617	Ch.Box Inlet A-2	FIG.5.86			
618	Level	LL-25	LM 618	Ch.Box Inlet B-1				
619	Level	LL-26	LM 619	Ch.Box Inlet B-2				
620	Level	LL-27	LM 620	Ch.Box Inlet C-1	FIG.5.87			
621	Level	LL-28	LM 621	Ch.Box Inlet C-2	FIG.5.87			
622	Level	LL-29	LM 622	Ch.Box Inlet D-1				
623	Level	LL-30	LM 623	Ch.Box Inlet D-2				
624	Level	LL-31	LM 624	Lower Pl. North 1	FIG.5.88			
625	Level	LL-32	LM 625	Lower Pl. North 2	FIG.5.88			
626	Level	LL-33	LM 626	Lower Pl. North 3	FIG.5.88			
627	Level	LL-34	LM 627	Lower Pl. North 4	FIG.5.88			
628	Level	LL-35	LM 628	Lower Pl. North 5	FIG.5.88			
629	Level	LL-36	LM 629	Lower Pl. North 6	Failure			
630	Level	LL-37	LM 630	Lower Pl. South 1				
631	Level	LL-38	LM 631	Lower Pl. South 2				
632	Level	LL-39	LM 632	Lower Pl. South 3				
633	Level	LL-40	LM 633	Lower Pl. South 4				
634	Level	LL-41	LM 634	Lower Pl. South 5				
635	Level	LL-42	LM 635	Lower Pl. South 6				
636	Level	LL-43	LM 636	Guide Tube North 0	FIG.5.89			
637	Level	LL-44	LM 637	Guide Tube North 1	FIG.5.89			
638	Level	LL-45	LM 638	Guide Tube North 3	FIG.5.89			
639	Level	LL-46	LM 639	Guide Tube North 6	Failure			
640	Level	LL-47	LM 640	Guide Tube South 0				
641	Level	LL-48	LM 641	Guide Tube South 1				
642	Level	LL-49	LM 642	Guide Tube South 3				
643	Level	LL-50	LM 643	Guide Tube South 6				
644	Level	L- 1	LM 644	Downcomer D-Side 1	FIG.5.90			
645	Level	L- 2	LM 645	Downcomer D-Side 2	FIG.5.90			
646	Level	L- 3	LM 646	Downcomer D-Side 3	FIG.5.90			
647	Level	L- 4	LM 647	Downcomer D-Side 4	FIG.5.90			
648	Level	L- 5	LM 648	Downcomer D-Side 5	Failure			
649	Level	L- 6	LM 649	Downcomer B-Side 1				
650	Level	L- 7	LM 650	Downcomer B-Side 2				

Table 3.2 Measurement List for RUN 955 (Continued)

651Ch.- 700Ch.

Ch.	Item	Symbol	ID.		Location	Fig.No.	Range			Unit	Accuracy
651	Level	L- 8	LM	651	Downcomer B-Side 3						
652	Level	L- 9	LM	652	Downcomer B-Side 4						
653	Level	L-10	LM	653	Downcomer B-Side 5	Failure					
654	Void	VF- 1	VD	654	A54 Tie Rod Pos.1	Not Measured	0.0	-	1.00		
655	Void	VF- 2	VD	655	A54 Tie Rod Pos.2	Not Measured	0.0	-	1.00		
656	Void	VF- 3	VD	656	A54 Tie Rod Pos.3	Not Measured	0.0	-	1.00		
657	Void	VF- 4	VD	657	A54 Tie Rod Pos.4	Not Measured	0.0	-	1.00		
658	Void	VF- 5	VD	658	A54 Tie Rod Pos.5	Not Measured	0.0	-	1.00		
659	Void	VF- 6	VD	659	A54 Tie Rod Pos.6	Not Measured	0.0	-	1.00		
660	Void	VF- 7	VD	660	A54 Tie Rod Pos.7	Not Measured	0.0	-	1.00		
661	Void	VF- 8	VD	661	B54 Tie Rod Pos.1	Not Measured	0.0	-	1.00		
662	Void	VF- 9	VD	662	B54 Tie Rod Pos.2	Not Measured	0.0	-	1.00		
663	Void	VF-10	VD	663	B54 Tie Rod Pos.3	Not Measured	0.0	-	1.00		
664	Void	VF-11	VD	664	B54 Tie Rod Pos.4	Not Measured	0.0	-	1.00		
665	Void	VF-12	VD	665	B54 Tie Rod Pos.5	Not Measured	0.0	-	1.00		
666	Void	VF-13	VD	666	B54 Tie Rod Pos.6	Not Measured	0.0	-	1.00		
667	Void	VF-14	VD	667	B54 Tie Rod Pos.7	Not Measured	0.0	-	1.00		
668	Void	VF-15	VD	668	C54 Tie Rod Pos.1	Not Measured	0.0	-	1.00		
669	Void	VF-16	VD	669	C54 Tie Rod Pos.2	Not Measured	0.0	-	1.00		
670	Void	VF-17	VD	670	C54 Tie Rod Pos.3	Not Measured	0.0	-	1.00		
671	Void	VF-18	VD	671	C54 Tie Rod Pos.4	Not Measured	0.0	-	1.00		
672	Void	VF-19	VD	672	C54 Tie Rod Pos.5	Not Measured	0.0	-	1.00		
673	Void	VF-20	VD	673	C54 Tie Rod Pos.6	Not Measured	0.0	-	1.00		
674	Void	VF-21	VD	674	C54 Tie Rod Pos.7	Not Measured	0.0	-	1.00		
675	Void	VF-22	VD	675	D54 Tie Rod Pos.7	Not Measured	0.0	-	1.00		
676	Void	VF-23	VD	676	D54 Tie Rod Pos.7	Not Measured	0.0	-	1.00		
677	Void	VF-24	VD	677	D54 Tie Rod Pos.7	Not Measured	0.0	-	1.00		
678	Void	VF-25	VD	678	D54 Tie Rod Pos.7	Not Measured	0.0	-	1.00		
679	Void	VF-26	VD	679	D54 Tie Rod Pos.7	Not Measured	0.0	-	1.00		
680	Void	VF-27	VD	680	D54 Tie Rod Pos.7	Not Measured	0.0	-	1.00		
681	Void	VF-28	VD	681	D54 Tie Rod Pos.7	Not Measured	0.0	-	1.00		
682	Void	VE- 1	VD	682	Channel A Outlet 1	Not Measured	0.0	-	1.00		
683	Void	VE- 2	VD	683	Channel A Outlet 2	Not Measured	0.0	-	1.00		
684	Void	VE- 3	VD	684	Channel A Outlet 3	Not Measured	0.0	-	1.00		
685	Void	VE- 4	VD	685	Channel B Outlet 1	Not Measured	0.0	-	1.00		
686	Void	VE- 5	VD	686	Channel B Outlet 2	Not Measured	0.0	-	1.00		
687	Void	VE- 6	VD	687	Channel B Outlet 3	Not Measured	0.0	-	1.00		
688	Void	VE- 7	VD	688	Channel C Outlet 1	Not Measured	0.0	-	1.00		
689	Void	VE- 8	VD	689	Channel C Outlet 2	Not Measured	0.0	-	1.00		
690	Void	VE- 9	VD	690	Channel C Outlet 3	Not Measured	0.0	-	1.00		
691	Void	VE-10	VD	691	Channel D Outlet 1	Not Measured	0.0	-	1.00		
692	Void	VE-11	VD	692	Channel D Outlet 2	Not Measured	0.0	-	1.00		
693	Void	VE-12	VD	693	Channel D Outlet 3	Not Measured	0.0	-	1.00		
694	Void	VE-13	VD	694	Lower Plenum Bottom 1	Not Measured	0.0	-	1.00		
695	Void	VE-14	VD	695	Lower Plenum Bottom 2	Not Measured	0.0	-	1.00		
696	Void	VE-15	VD	696	Lower Plenum Bottom 3	Not Measured	0.0	-	1.00		
697	Void	VP- 1	VD	697	Lower Plenum Inlet	Not Measured	0.0	-	1.00		
698	Void	VP- 2	VD	698	Lower Plenum Inlet	Not Measured	0.0	-	1.00		

Table 3.3 Core instrumentation map

Item	Pos. / DL / Rod NO.	Core Outlet	Pos.1	Pos.2	Pos.3	Pos.4	Pos.5	Pos.6	Pos.7	Core Inlet
		3660	3417	3114.5	2879.5	2527	2174.5	1939.5	1637	1454
Surface Temp.	A11		TF 1	TF 2	TF 3	TF 4	TF 5	TF 6	TF 7	
	A12		TF 8	TF 9	TF 10	TF 11	TF 12	TF 13	TF 14	
	A13		TF 15	TF 16	TF 17	TF 18	TF 19	TF 20	TF 21	
	A14		TF 22	TF 23	TF 24	TF 25	TF 26	TF 27	TF 28	
	A15		TF 29			TF 30				
	A17		TF 31			TF 32				
	A22		TF 33	TF 34	TF 35	TF 36	TF 37	TF 38	TF 39	
	A23		TF 40	TF 41	TF 42	TF 43	TF 44	TF 45	TF 46	
	A24		TF 47	TF 48	TF 49	TF 50	TF.51	TF 52	TF 53	
	A26		TF 54			TF 55				
	A28		TF 56			TF 57				
	A31		TF 58			TF 59				
	A33		TF 60	TF 61	TF 62	TF 63	TF 64	TF 65	TF 66	
	A34		TF 67	TF 68	TF 69	TF 70	TF 71	TF 72	TF 73	
	A35		TF 74			TF 75				
	A37		TF 76			TF 77				
	A42		TF 78			TF 79				
Fluid Temp.	A44	TC 1	TF180	TF181	TF182	TF183	TF184	TF185	TF186	TC 2
Surface Temp.	A45		TF 80			TF 81				
	A46		TF 82			TF 83				
	A48		TF 84			TF 85				
	A51		TF 86			TF 87				
	A53		TF 88			TF 89				
	A54		TF 90							
	A57		TF 91			TF 92				
	A62		TF 93			TF 94				
	A64		TF 95			TF 96				
	A66		TF 97			TF 98				
	A68		TF 99			TF100				
	A71		TF101			TF102				
	A73		TF103			TF104				
	A75		TF105			TF106				
	A77		TF107			TF108				

Table 3.3 Core instrumentation map (Continued)

Item	Pos. / Rod NO. / DL	Core Outlet	Pos.1	Pos.2	Pos.3	Pos.4	Pos.5	Pos.6	Pos.7	Core Inlet
		3660	3417	3114.5	2879.5	2527	2174.5	1939.5	1637	1454
Surface Temp.	A82		TF109			TF110				
	A84		TF111			TF112				
	A86		TF113			TF114				
	A88		TF115			TF116				
	B11					TF117				
	B13					TF118				
	B15		TF119	TF120	TF121	TF122	TF123	TF124	TF125	
	B31					TF126				
	B33					TF127				
	B35					TF128				
Fluid Temp.	B44	TC 3	TF187	TF188	TF189	TF190	TF191	TF192	TF193	TC 4
Surface Temp.	B51					TF129				
	B53					TF130				
	B85		TF131	TF132	TF133	TF134	TF135	TF136	TF137	
	C11					TF138				
	C13					TF139				
	C15					TF140				
	C31					TF141				
	C33		TF142	TF143	TF144	TF145	TF146	TF147	TF148	
	C35					TF149				
Fluid Temp.	C44	TC 5	TF194	TF195	TF196	TF197	TF198	TF199	TF200	TC 6
Surface Temp.	C51					TF150				
	C53					TF151				
	C77		TF152	TF153	TF154	TF155	TF156	TF157	TF158	
	D11					TF159				
	D13					TF160				
	D27		TF161	TF162	TF163	TF164	TF165	TF166	TF167	
	D31					TF168				
	D33					TF169				
	D35					TF170				
Fluid Temp.	D44	TC 7	TF201	TF202	TF203	TF204	TF205	TF206	TF207	TC 8
Surface Temp.	D51					TF171				
	D53					TF172				
	D88		TF173	TF174	TF175	TF176	TF177	TF178	TF179	

Table 3.3 Core instrumentation map (Continued)

Item	Pos. / Rod NO. / DL	Core Outlet	Pos.1	Pos.2	Pos.3	Pos.4	Pos.5	Pos.6	Pos.7	Core Inlet
		3660	3417	3114.5	2879.5	2527	2174.5	1939.5	1673	1454
Void	A55		VF 1	VF 2	VF 3	VF 4	VF 5	VF 6	VF 7	
	B55		VF 8	VF 9	VF 10	VF 11	VF 12	VF 13	VF 14	
	C55		VF 15	VF 16	VF 17	VF 18	VF 19	VF 20	VF 21	
	D55		VF 22	VF 23	VF 24	VF 25	VF 26	VF 27	VF 28	
Channel Box Surface Temp.	A1*		TB 1	TB 2	TB 3	TB 4	TB 5	TB 6	TB 7	
	A2*		TB 8	TB 9	TB 10	TB 11	TB 12	TB 13	TB 14	
	B*		TB 15	TB 16	TB 17	TB 18	TB 19	TB 20	TB 21	
	C*		TB 22	TB 23	TB 24	TB 25	TB 26	TB 27	TB 28	
	D*		TB 29	TB 30	TB 31	TB 32	TB 33	TB 34	TB 35	
Liquid Level in the Channel Box	A1*		LB 1	LB 2	LB 3	LB 4	LB 5	LB 6	LB 7	
	A2*		LB 8	LB 9	LB 10	LB 11	LB 12	LB 13	LB 14	
	B*		LB 15	LB 16	LB 17	LB 18	LB 19	LB 20	LB 21	
	C*		LB 22	LB 23	LB 24	LB 25	LB 26	LB 27	LB 28	
	D*		LB 29	LB 30	LB 31	LB 32	LB 33	LB 34	LB 35	

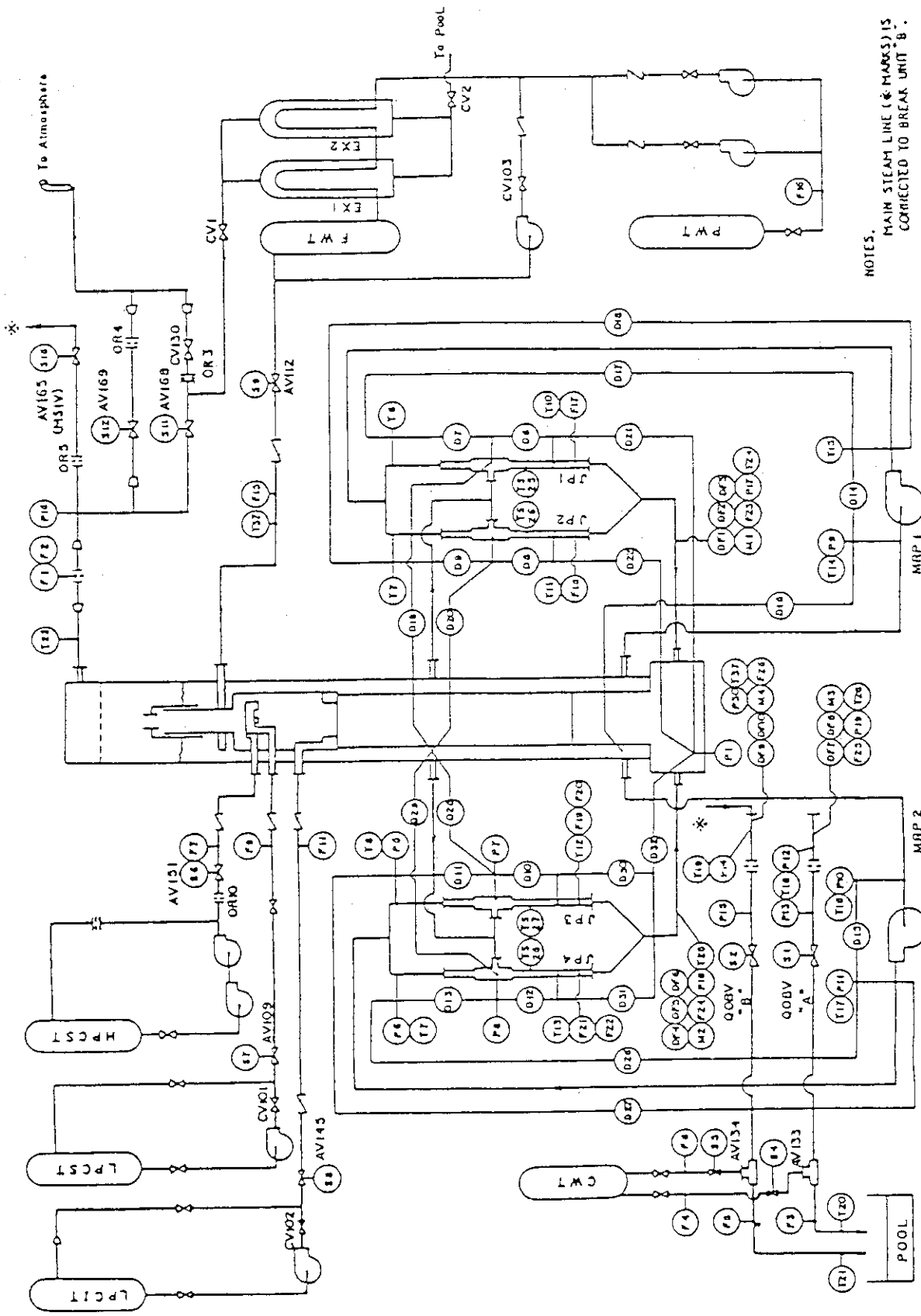

Fig. 3.1 Instrumentation location of ROSA-III test facility

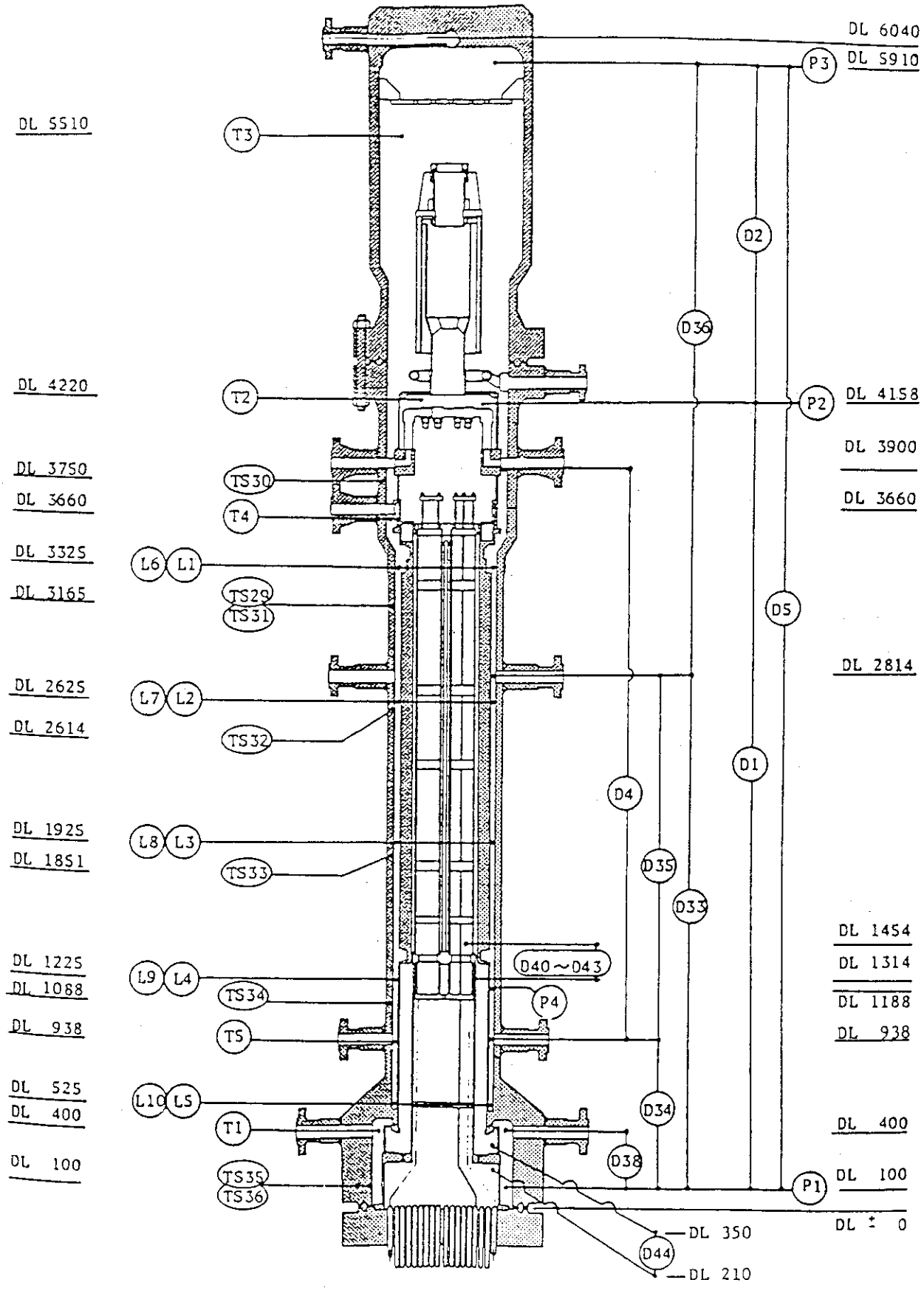

Fig. 3.2 Instrumentation location in pressure vessel

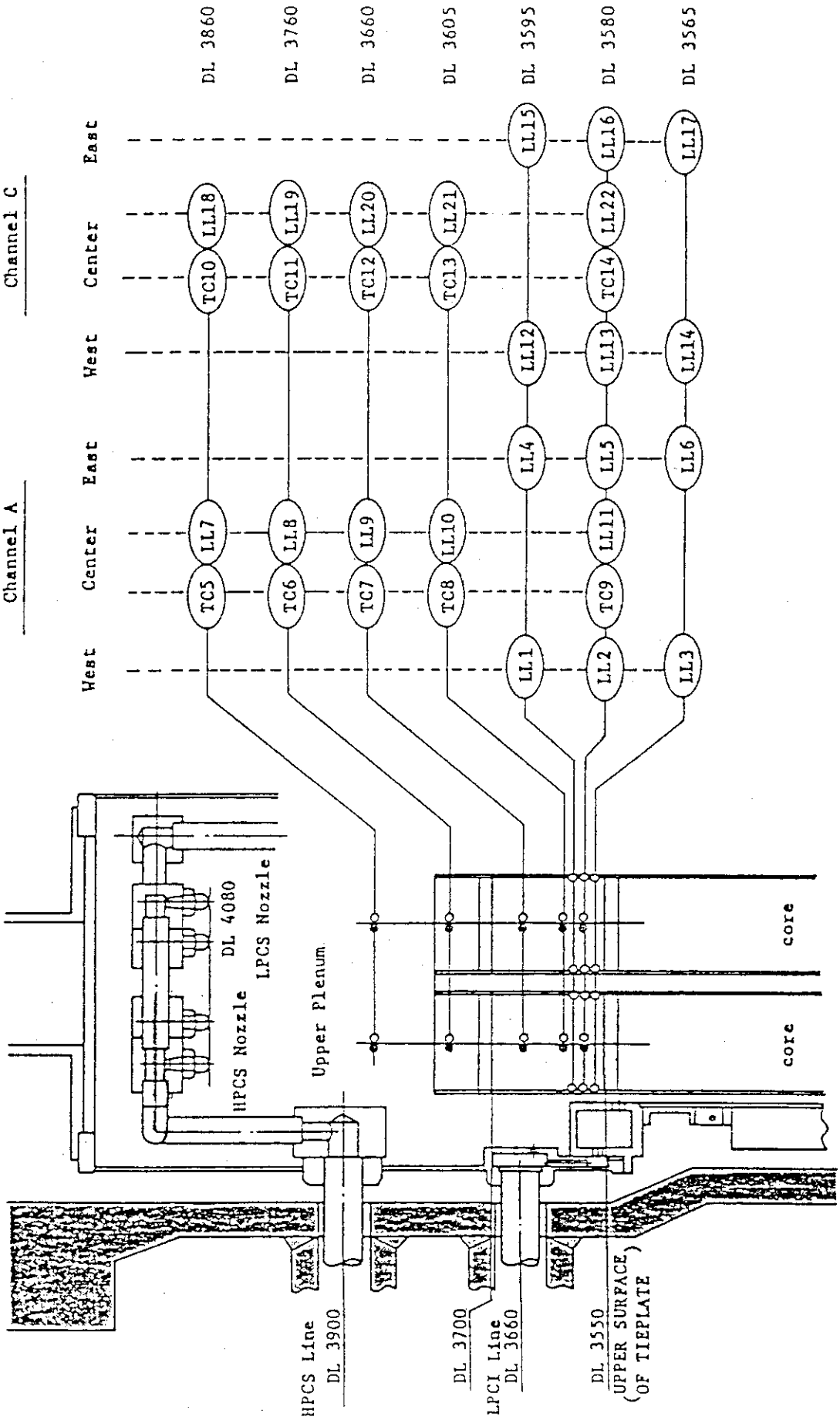

Fig. 3.3 Upper plenum instrumentation

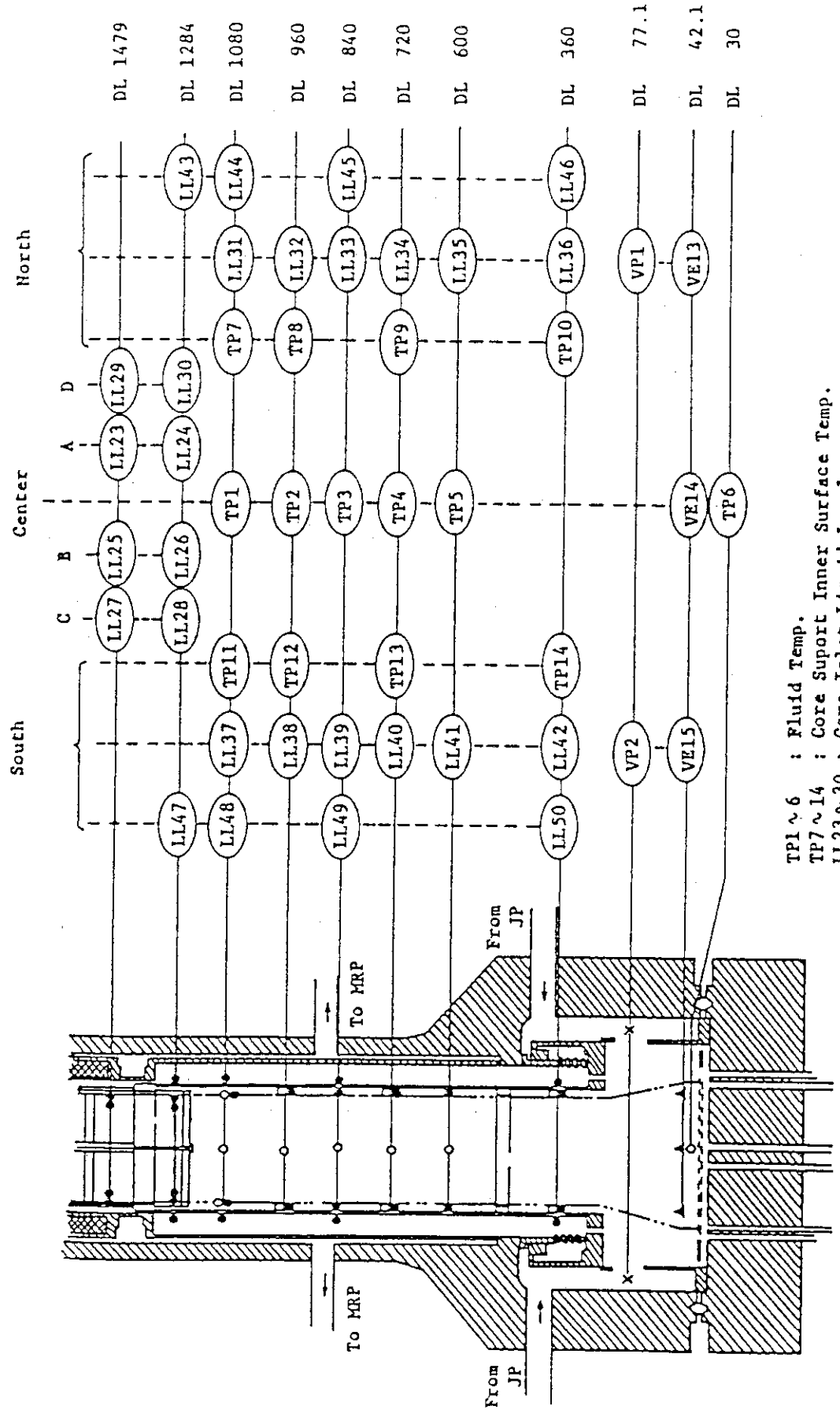

Fig. 3.4 Lower plenum instrumentation

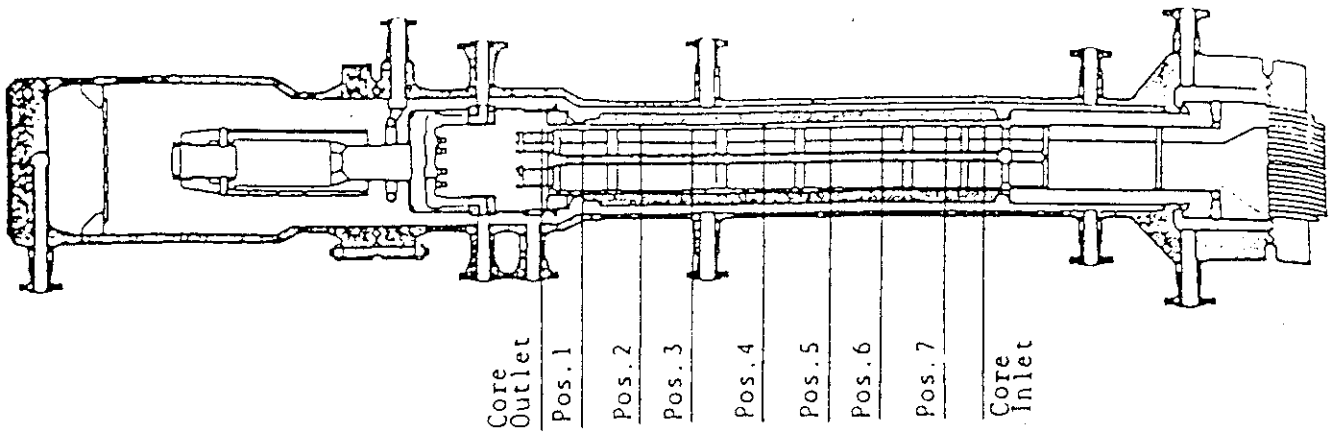

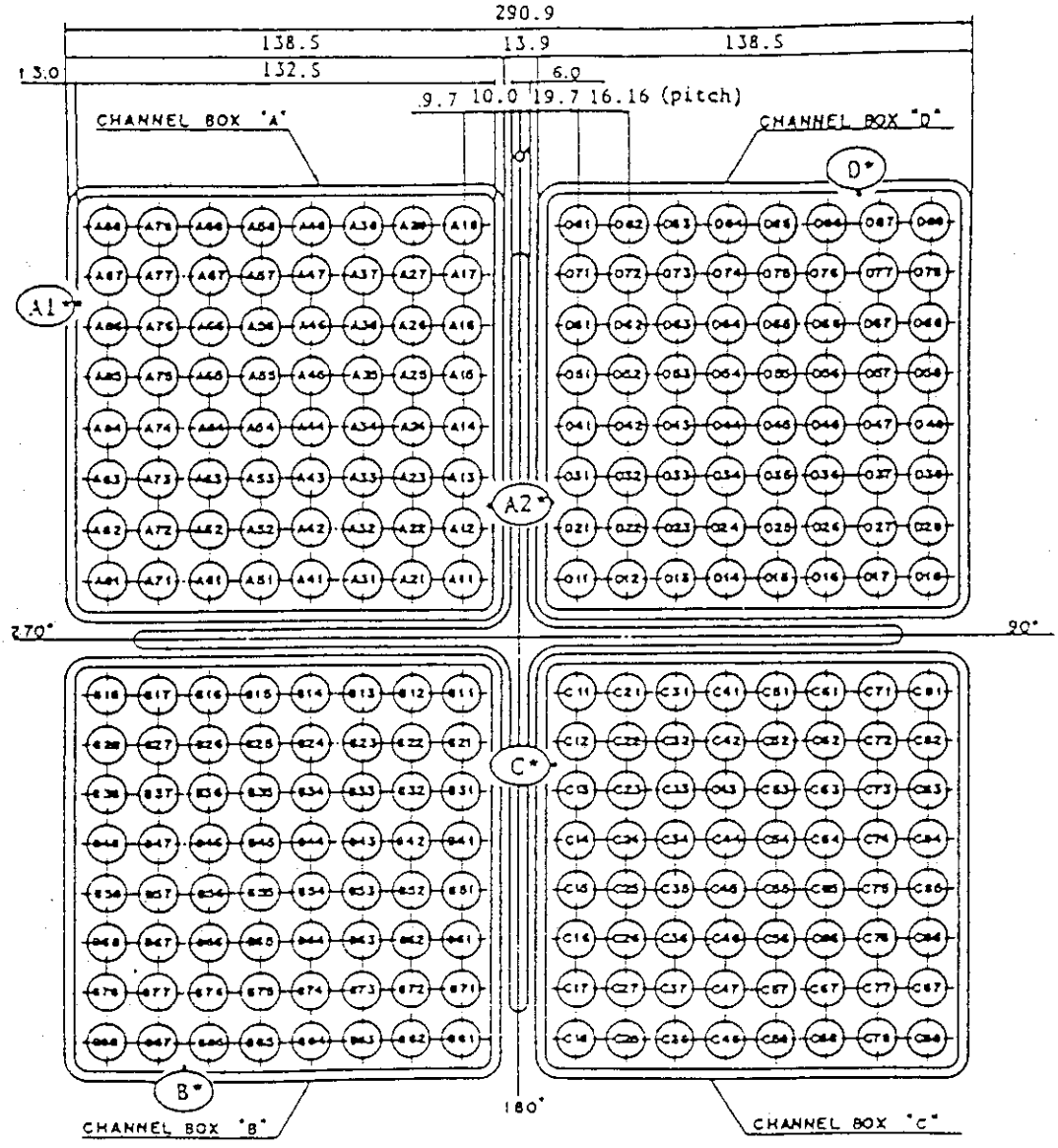

Heater rod O.D. is 12.27mm

A5S4, B5S4, C5S4 and D5S4 are water rod simulators with void probes, O.D.= 15.01mm

A4S, B4S, C4S and D4S are water rod simulators with thermocouples, O.D.= 15.01mm

Fig. 3.5 Core instrumentation (cf. Table 3.3)

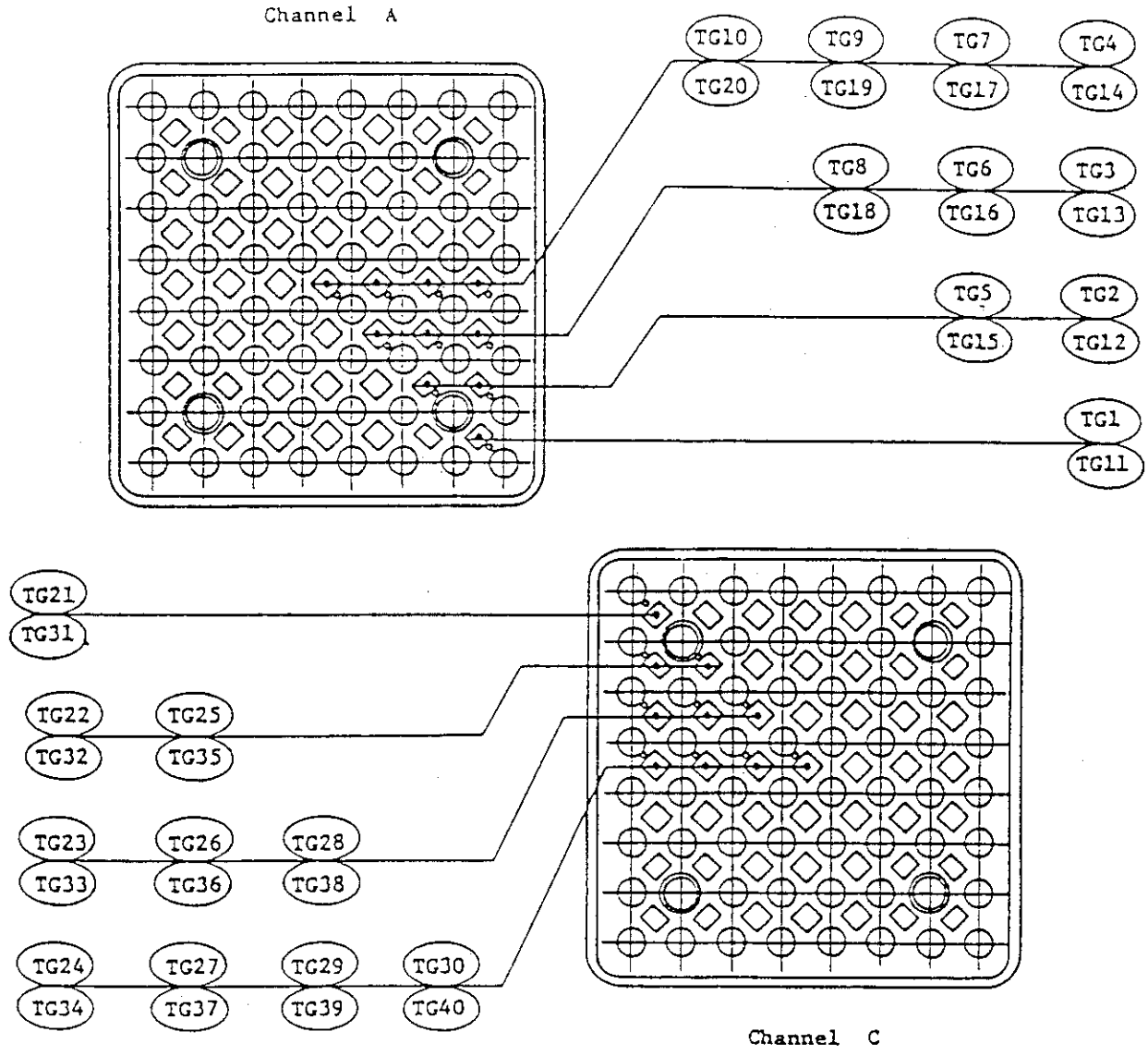

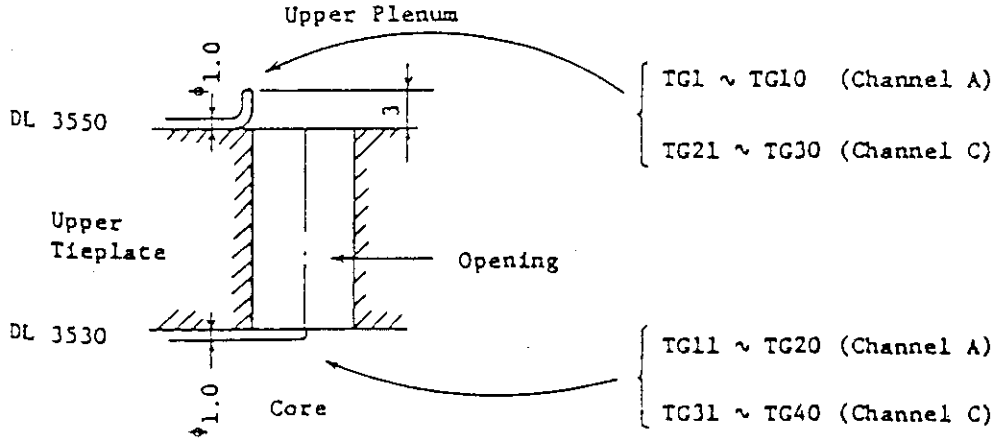

Fig. 3.6 Upper tieplate instrumentations

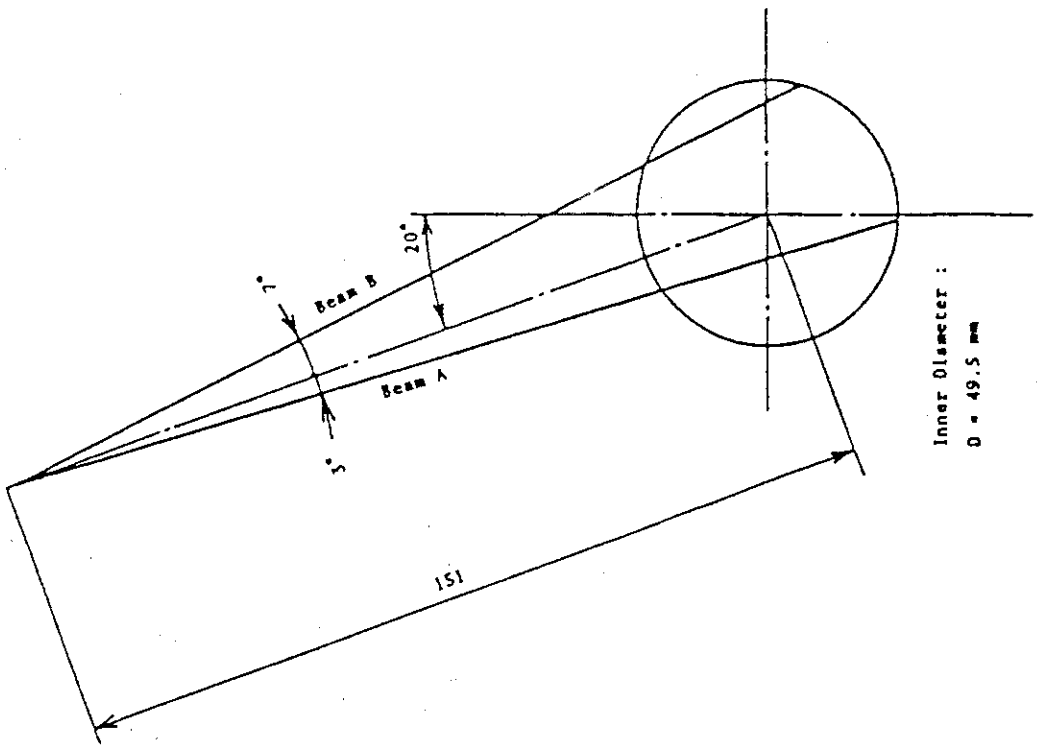

Fig. 3.8 Beam directions of two-beam gamma densitometer

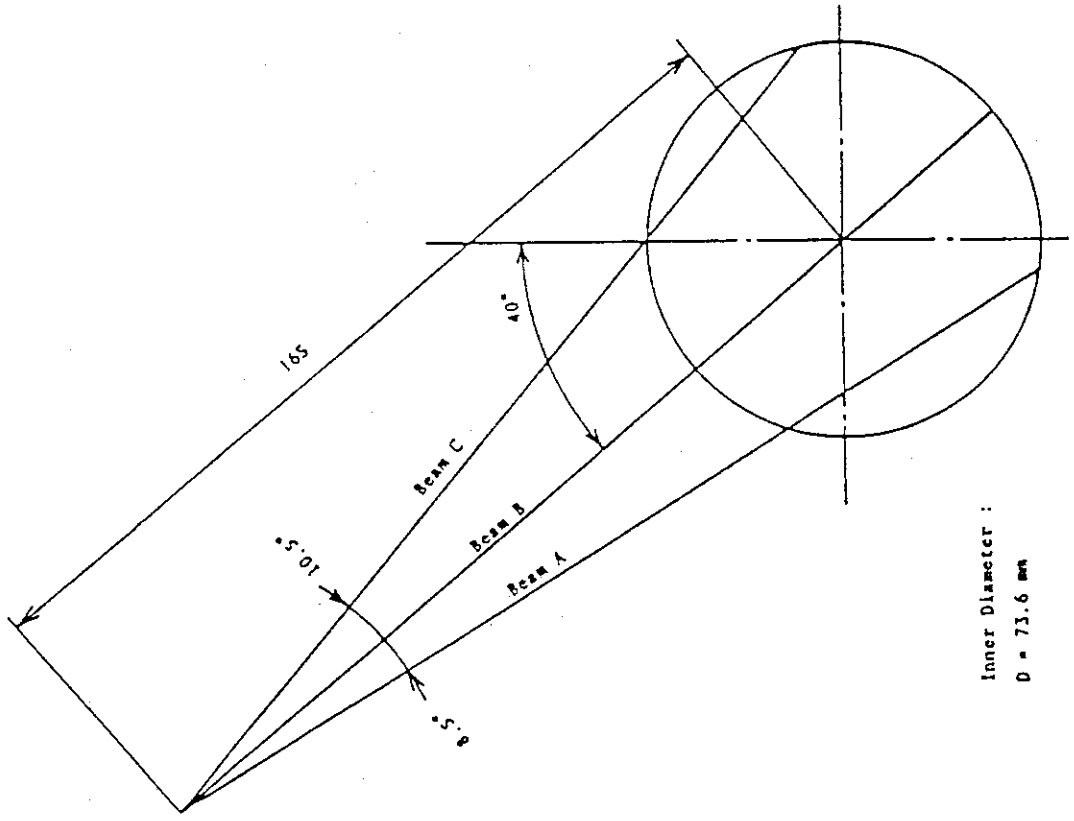

Fig. 3.7 Beam directions of three-beam gamma densitometer

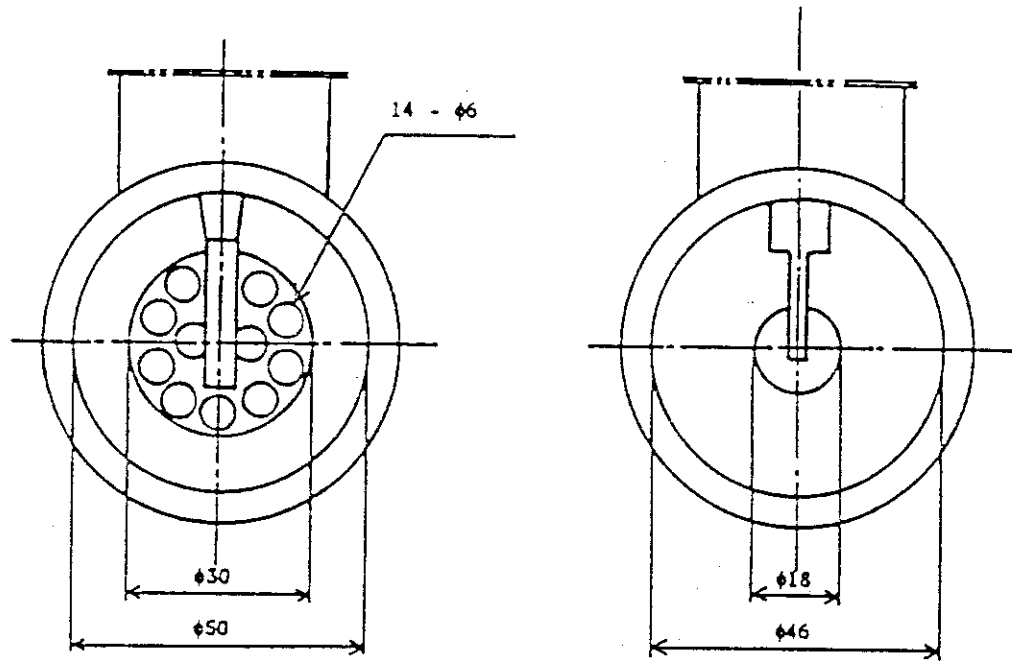

(a) High Range Drag Disc

(b) Low Range Drag Disc

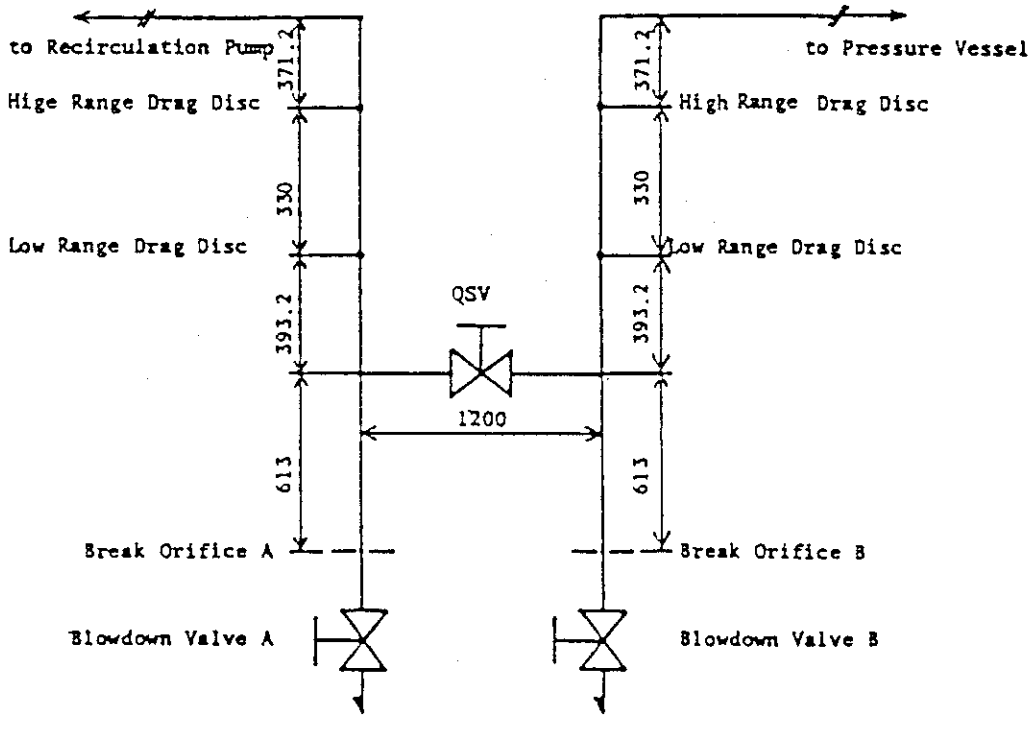

(c) Location of Drag Discs

Fig. 3.9 Arrangement and location of drag disks

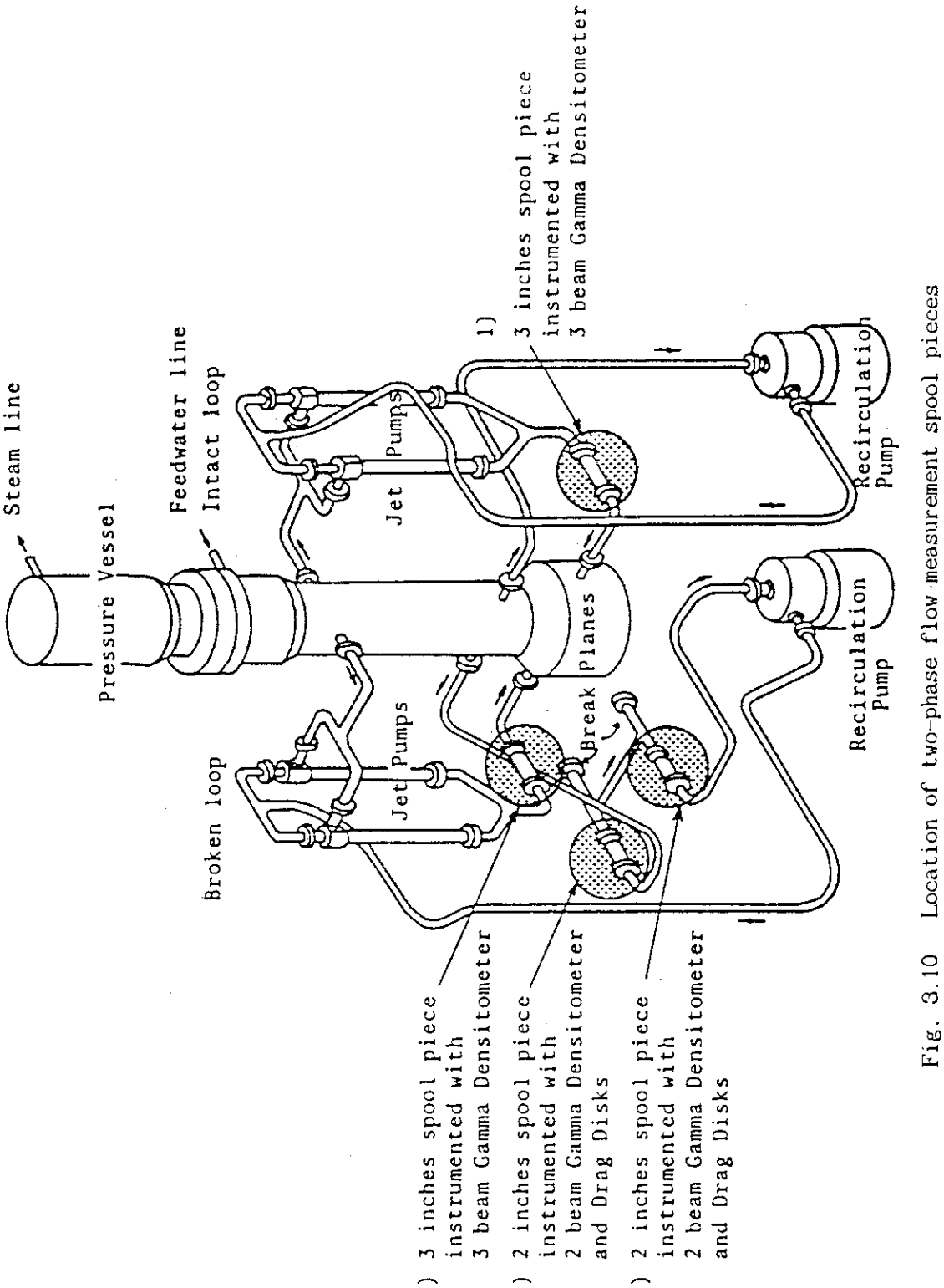

Fig. 3.10 Location of two-phase flow measurement spool pieces

Table 4.1 Test conditions of RUN 955

Parameter	Unit	Measured Value
Break Conditions		
Location		MSL outside RCV
Orifice Diameter	mm	31.0
1/424 Scaled Area	%	100
Initial Conditions		
Steam Dome Pressure	MPa	7.36
Lower Plenum Temperature	K	552.6
Lower Plenum Subcooling	K	10.7
Core Inlet Flow Rute	kg/s	16.8
Total Core Power	MW	3.98
Max. Lineer Heat Rate		
Channel A (LPF=1.1)	kW/m	16.74
Channel A (" =1.0)	"	15.21
Channel A (" =0.875)	"	13.31
Channels B,C,D (" =1.1)	"	11.96
Channels B,C,D (" =1.0)	"	10.87
Channels B,C,D (" =0.875)	"	9.51
Upper Plenum Quality	%	12.6
Water Level	m	5.04
Steam Flow Rate	kg/s	2.06
Feedwater Flow Rate	"	2.06
Feedwater Temperature	K	489
Transient Conditions		
MSIV Closure Time	s	3
SRV Operation Pressure	MPa	8.0
ECCS Conditions		
HPCS Actuation		Failure
LPCS Actuation Time	s	516
Initiation Pressure	MPa	2.2
Trip Logic	s	L1 + 40
Water Temperature	K	313
LPCI Actuation Time	s	597
Initiation Pressure	MPa	1.7
Trip Logic	s	L1 + 40
Water Temperature	K	313
ADS Actuation Time	s	150
Trip Logic		L2 + 120
Orifice Diameter	mm	15.5

Table 4.2 Major events and test procedures of RUN 955

Time (s)	Events
-118	· Initiation of data recording
- 12	· Initiation of data plotting
0.0	· Initiation of break line valves opening (AV-165, QOBV)
	· Initiation of valve closure (CV-1, 2)
	· Primary pump coast down (MRP1, 2)
1.6	· Initiation of feedwater line closure (Completed at 4.0 s)
3.2	· Initiation of MSIV closure
8.0	· SRV operation at 8.0 MPa
9.0	· Initiation of core power decrease
28	· L2 level trip in downcomer
150	· ADS actuation
178	· Initiation of lower plenum flashing
330	· Initiation of core dryout
440	· L1 level trip in downcomer
516	· LPCS actuation
540	· PCT at position 2 of A88 rod (646 K)
546	· Completion of core quenching
591	· LPCI actuation
788	· Termination of data plotting
1150	· Termination of data recording

Table 4.3 Characteristics of steam discharge line valves

Valve		Close to Open	Open to Close
AV165	(Transient Line)	0.1 s	1.5 s
AV168	(Steady Line)	-	0.1 s
AV169	(ADS)	0.3 s	2.0 s

Table 4.4 Control sequence for steam line valves in RUN 955

Valves	Simulation	Before Break	After Break
CV-130	SRV	Open	Control
AV-168		Open	Open
AV-165	Break	Close	Open by break signal and close at 3s
AV-169	ADS	Close	Open by L2 + 120s
CV-1		Open	Close
CV-2		Open	Close

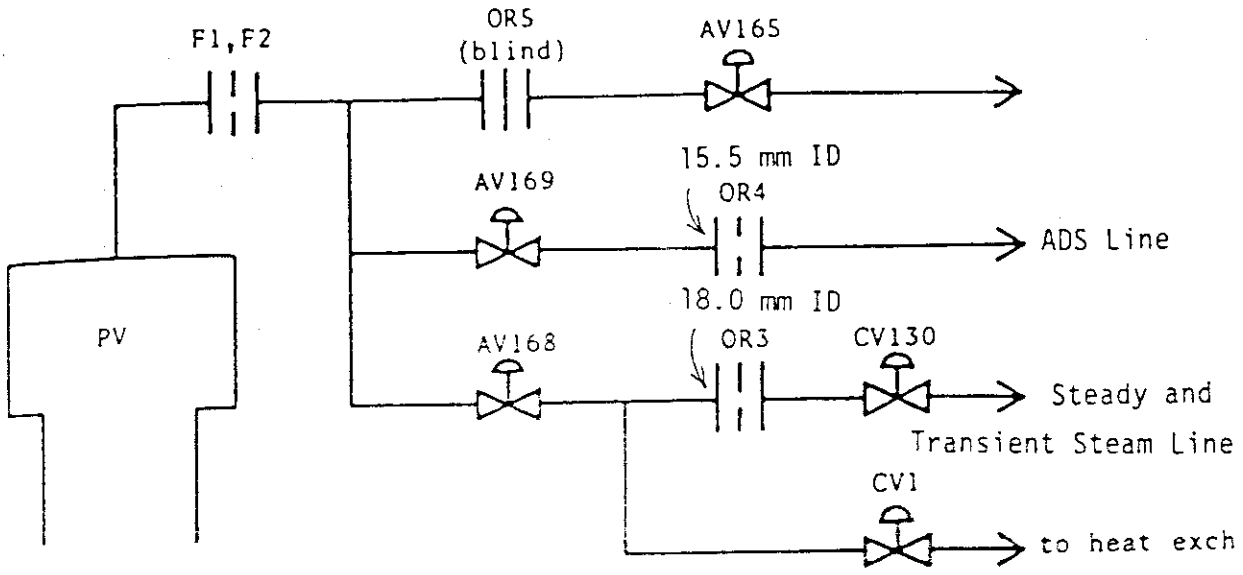

Fig. 4.1 Main steam line schematic

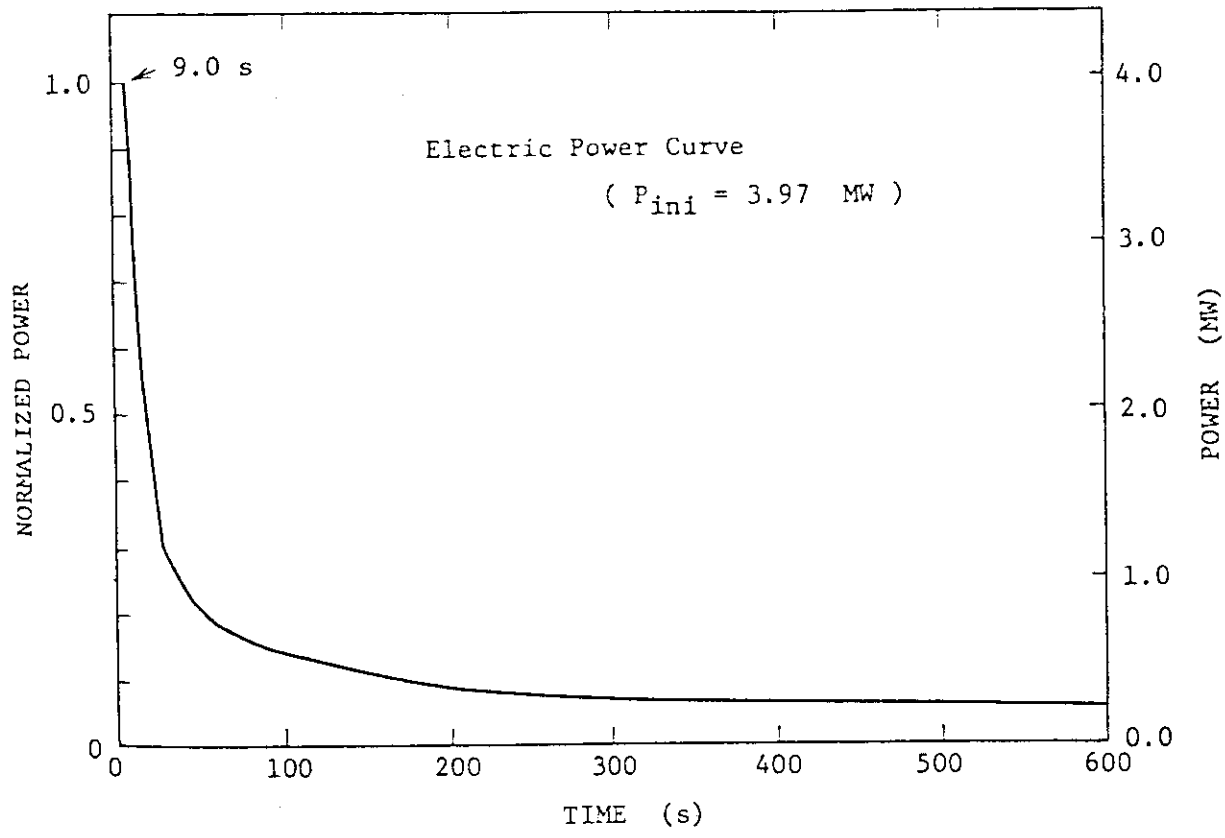

Fig. 4.2 Normalized power transient for ROSA-III test

Table 5.1 Maximum Cladding Temperature Distribution in the Core of RUN 955

	Pos.1	Pos.2	Pos.3	Pos.4	Pos.5	Pos.6	Pos.7
A-11 rod	TE 201	TE 202	TE 203	TE 204	TE 205	TE 206	TE 207
PCT (K)	573.1	621.1	643.9	580.3	577.9	574.3	576.7
Time (s)	9.6	522.4	529.6	9.6	8.8	9.6	9.6
A-12 rod	TE 208	TE 209	TE 210	TE 211	TE 212	TE 213	TE 214
PCT (K)	571.9	593.5	615.1	579.1	575.5	575.5	571.9
Time (s)	10.4	519.2	524.8	9.6	8.8	8.8	9.6
A-13 rod	TE 215	TE 216	TE 217	TE 218	TE 219	TE 220	TE 221
PCT (K)	574.3	606.7	617.5	579.1	576.7	576.7	574.3
Time (s)	9.6	520.8	526.4	8.8	8.8	8.8	9.6
A-14 rod	TE 222	TE 223	TE 224	TE 225	TE 226	TE 227	TE 228
PCT (K)	------	------	------	------	------	------	------
Time (s)	------	------	------	------	------	------	------
A-15 rod	TE 229			TE 230			
PCT (K)	------			------			
Time (s)	------			------			
A-17 rod	TE 231			TE 232			
PCT (K)	------			575.5			
Time (s)	------			8.8			
A-22 rod	TE 233	TE 234	TE 235	TE 236	TE 237	TE 238	TE 239
PCT (K)	588.7	645.1	634.3	577.6	576.8	578.8	574.1
Time (s)	519.2	528.0	536.0	9.6	8.8	10.4	8.8
A-24 rod	TE 240	TE 241	TE 242	TE 243	TE 244	TE 245	TE 246
PCT (K)	------	------	------	------	------	------	------
Time (s)	------		------	------	------	------	------

Table 5.1 Maximum Cladding Temperature Distribution in the Core of RUN 955 (Continued)

	Pos.1	Pos.2	Pos.3	Pos.4	Pos.5	Pos.6	Pos.7
A-26 rod	TE 247			TE 248			
PCT (K)	------			------			
Time (s)	------			------			
A-28 rod	TE 249			TE 250			
PCT (K)	------			577.6			
Time (s)	------			8.8			
A-31 rod	TE 251			TE 252			
PCT (K)	------			577.6			
Time (s)	------			9.6			
A-33 rod	TE 253	TE 254	TE 255	TE 256	TE 257	TE 258	TE 259
PCT (K)	575.2	576.4	590.5	572.9	572.0	573.9	571.0
Time (s)	10.4	8.8	527.2	8.8	8.0	8.8	8.8
A-34 rod	TE 260	TE 261	TE 262	TE 263	TE 264	TE 265	TE 266
PCT (K)	------	------	------	------	------	------	------
Time (s)	------	------	------	------	------	------	------
A-37 rod	TE 267			TE 268			
PCT (K)	------			------			
Time (s)	------			------			
A-42 rod	TE 269			TE 270			
PCT (K)	------			------			
Time (s)	------			------			
A-44 rod	TE 271	TE 272	TE 273	TE 274	TE 275	TE 276	TE 277
PCT (K)	------	------	------	------	------	------	------
Time (s)	------	------	------	------	------	------	------

Table 5.1 Maximum Cladding Temperature Distribution in the Core of RUN 955 (Continued)

	Pos.1	Pos.2	Pos.3	Pos.4	Pos.5	Pos.6	Pos.7
A-48 rod	TE 278			TE 279			
PCT (K)	------			------			
Time (s)	------			------			
A-51 rod	TE 280			TE 281			
PCT (K)	------			------			
Time (s)	------			------			
A-53 rod	TE 282			TE 283			
PCT (K)	------			------			
Time (s)	------			------			
A-57 rod	TE 284			TE 285			
PCT (K)	------			576.8			
Time (s)	------			8.8			
A-62 rod	TE 286			TE 287			
PCT (K)	------			------			
Time (s)	------			------			
A-66 rod	TE 288			TE 289			
PCT (K)	------			------			
Time (s)	------			------			
A-68 rod	TE 290			TE 291			
PCT (K)	------			574.9			
Time (s)	------			8.8			
A-71 rod	TE 292			TE 293			
PCT (K)	------			571.0			
Time (s)	------			8.8			

Table 5.1 Maximum Cladding Temperature Distribution in the Core of RUN 955 (Continued)

	Pos.1	Pos.2	Pos.3	Pos.4	Pos.5	Pos.6	Pos.7
A-73 rod	TE 294			TE 295			
PCT (K)	------			574.9			
Time (s)	------			8.8			
A-75 rod	TE 296			TE 297			
PCT (K)	------			------			
Time (s)	------			------			
A-77 rod	TE 298	TE 299	TE 300	TE 301	TE 302	TE 303	TE 304
PCT (K)	599.9	642.9	628.6	569.1	572.0	573.0	------
Time (s)	531.2	536.0	536.8	8.8	16.0	8.8	------
A-82 rod	TE 305			TE 306			
PCT (K)	------			------			
Time (s)	------			------			
A-84 rod	TE 307			TE 308			
PCT (K)	572.0			576.8			
Time (s)	8.8			8.8			
A-85 rod	TE 309	TE 310	TE 311	TE 312	TE 313	TE 314	TE 315
PCT (K)	------	------	------	------	------	------	------
Time (s)	------	------	------	------	------	------	------
A-87 rod	TE 316	TE 317	TE 318	TE 319	TE 320	TE 321	TE 322
PCT (K)	573.9	641.9	641.0	572.0	574.9	574.9	571.0
Time (s)	8.8	534.4	536.0	8.8	8.8	8.8	8.0
A-88 rod	TE 323	TE 324	TE 325	TE 326	TE 327	TE 328	TE 329
PCT (K)	573.0	645.7	641.9	576.8	575.9	574.9	574.9
Time (s)	8.0	540.0	536.8	8.8	8.8	8.8	8.8

Table 5.1 Maximum Cladding Temperature Distribution in the Core of RUN 955 (Continued)

	Pos.1	Pos.2	Pos.3	Pos.4	Pos.5	Pos.6	Pos.7
B-11 rod	TE 330	TE 331	TE 332	TE 333	TE 334	TE 335	TE 336
PCT (K)	572.0	572.0	589.3	572.0	572.0	574.9	------
Time (s)	8.8	8.8	524.8	8.8	8.0	8.8	------
B-13 rod				TE 337			
PCT (K)				574.9			
Time (s)				8.8			
B-22 rod	TE 338	TE 339	TE 340	TE 341	TE 342	TE 343	TE 344
PCT (K)	573.0	574.9	597.0	574.9	574.9	573.0	574.9
Time (s)	8.8	8.8	526.4	8.8	8.8	8.8	8.8
B-31 rod				TE 345			
PCT (K)				------			
Time (s)				------			
B-33 rod				TE 346			
PCT (K)				------			
Time (s)				------			
B-51 rod				TE 347			
PCT (K)				------			
Time (s)				------			
B-53 rod				TE 348			
PCT (K)				------			
Time (s)				------			
B-66 rod				TE 349			
PCT (K)				------			
Time (s)				------			

Table 5.1 Maximum Cladding Temperature Distribution in the Core of RUN 955 (Continued)

	Pos.1	Pos.2	Pos.3	Pos.4	Pos.5	Pos.6	Pos.7
B-77 rod	TE 350	TE 351	TE 352	TE 353	TE 354	TE 355	TE 356
PCT (K)	571.0	608.5	602.8	573.9	573.9	574.9	573.0
Time (s)	8.8	524.8	526.4	8.8	8.8	8.8	9.6
B-86 rod				TE 357			
PCT (K)				------			
Time (s)				------			
C-11 rod	TE 358	TE 359	TE 360	TE 361	TE 362	TE 363	TE 364
PCT (K)	574.9	572.0	597.0	572.0	570.1	573.9	567.2
Time (s)	8.8	8.8	525.6	8.8	9.6	8.8	8.8
C-13 rod	TE 365	TE 366	TE 367	TE 368	TE 369	TE 370	TE 371
PCT (K)	568.1	572.0	600.8	573.0	574.9	573.9	572.0
Time (s)	8.8	8.8	529.6	8.8	8.8	8.8	8.8
C-15 rod				TE 372			
PCT (K)				------			
Time (s)				------			
C-22 rod	TE 373	TE 374	TE 375	TE 376	TE 377	TE 378	TE 379
PCT (K)	571.0	598.0	599.9	575.9	574.9	575.9	571.0
Time (s)	8.8	520.8	528.0	9.6	8.8	8.8	10.4
C-31 rod				TE 380			
PCT (K)				------			
Time (s)				------			
C-33 rod	TE 381	TE 382	TE 383	TE 384	TE 385	TE 386	TE 387
PCT (K)	571.0	573.0	572.0	573.0	573.0	571.0	568.1
Time (s)	8.8	8.8	8.8	8.8	8.0	8.8	9.6

Table 5.1 Maximum Cladding Temperature Distribution in the Core of RUN 955 (Continued)

	Pos.1	Pos.2	Pos.3	Pos.4	Pos.5	Pos.6	Pos.7
C-35 rod				TE 388			
PCT (K)				------			
Time (s)				------			
C-66 rod				TE 389			
PCT (K)				------			
Time (s)				------			
C-68 rod				TE 390			
PCT (K)				------			
Time (s)				------			
C-77 rod	TE 391	TE 392	TE 393	TE 394	TE 395	TE 396	TE 397
PCT (K)	575.9	614.3	605.6	574.9	574.9	572.0	571.0
Time (s)	524.8	537.6	534.4	8.8	8.8	8.8	9.6
D-11 rod				TE 398			
PCT (K)				573.9			
Time (s)				29.6			
D-13 rod				TE 399			
PCT (K)				576.8			
Time (s)				31.2			
D-22 rod	TE 400	TE 401	TE 402	TE 403	TE 404	TE 405	TE 406
PCT (K)	571.0	602.8	599.9	574.9	574.9	573.9	570.1
Time (s)	8.8	525.6	525.6	8.0	8.8	8.8	8.8
D-31 rod				TE 407			
PCT (K)				------			
Time (s)				------			

Table 5.1 Maximum Cladding Temperature Distribution in the Core of RUN 955 (Continued)

	Pos.1	Pos.2	Pos.3	Pos.4	Pos.5	Pos.6	Pos.7
D-33 rod				TE 408			
PCT (K)				------			
Time (s)				------			
D-51 rod				TE 409			
PCT (K)				------			
Time (s)				------			
D-53 rod				TE 410			
PCT (K)				------			
Time (s)				------			
D-66 rod				TE 411			
PCT (K)				------			
Time (s)				------			
D-77 rod				TE 412			
PCT (K)				574.9			
Time (s)				8.8			
D-86 rod				TE 413			
PCT (K)				574.9			
Time (s)				8.0			

Table 5.1 Maximum Cladding Temperature Distribution in the Core of RUN 955 (Continued)

** Order of PCT (RUN 955) **

No. 1	A-88 rod	Pos. 2	PCT =	645.7 (K)	Time =	540.0 (s)
No. 2	A-22 rod	Pos. 2	PCT =	645.1 (K)	Time =	528.0 (s)
No. 3	A-11 rod	Pos. 3	PCT =	643.9 (K)	Time =	529.6 (s)
No. 4	A-77 rod	Pos. 2	PCT =	642.9 (K)	Time =	536.0 (s)
No. 5	A-87 rod	Pos. 2	PCT =	641.9 (K)	Time =	534.4 (s)
No. 6	A-88 rod	Pos. 3	PCT =	641.9 (K)	Time =	536.8 (s)
No. 7	A-87 rod	Pos. 3	PCT =	641.0 (K)	Time =	536.0 (s)
No. 8	A-22 rod	Pos. 3	PCT =	634.3 (K)	Time =	536.0 (s)
No. 9	A-77 rod	Pos. 3	PCT =	628.6 (K)	Time =	536.8 (s)
No.10	A-11 rod	Pos. 2	PCT =	621.1 (K)	Time =	522.4 (s)

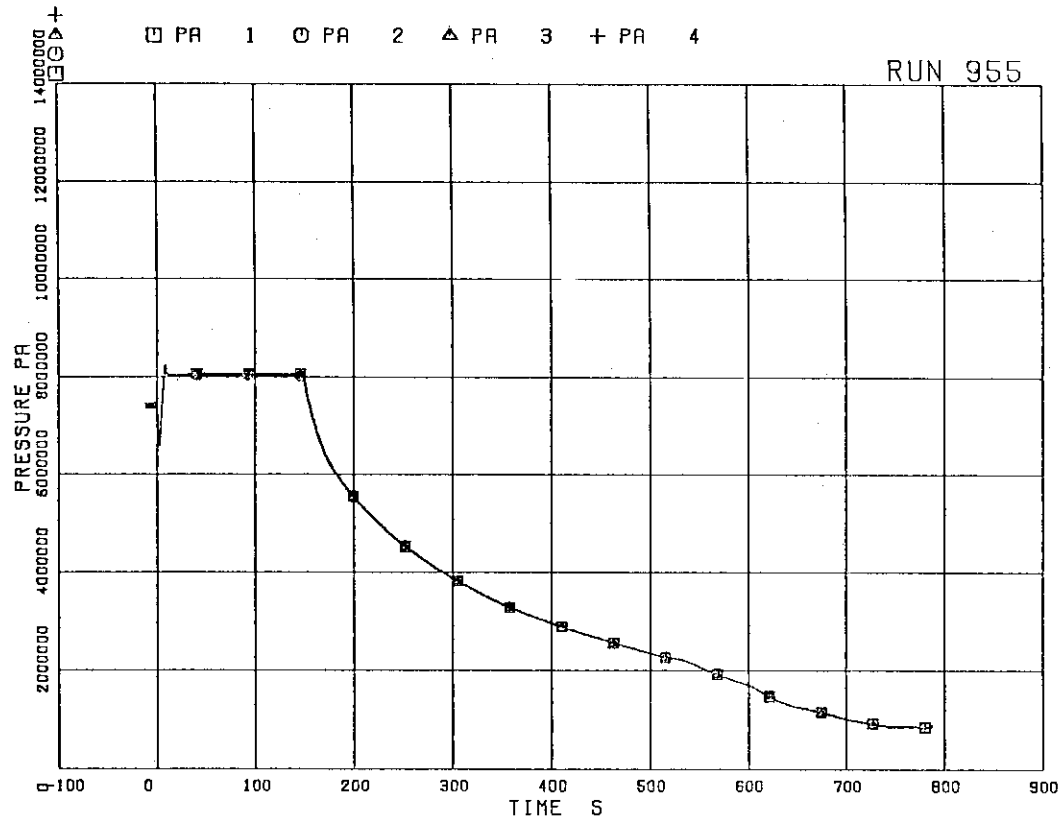

FIG.5. 1 PRESSURES IN PV (PRESSURE VESSEL)

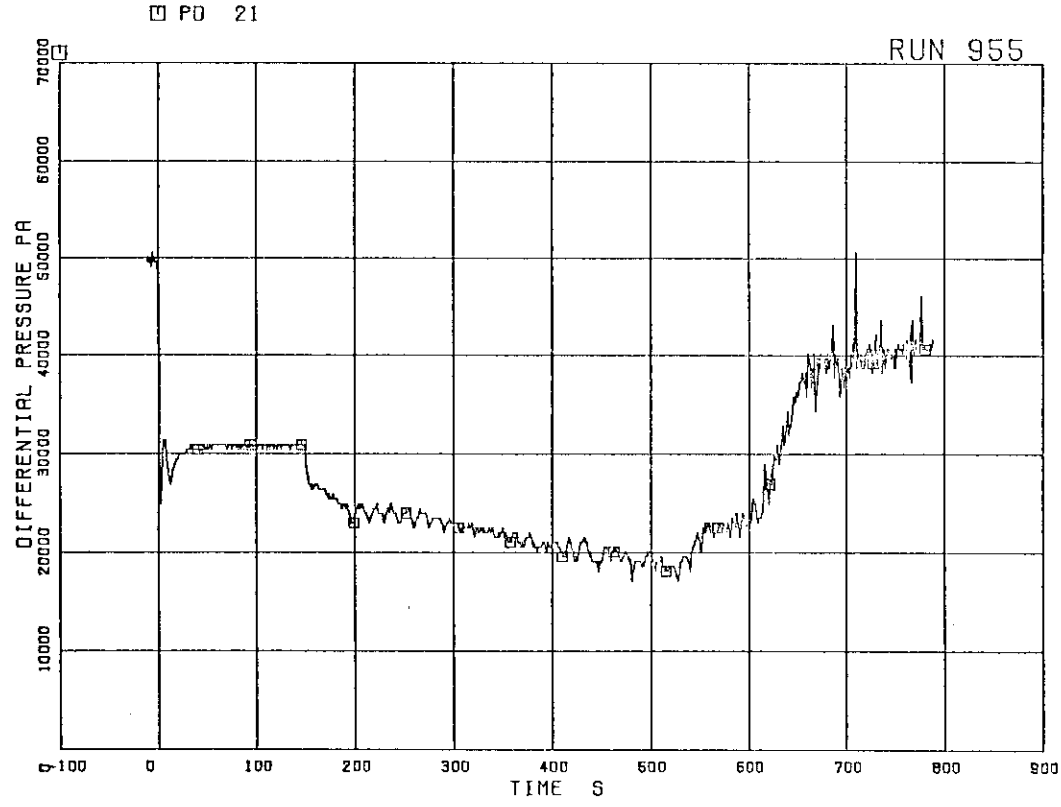

FIG.5. 2 DIFFERENTIAL PRESSURE BETWEEN LOWER PLENUM AND UPPER PLENUM

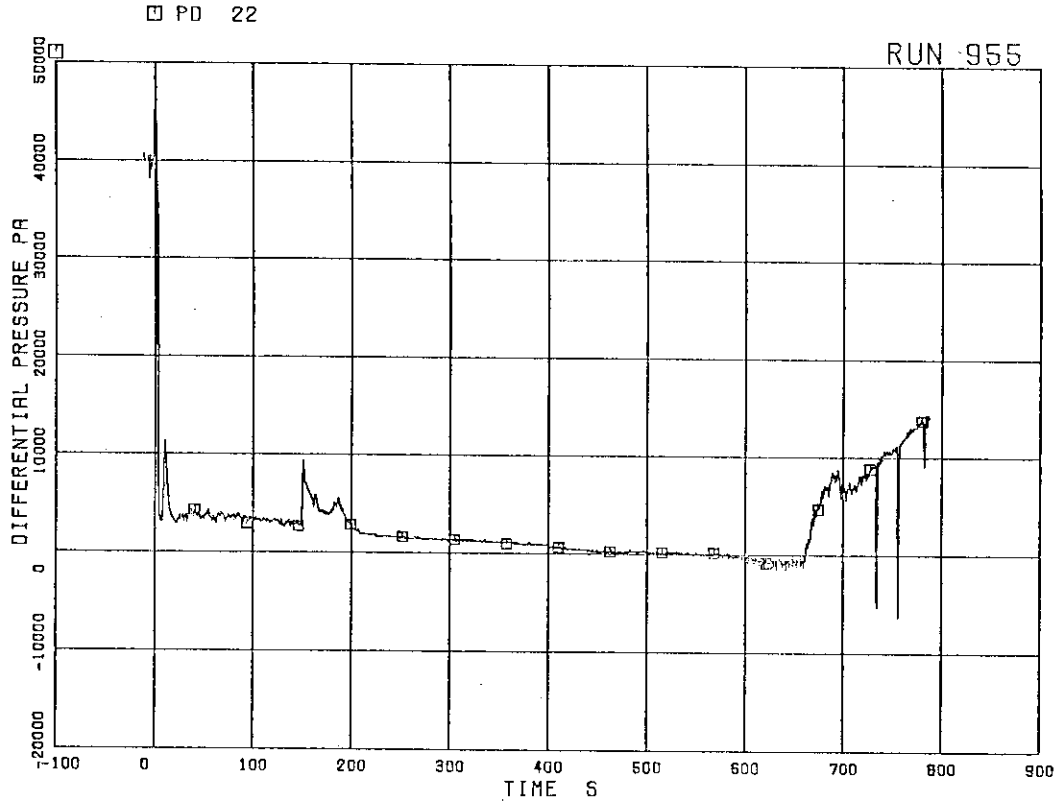

FIG.5. 3 DIFFERENTIAL PRESSURE BETWEEN UPPER PLENUM AND STEAM DOME

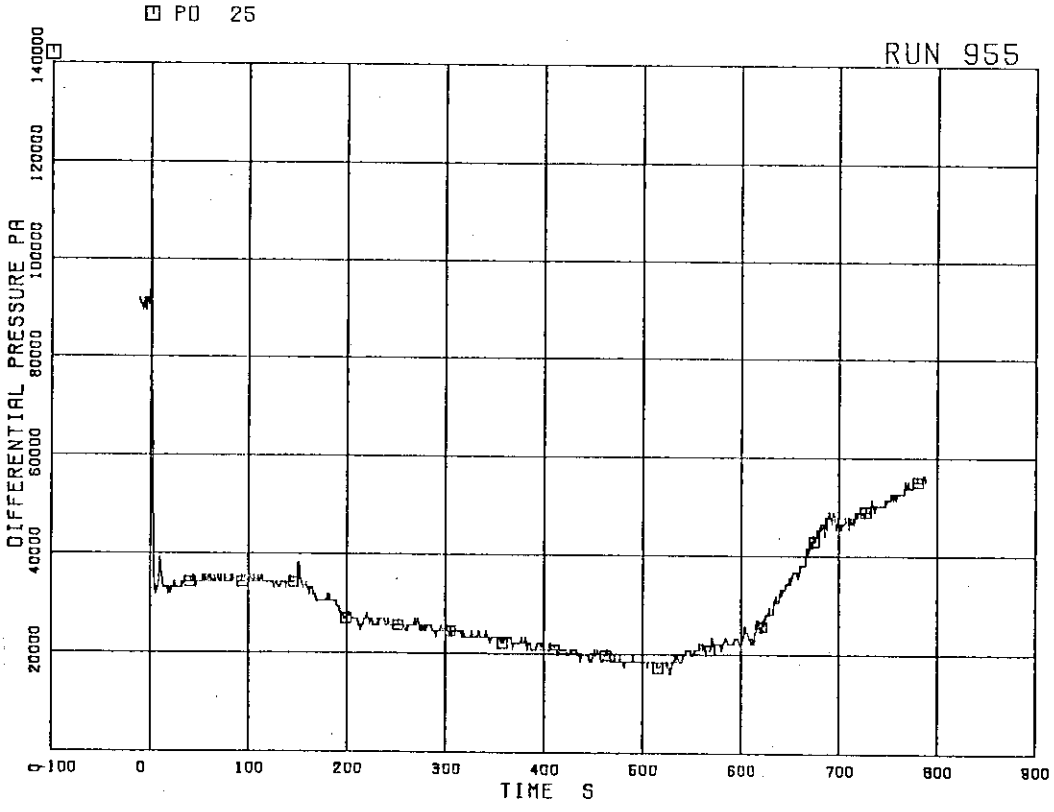

FIG.5. 4 DIFFERENTIAL PRESSURE BETWEEN PV BOTTOM AND TOP

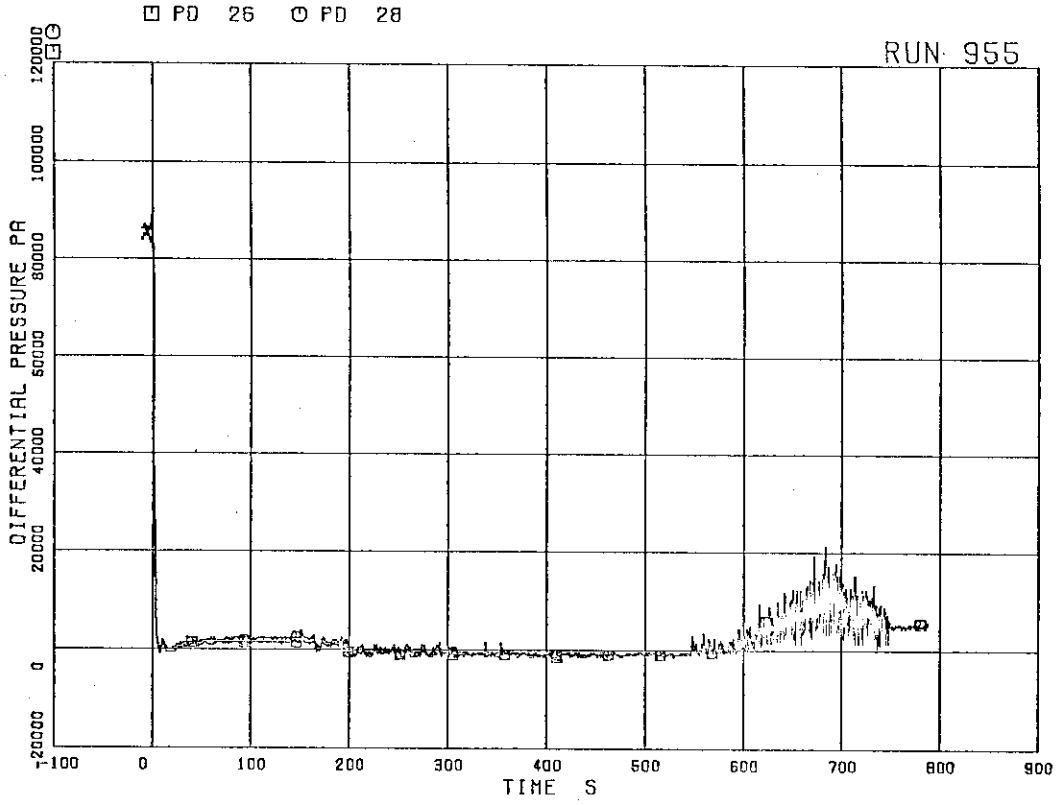

FIG.5. 5 DIFFERENTIAL PRESSURE BETWEEN JP-1,2 DISCHARGE AND SUCTION

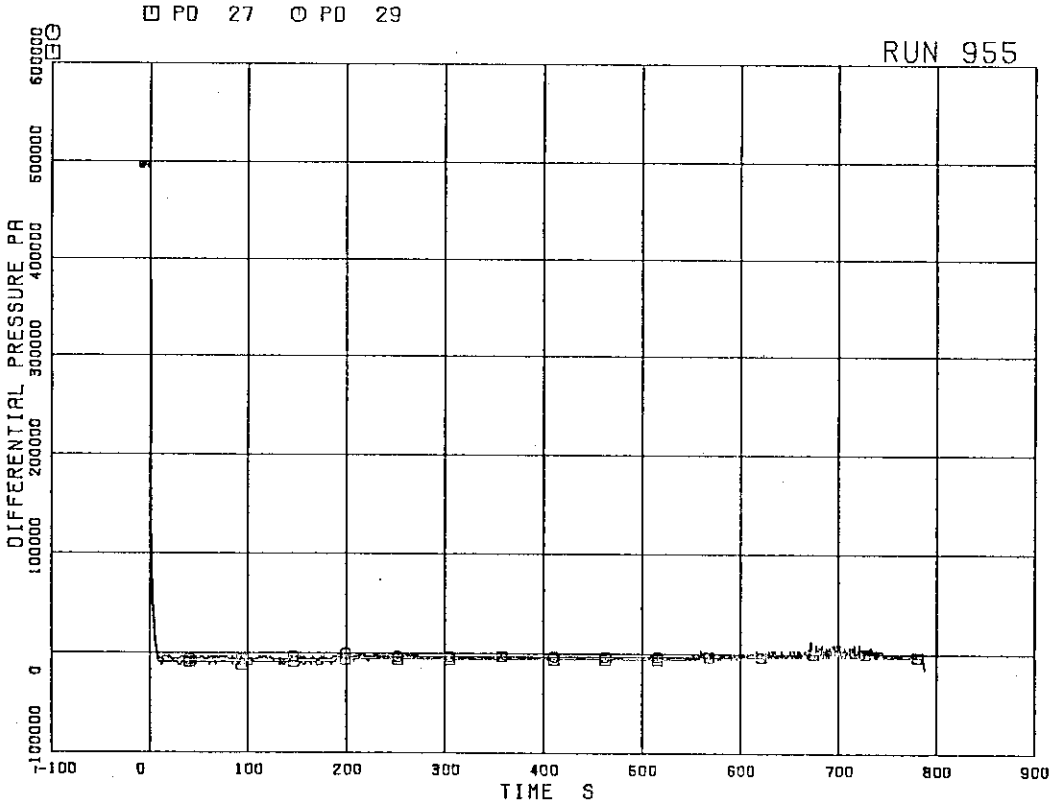

FIG.5. 6 DIFFERENTIAL PRESSURE BETWEEN JP-1,2 DRIVE AND SUCTION

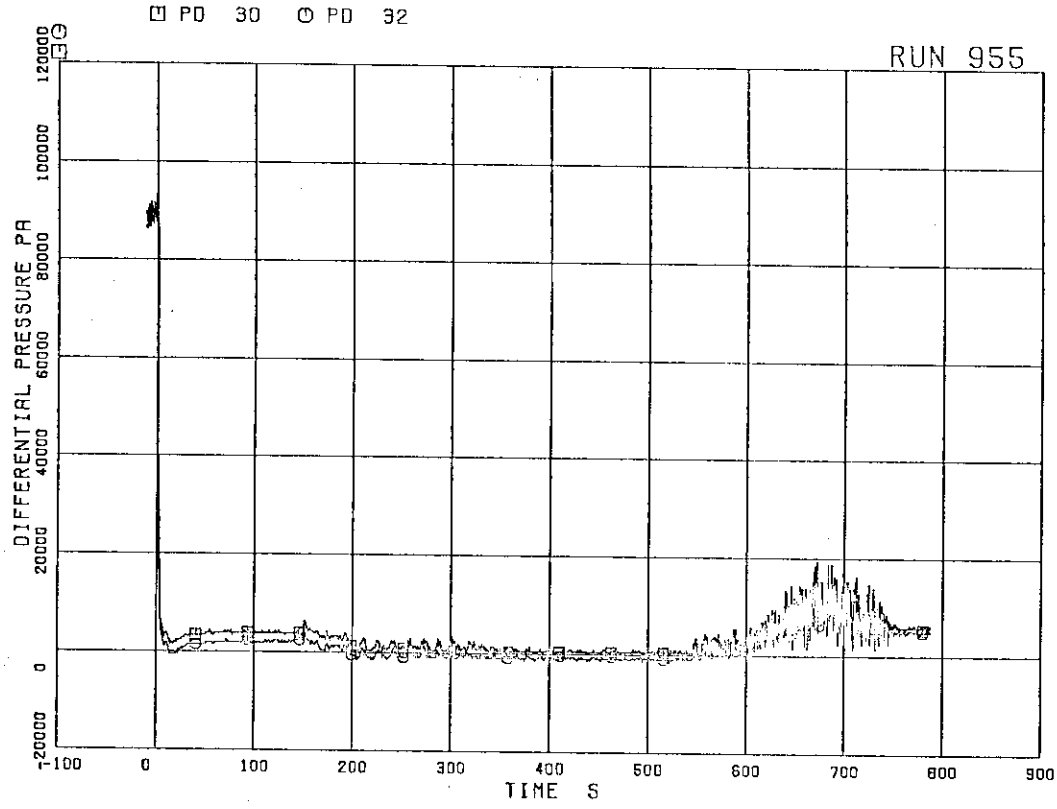

FIG.5. 7 DIFFERENTIAL PRESSURE BETWEEN JP-3,4 DISCHARGE AND SUCTION

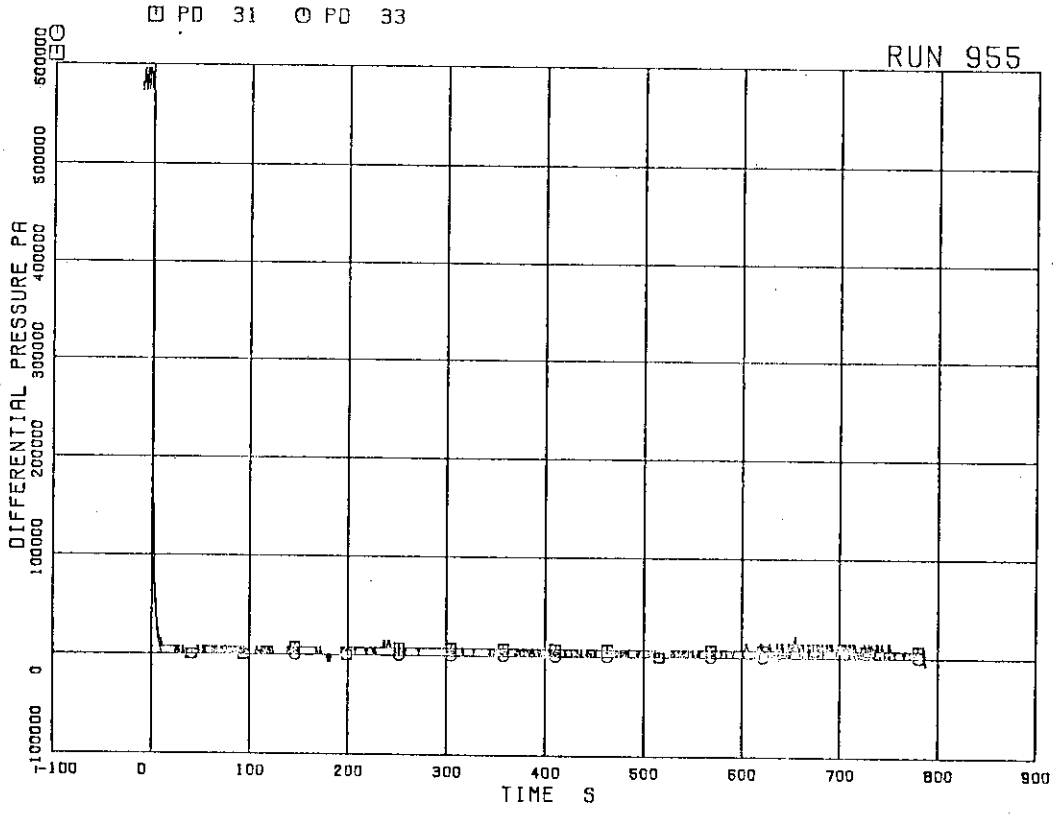

FIG.5. 8 DIFFERENTIAL PRESSURE BETWEEN JP-3,4 DRIVE AND SUCTION

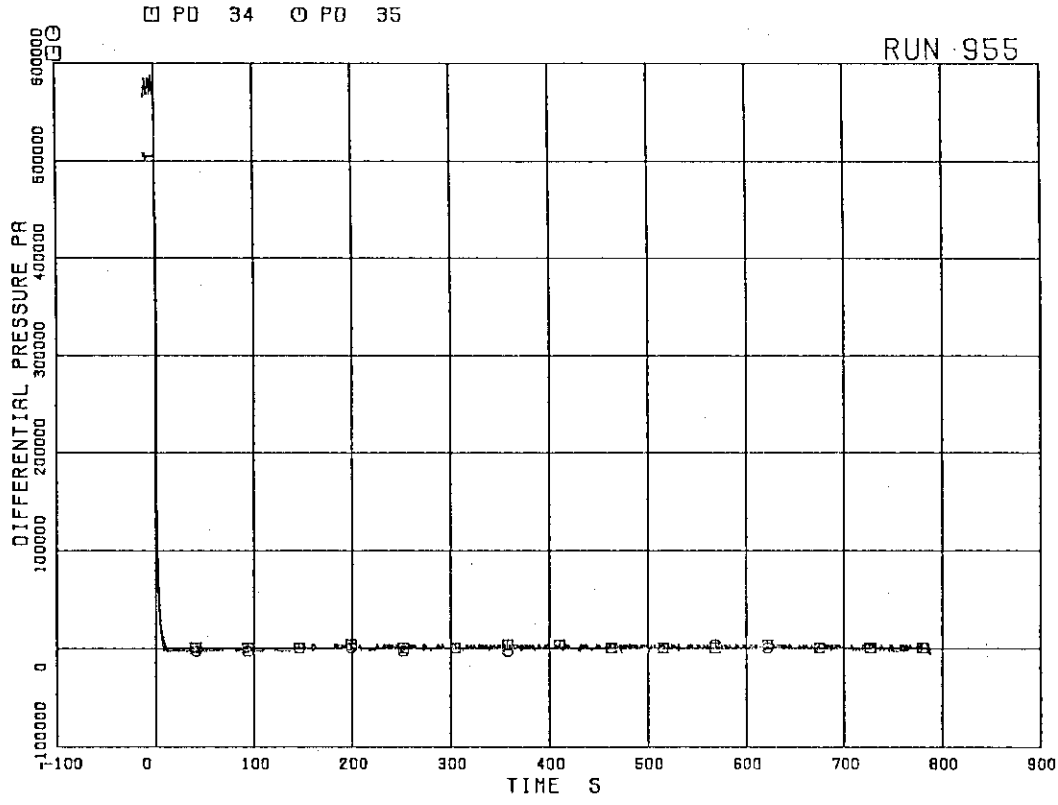

FIG.5. 9 DIFFERENTIAL PRESSURE BETWEEN MRP DELIVERY AND SUCTION

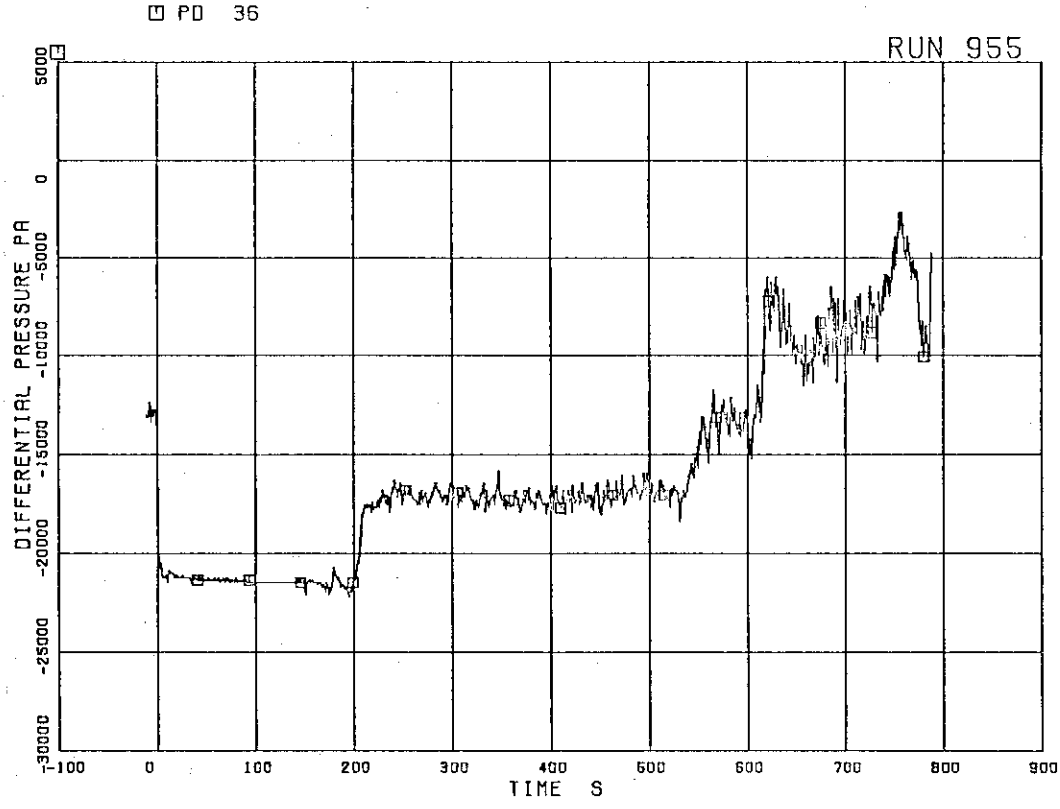

FIG.5. 10 DIFFERENTIAL PRESSURE BETWEEN DOWNCOMER BOTTOM AND MRP1 SUCTION

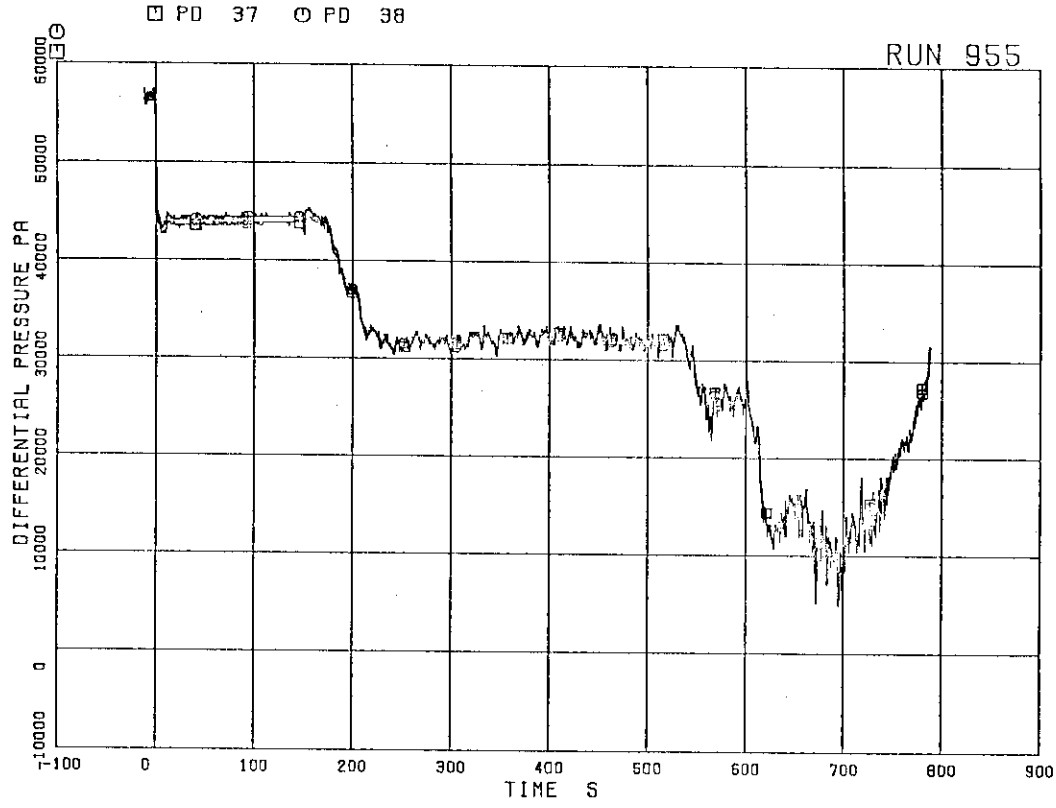

FIG.5. 11 DIFFERENTIAL PRESSURE BETWEEN MRP DELIVERY AND JP-1,2 DRIVE

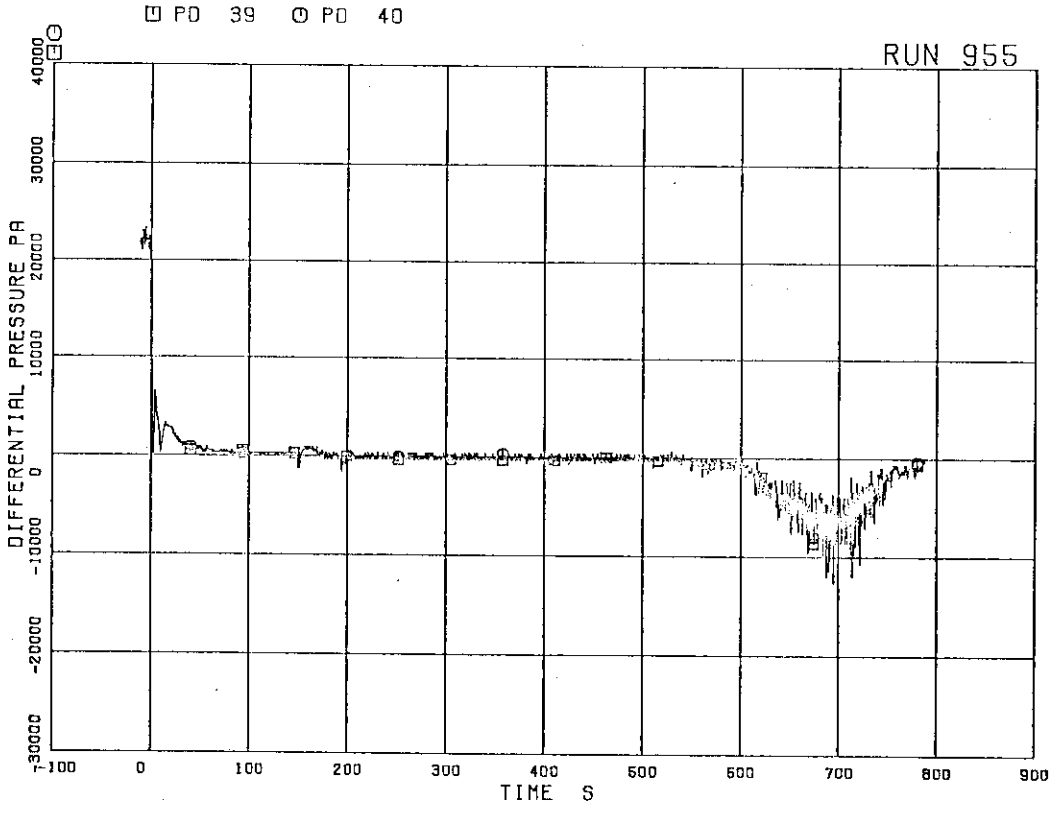

FIG.5. 12 DIFFERENTIAL PRESSURE BETWEEN DOWNCOMER MIDDLE AND JP-1.2 SUCTION

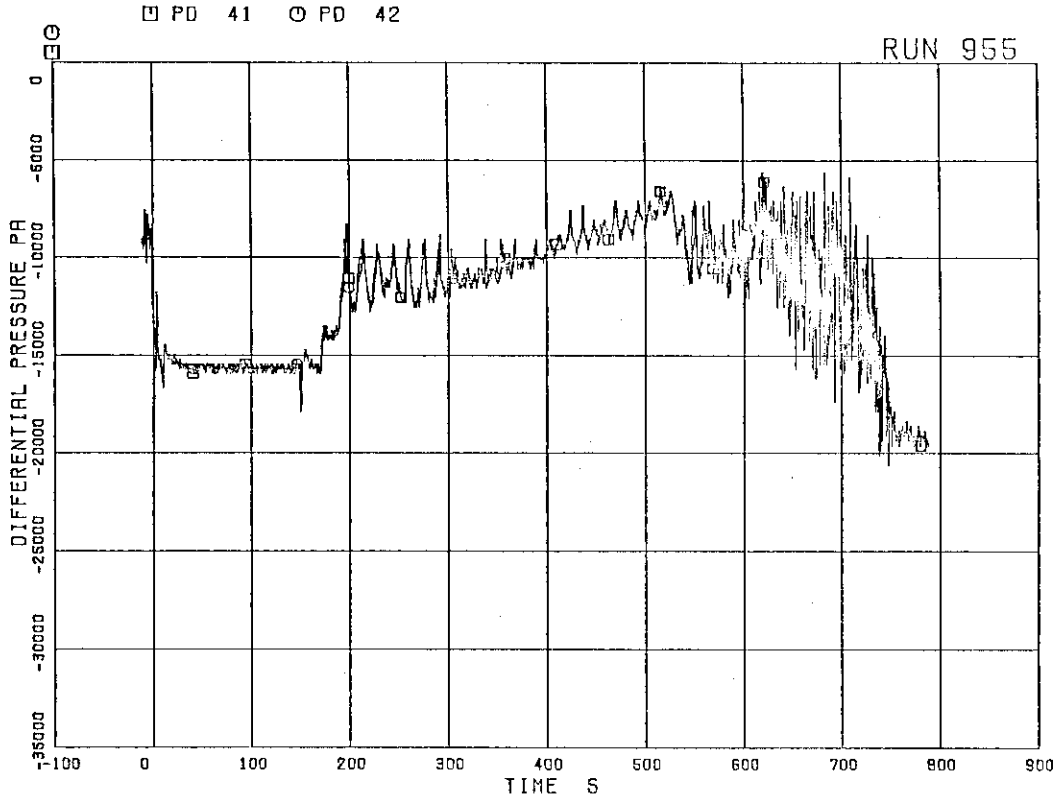

FIG.5. 13 DIFFERENTIAL PRESSURE BETWEEN JP-1,2 DISCHARGE AND LOWER PLENUM

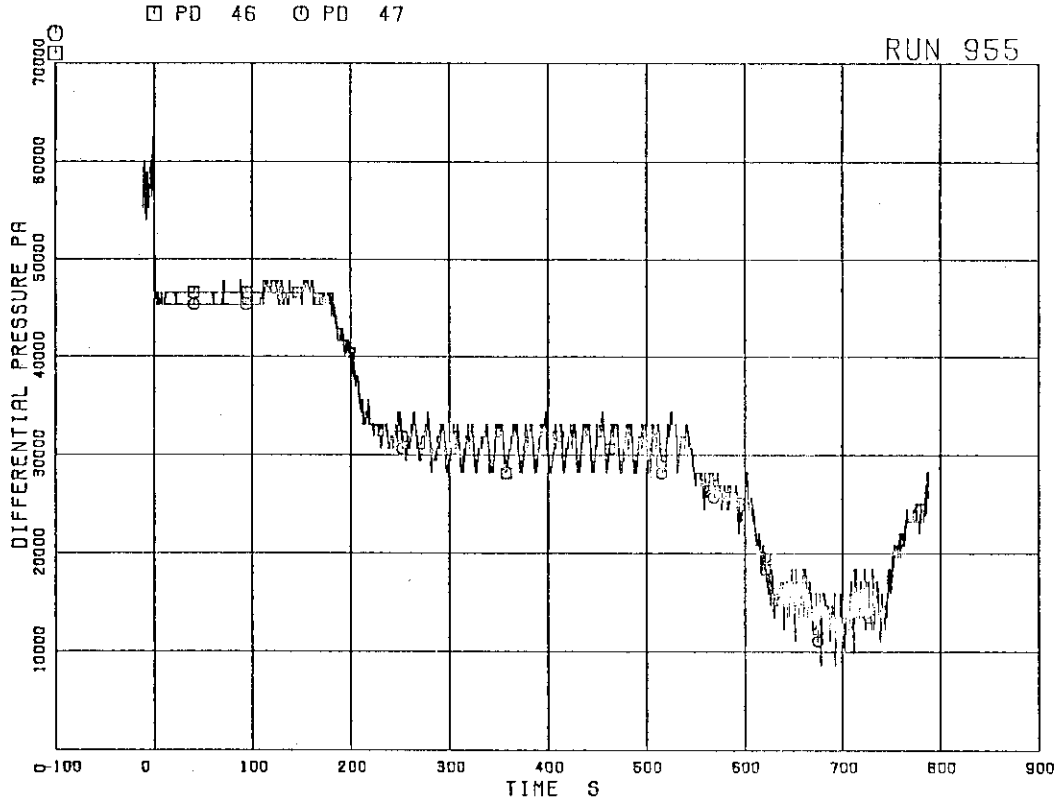

FIG.5. 14 DIFFERENTIAL PRESSURE BETWEEN MRP DELIVERY AND JP-3,4 DRIVE

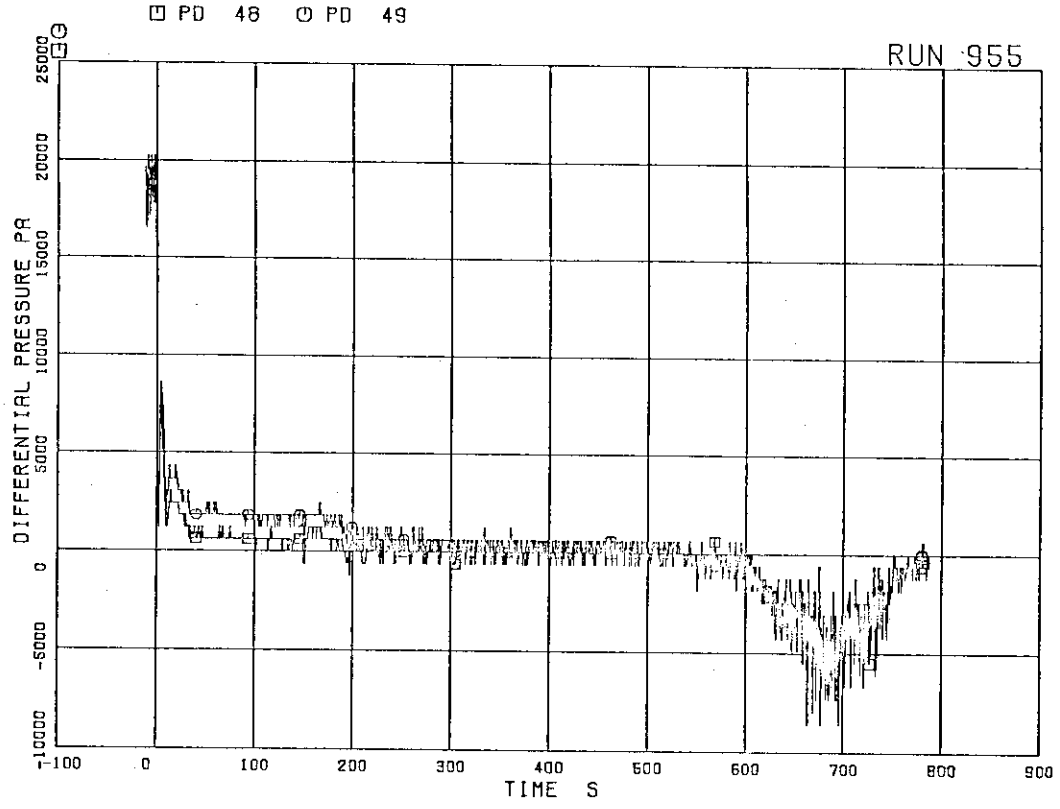

FIG.5. 15 DIFFERENTIAL PRESSURE BETWEEN DOWNCOMER MIDDLE AND JP-3,4 SUCTION

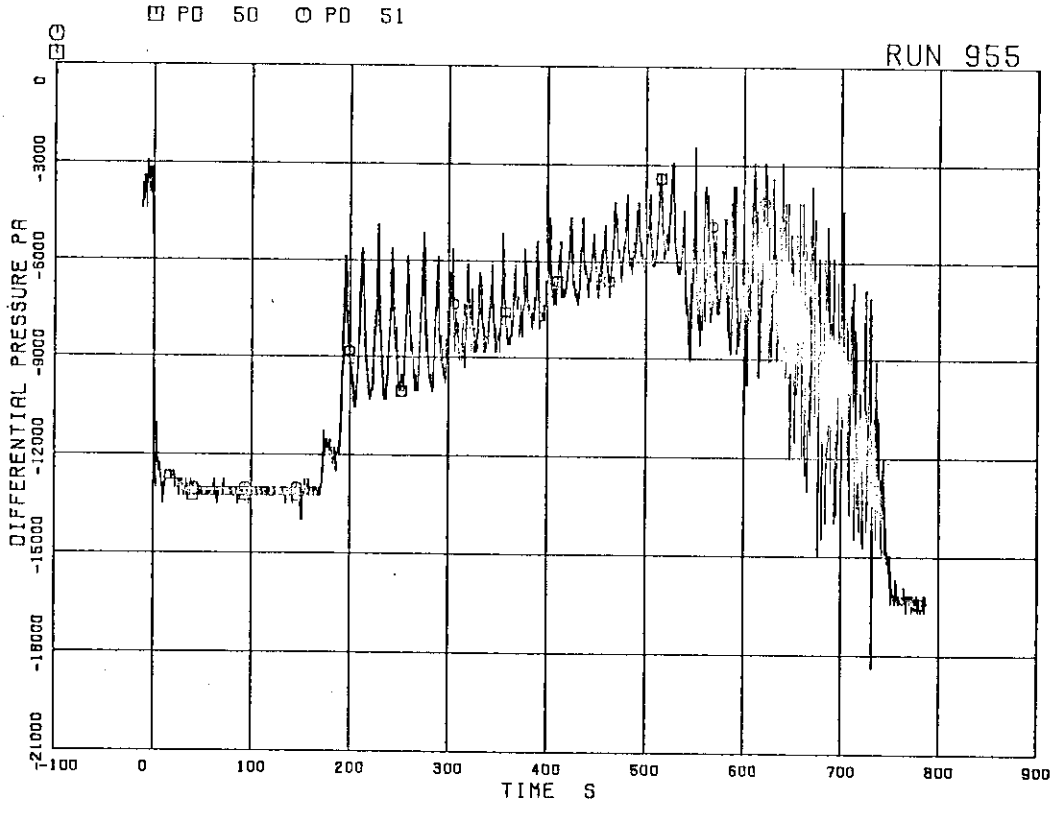

FIG.5. 16 DIFFERENTIAL PRESSURE BETWEEN JP-3,4 DISCHARGE AND CONFLURNCE

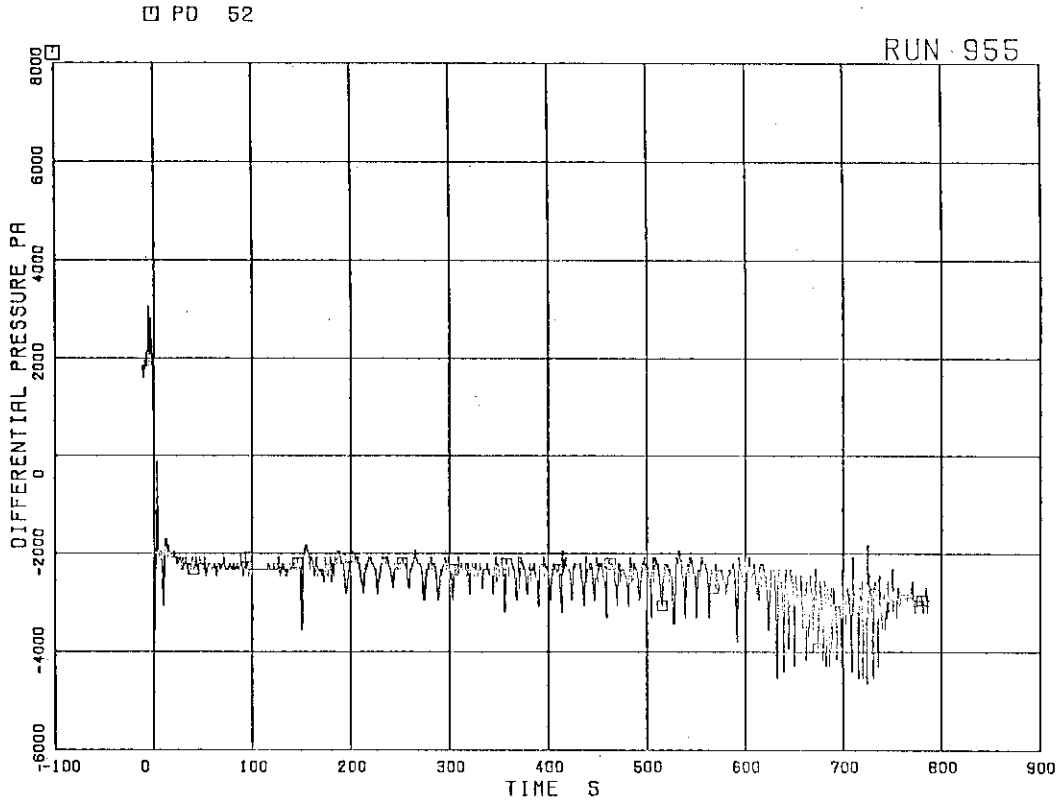

FIG.5. 17 DIFFERENTIAL PRESSURE BETWEEN CONFLUENCE IN BROKEN LOOP AND LP

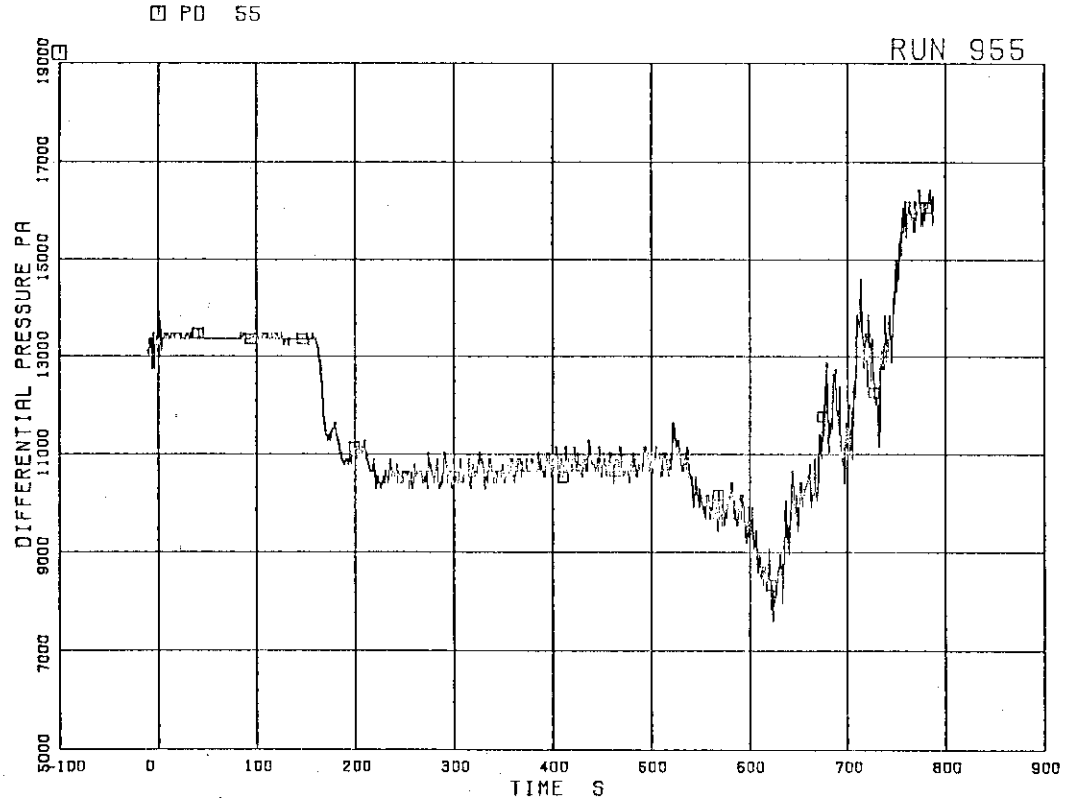

FIG.5. 18 DIFFERENTIAL PRESSURE BETWEEN DOWNCOMER BOTTOM AND DOWNCOMER MIDDLE

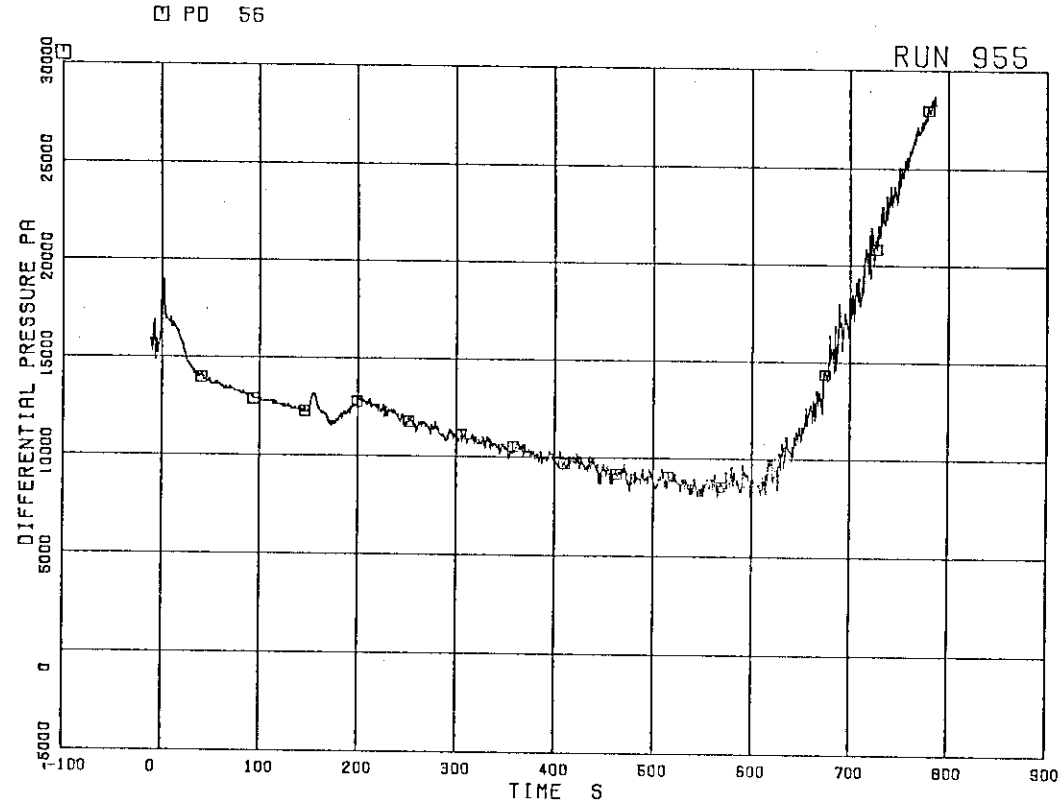

FIG.5. 19 DIFFERENTIAL PRESSURE BETWEEN DOWNCOMER MIDDLE AND STEAM DOME

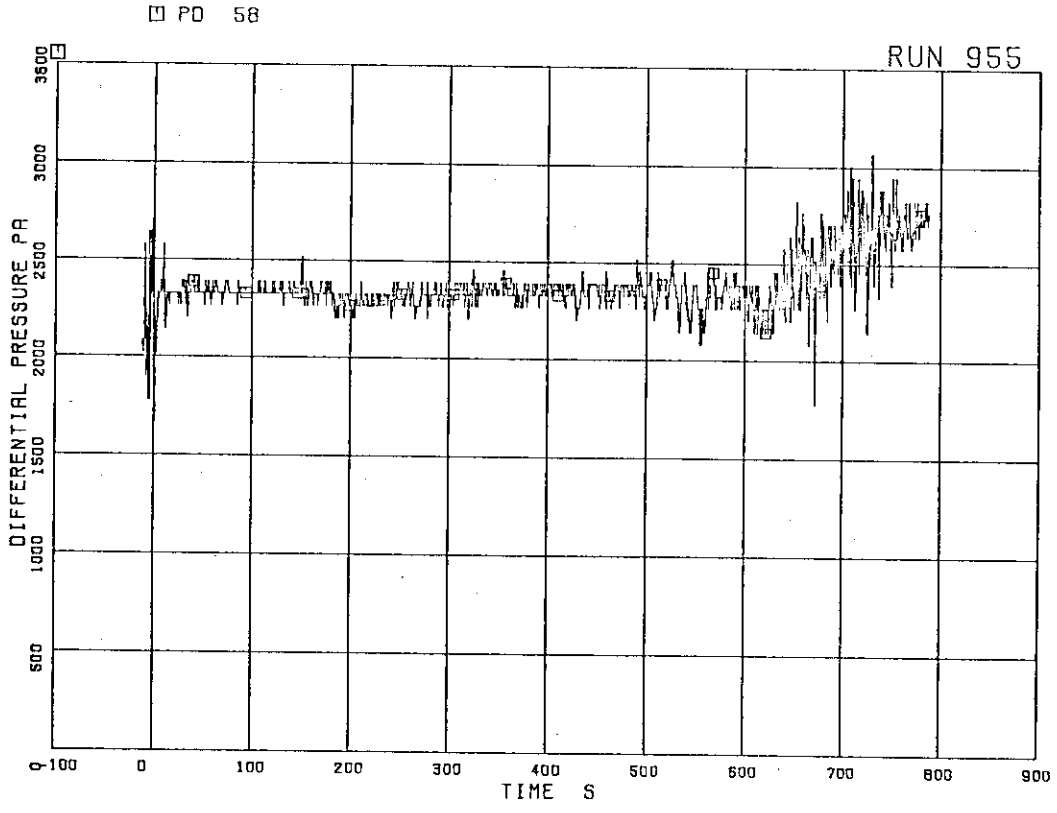

FIG.5. 20 DIFFERENTIAL PRESSURE BETWEEN LP BOTTOM AND LP MIDDLE

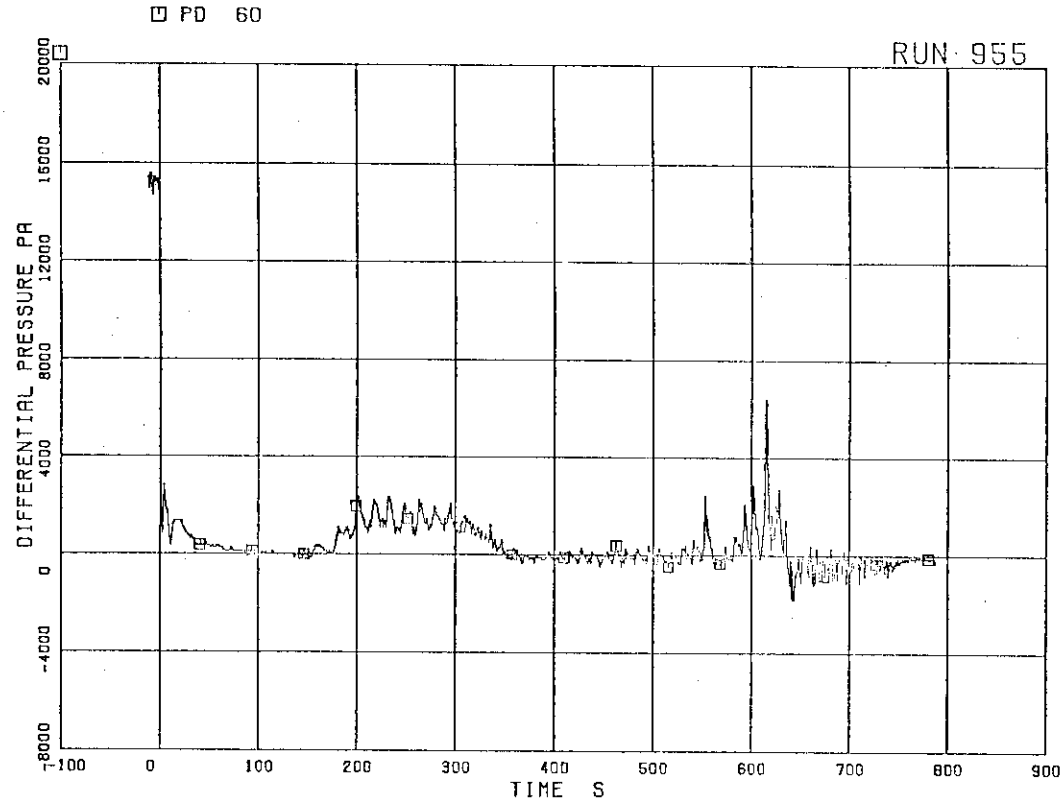

FIG.5. 21 DIFFERENTIAL PRESSURE ACROSS CHANNEL INLET ORIFICE A

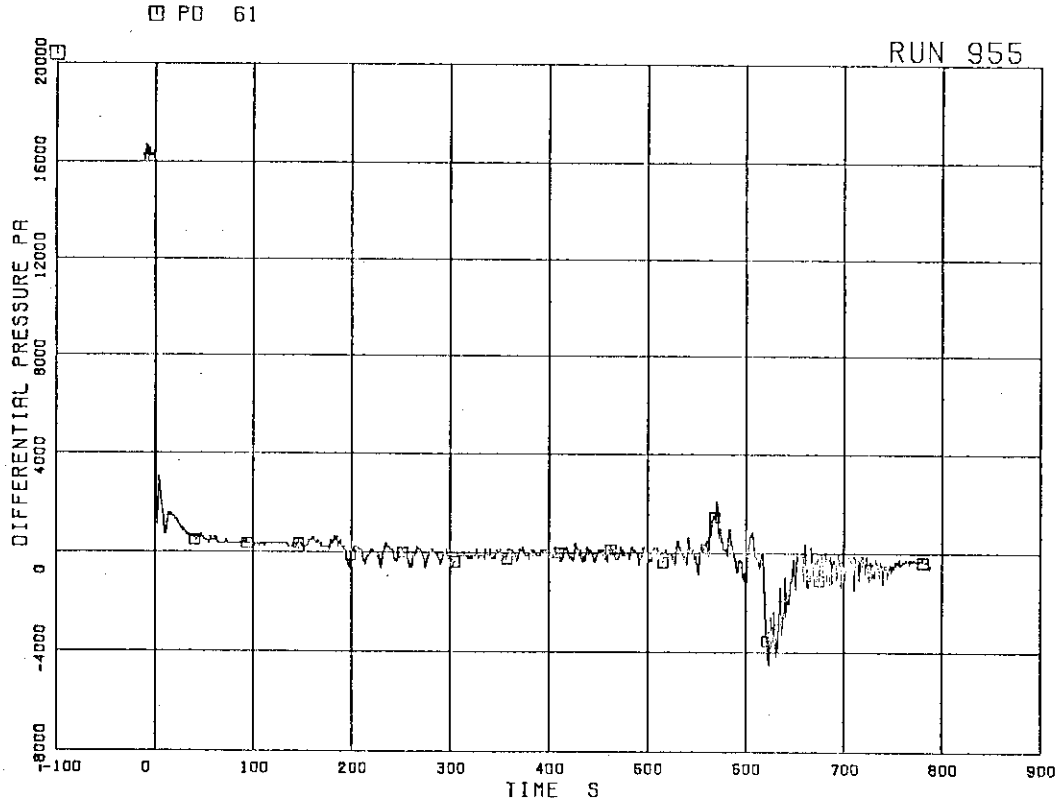

FIG.5. 22 DIFFERENTIAL PRESSURE ACROSS CHANNEL INLET ORIFICE B

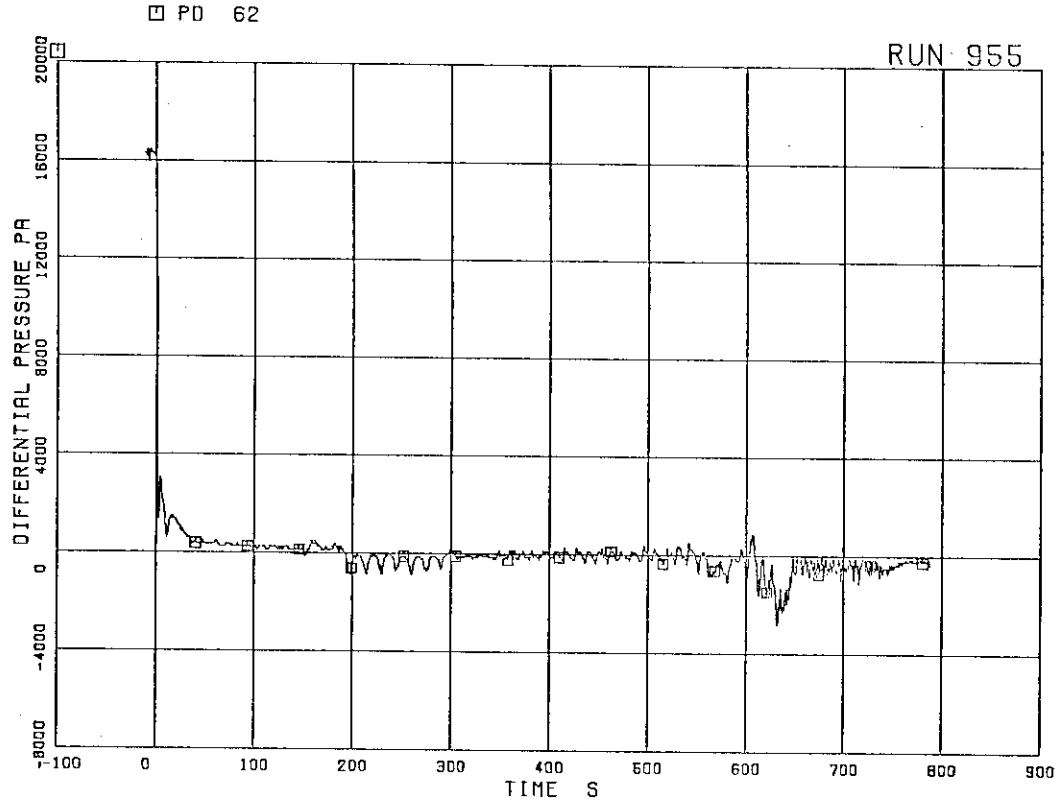

FIG.5. 23 DIFFERENTIAL PRESSURE ACROSS CHANNEL INLET ORIFICE C

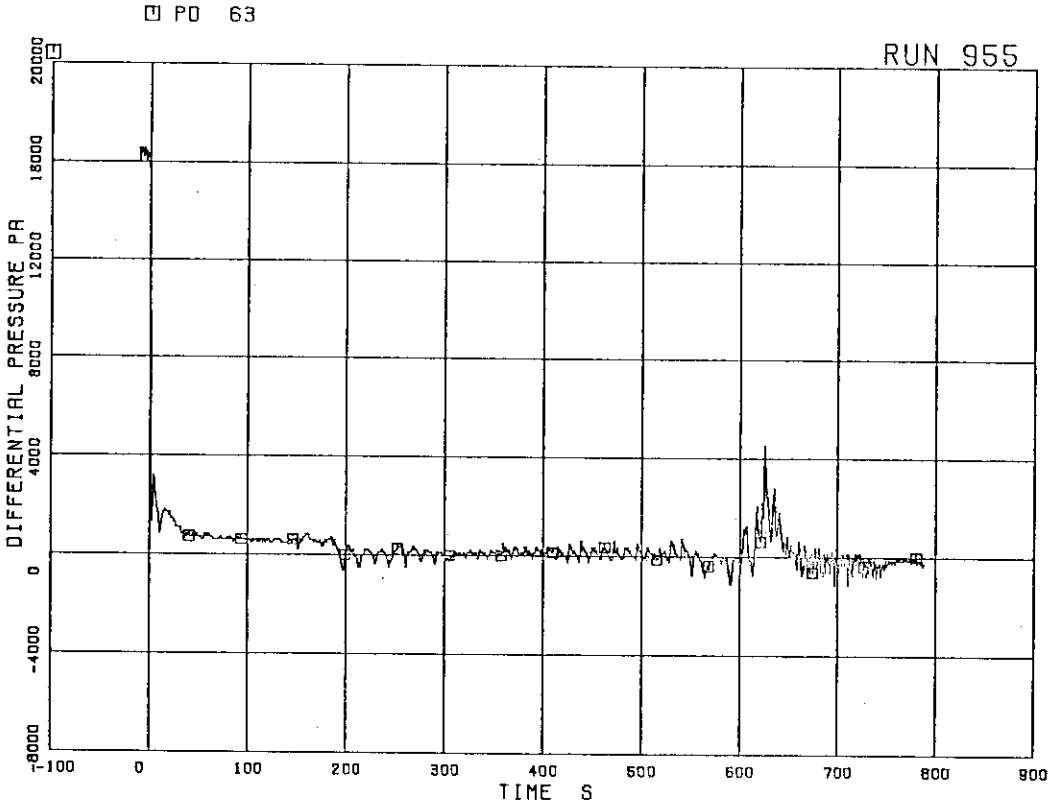

FIG.5. 24 DIFFERENTIAL PRESSURE ACROSS CHANNEL INLET ORIFICE D

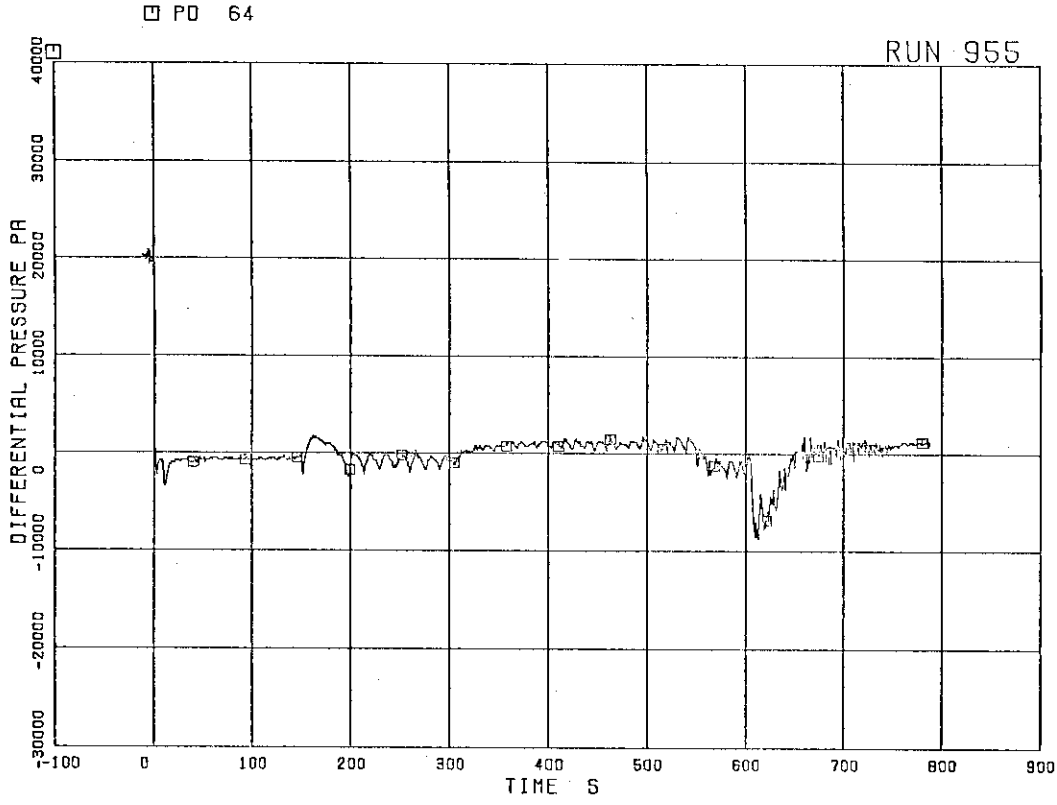

FIG.5. 25 DIFFERENTIAL PRESSURE ACROSS BYPASS HOLE

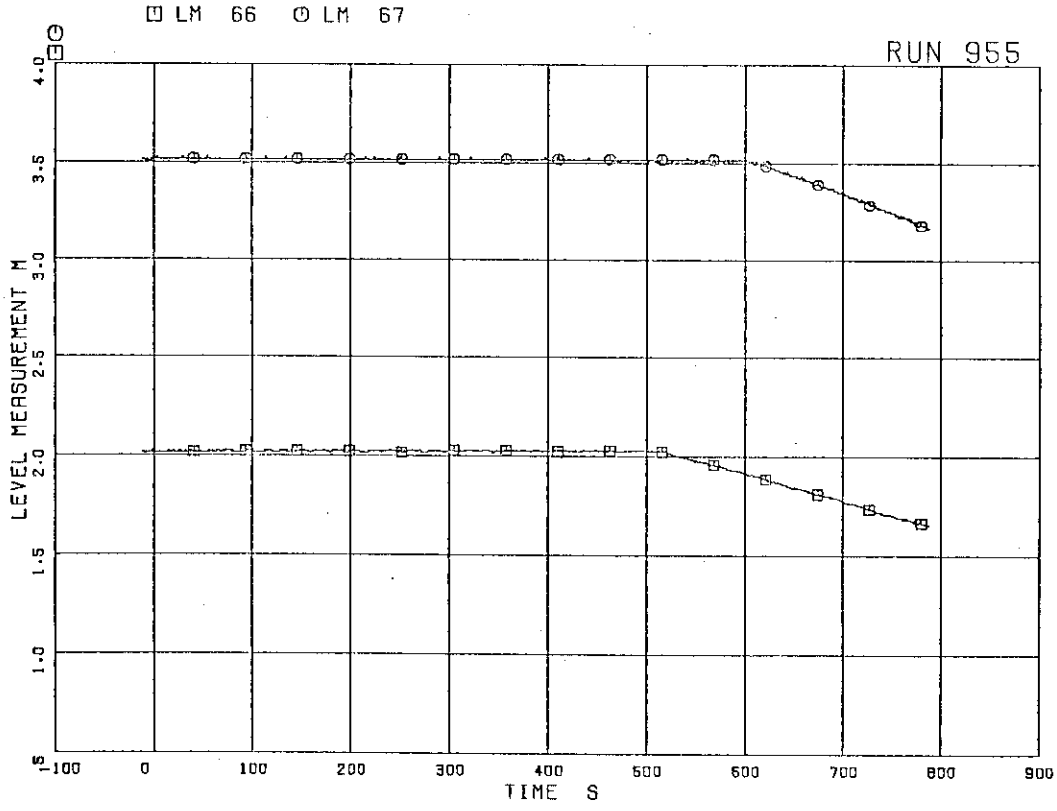

FIG.5. 26 LIQUID LEVELS IN ECCS TANKS

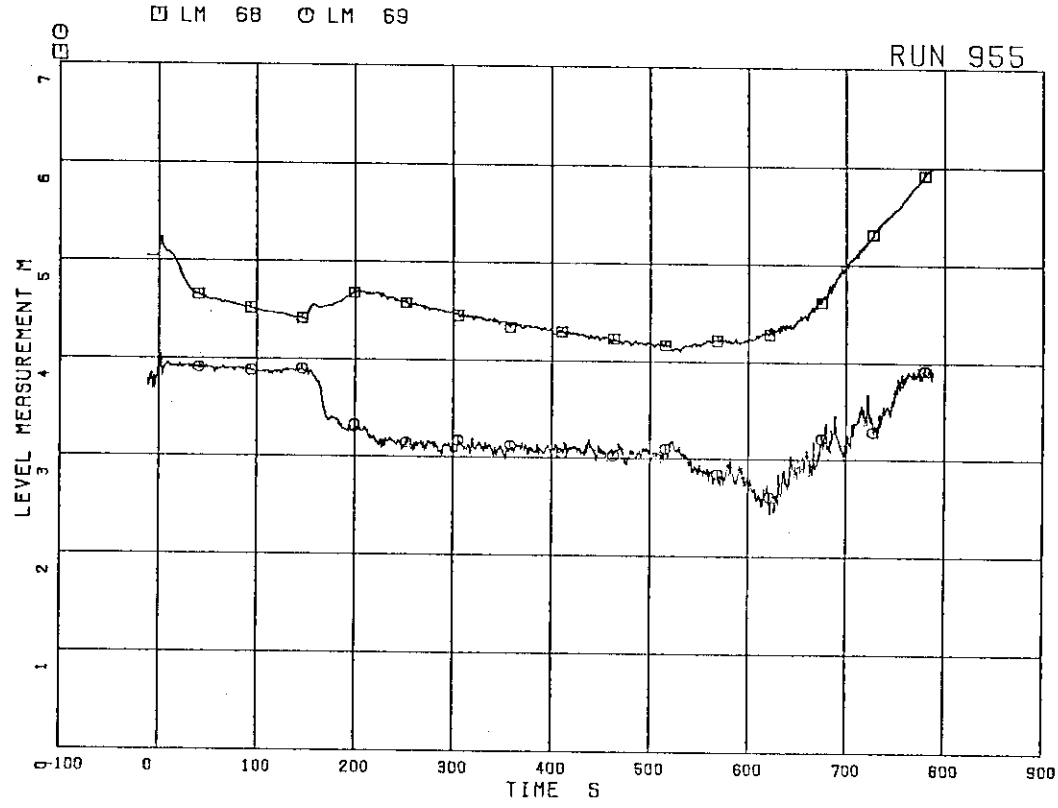

FIG.5. 27 LIQUID LEVEL IN DOWNCOMER

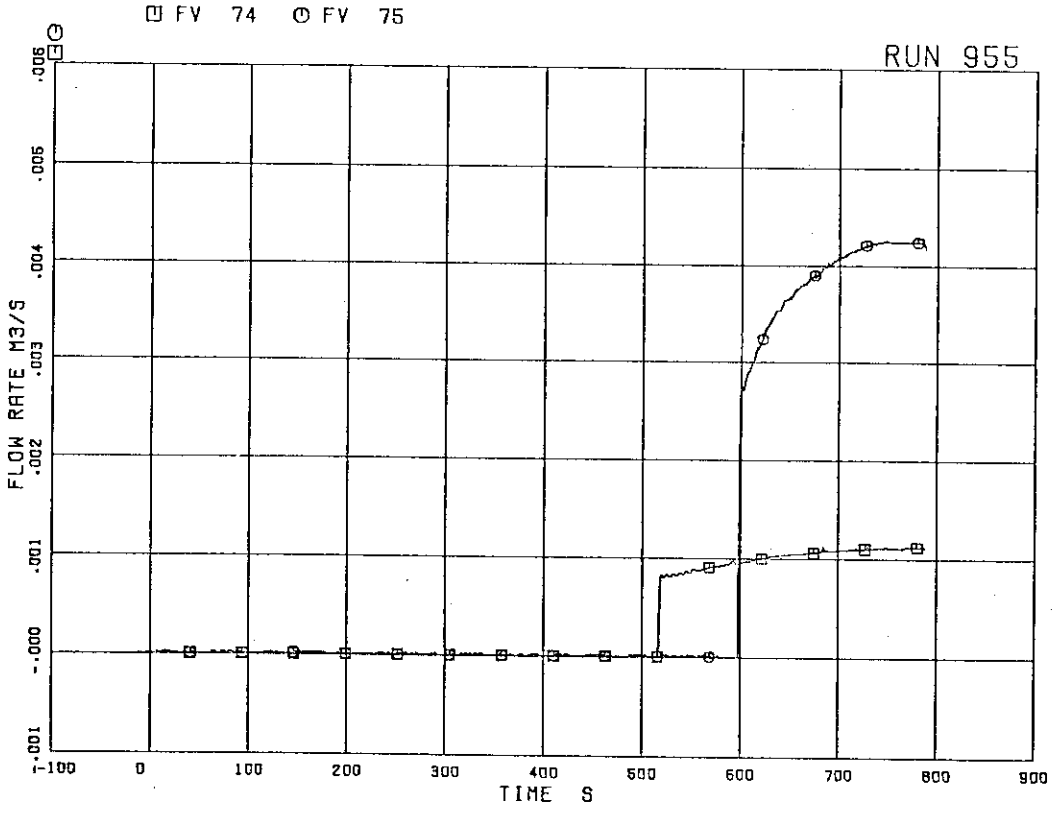

FIG.5. 28 ECC INJECTION FLOW RATES

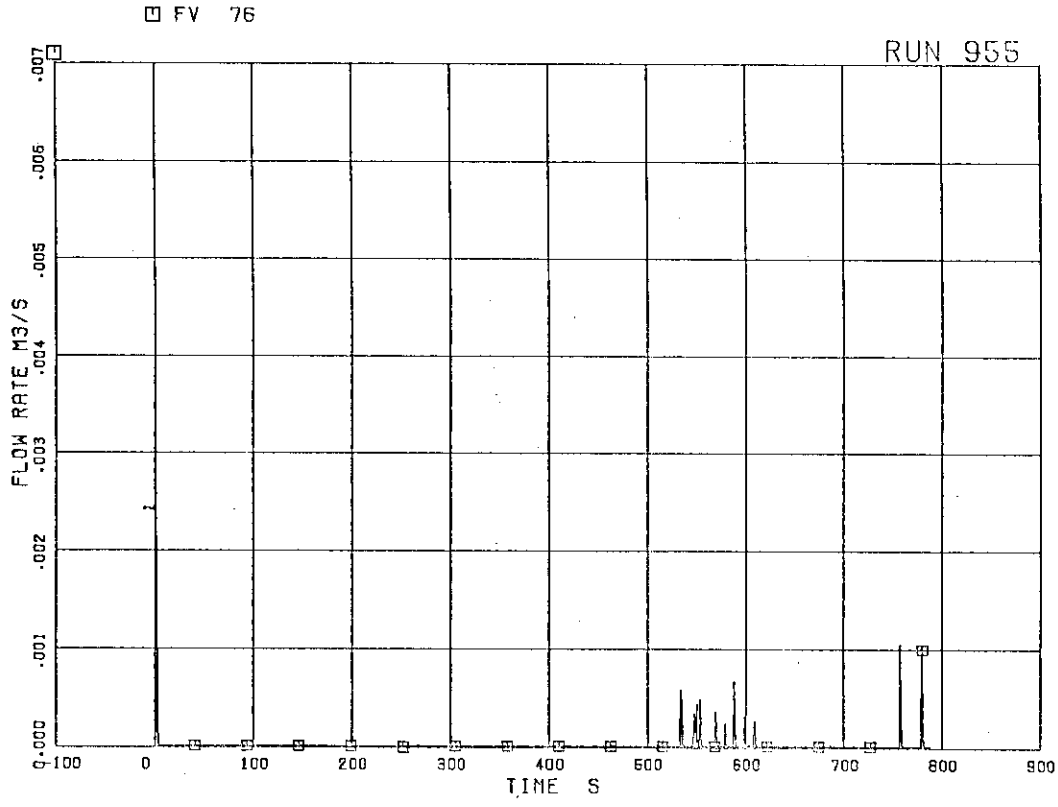

FIG.5. 29 FEEDWATER FLOW RATE

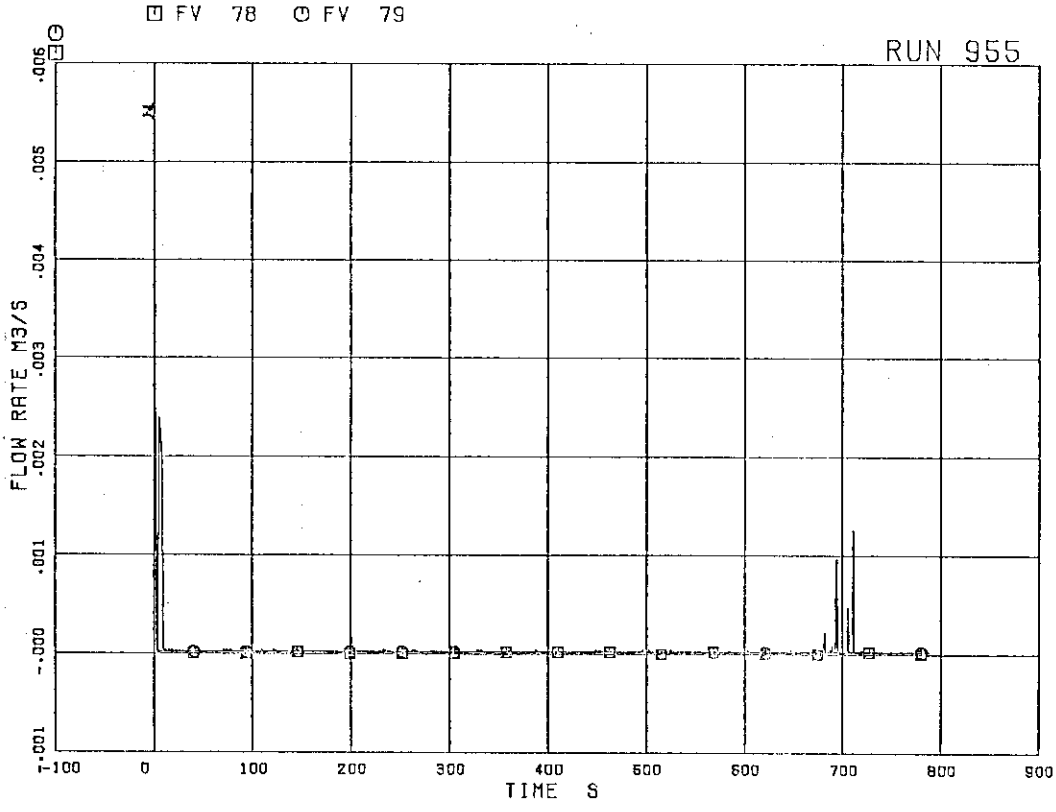

FIG.5. 30 JP-1,2 DISCHARGE FLOW RATES

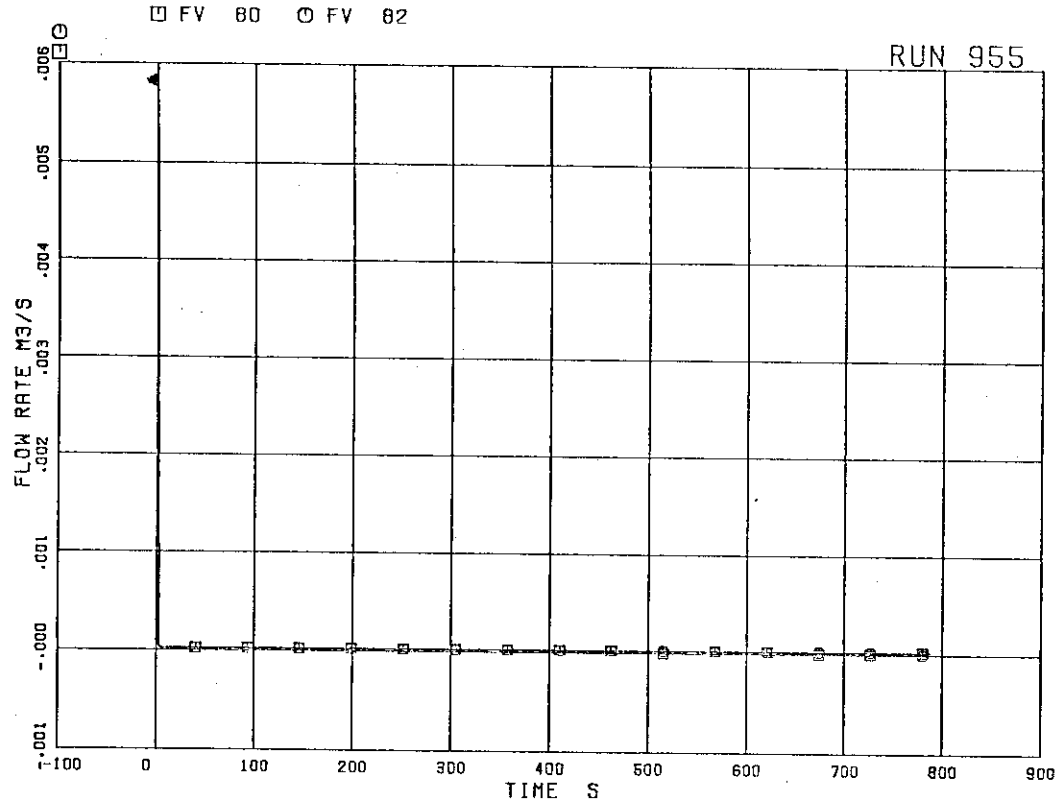

FIG.5. 31 JP-3.4 DISCHARGE FLOW RATES (HIGH RANGE)

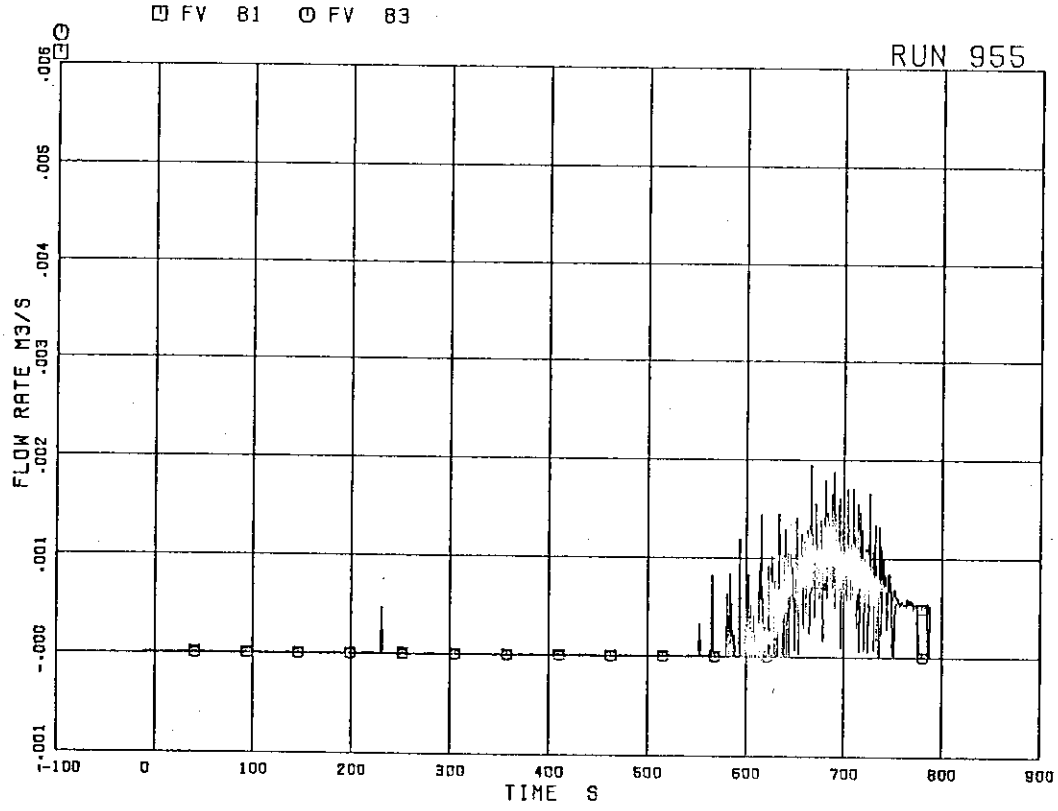

FIG.5. 32 JP-3.4 DISCHARGE FLOW RATES (LOW RANGE)

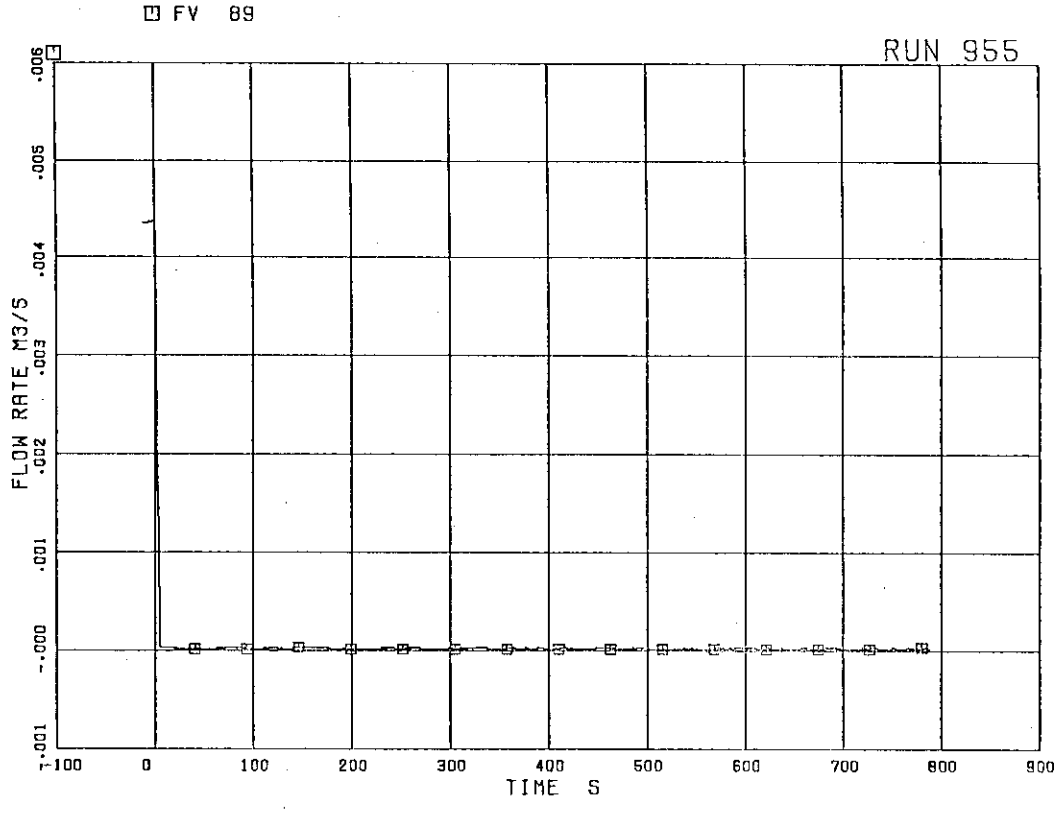

FIG.5. 33 MRP DISCHARGE FLOW RATE

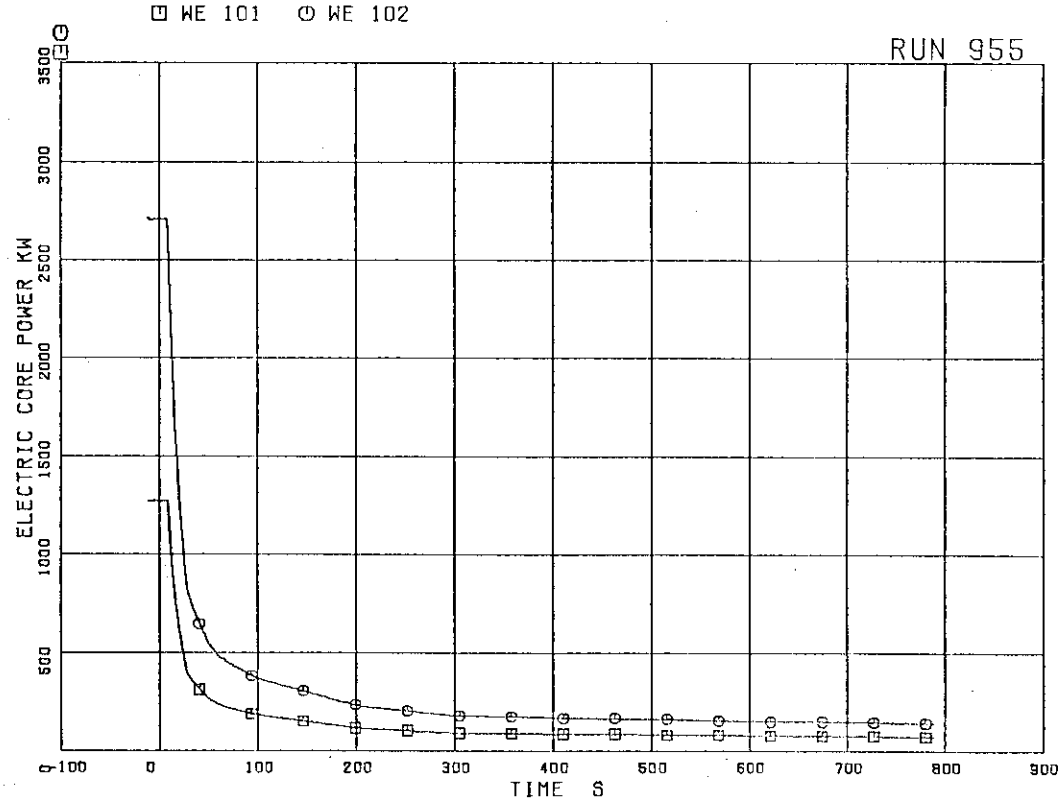

FIG.5. 34 ELECTRIC CORE POWER

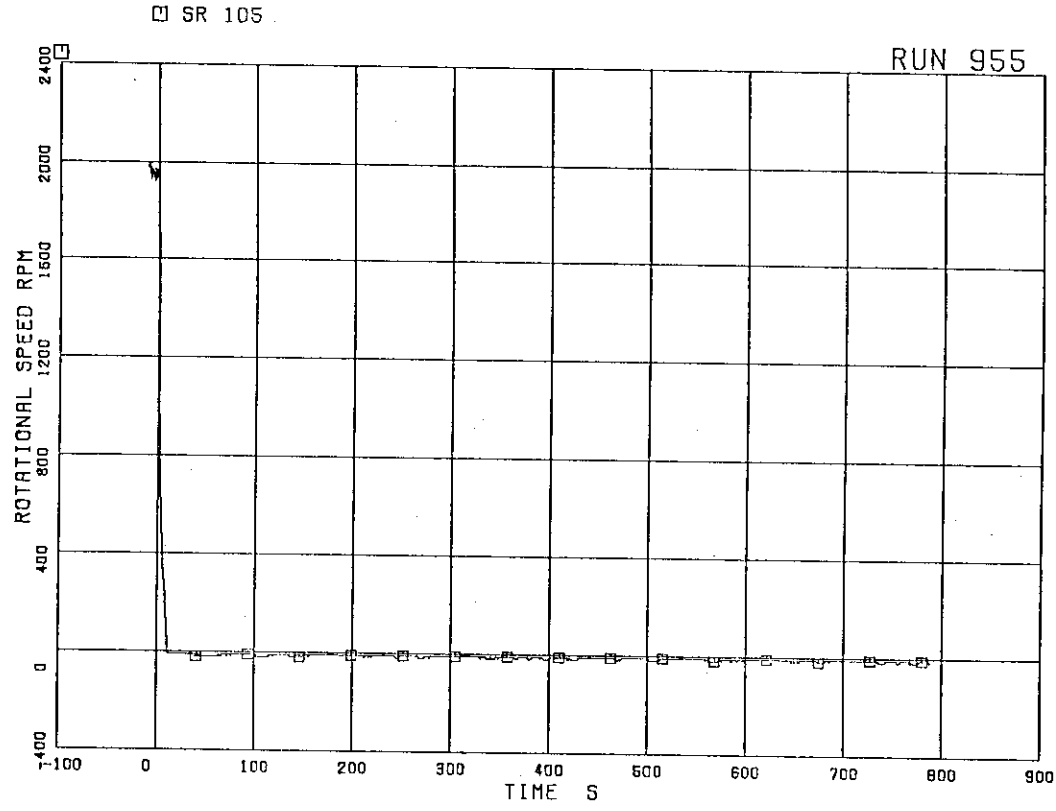

FIG.5. 35 MRP PUMP SPEED

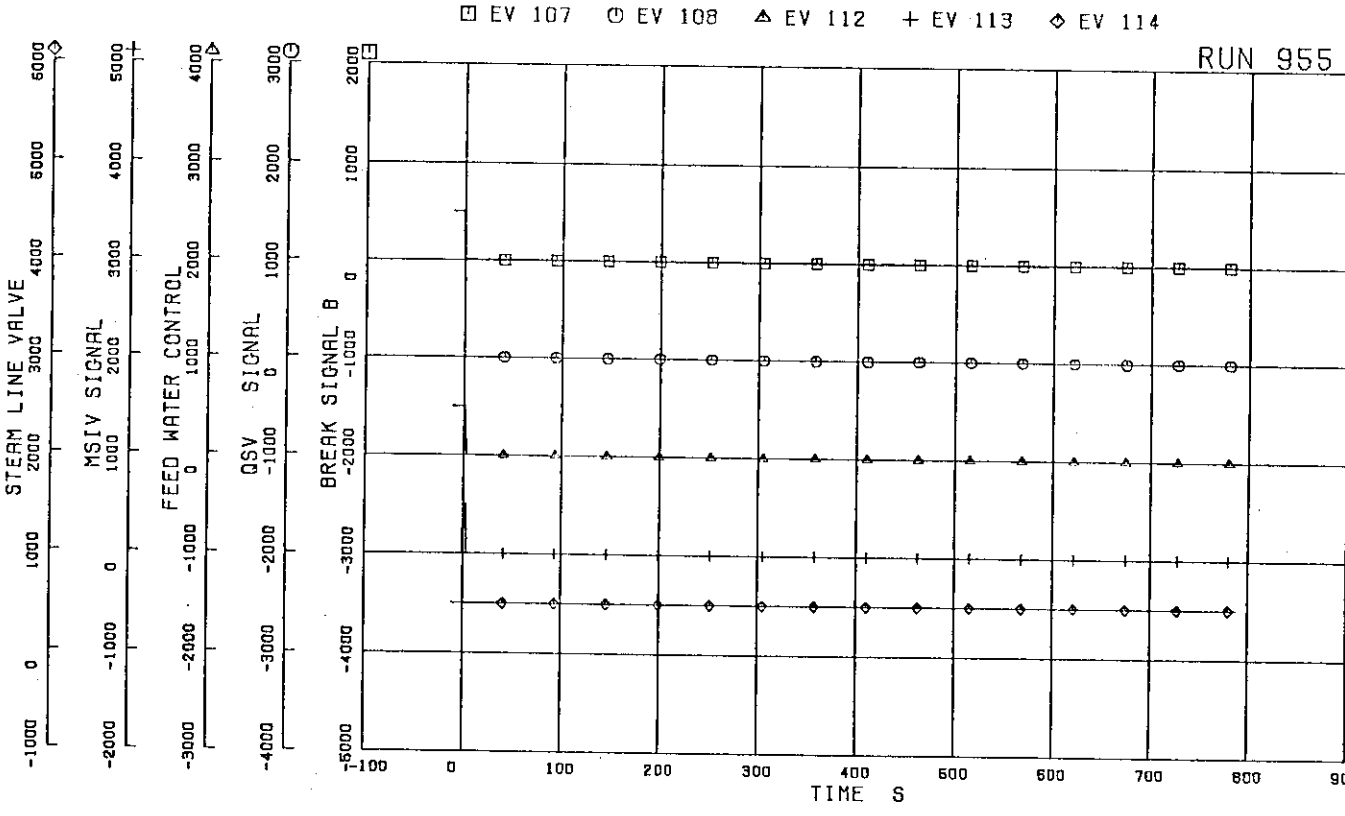

FIG.5. 36 VALVE OPERATION SIGNALS

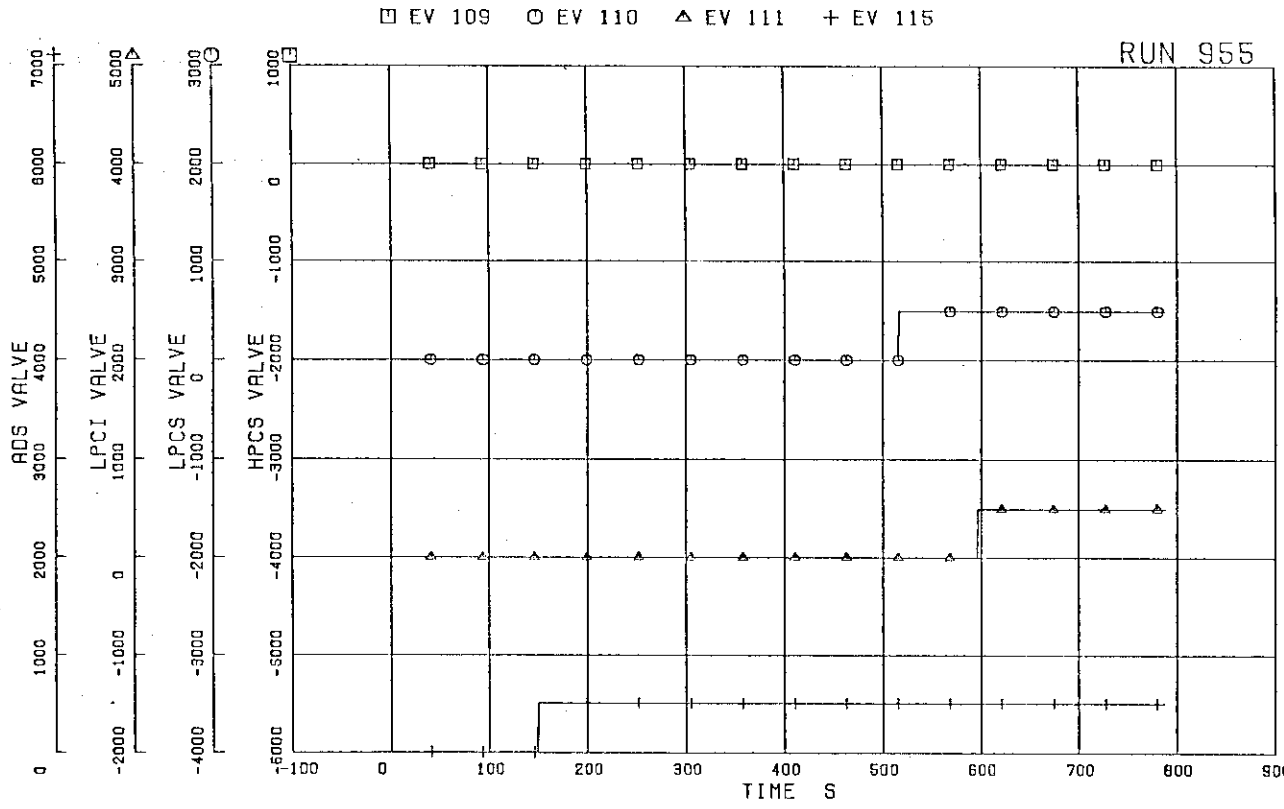

FIG.5. 37 ECCS OPERATION SIGNALS

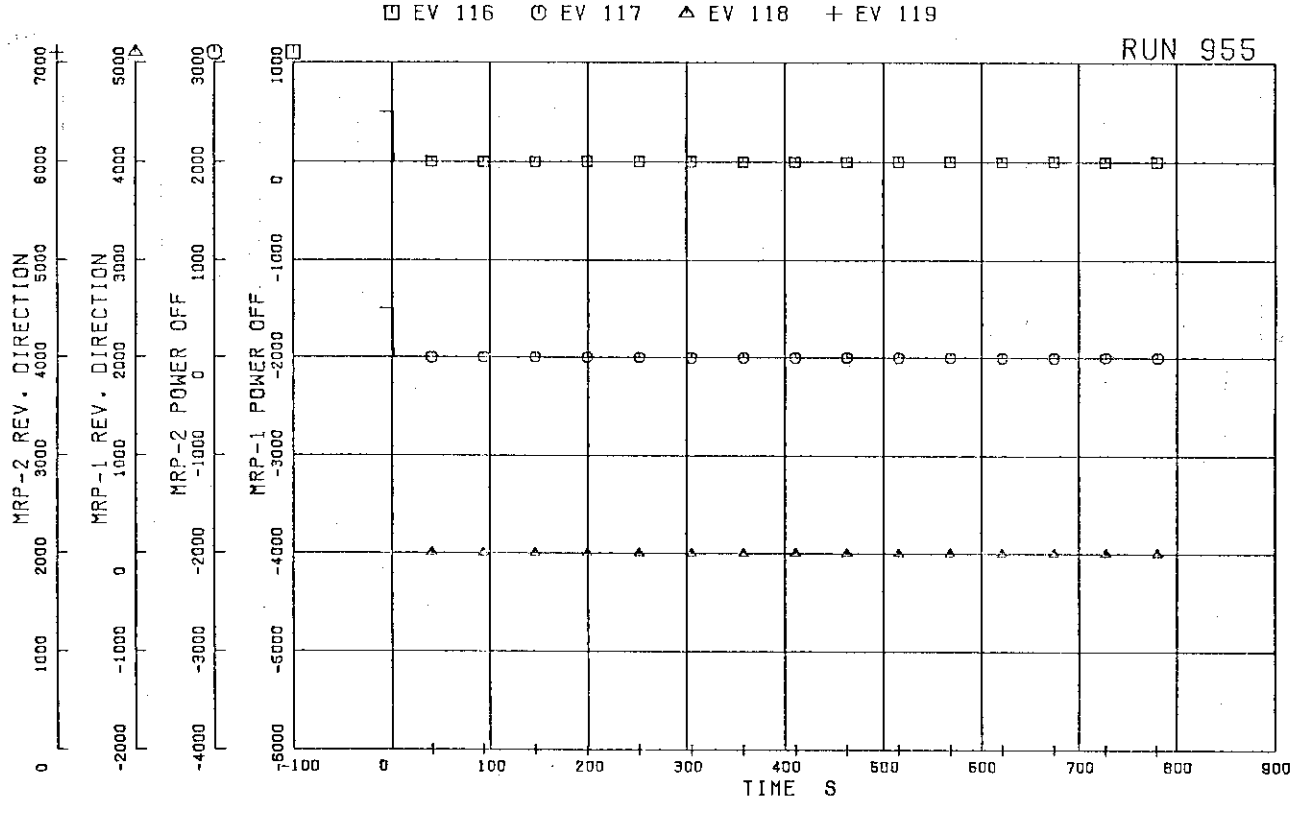

FIG.5. 38 MRP OPERATION SIGNALS

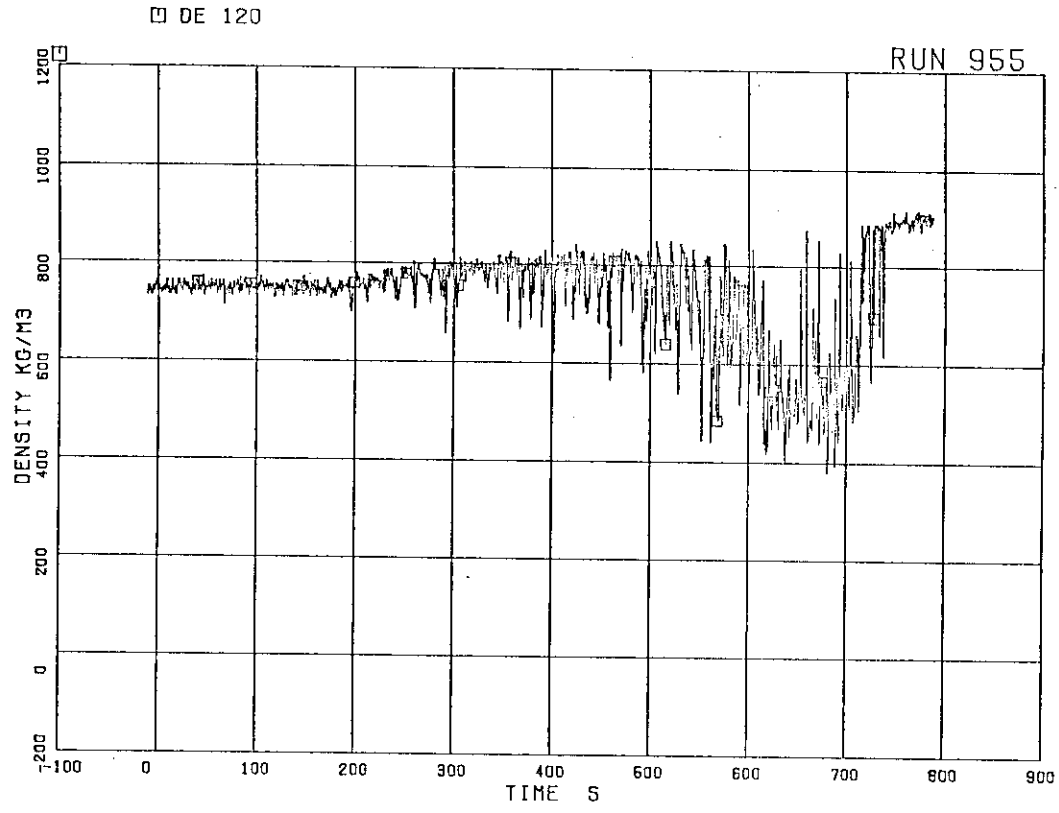

FIG.5. 39 FLUID DENSITY AT JP-1.2 OUTLET, BEAM A

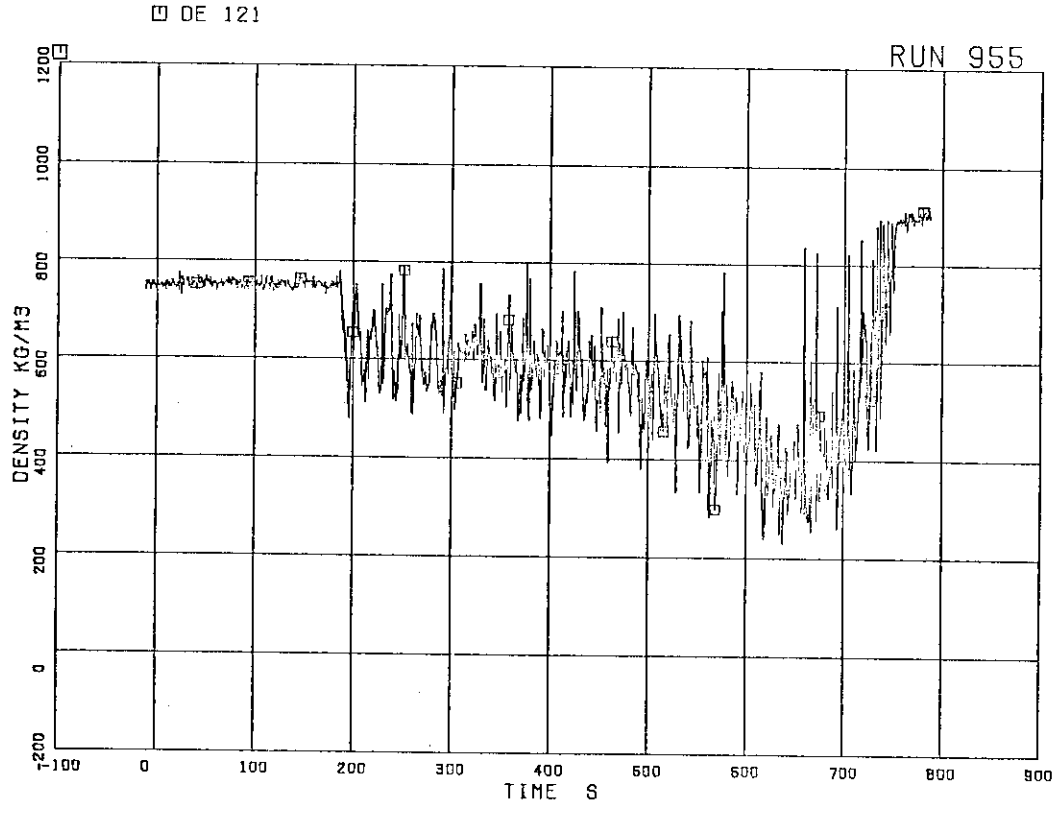

FIG.5. 40 FLUID DENSITY AT JP-1.2 OUTLET, BEAM B

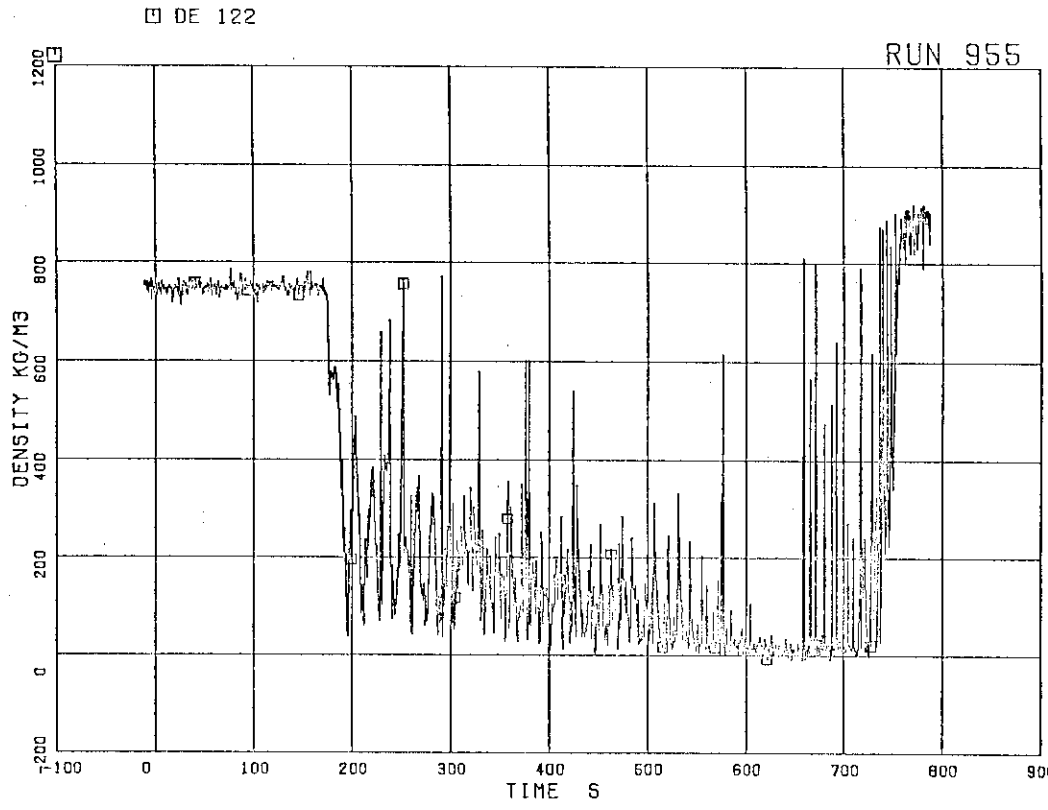

FIG.5. 41 FLUID DENSITY AT JP-1,2 OUTLET, BEAM C

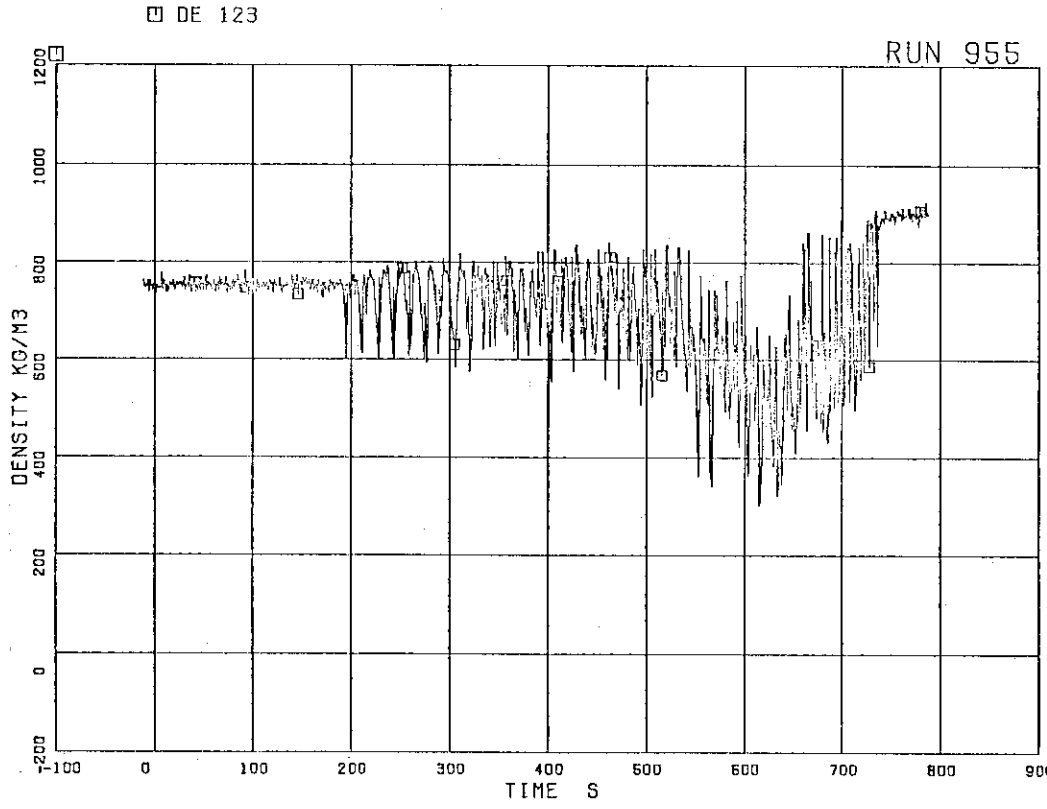

FIG.5. 42 FLUID DENSITY AT JP-3,4 OUTLET, BEAM A

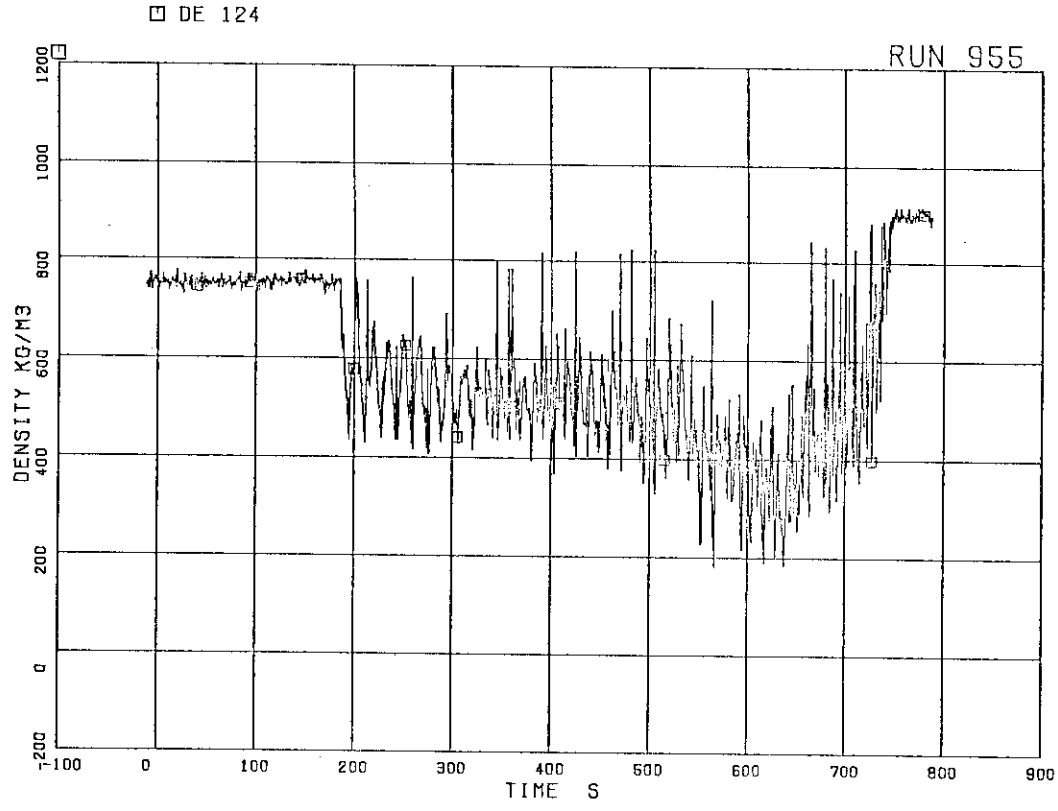

FIG.5. 43 FLUID DENSITY AT JP-3,4 OUTLET, BEAM B

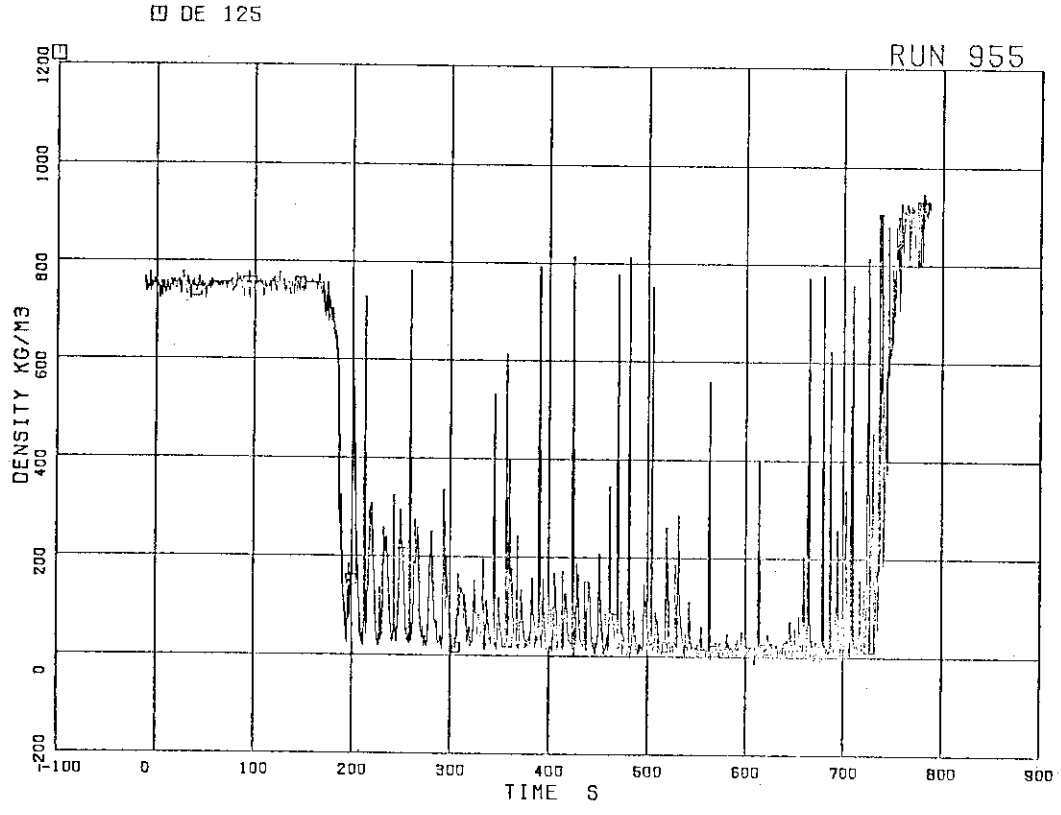

FIG.5. 44 FLUID DENSITY AT JP-3,4 OUTLET, BEAM C

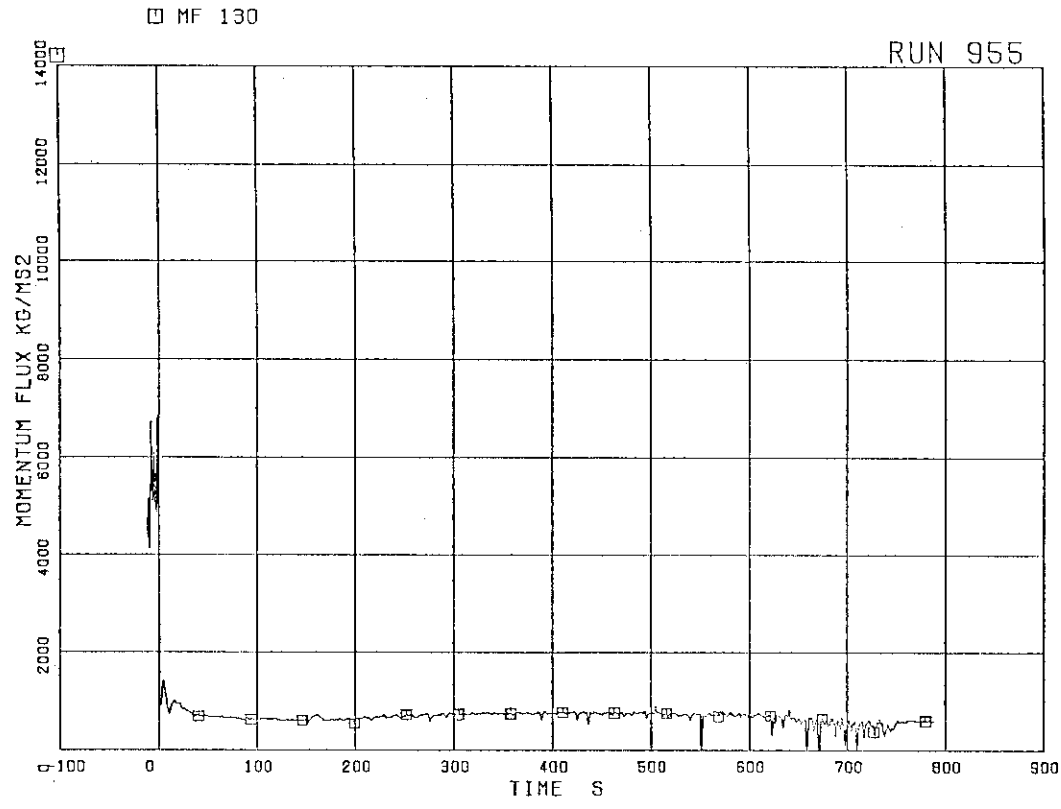

FIG.5. 45 MOMENTUM FLUX AT JP-1,2 OUTLET SPOOL

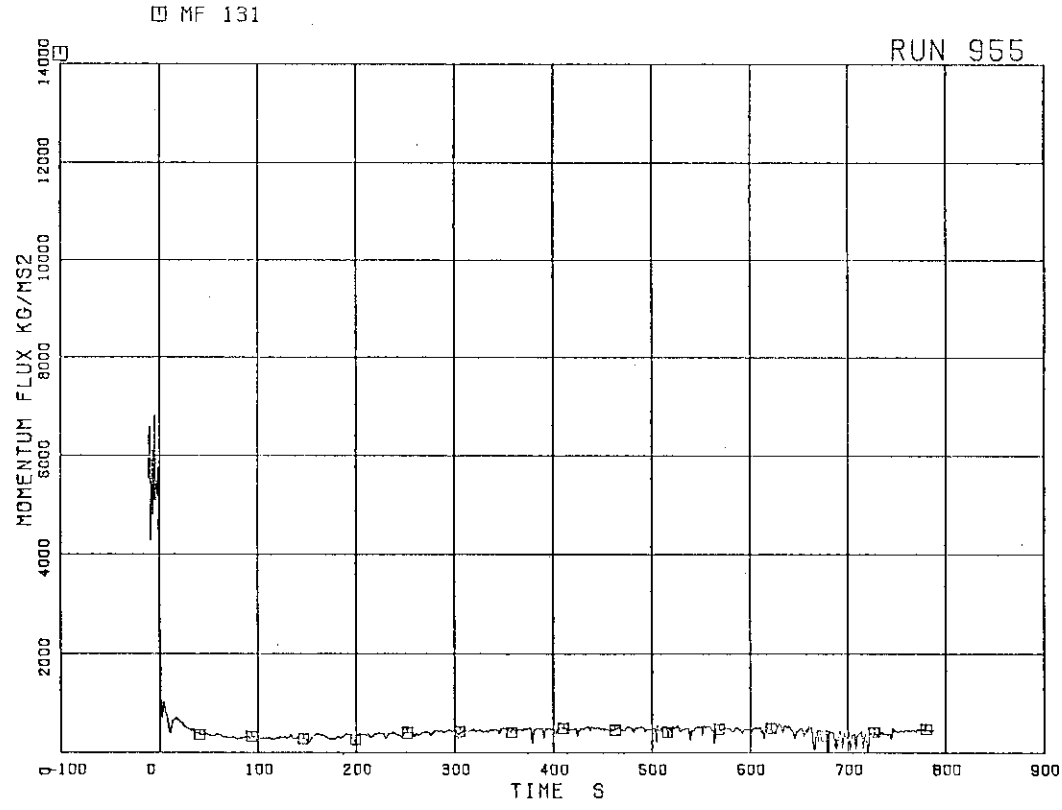

FIG.5. 46 MOMENTUM FLUX AT JP-3,4 OUTLET SPOOL

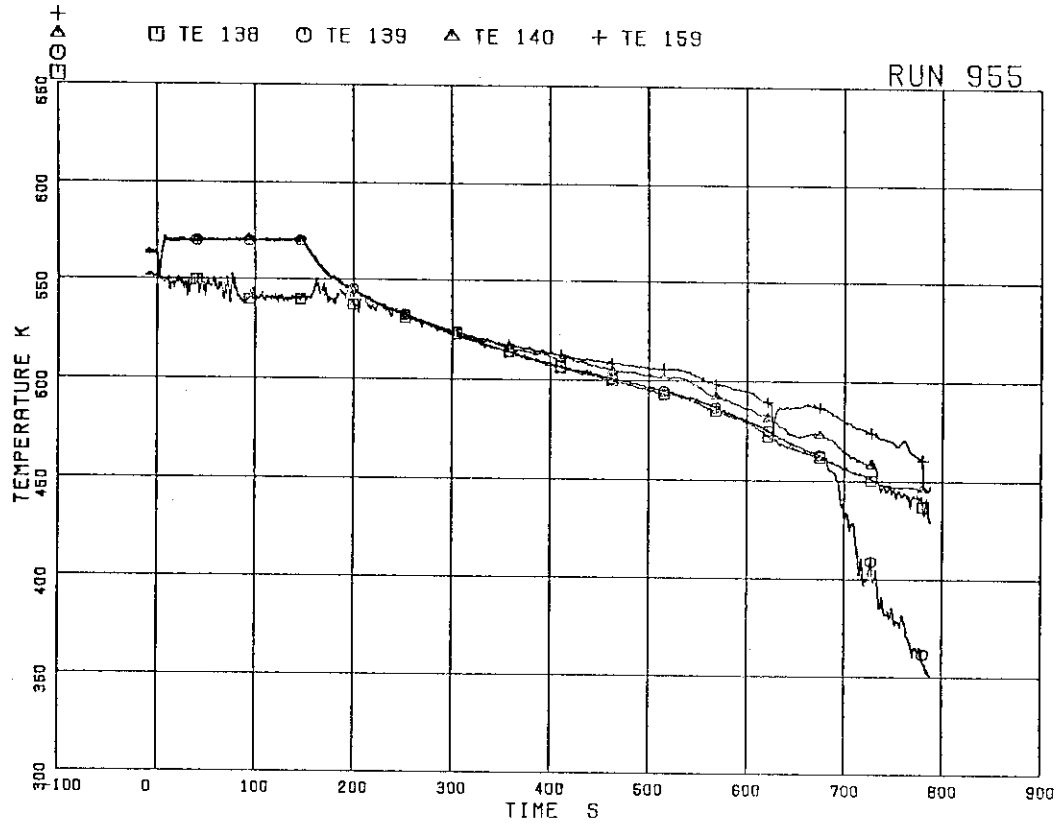

FIG.5. 47 FLUID TEMPERATURES IN PV AND MSL

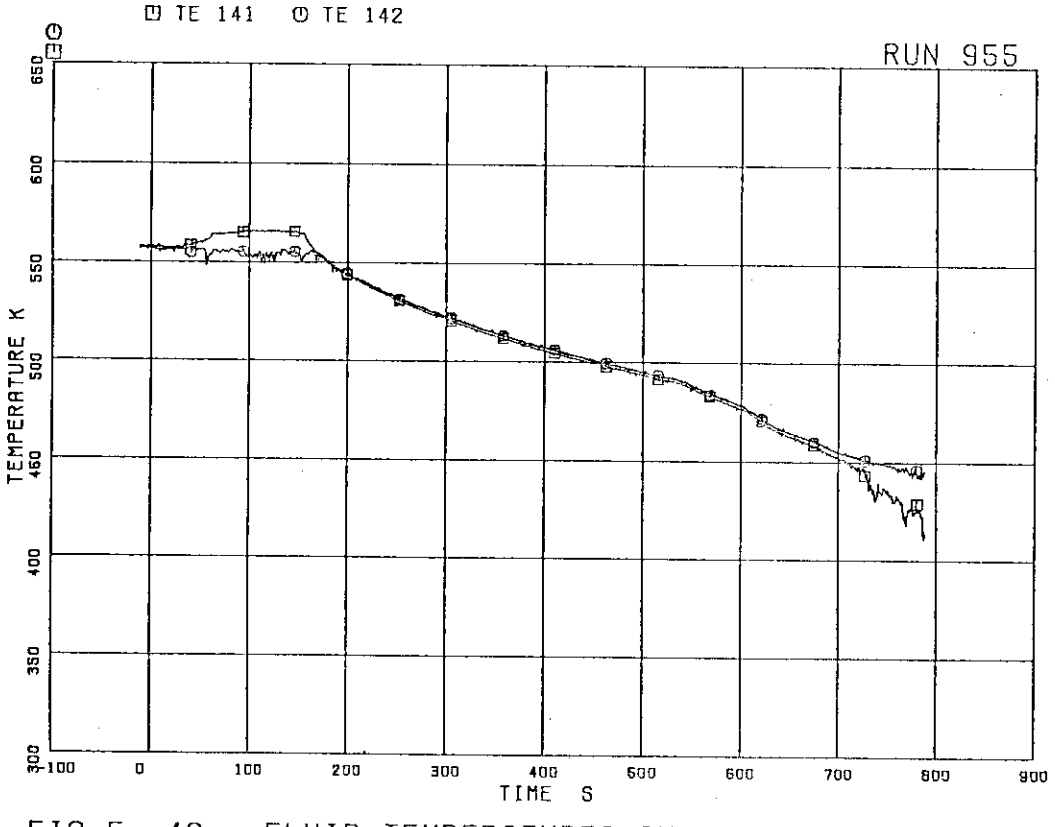

FIG.5. 48 FLUID TEMPERATURES IN DOWNCOMER

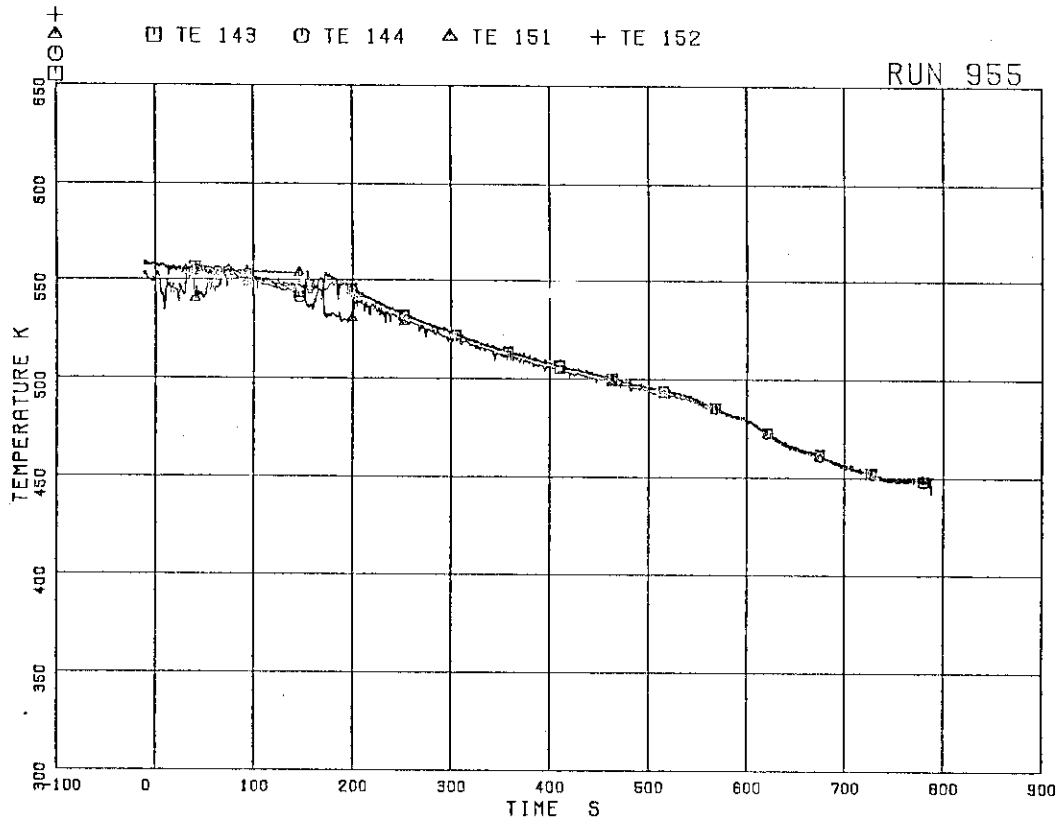

FIG.5. 49 FLUID TEMPERATURES IN INTACT RECIRCULATION LOOP

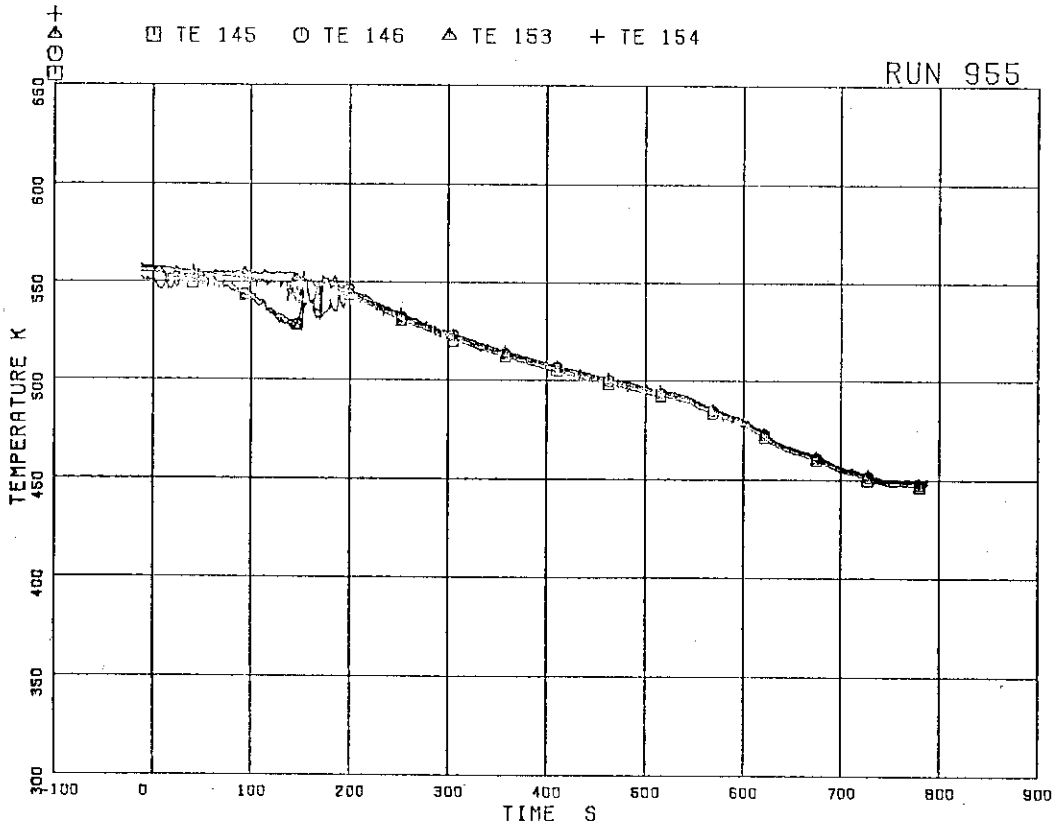

FIG.5. 50 FLUID TEMPERATURES IN BROKEN RECIRCULATION LOOP

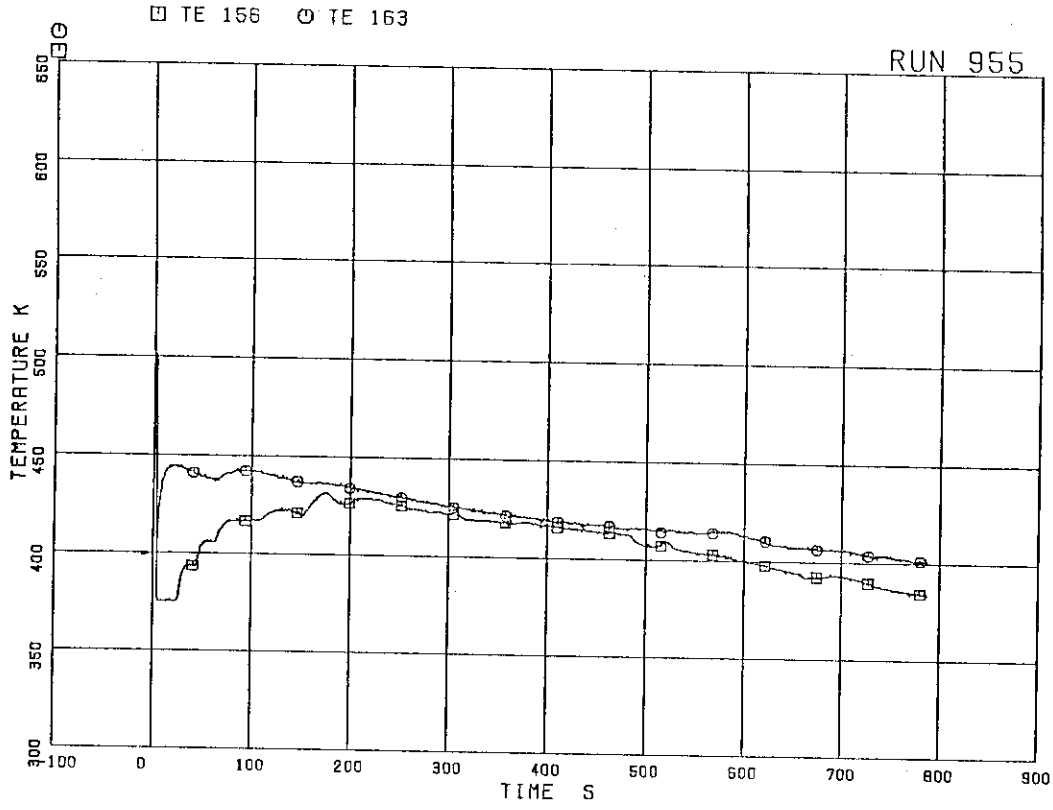

FIG.5. 51 FLUID TEMPERATURES NEAR BREAK B

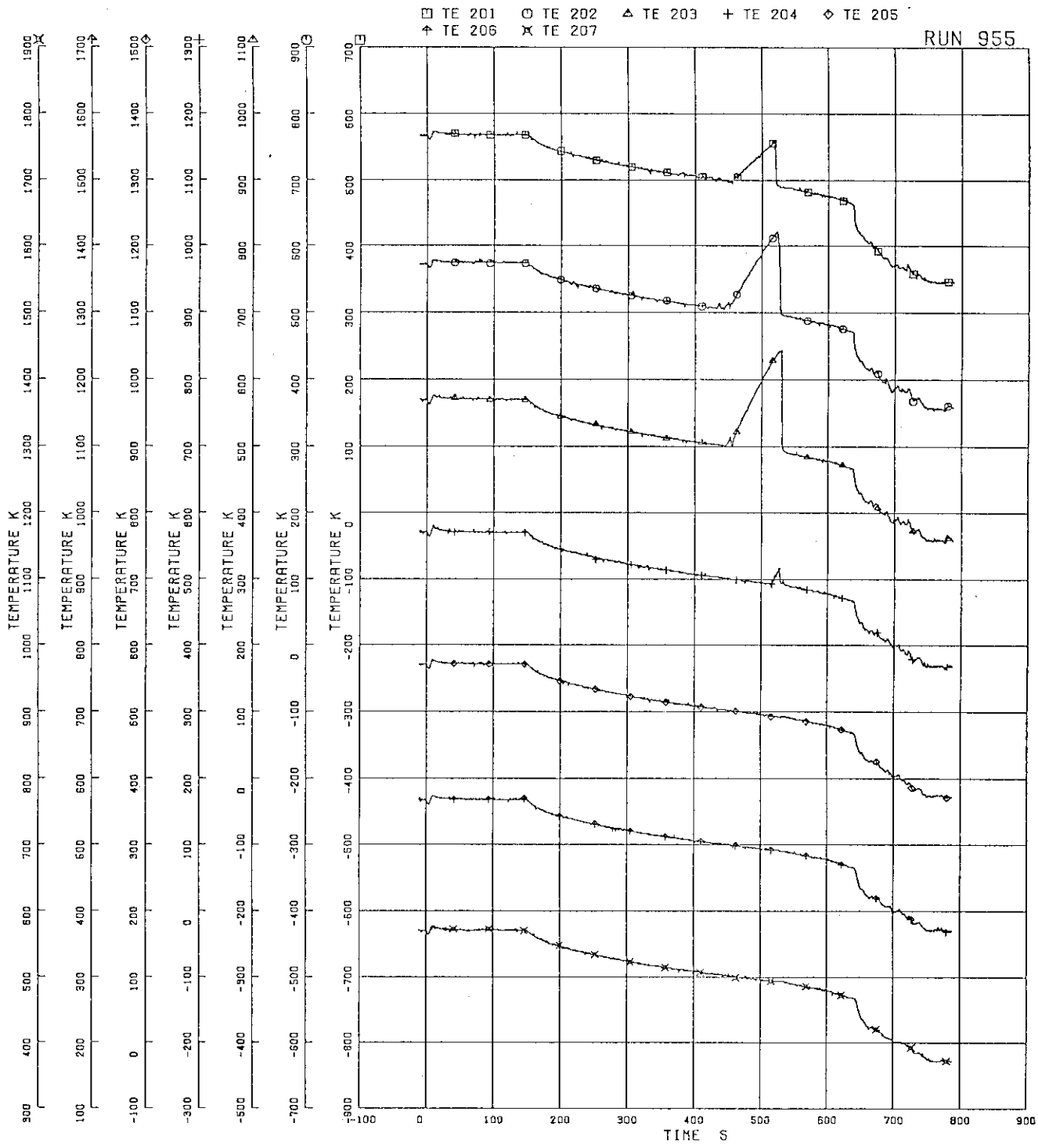

FIG.5. 52 FUEL ROD SURFACE TEMPERATURES OF A11 ROD

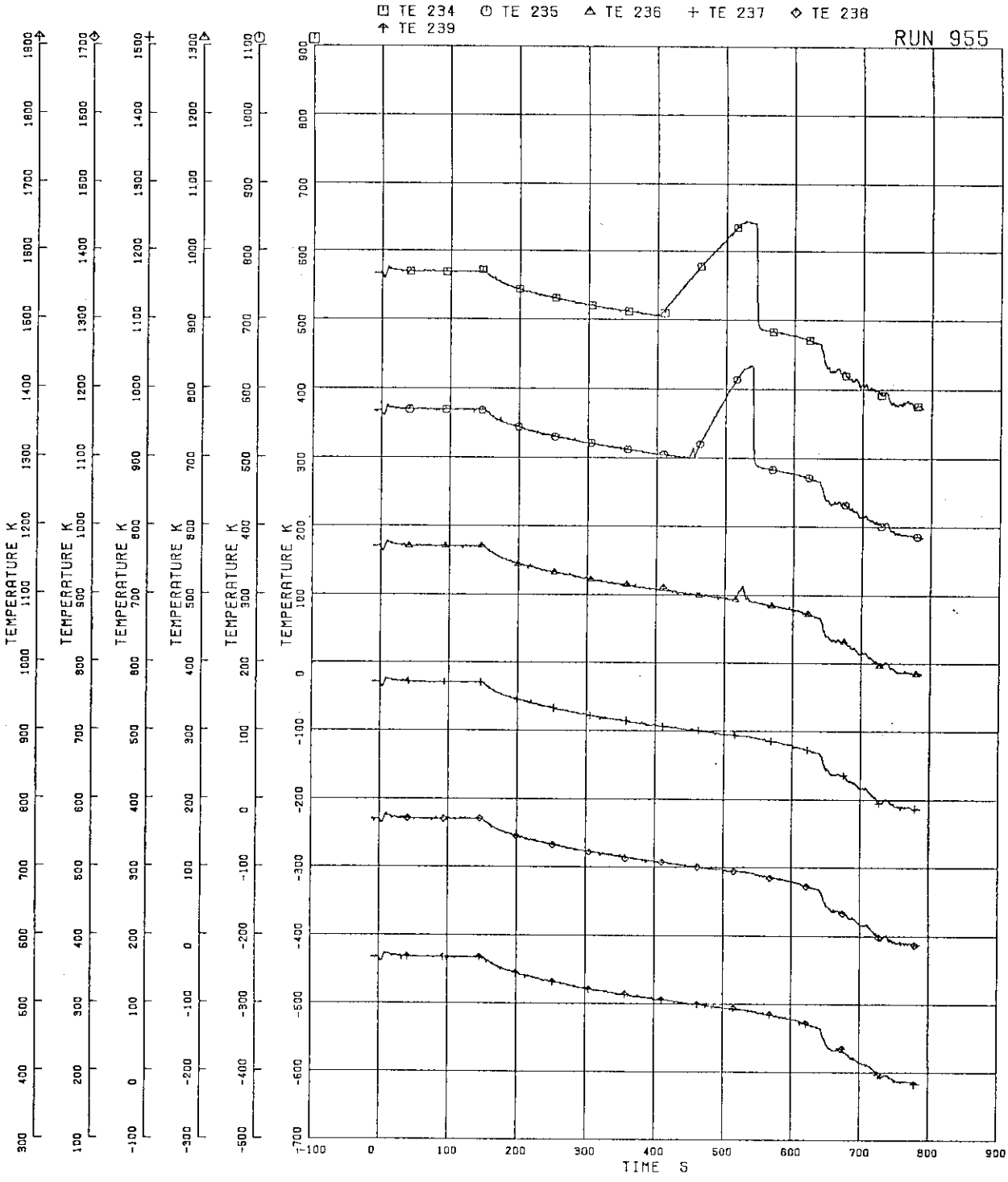

FIG.5. 53 FUEL ROD SURFACE TEMPERATURES OF A22 ROD

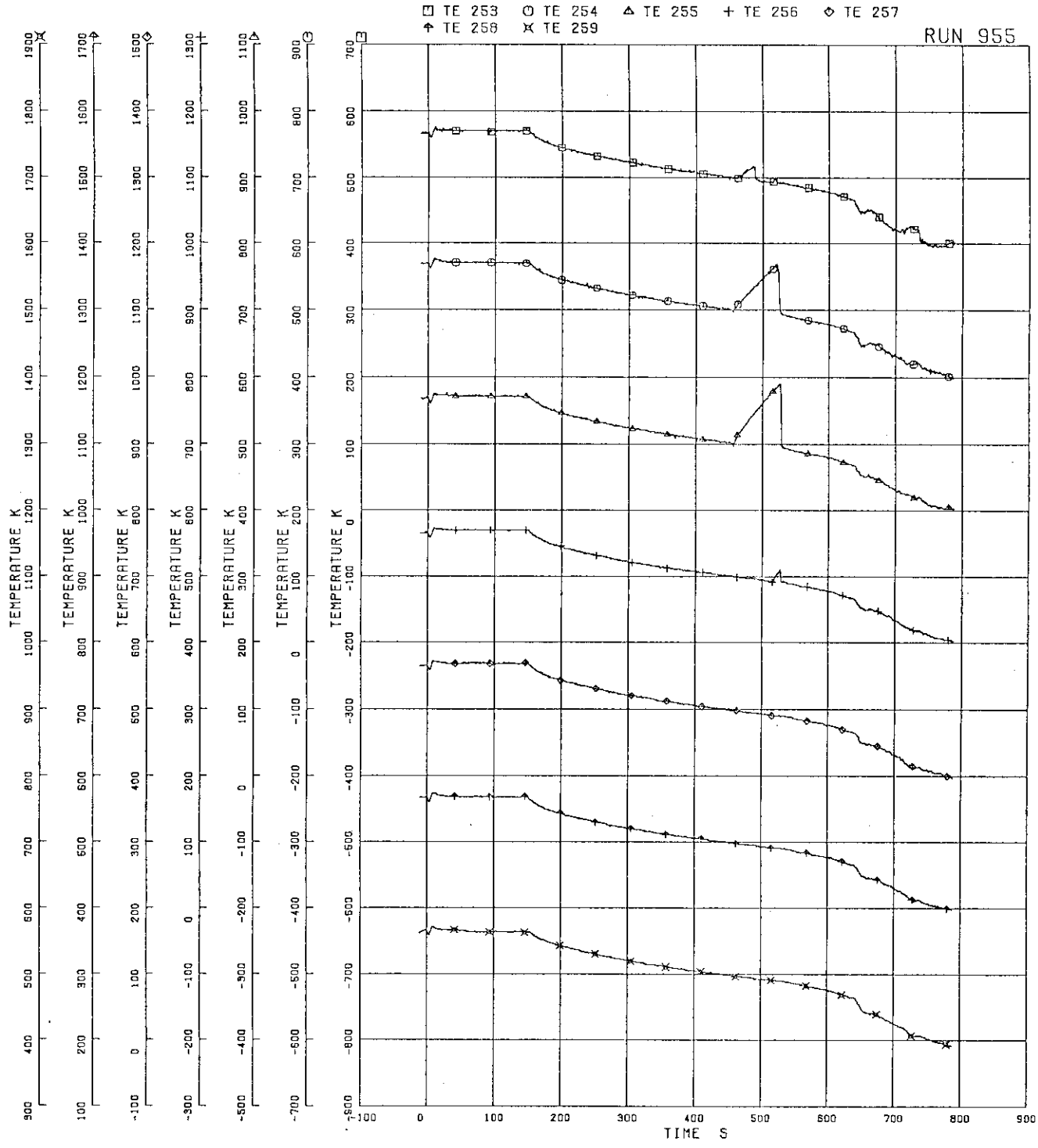

FIG.5. 54 FUEL ROD SURFACE TEMPERATURES OF A33 ROD

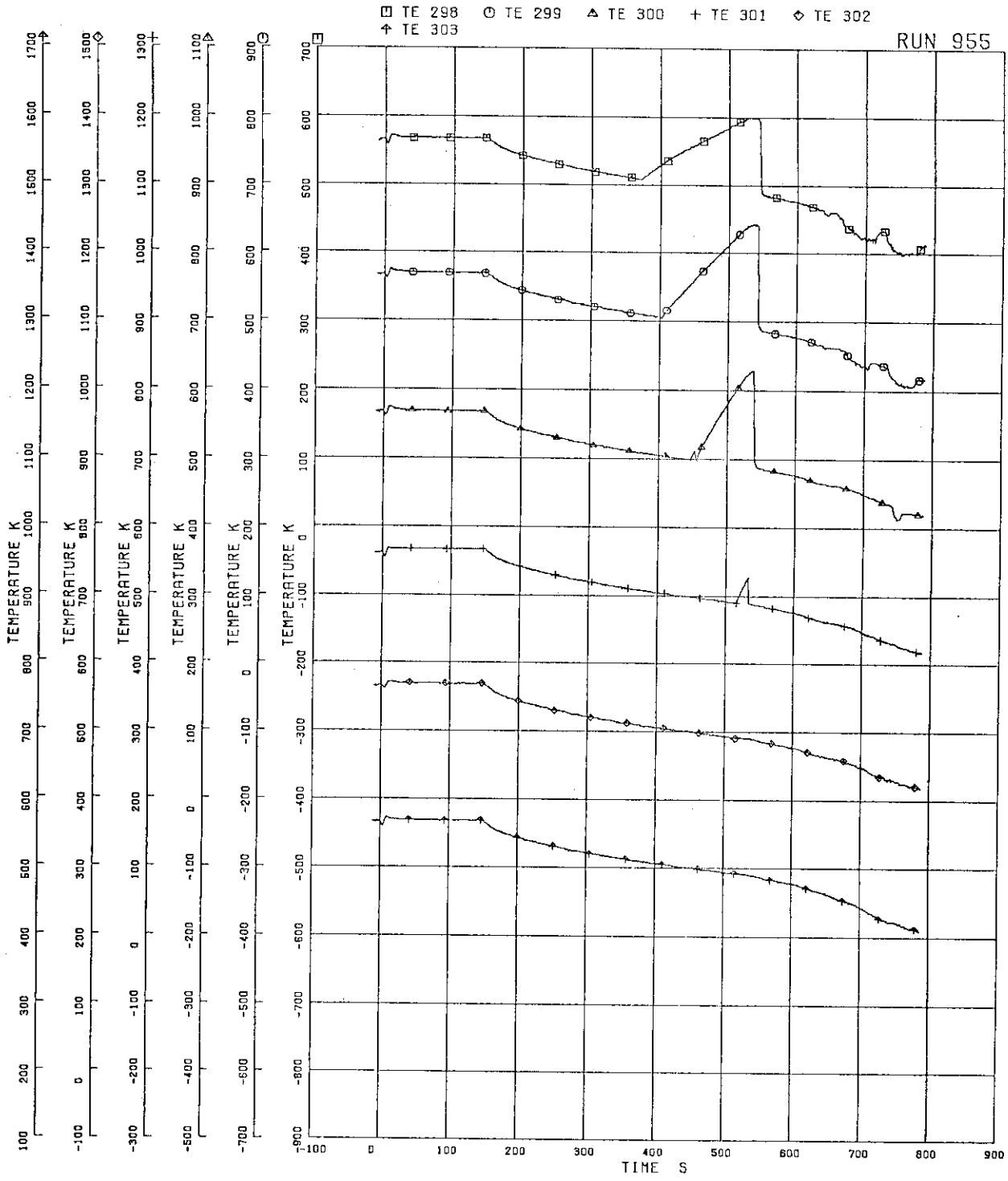

FIG.5. 55 FUEL ROD SURFACE TEMPERATURES OF A77 ROD

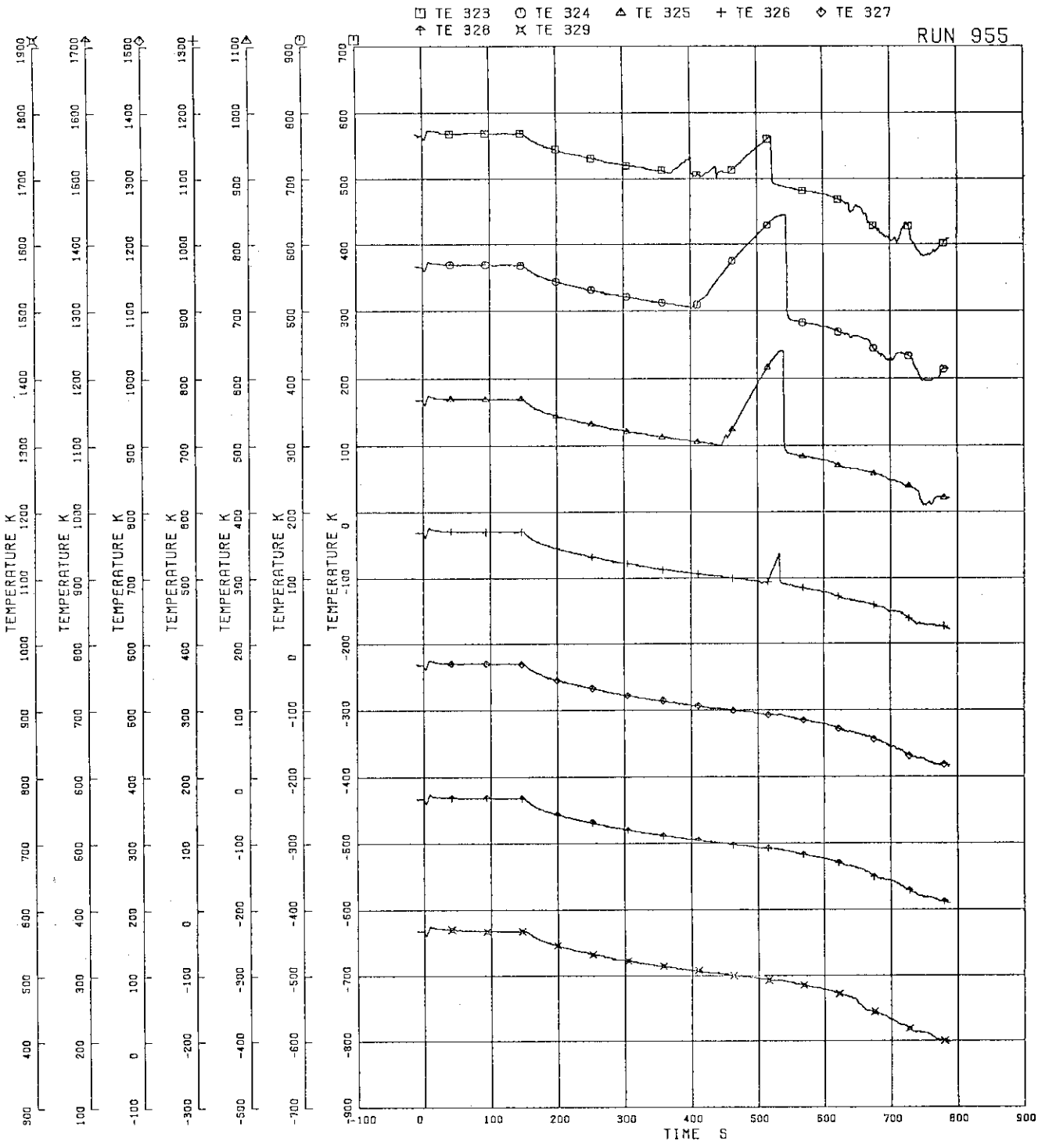

FIG.5. 56 FUEL ROD SURFACE TEMPERATURES OF A88 ROD

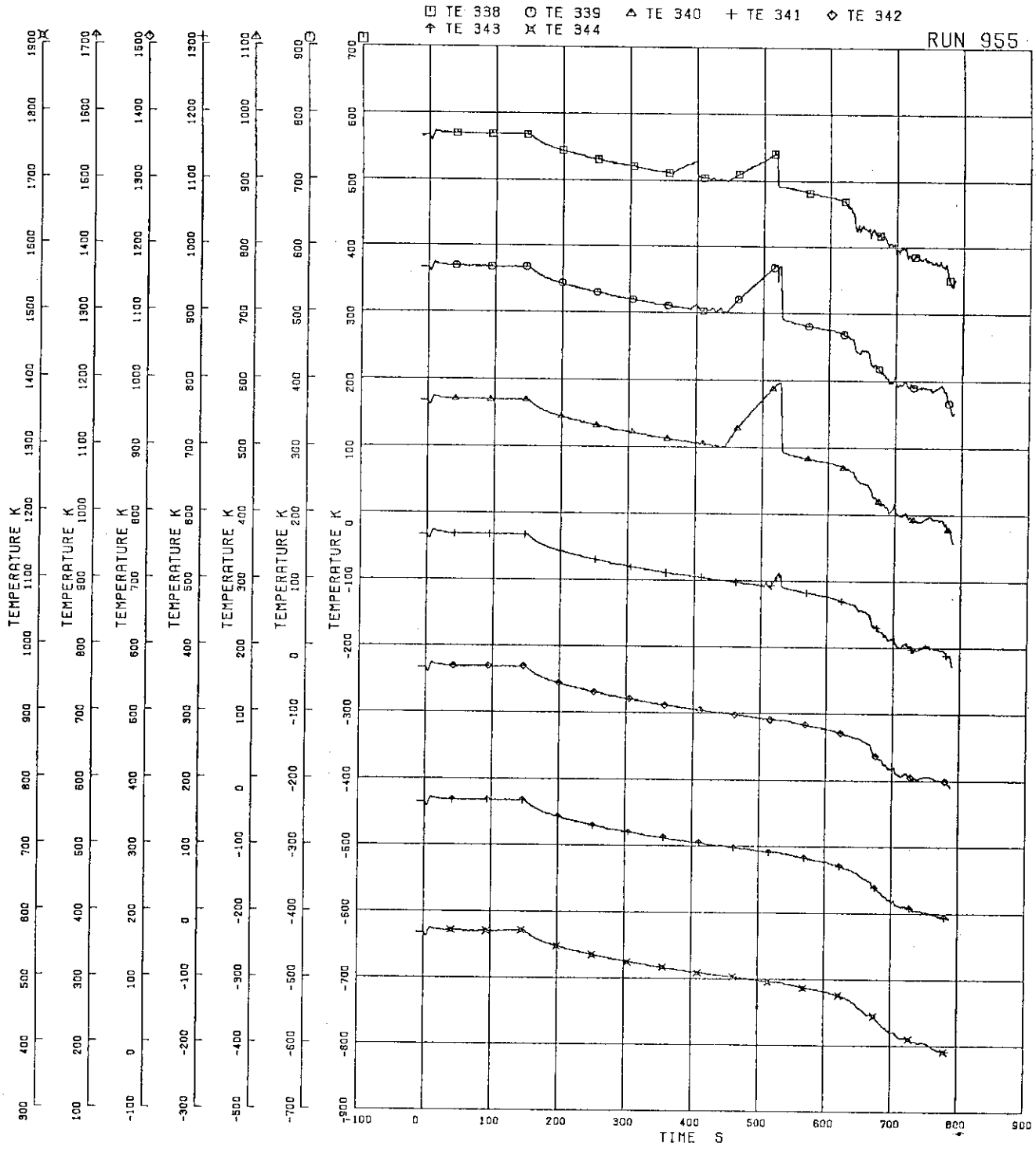

FIG.5. 57 FUEL ROD SURFACE TEMPERATURES OF B22 ROD

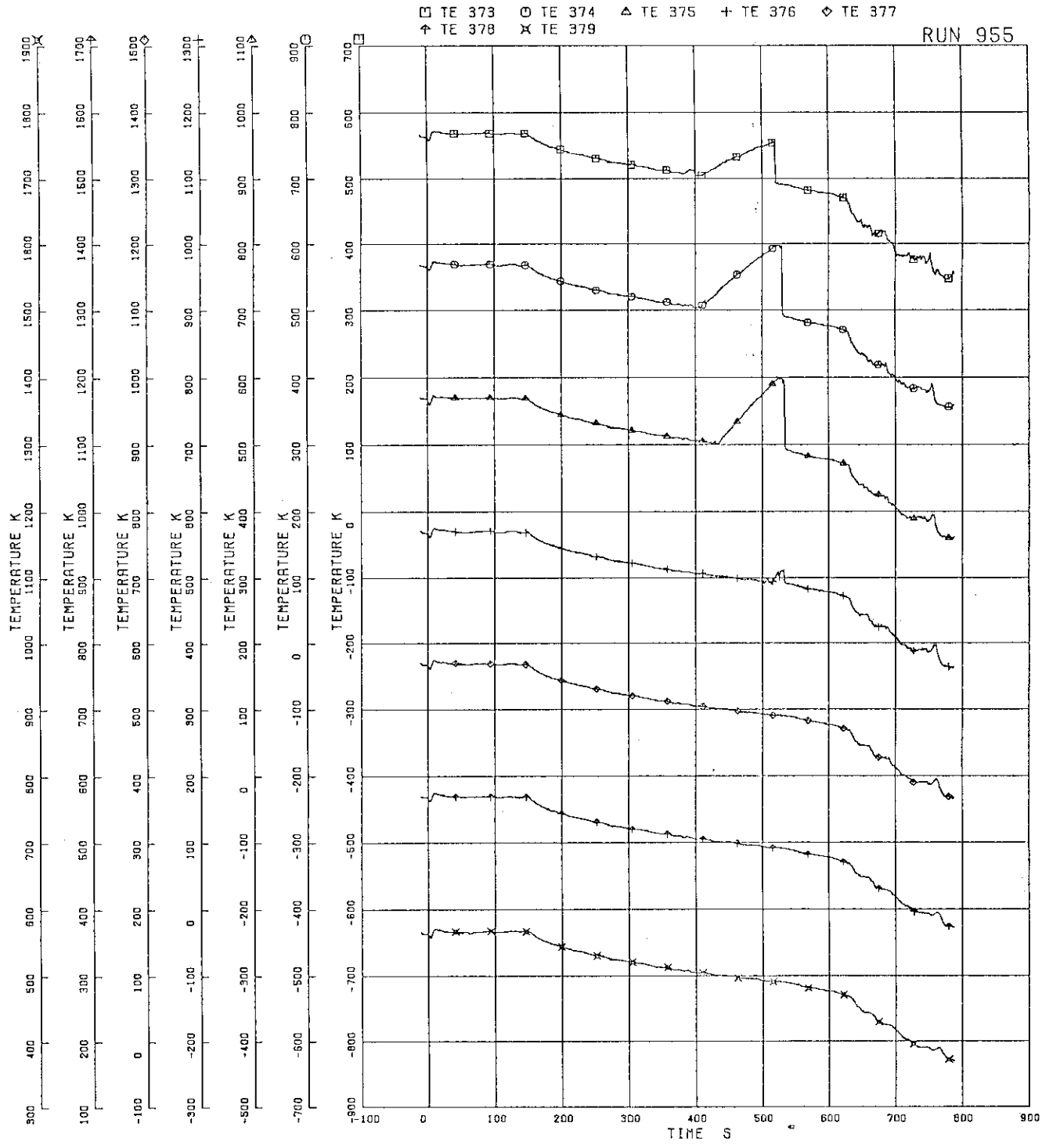

FIG.5. 58 FUEL ROD SURFACE TEMPERATURES OF C22 ROD

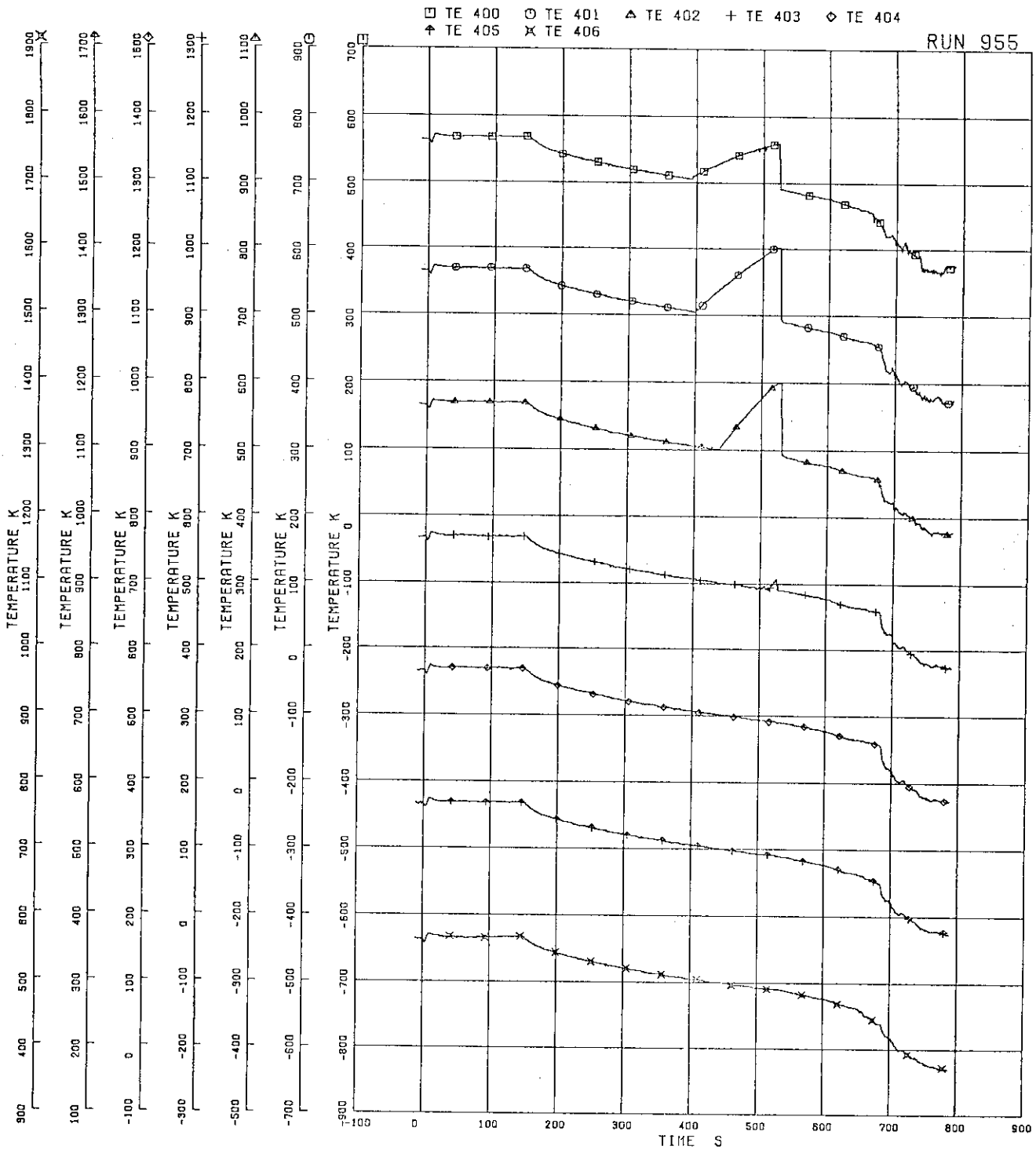

FIG.5. 59 FUEL ROD SURFACE TEMPERATURES OF D22 ROD

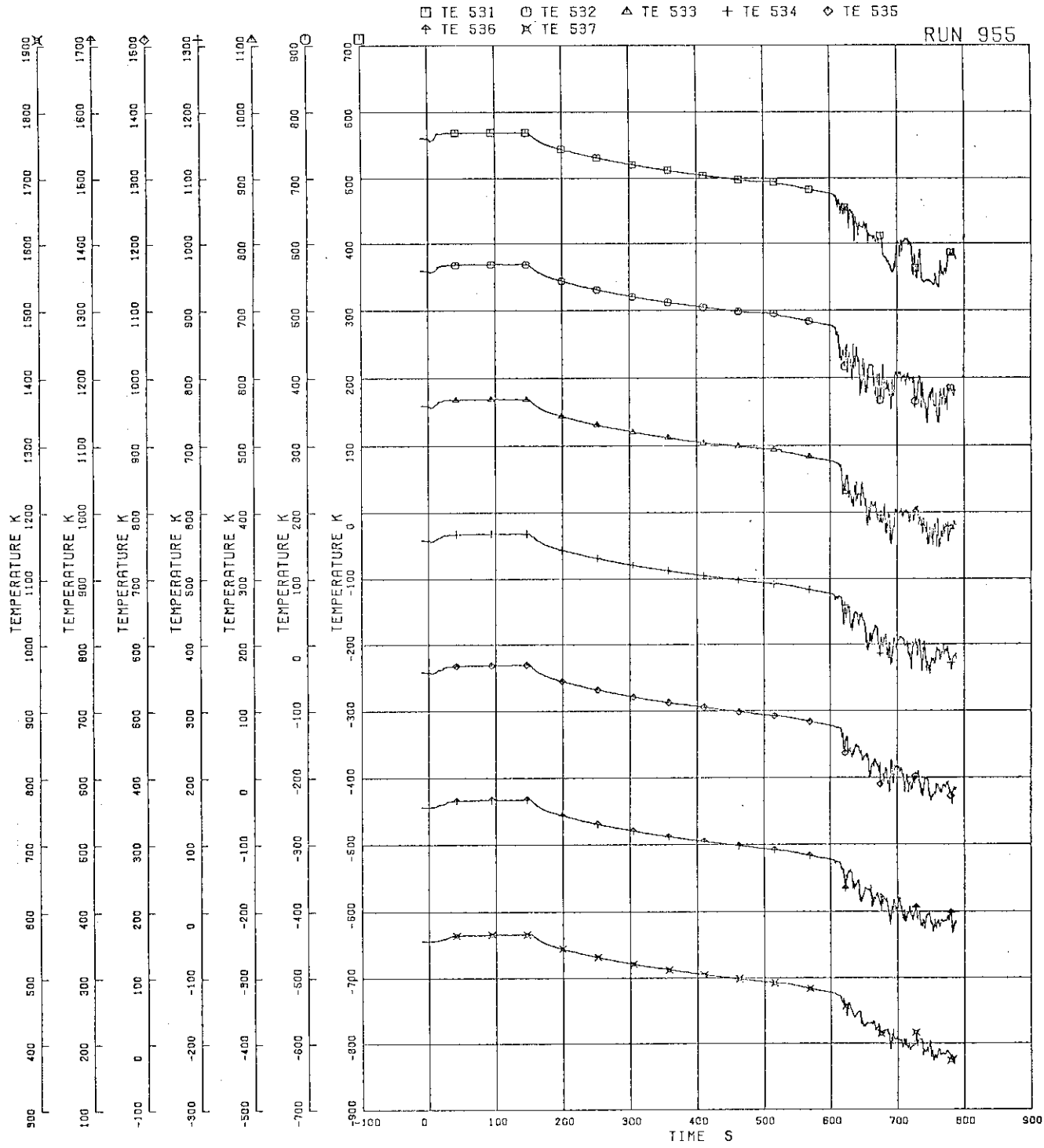

FIG.5. 60 OUTER SURFACE TEMPERATURES OF CHANNEL BOX A

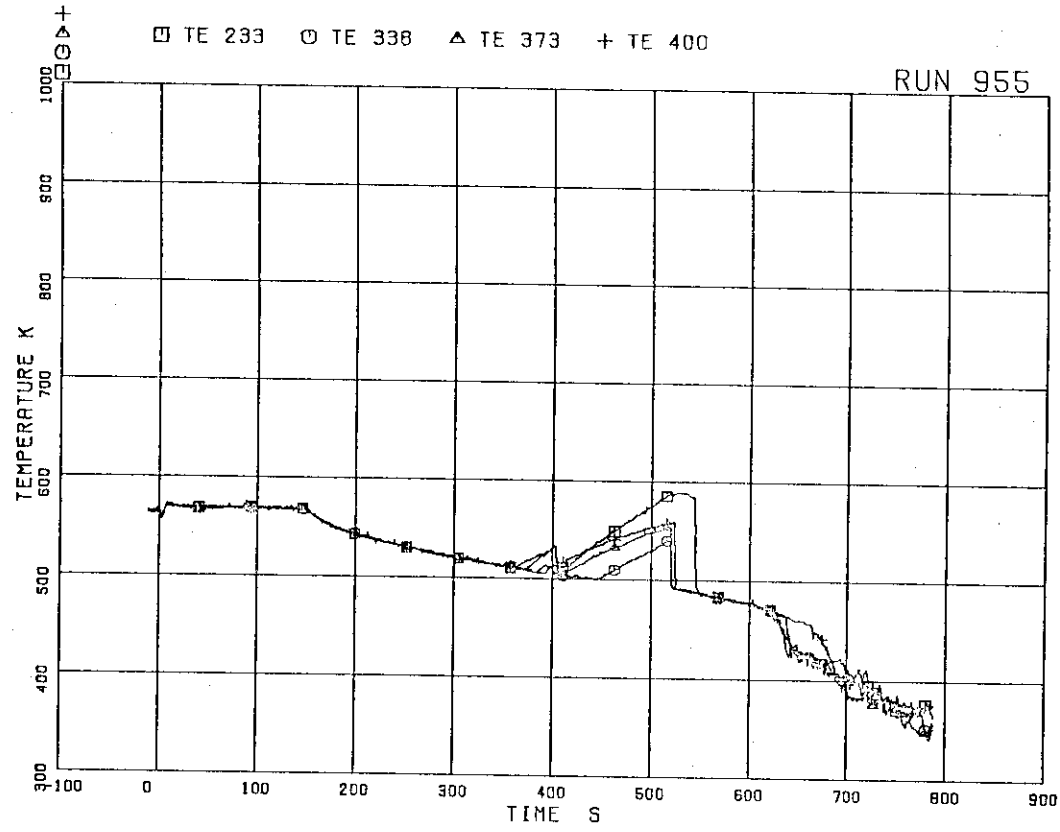

FIG.5. 61 SURFACE TEMPERATURES OF FUEL RODS A22,B22,C22,D22 AT POSITION 1

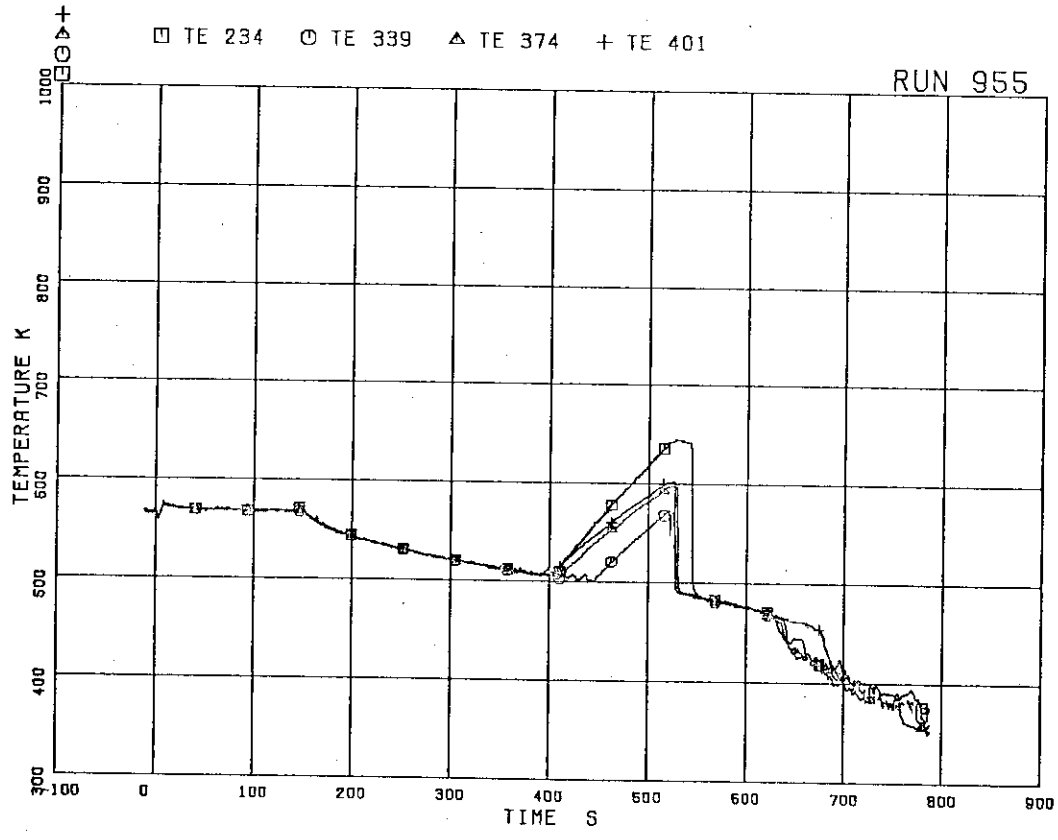

FIG.5. 62 SURFACE TEMPERATURES OF FUEL RODS A22,B22,C22,D22 AT POSITION 2

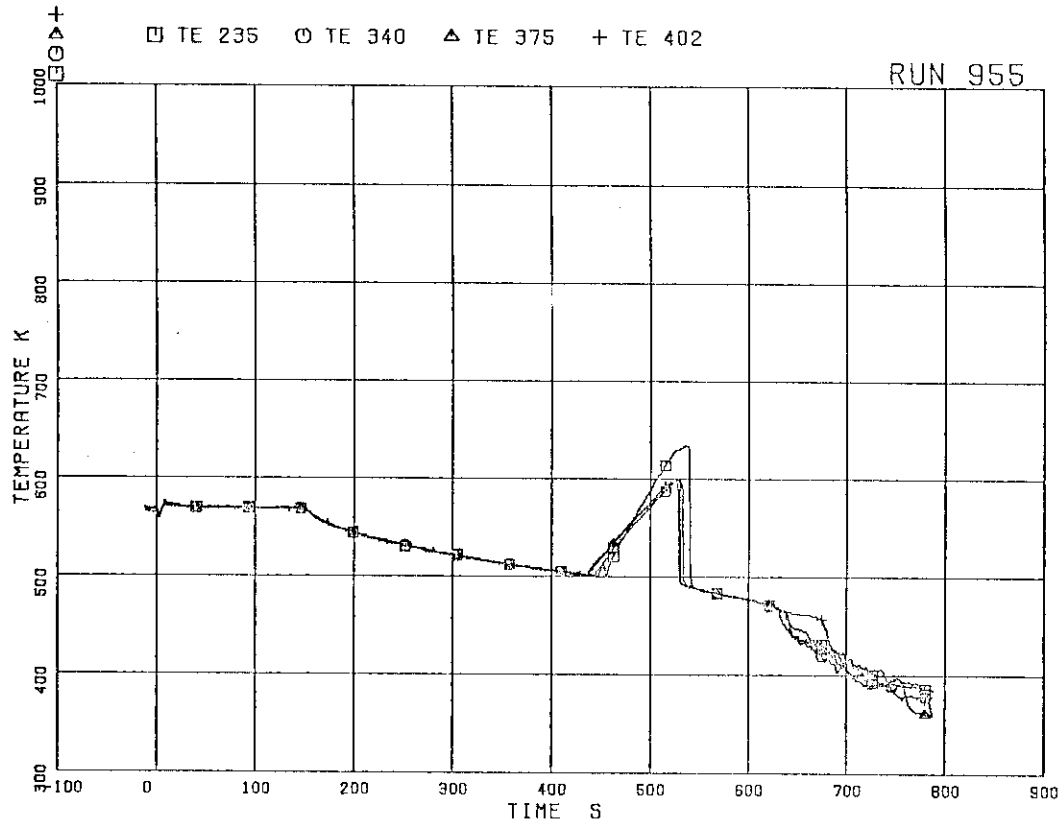

FIG.5. 63 SURFACE TEMPERATURES OF FUEL RODS A22,B22,C22,D22 AT POSITION 3

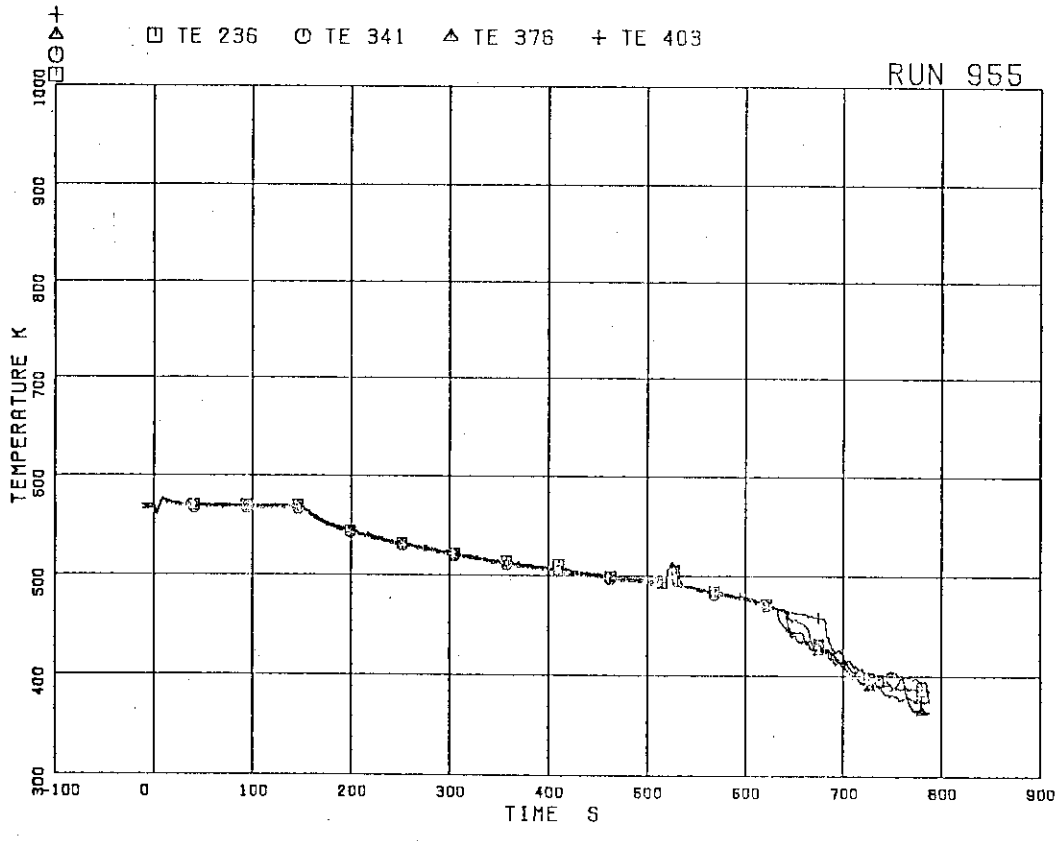

FIG.5. 64 SURFACE TEMPERATURES OF FUEL RODS A22,C22,D22 AT POSITION 4

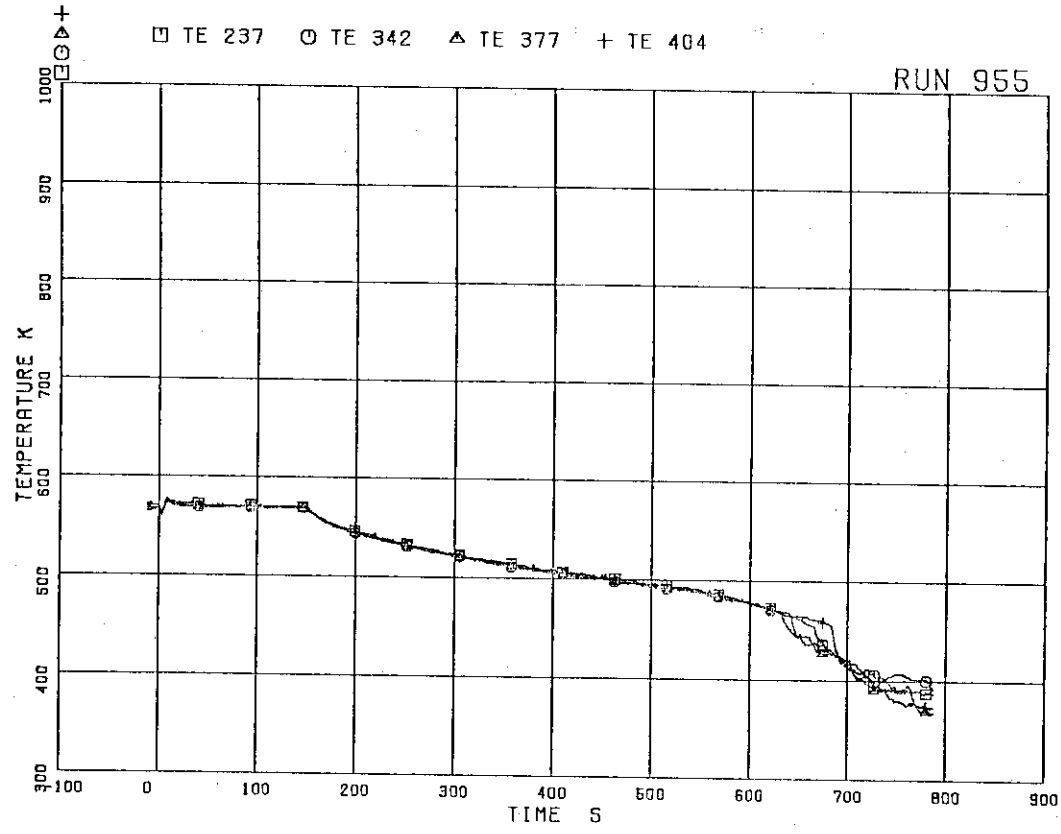

FIG.5. 65 SURFACE TEMPERATURES OF FUEL RODS A22,B22,C22,D22 AT POSITION 5

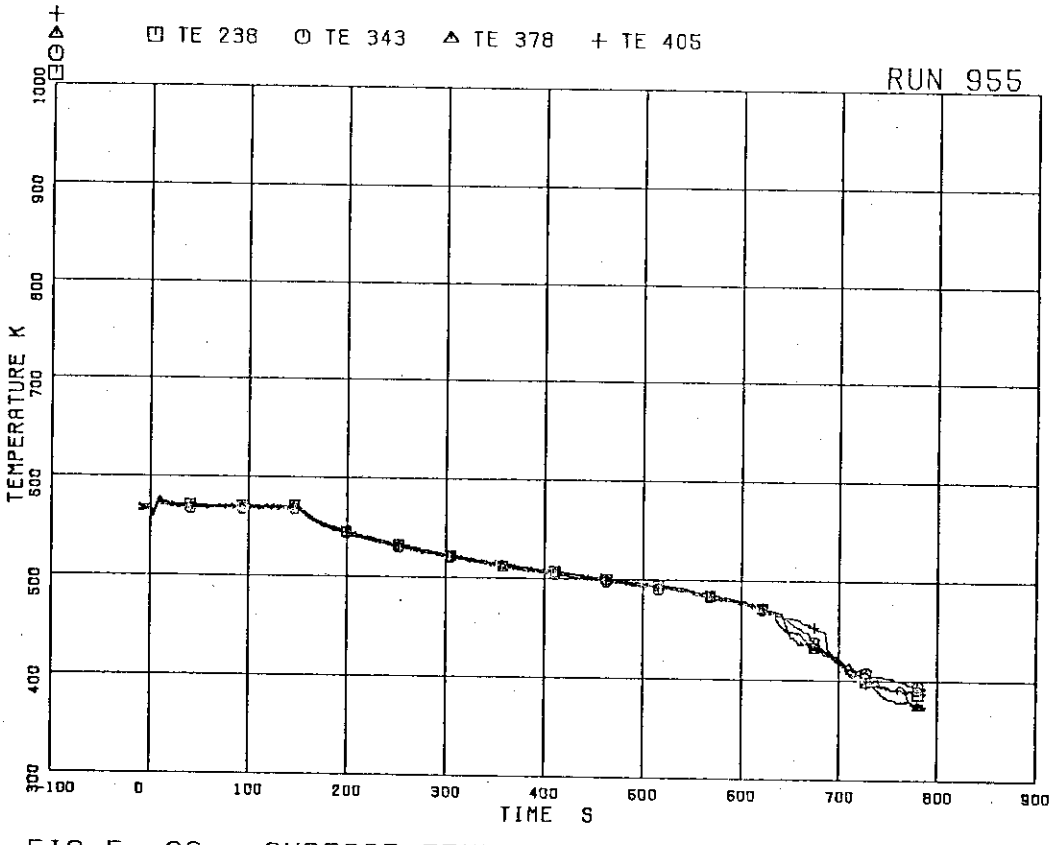

FIG.5. 66 SURFACE TEMPERATURES OF FUEL RODS A22,B22,C22,D22 AT POSITION 6

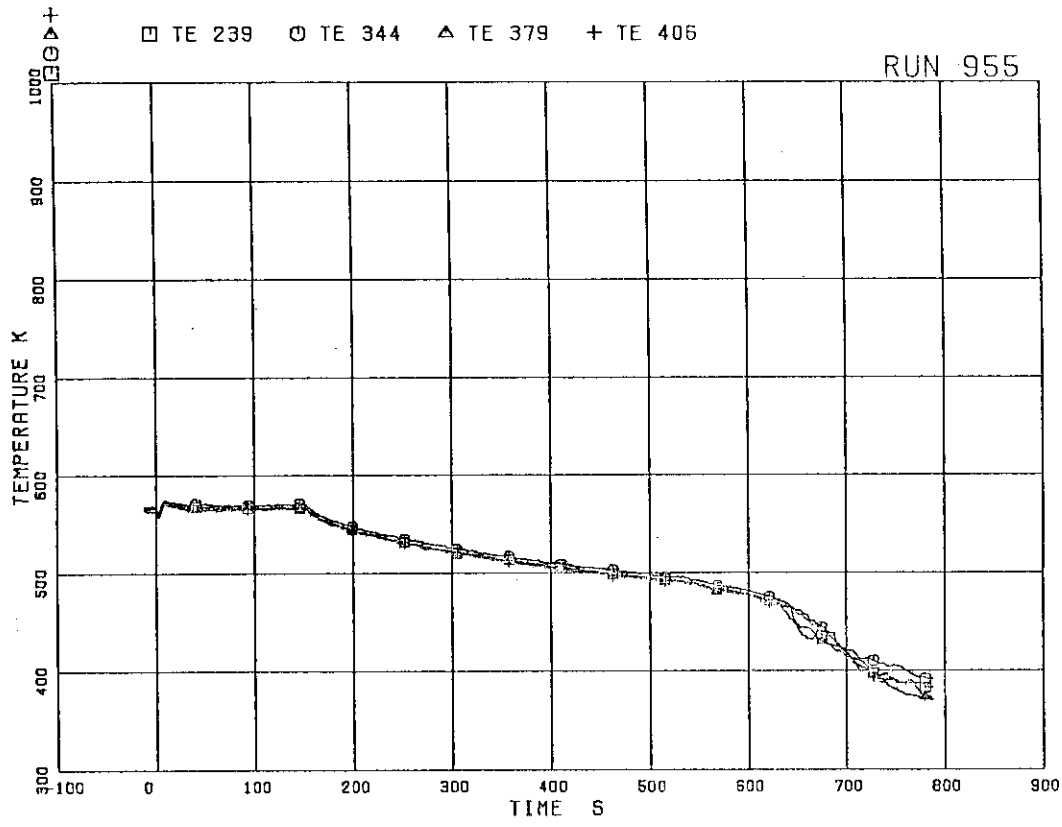

FIG.5. 67 SURFACE TEMPERATURES OF FUEL RODS A22,B22,C22,D22 AT POSITION 7

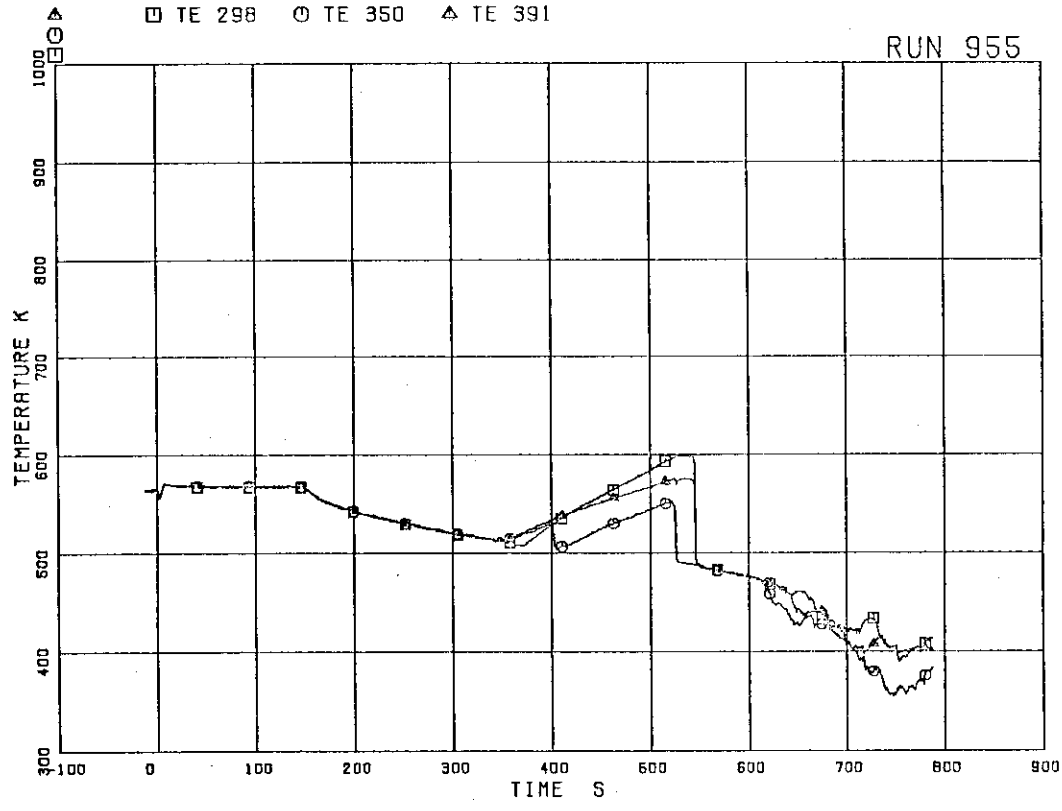

FIG.5. 68 SURFACE TEMPERATURES OF FUEL RODS A77,B77,C77 AT POSITION 1

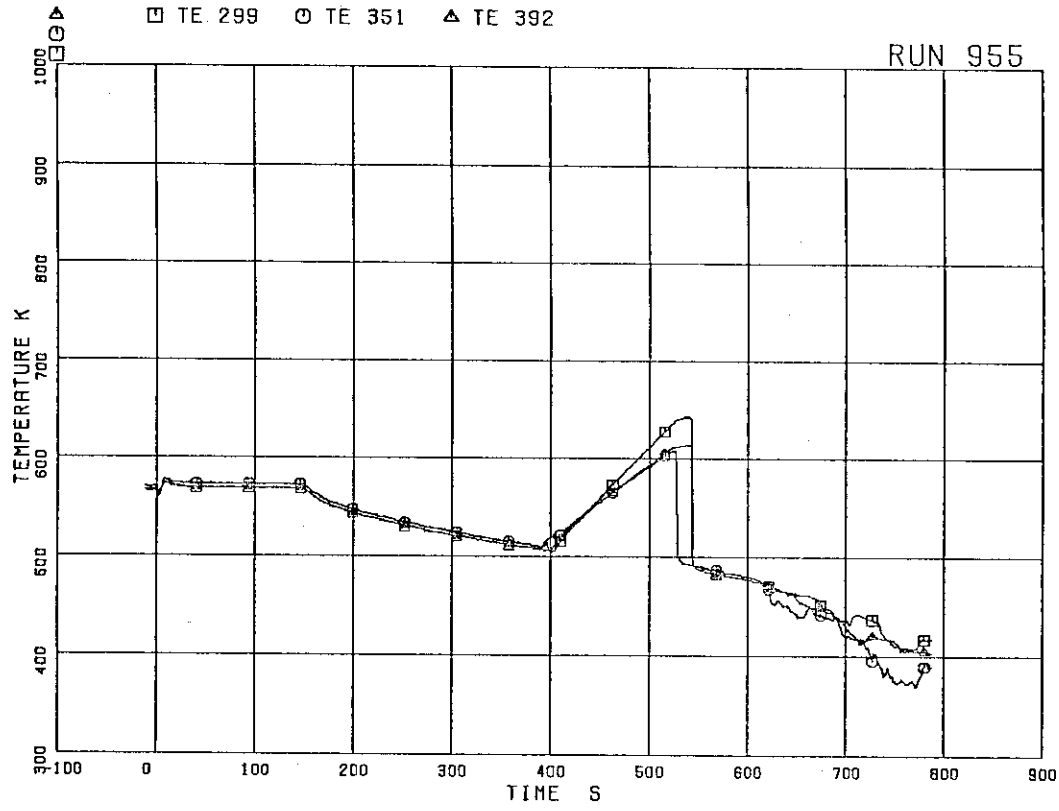

FIG.5. 69 SURFACE TEMPERATURES OF FUEL RODS A77,B77,C77 AT POSITION 2

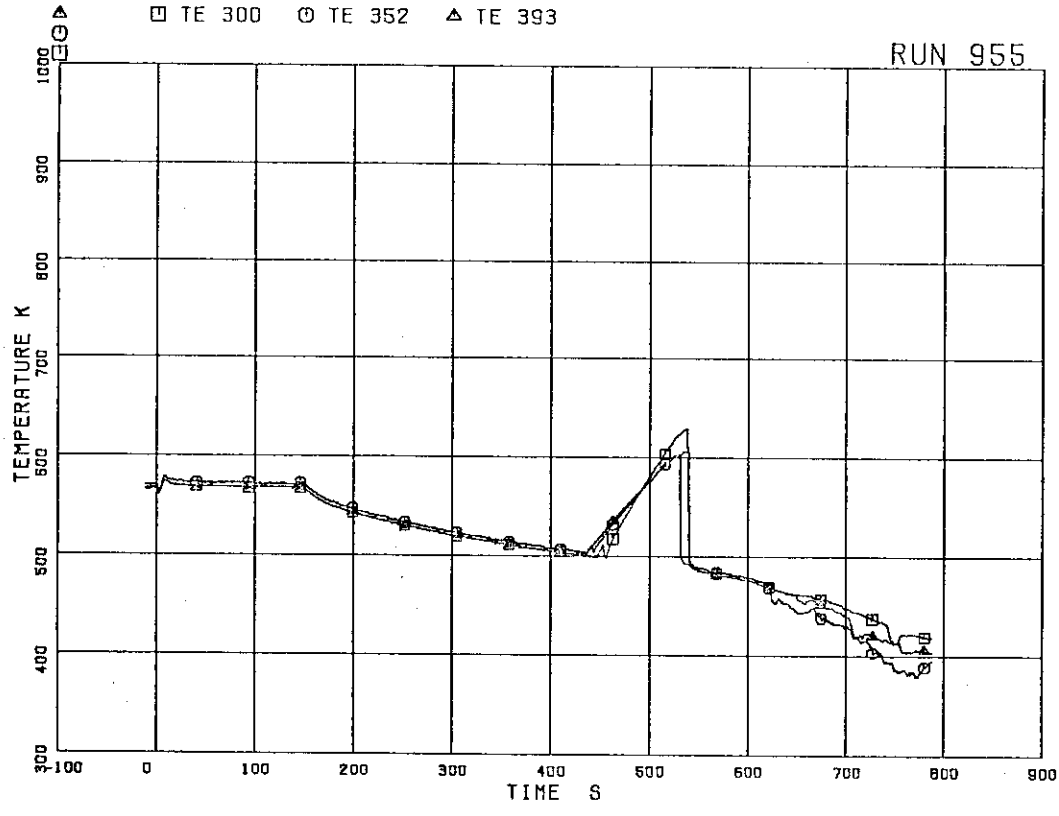

FIG.5. 70 SURFACE TEMPERATURES OF FUEL RODS A77,B77,C77 AT POSITION 3

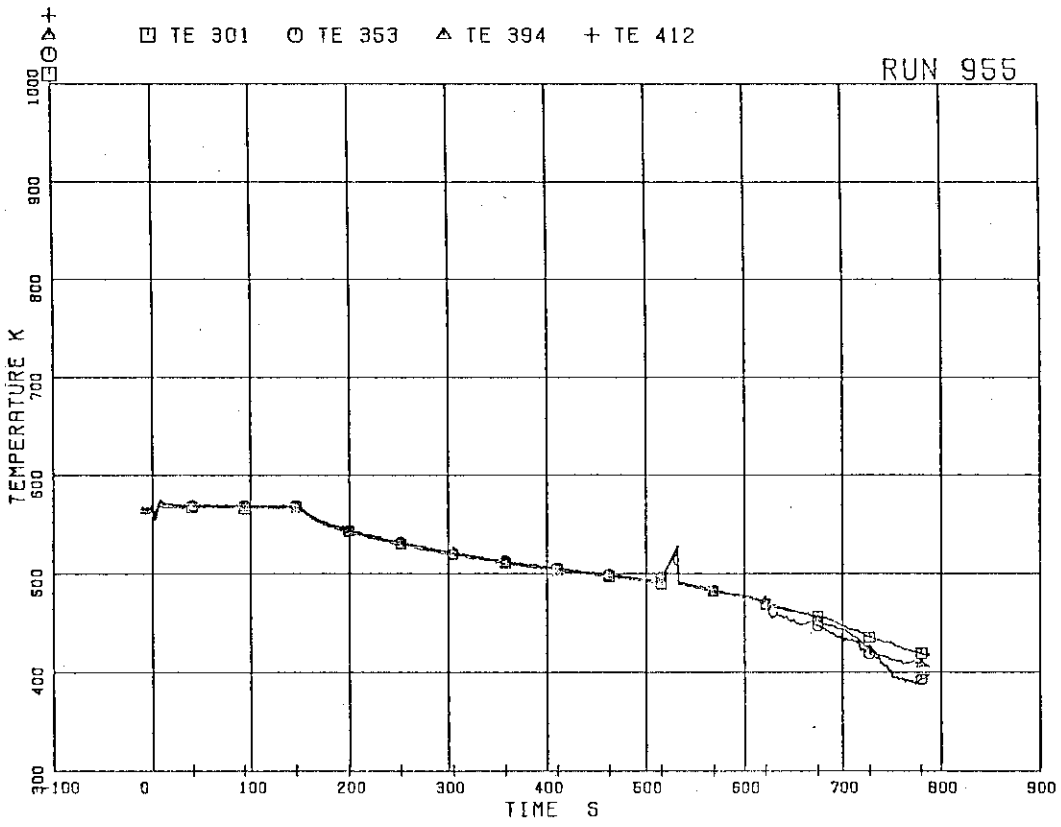

FIG.5. 71 SURFACE TEMPERATURES OF FUEL RODS A77,B77,C77 AT POSITION 4

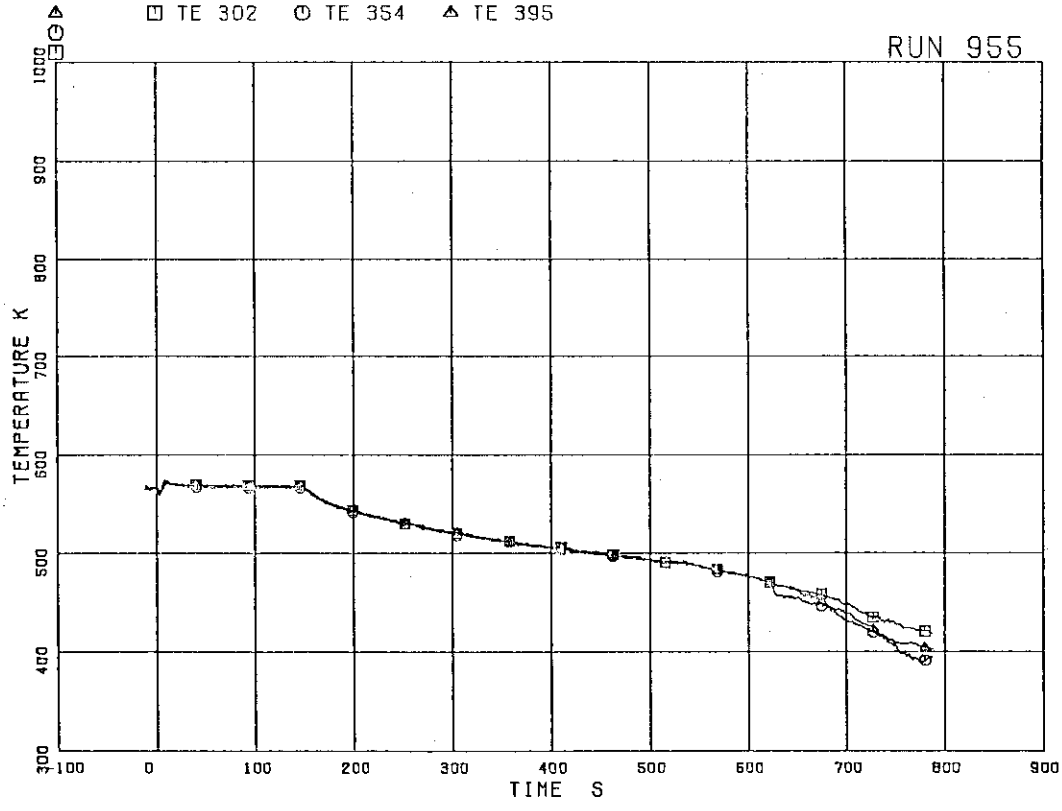

FIG.5. 72 SURFACE TEMPERATURES OF FUEL RODS A77,B77,C77 AT POSITION 5

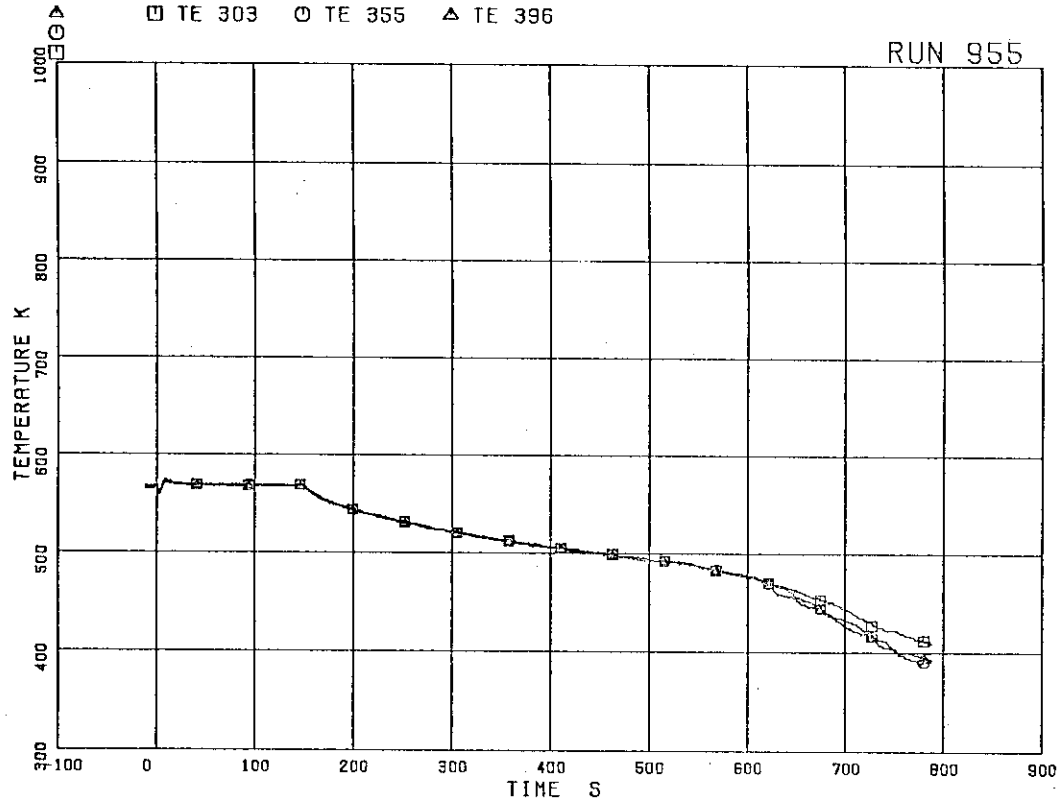

FIG.5. 73 SURFACE TEMPERATURES OF FUEL RODS
A77,B77,C77 AT POSITION 6

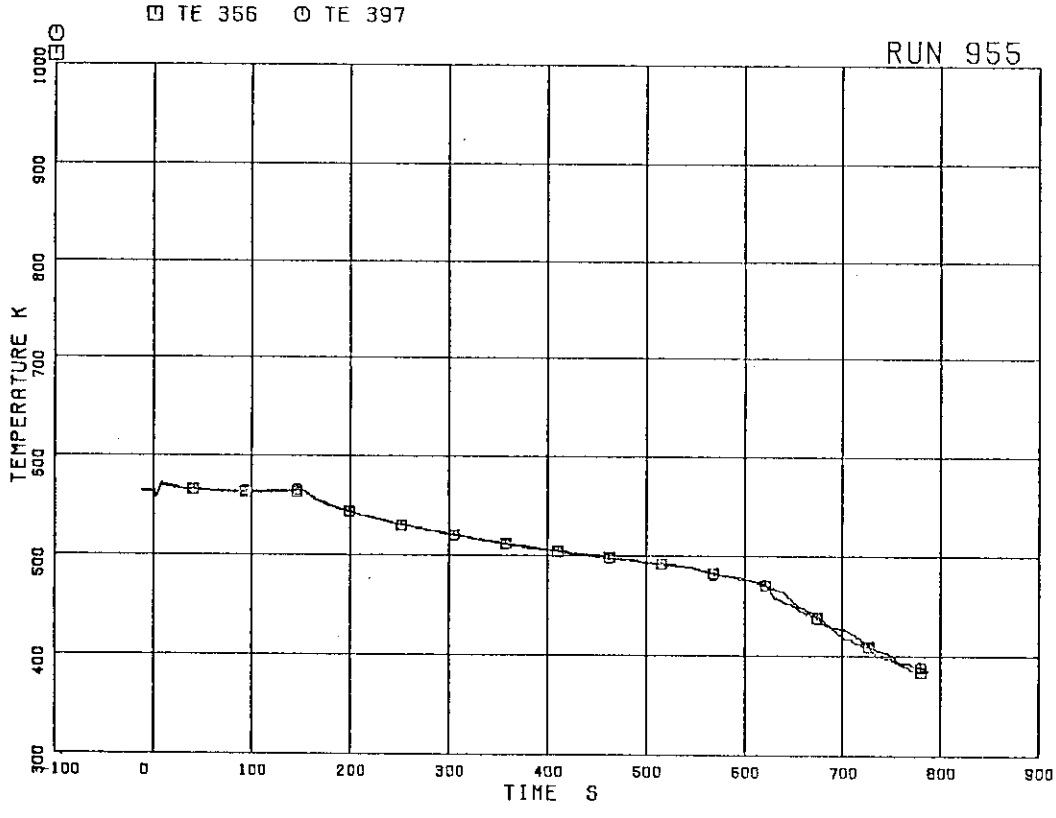

FIG.5. 74 SURFACE TEMPERATURES OF FUEL RODS
B77,C77 RODS AT POSITION 7

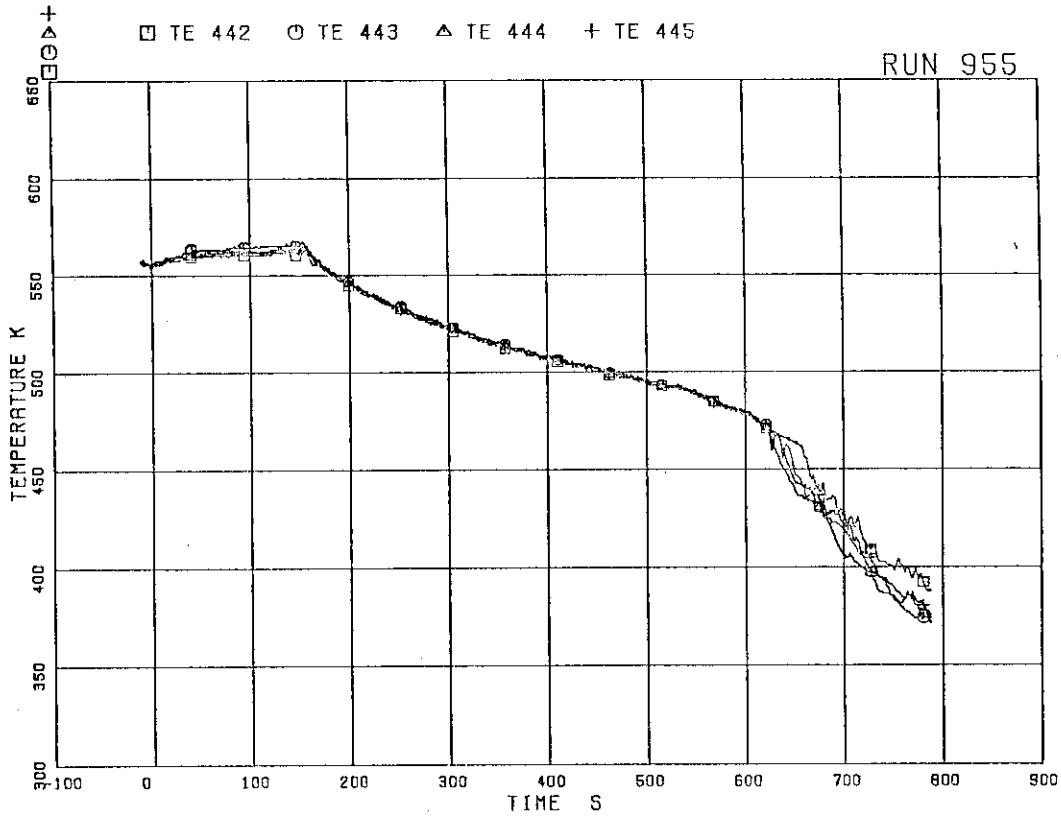

FIG.5. 75 FLUID TEMPERATURES AT CHANNEL INLET

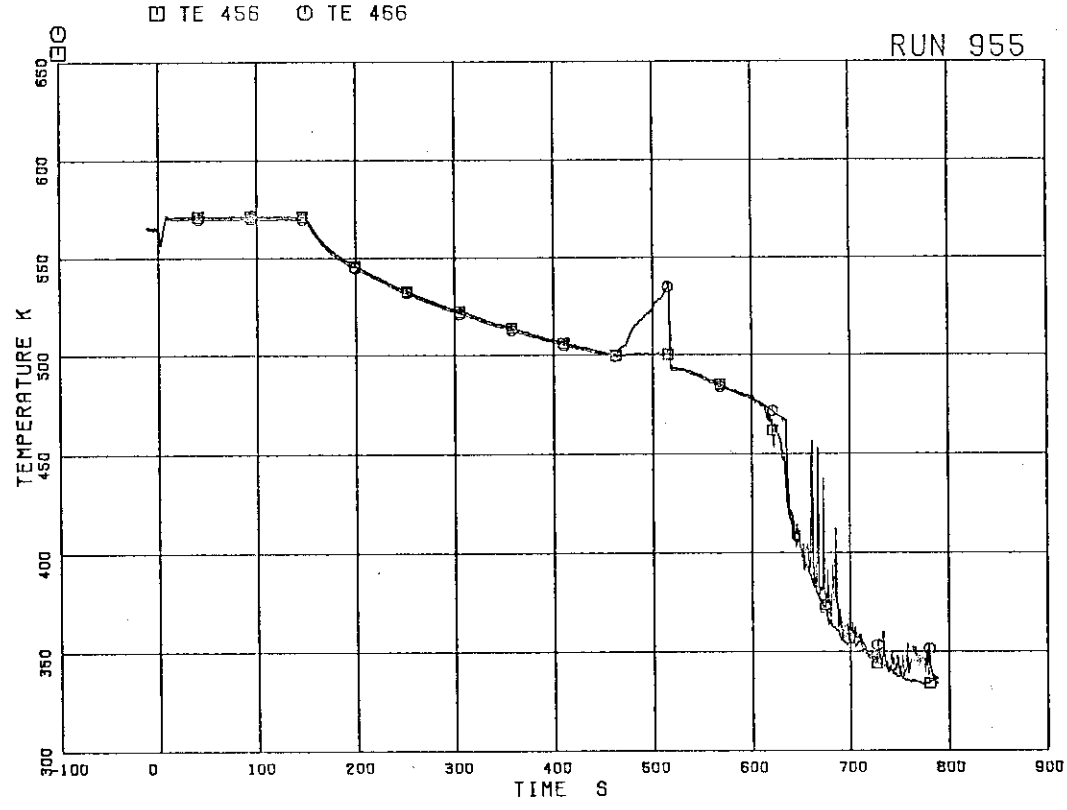

FIG.5. 76 FLUID TEMPERATURES AT UTP IN CHANNEL A, OPENING 1

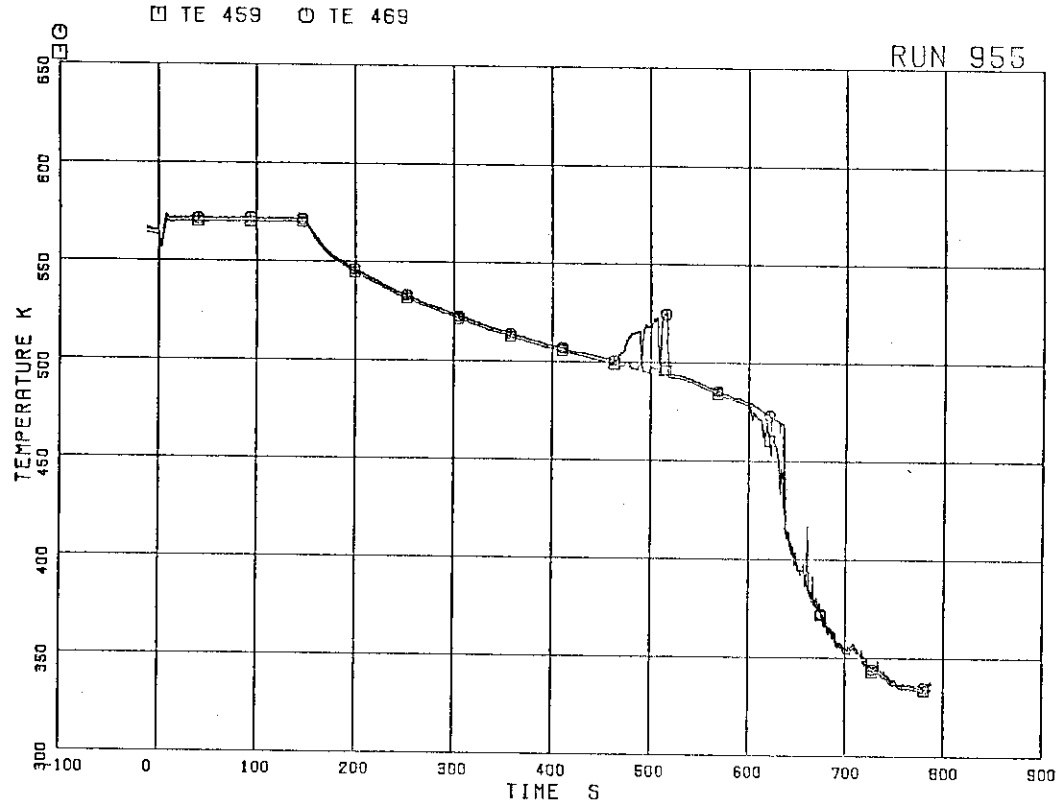

FIG.5. 77 FLUID TEMPERATURES AT UTP IN CHANNEL A, OPENING 4

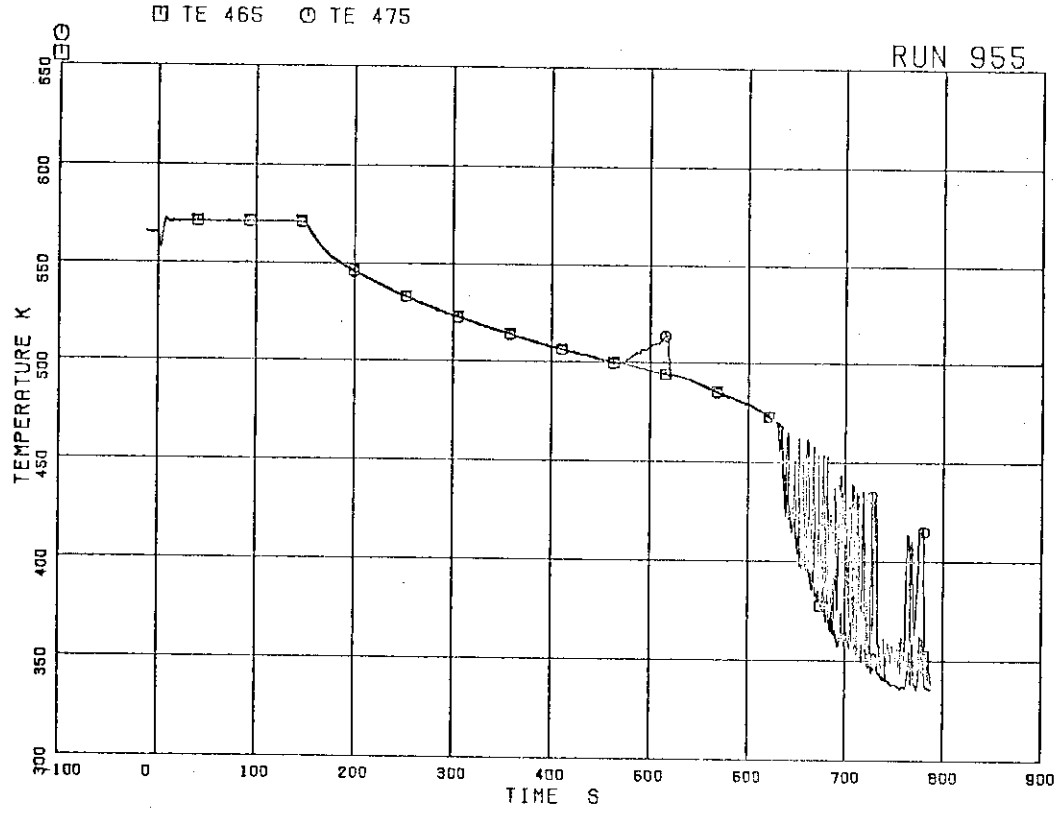

FIG.5. 78 FLUID TEMPERATURES AT UTP IN CHANNEL A, OPENING 10

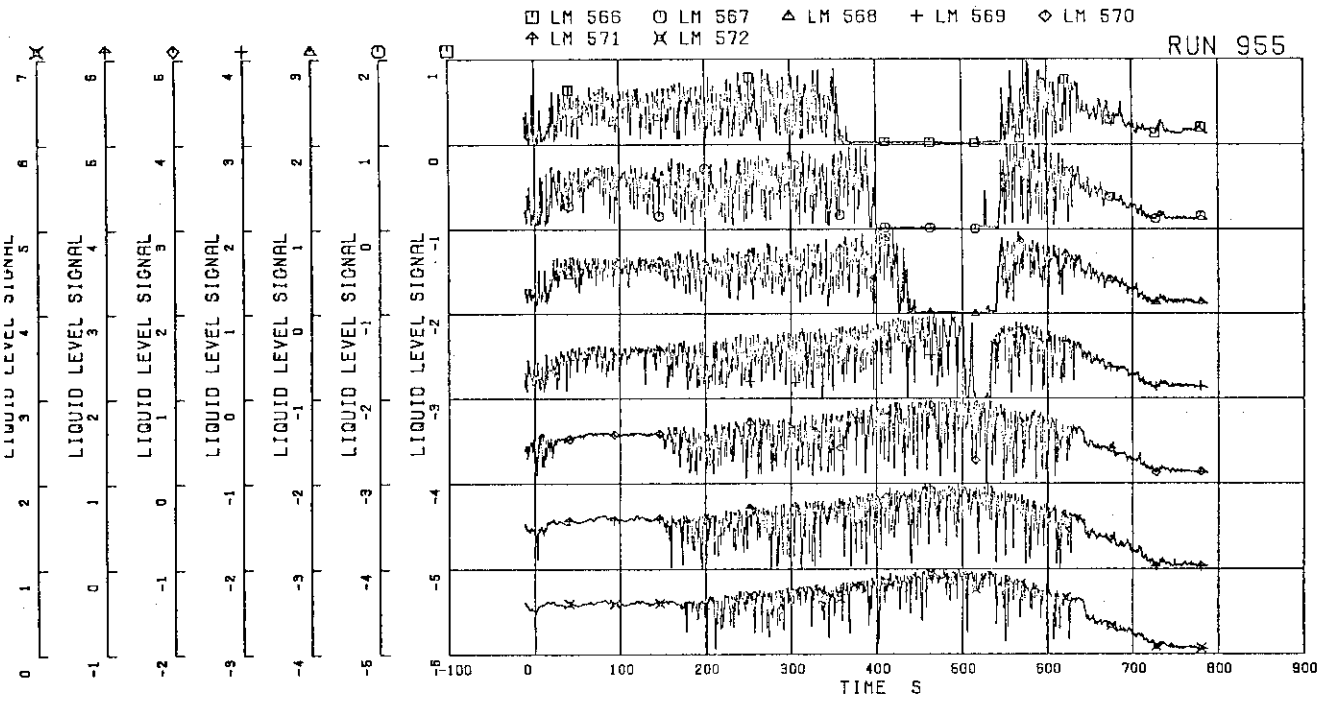

FIG.5. 79 LIQUID LEVEL SIGNALS IN CHANNEL BOX A, LOCATION A2

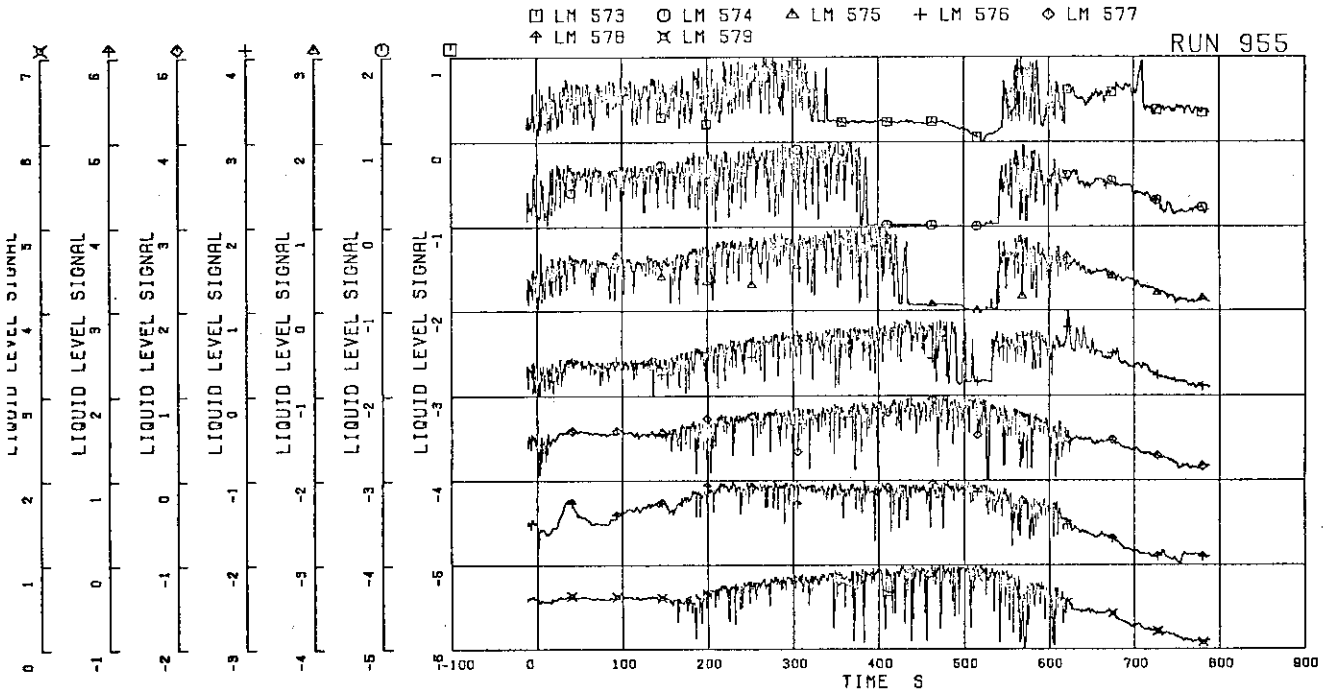

FIG.5. 80 LIQUID LEVEL SIGNALS IN CHANNEL BOX B

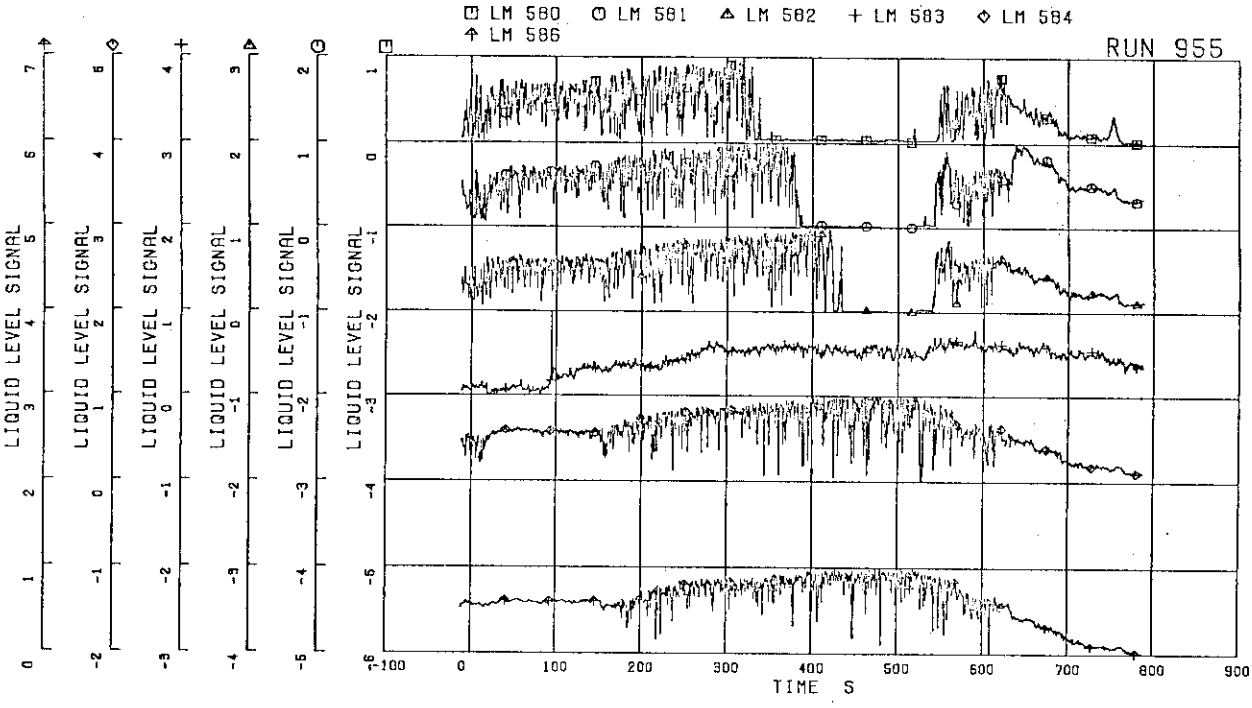

FIG.5. 81 LIQUID LEVEL SIGNALS IN CHANNEL BOX C

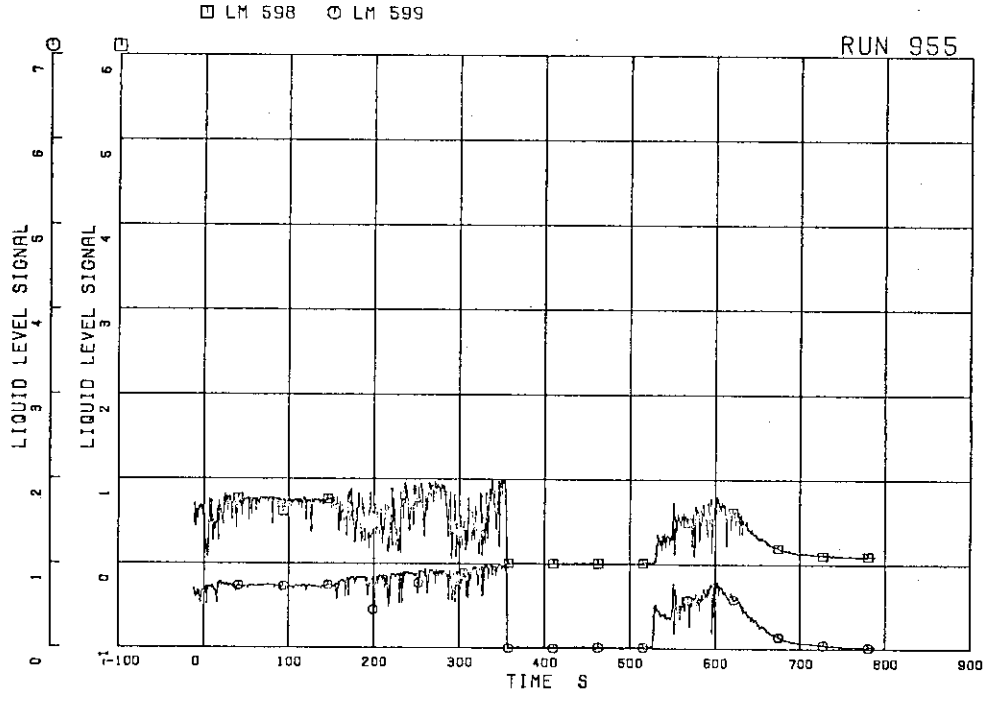

FIG.5. 82 LIQUID LEVEL SIGNALS IN CHANNEL A OUTLET LOCATION A2

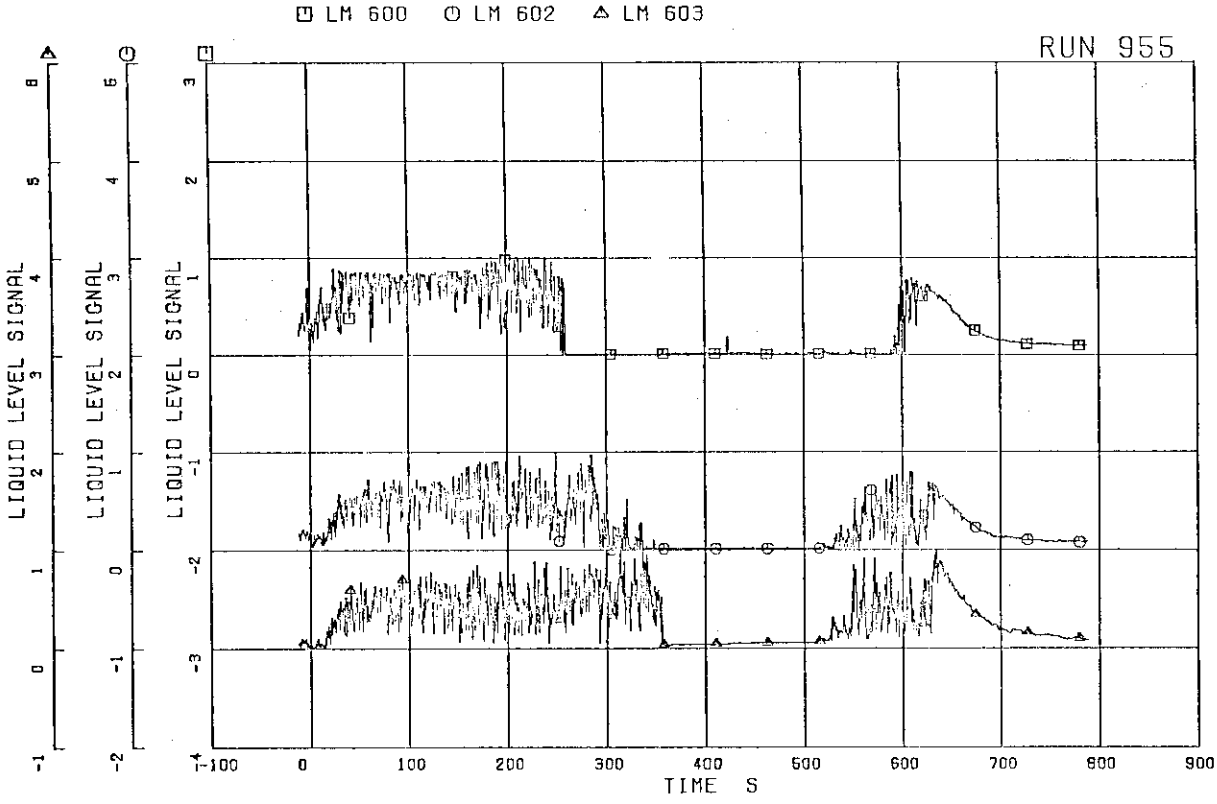

FIG.5. 83 LIQUID LEVEL SIGNALS IN CHANNEL A OUTLET CENTER

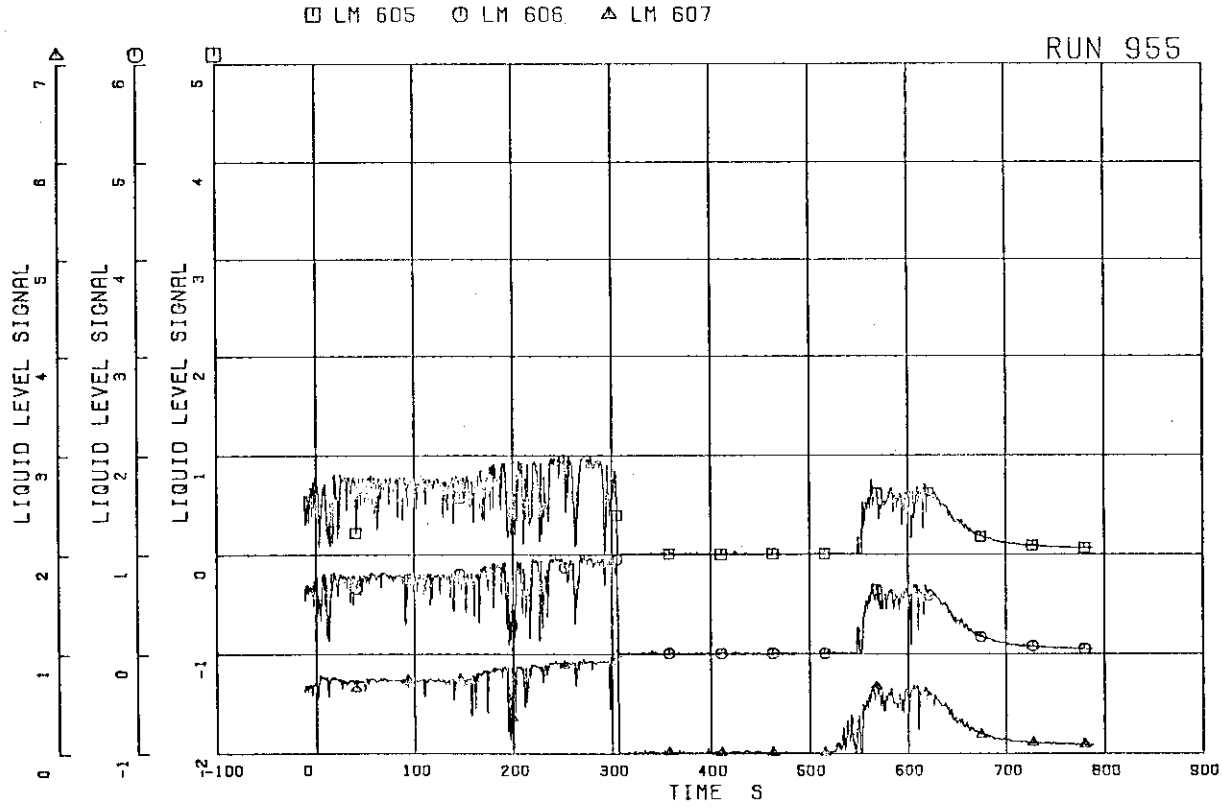

FIG.5. 84 LIQUID LEVEL SIGNALS IN CHANNEL C OUTLET LOCATION C2

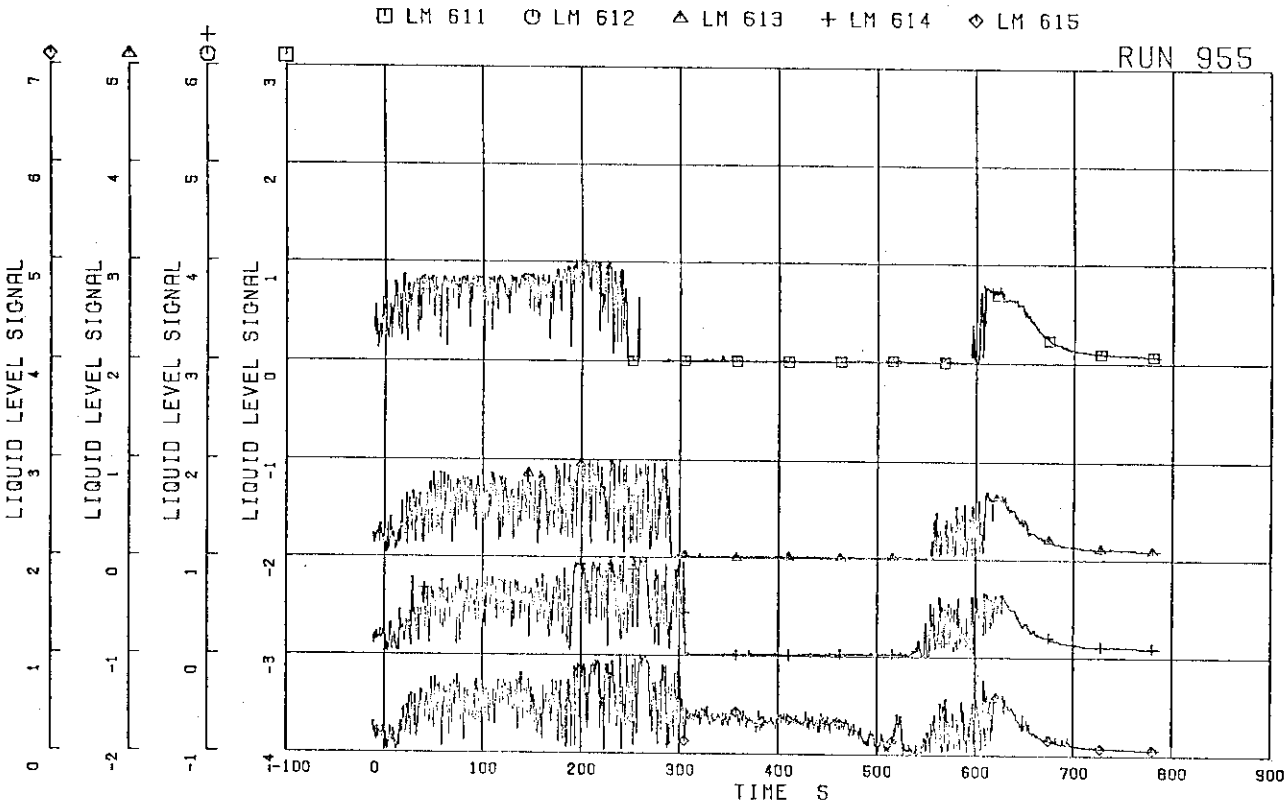

FIG.5. 85 LIQUID LEVEL SIGNALS IN CHANNEL C OUTLET CENTER

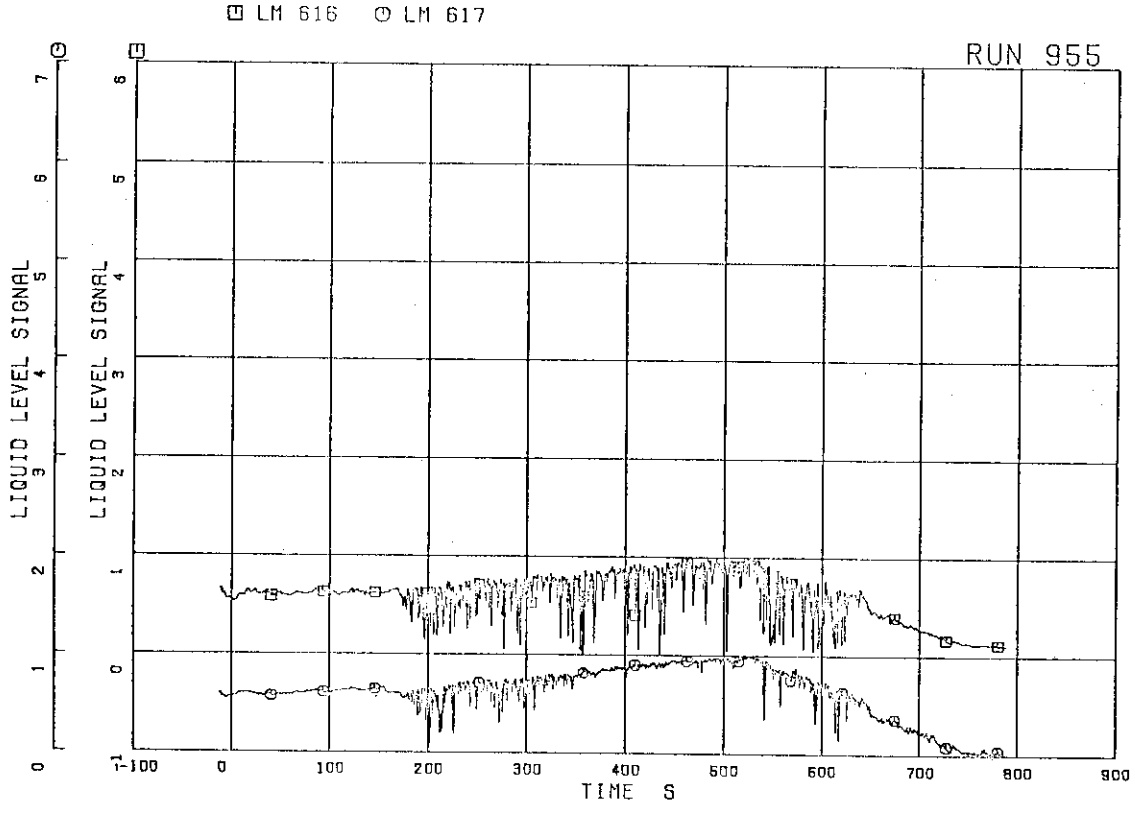

FIG.5. 86 LIQUID LEVEL SIGNALS IN CHANNEL A INLET

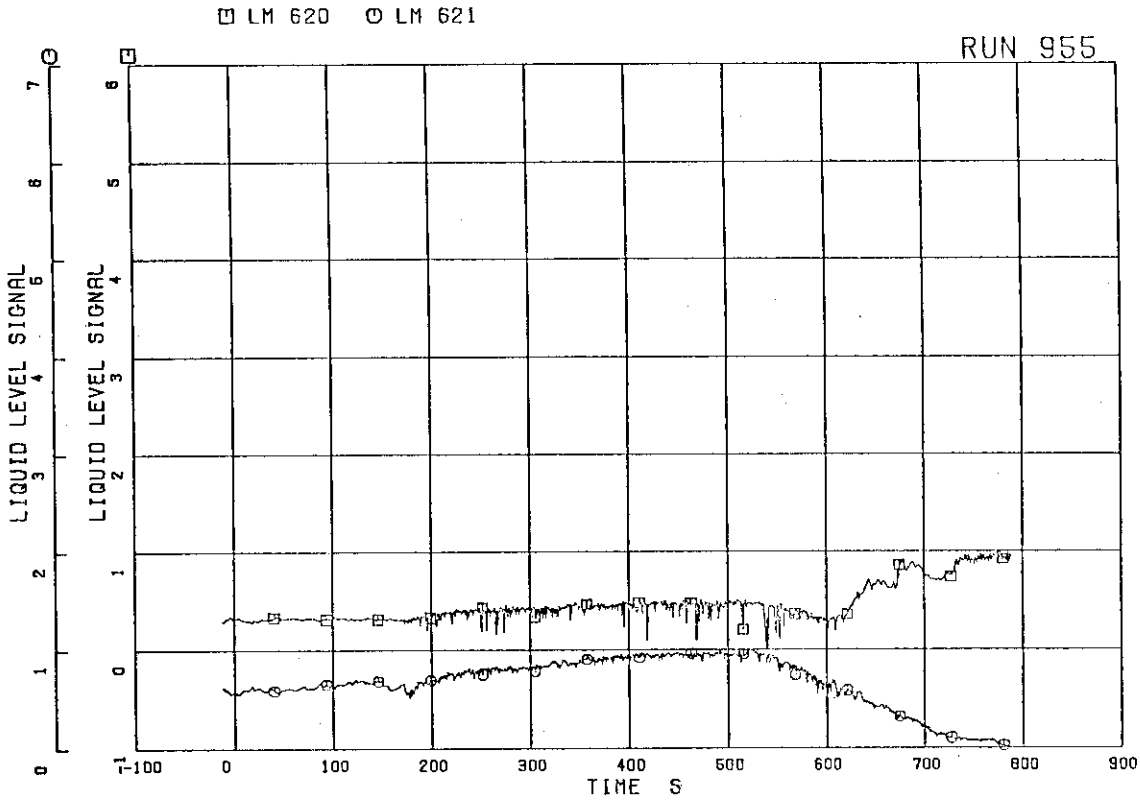

FIG.5. 87 LIQUID LEVEL SIGNALS IN CHANNEL C INLET

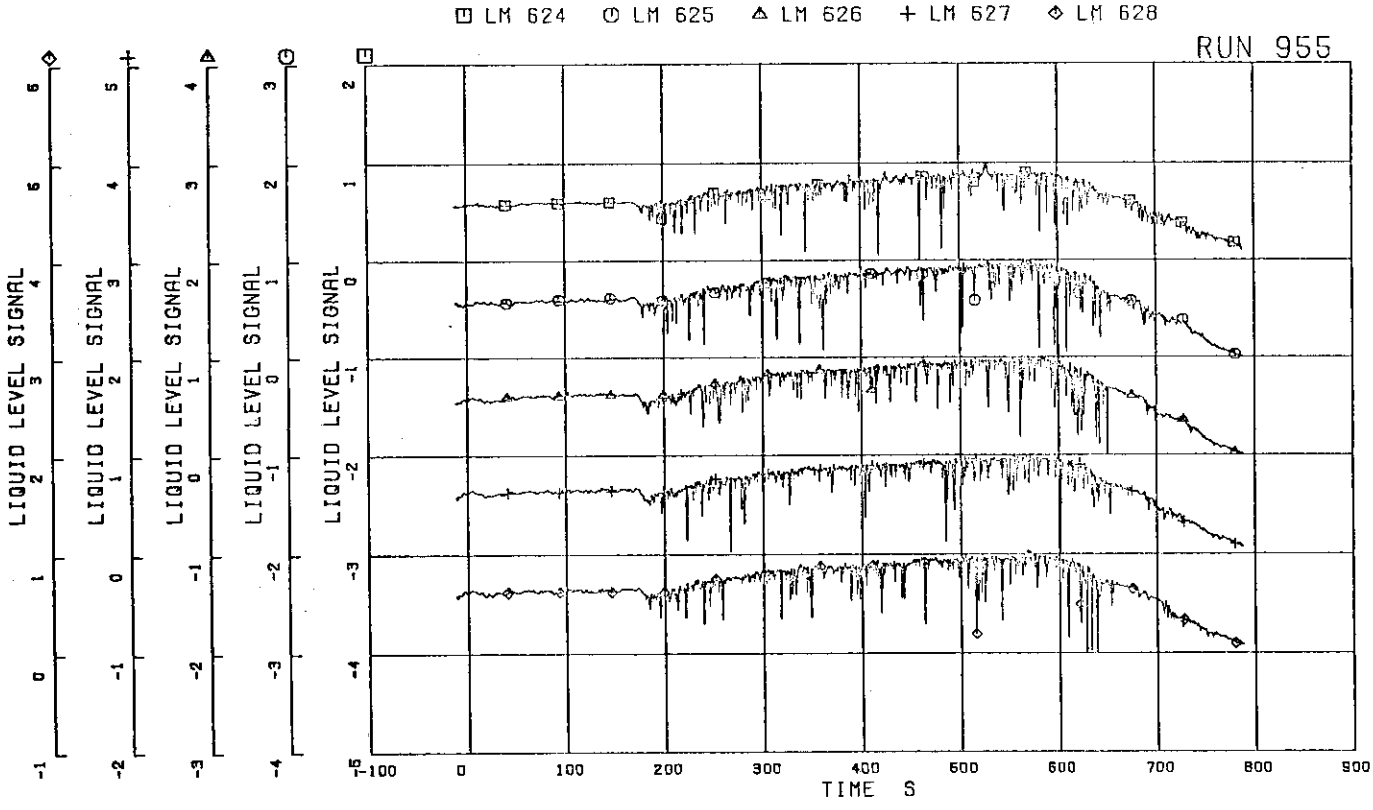

FIG.5. 88 LIQUID LEVEL SIGNALS IN LOWER PLENUM, NORTH

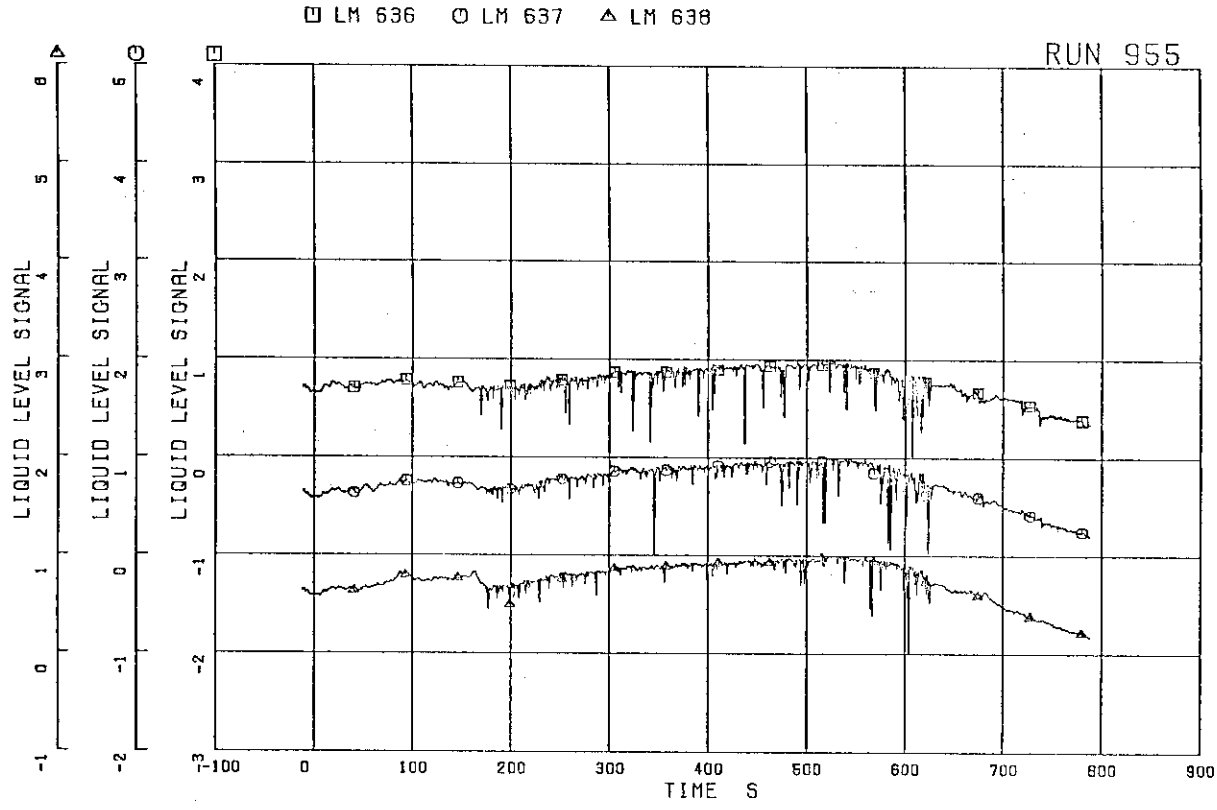

FIG.5. 89 LIQUID LEVEL SIGNALS IN GUIDE TUBE, NORTH

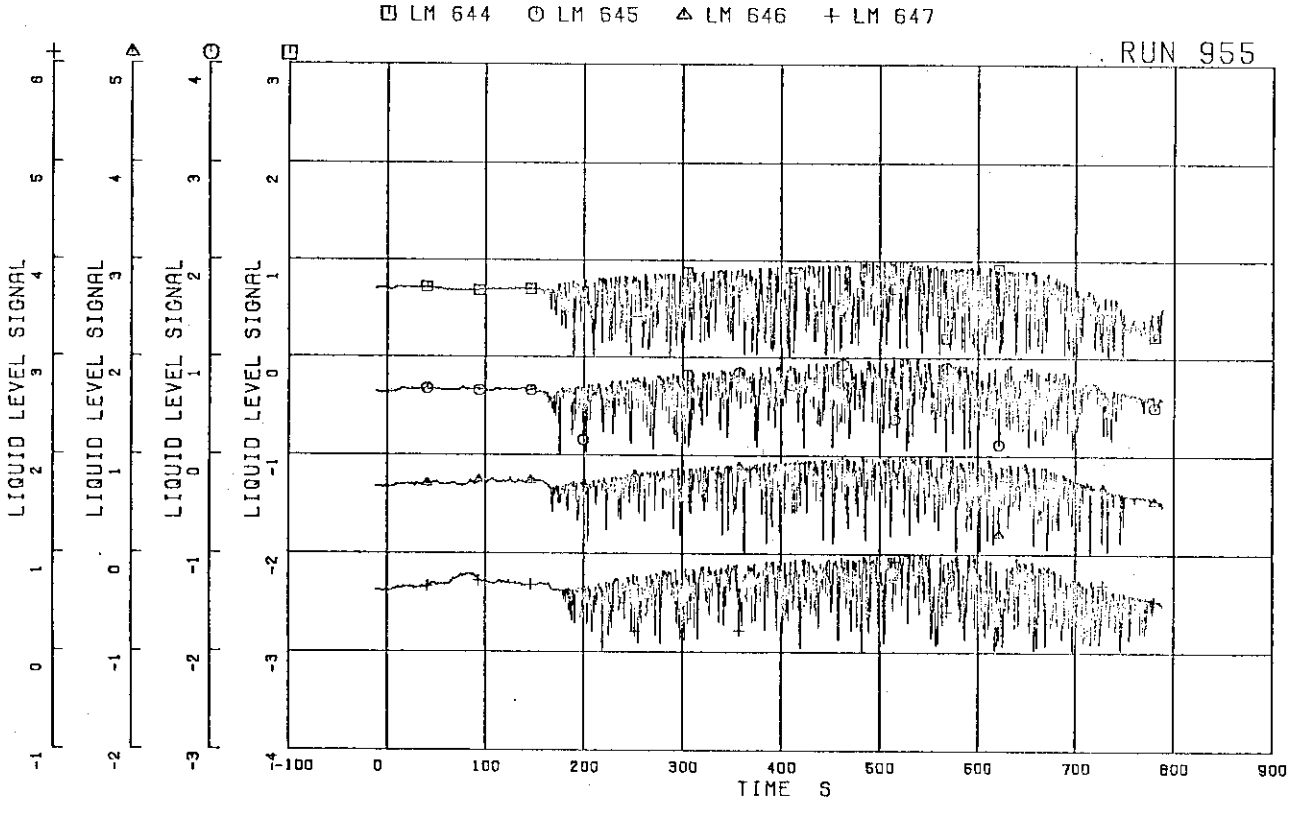

FIG.5. 90 LIQUID LEVEL SIGNALS IN DOWNCOMER, D SIDE

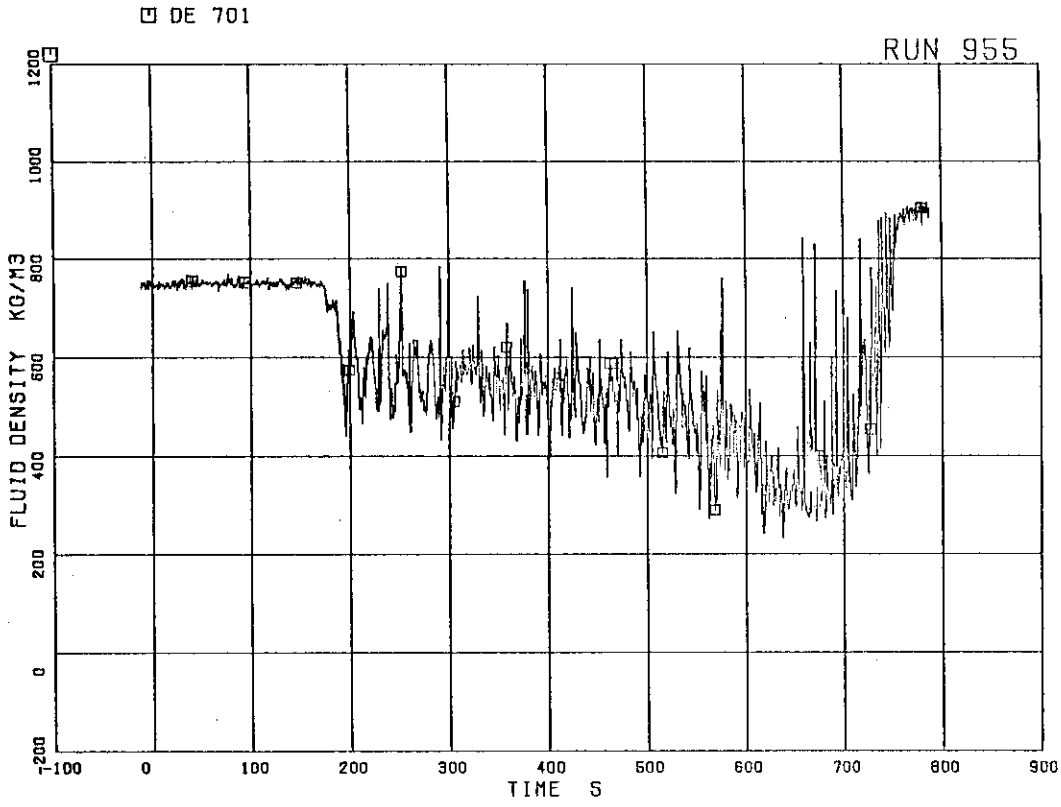

FIG.5. 91 AVERAGE DENSITY AT JP-1,2 OUTLET

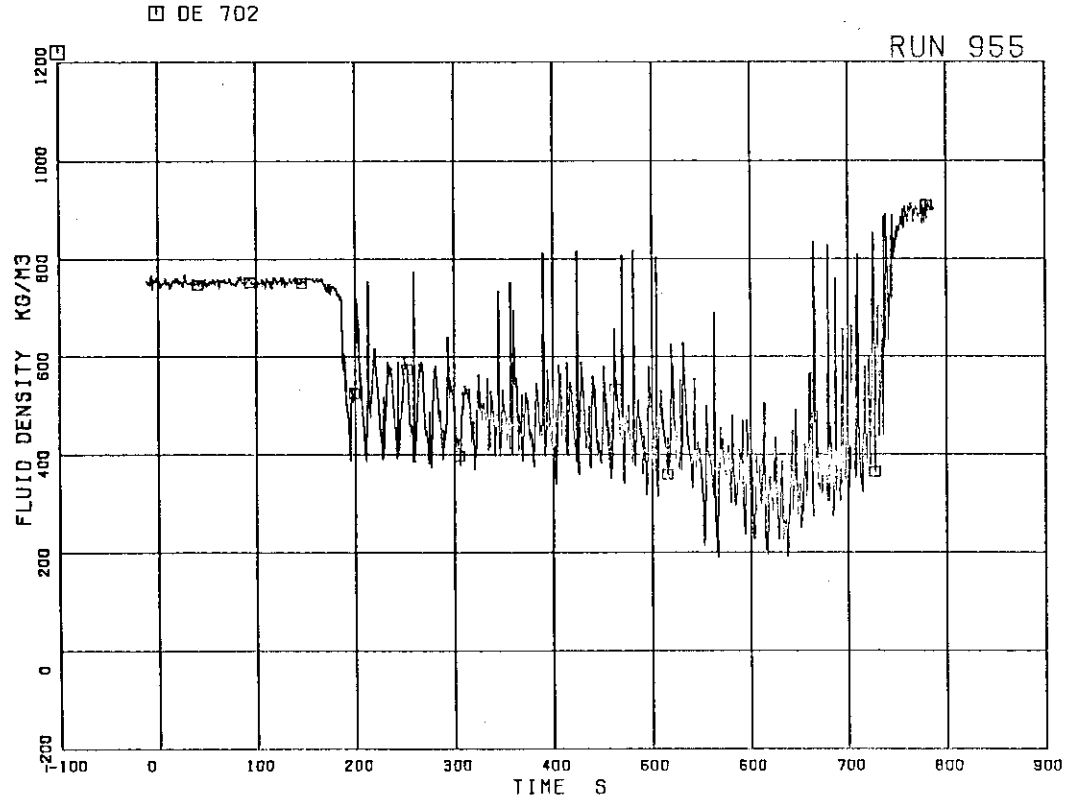

FIG.5. 92 AVERAGE DENSITY AT JP-3,4 OUTLET

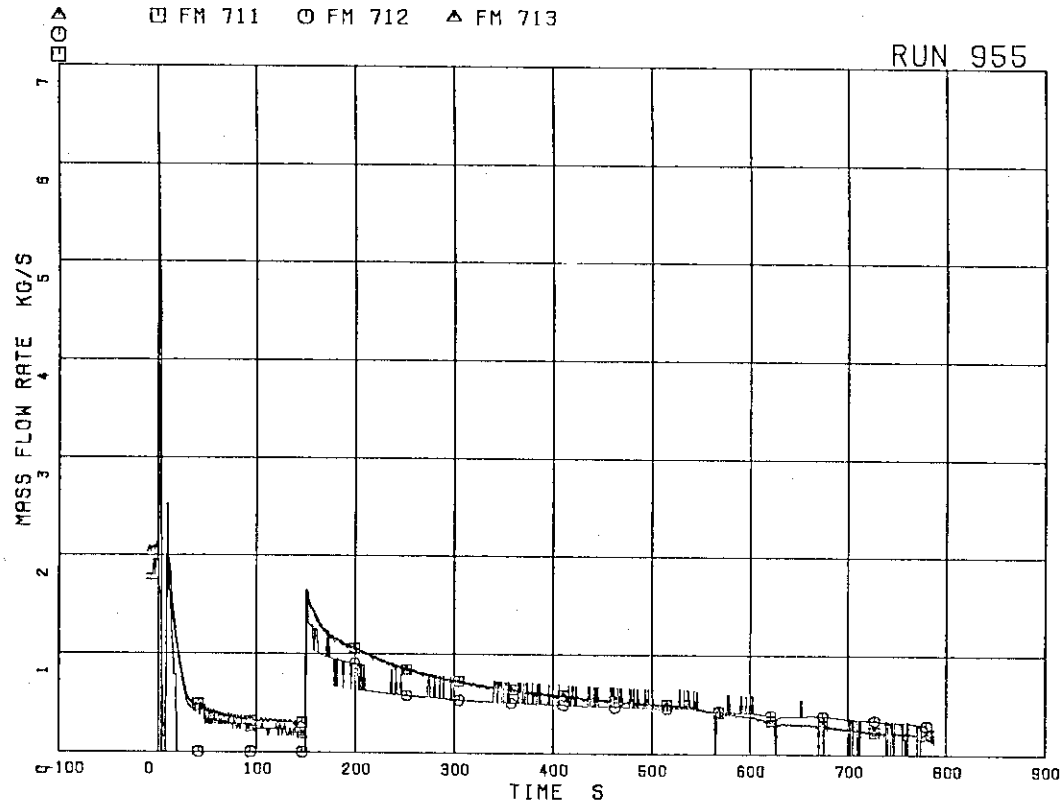

FIG.5. 93 STEAM DISCHARGE FLOW RATE THROUGH MSL

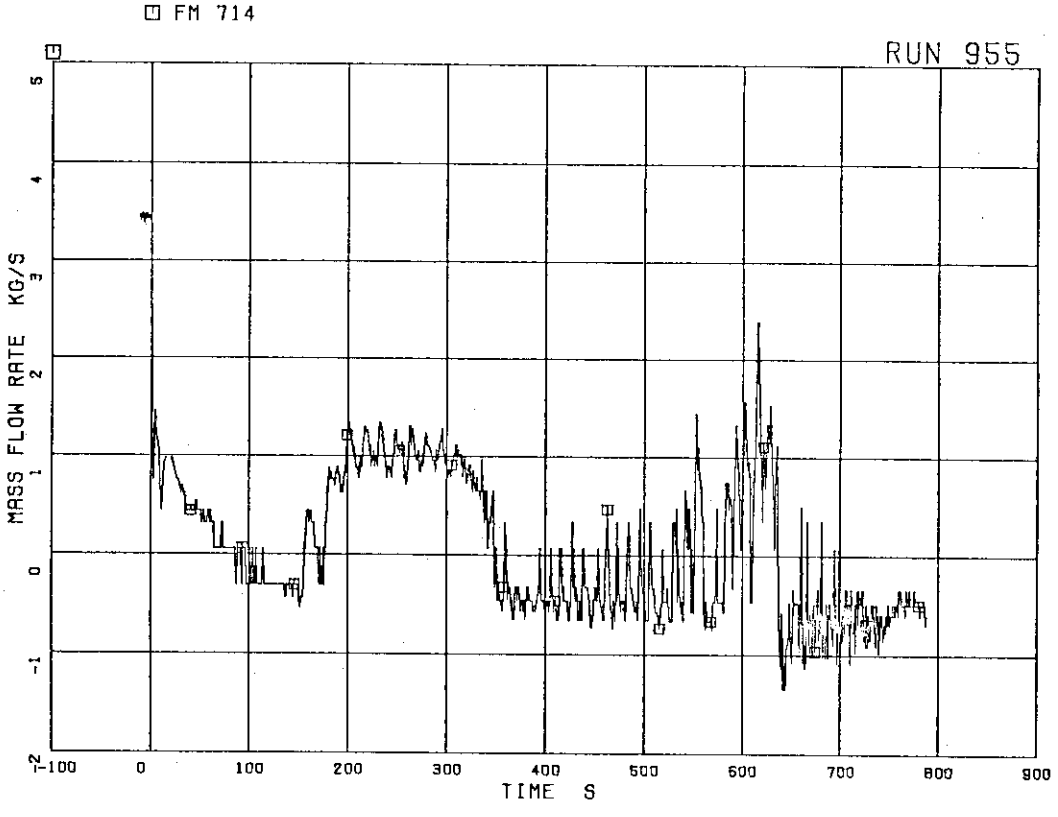

FIG.5. 94 FLOW RATE AT CHANNEL A INLET

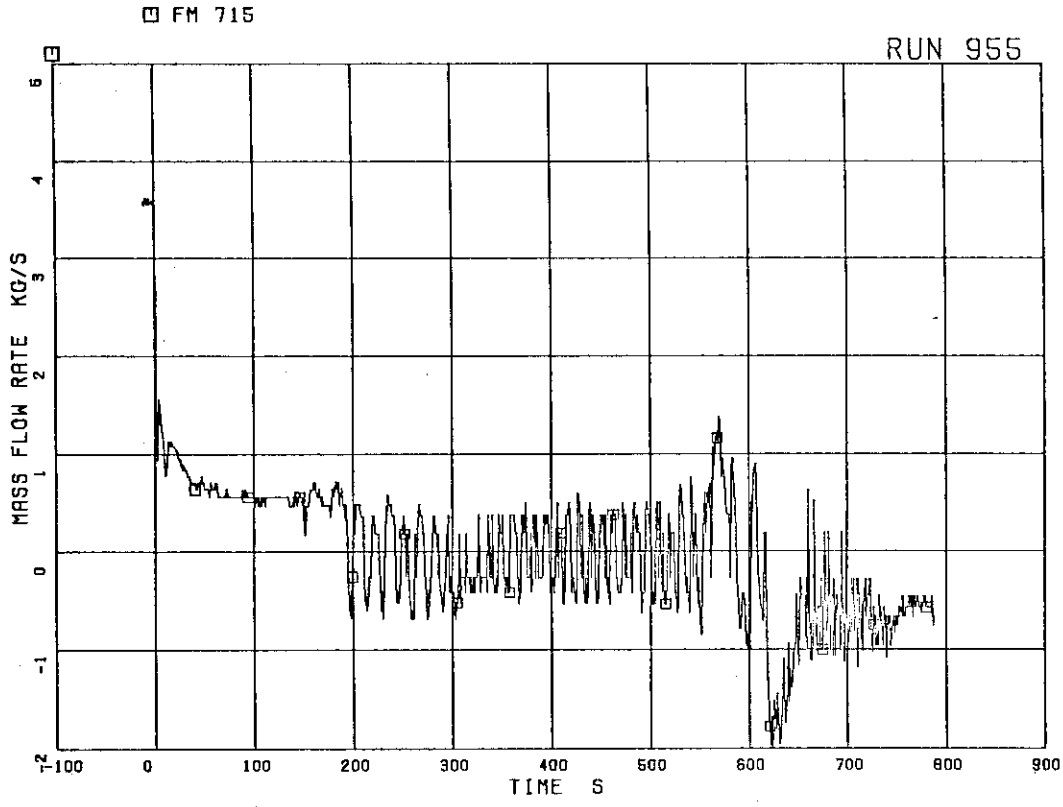

FIG.5. 95 FLOW RATE AT CHANNEL B INLET

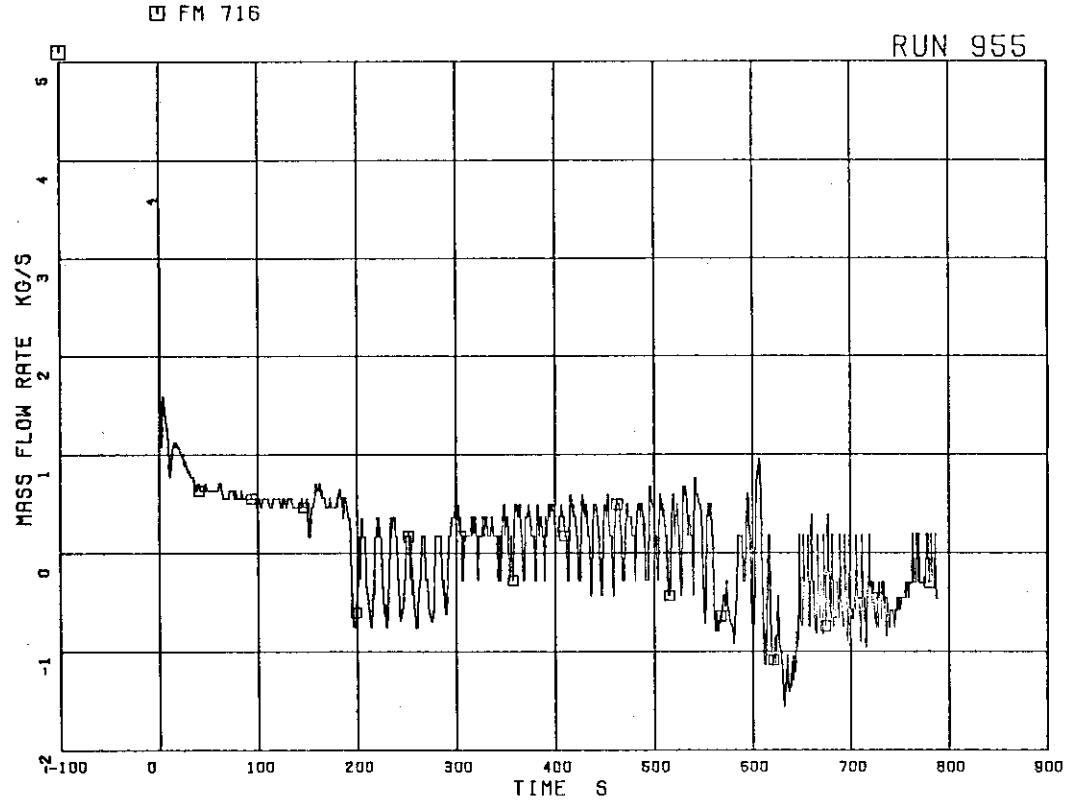

FIG.5. 96 FLOW RATE AT CHANNEL C INLET

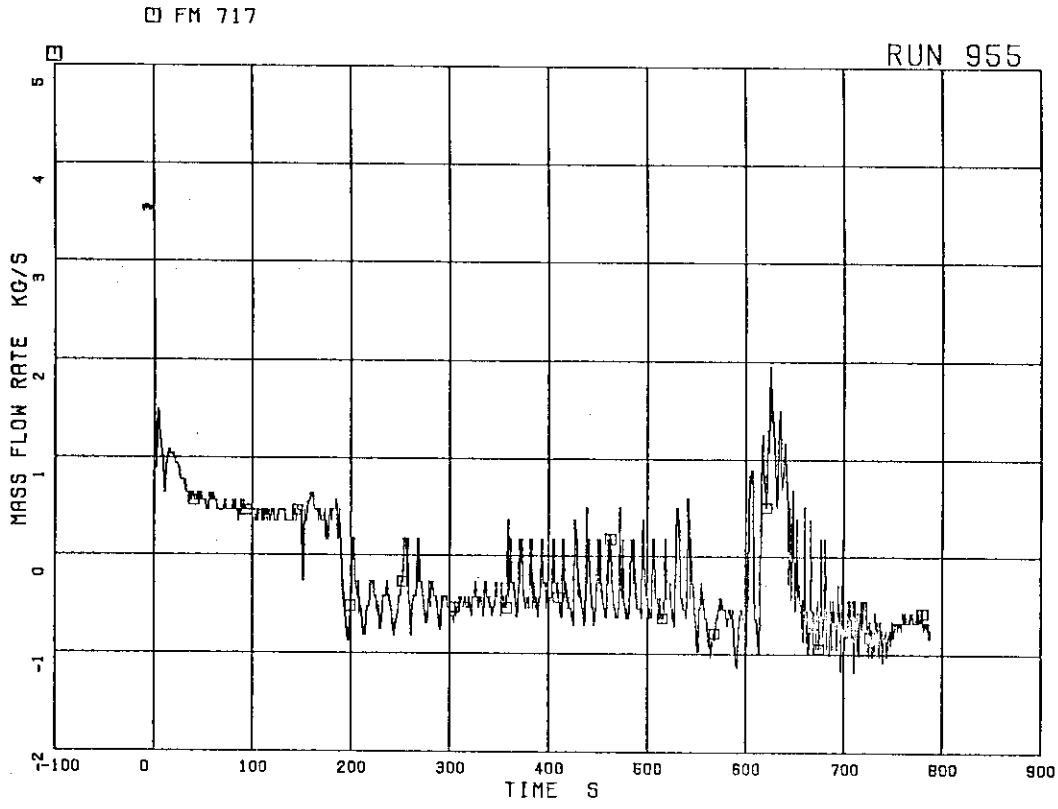

FIG.5. 97 FLOW RATE AT CHANNEL D INLET

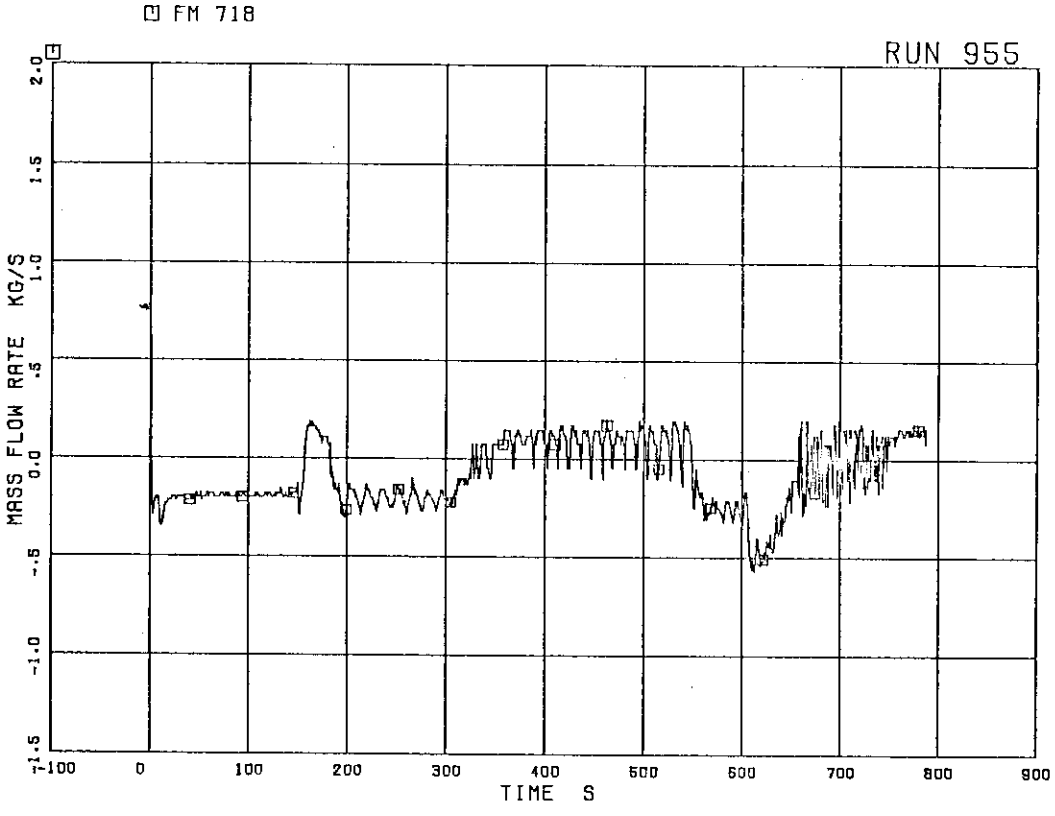

FIG.5. 98 FLOW RATE AT BYPASS HOLE

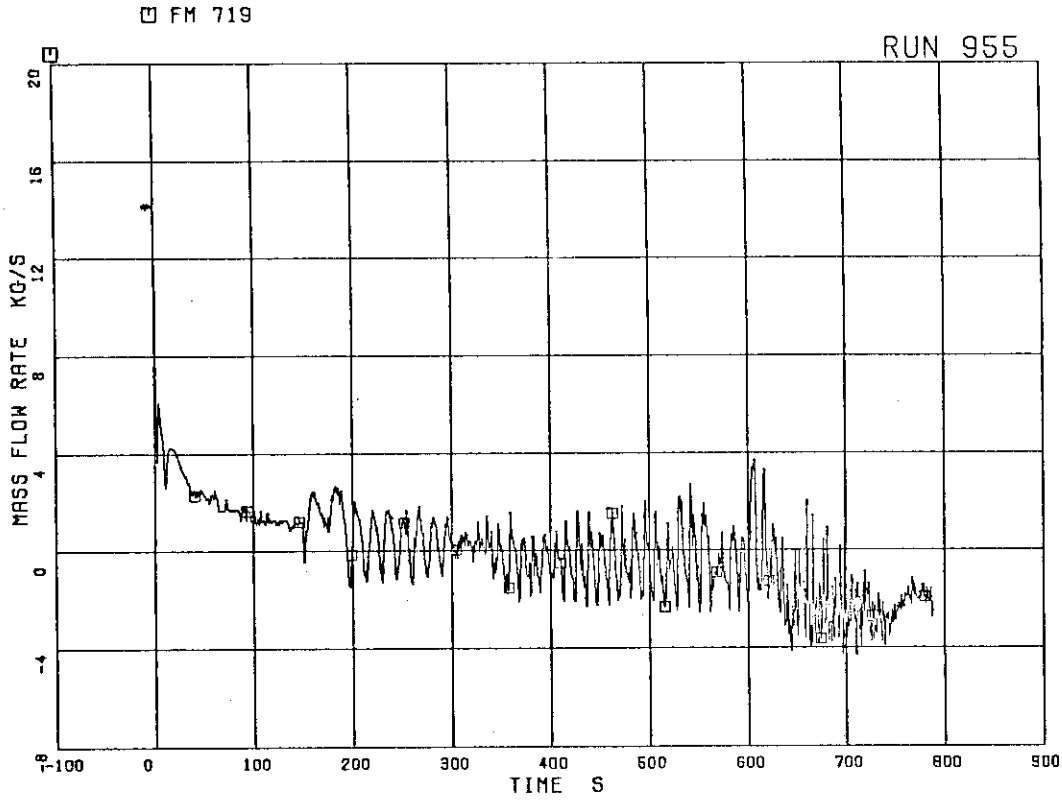

FIG.5. 99 TOTAL CHANNEL INLET FLOW RATE

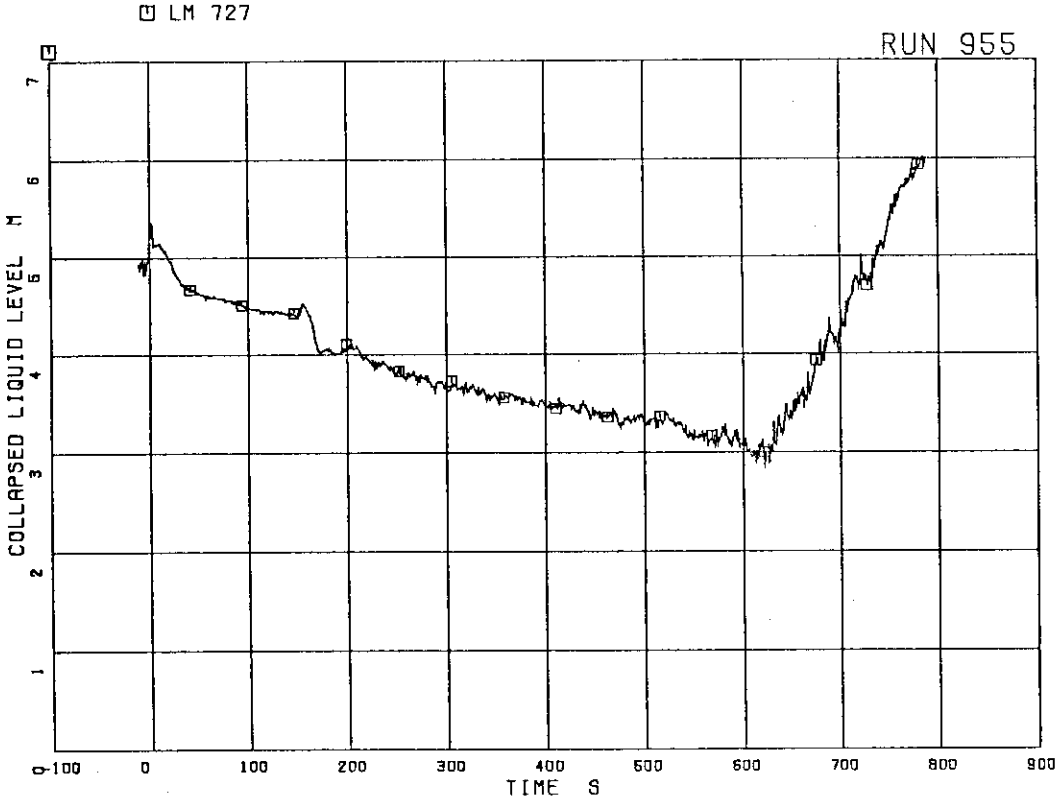

FIG.5.100 COLLAPSED LIQUID LEVEL IN DOWNCOMER

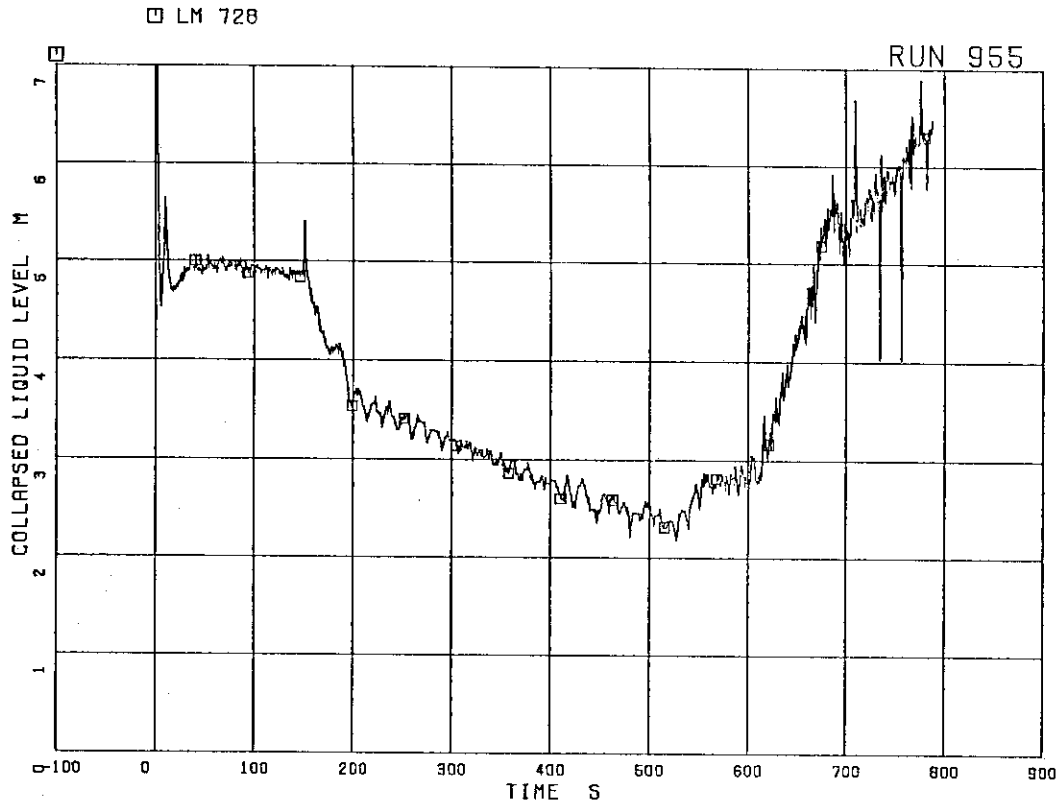

FIG.5.101 COLLAPSED LIQUID LEVEL INSIDE CORE SHROUD

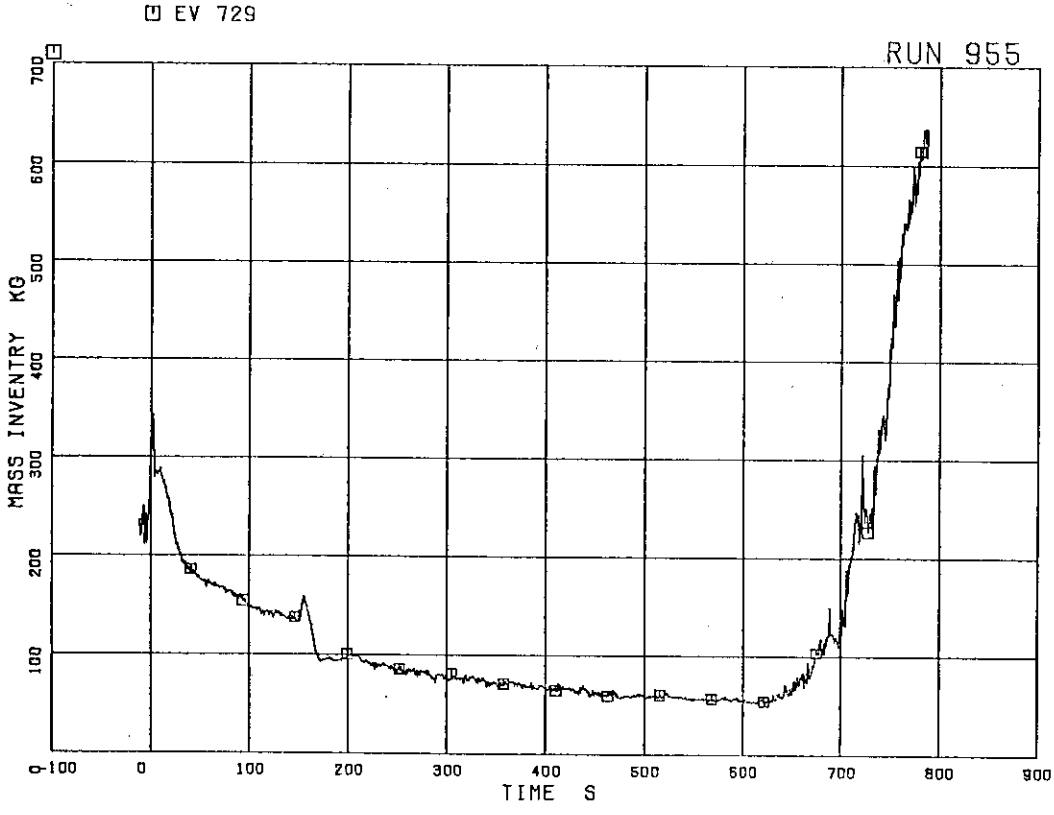

FIG.5.102 FLUID INVENTORY IN DOWNCOMER

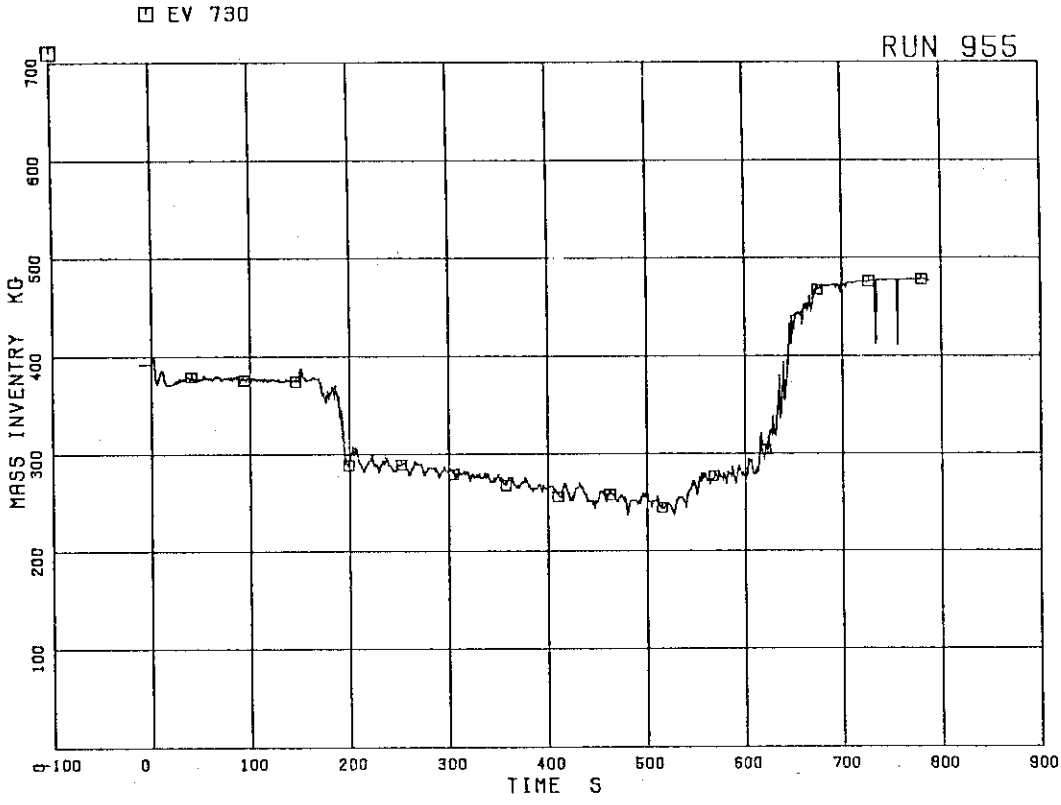

FIG.5.103 FLUID INVENTORY INSIDE CORE SHROUD

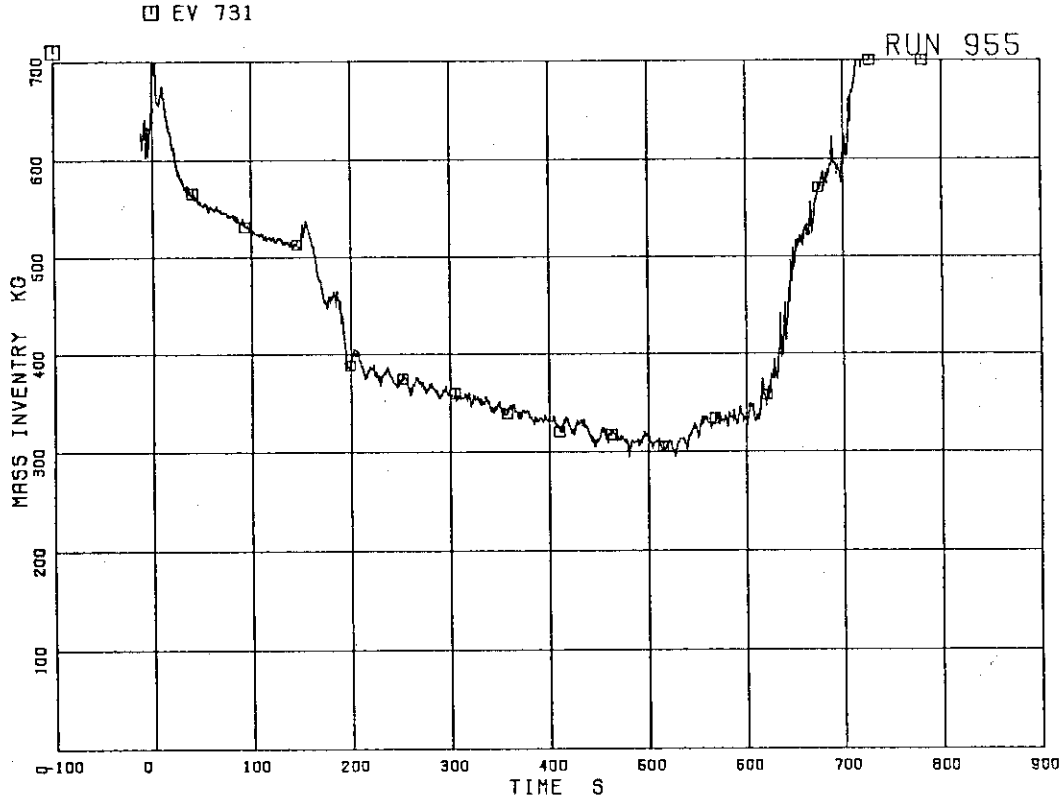

FIG.5.104 TOTAL FLUID INVENTORY IN PRESSURE VESSEL

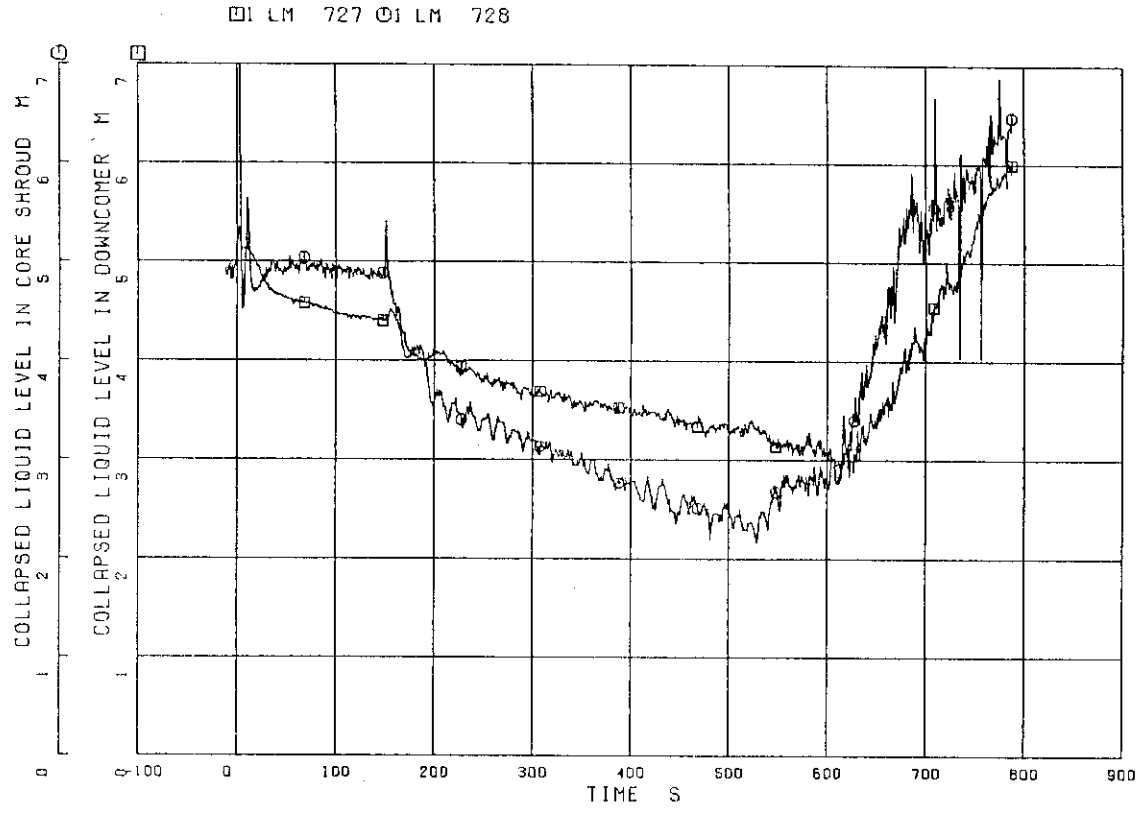

Fig. 5.105 Collapsed water levels in PV

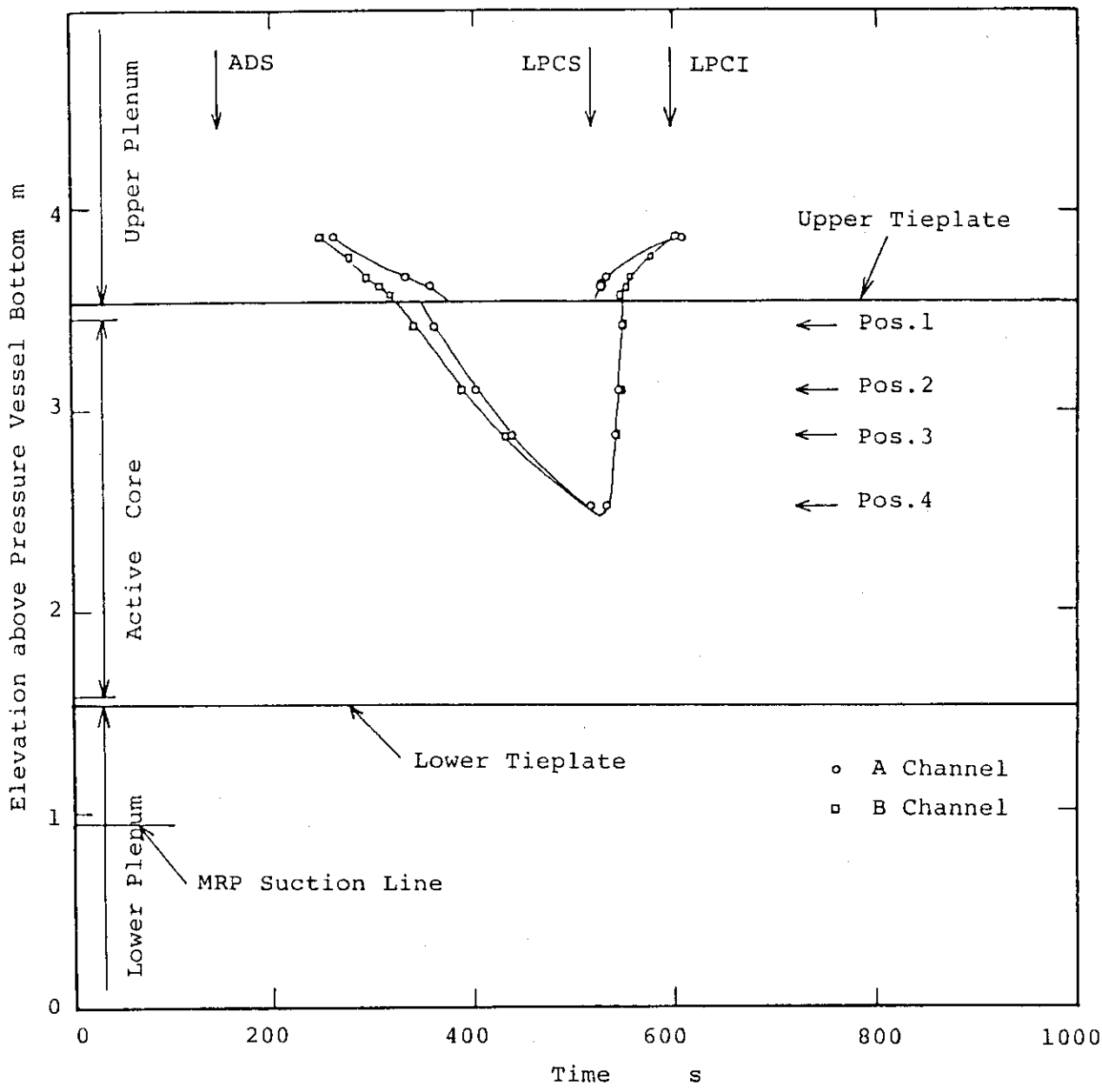

Fig. 5.106 Mixture levels in PV

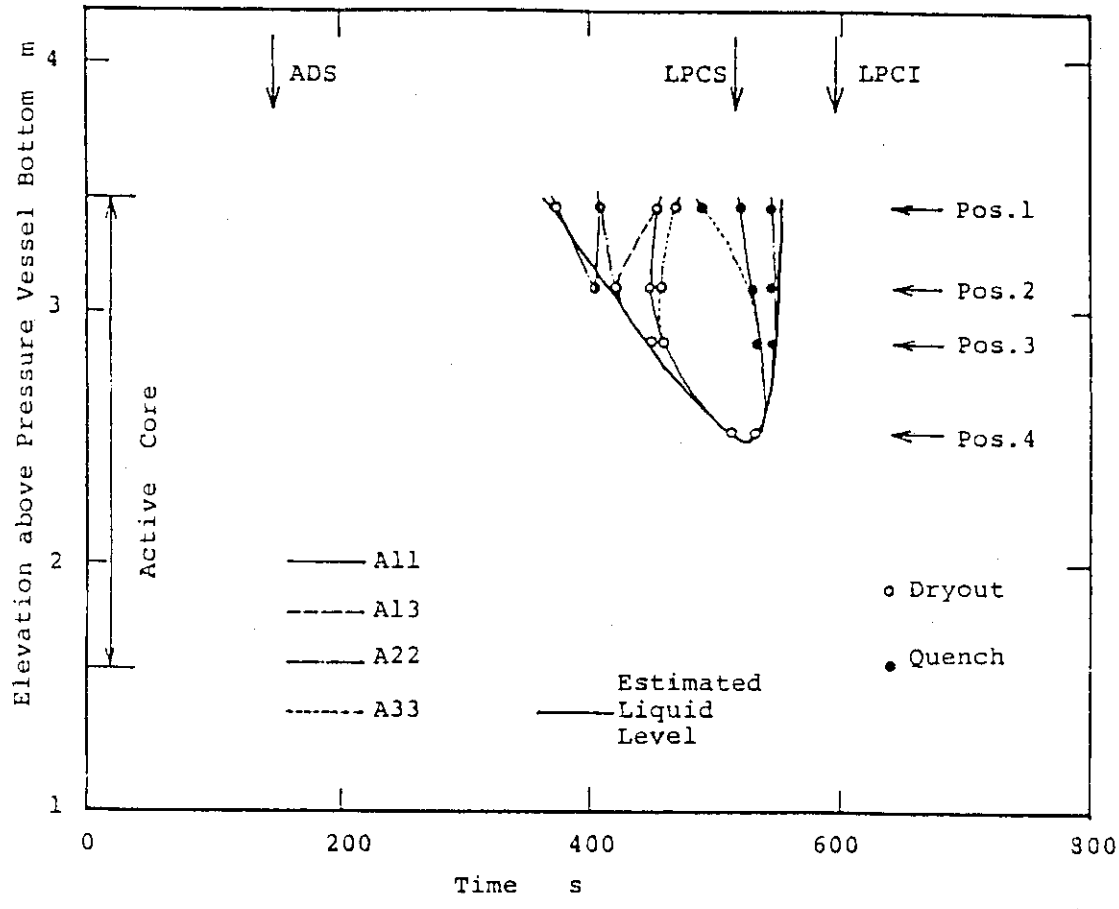

Fig. 5.107 Dryout and quench times of fuel rods in bundle A

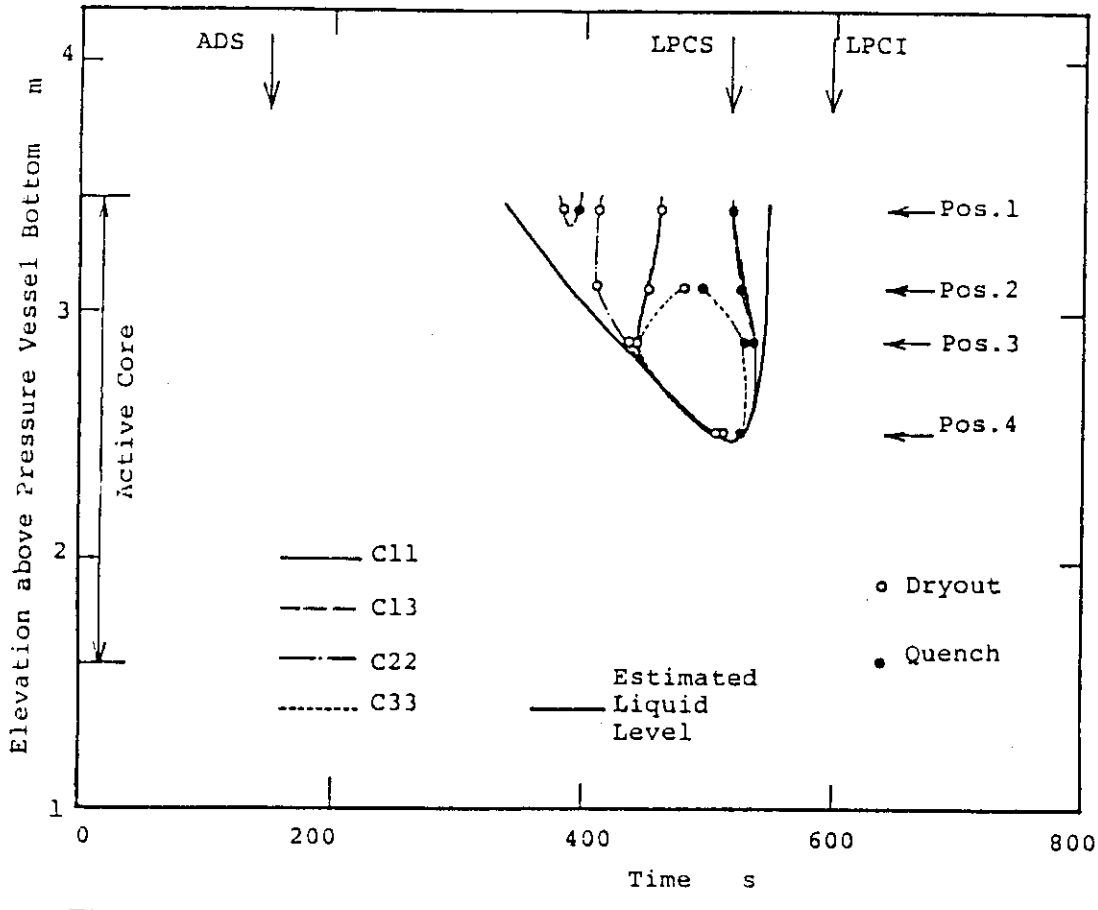

Fig. 5.108 Dryout and quench times of fuel rods in bundle C

Table 6.1 Steam mass discharged through main steam lines in RUN 955

Time (s)	Discharged Steam Mass after Break (kg)			
	Break Line (OR-5)	Steady Line (CV-130)	ADS Line (OR-4)	Total M_D
0	0	0	0	0
50	15*	42*	0	57
100	"	60	0	75
150	"	76	0	91
200	"	137		152
250	"	184		199
300	"	223		238
400	"	288		303
500	"	342		357
600	"	389		404
700	"	425		440

* Total steam mass of 20 kg discharged in the first 4 s before MSIV closure completion was divided into two parts according to their flow areas. Steam mass discharged through CV-130 during 4 and 50s was 37 kg.

Table 6.2 Average void fraction and water mass in main recirculation line and jet pumps in RUN 955

Time (s)	Saturated Water Density ρ (kg/m^3)	Void Fraction (α) in MRP outlet Line	Water Mass M (kg)*
0	(752)	0.0	129
200	766	0.17	109
250	786	0.32	92
300	802	0.33	92
400	822	0.33	94
500	839	0.36	92
600	860	0.48	76
700	887	0.81	29

* Fluid volume in main recirculation loops and jet pumps is 0.172 m^3. The water mass M in the transient phase was calculated by a following relation with suffix 0 for the initial state,

$$M = M_o \times (\rho/\rho_o) \times (1 - \alpha).$$

Table 6.3 Estimation of PV mass inventory by two methods in RUN 955
(remained mass and discharged mass)

Time	PV Mass*1 M_A (kg)	PV Mass*2 M_B (kg)	Difference $(M_A-M_B)/M_B$	Total System Mass M_T*3 (kg)	Transient Total Mass Ratio M_T/M_{To}	Note
0	623	579	0.08	708	1.00	MSIV trip at 3s
50	555	528	0.05	657	0.93	
100	525	510	0.03	639	0.90	
150	508	494	0.03	623	0.88	ADS trip at 150s
200	392 (458)*4	453	-0.13 (0.00)*4	562	0.79	
250	374 (421)*4	423	-0.12 (0.00)*4	515	0.73	
300	358 (392)*4	384	-0.07 (0.02)*4	476	0.67	
400	333	317	0.05	411	0.58	
500	308	265	0.16	357	0.50	
600	337	322	0.05	398	0.56	LPCS (516s) LPCI (591s)
700	600	800	-0.25	829	1.17	

*1 M_A is shown by total PV fluid mass in Fig. 5.104.

*2 M_B is obtained as M_T-M (Table 6.2).

*3 M_T is obtained as M_o-M_D (Table 6.1) + M_F (Feedwater) + M_I (ECCS water).

*4 Mass in the upper downcomer was corrected by the upper downcomer water level.

Table 6.4 Test conditions of RUNs 955, 920 and 923

Items	Unit	RUN 955	RUN 920	RUN 923
Break Conditions				
Location		MSL outside RCV	MRL Suction Line	MRL Suction Line
Break Diameter	mm	31.0	3.7	0.0
Area Ratio to 1/424 Scaled BWR MRL Area	%	140	2	0
Initial Conditions				
Steam Dome Pressure	MPa	7.36	7.35	7.35
Lower Plenum Subcooling	K	10.7	10.3	10.3
Core Inlet Flow Rate	kg/s	16.8	16.5	16.4
Core Power	MW	3.98	3.96	3.96
Upper Plenum Quality	%	12.6	12.5	12.6
Water Level	m	5.0	5.0	5.0
Transient Conditions				
MSIV Closure	s	3	L2 + 3	L2 + 3
Relief Valve Operation	MPa	8.0	8.2	8.1
Feedwater Stop	s	2 - 4	2 - 4	2 - 4
MRP Coast Down	s	0.0	0.0	0.0
ECCS Conditions				
HPCS		Failure	Failure	Failure
LPCS Actuation	MPa	2.2	2.3	2.2
LPCI Actuation	MPa	1.7	1.7	1.7
ADS Actuation	s	L2 + 120	L1 + 120	L1 + 120

L2 level : 4.76 m from PV bottom

L1 level : 4.25 m from PV bottom

Table 6.5 Comparison of major events among the three tests

Events	Time after Break (s)		
	RUN 955	RUN 920	RUN 923
MSIV Closure	3	29	35
SRV Operation	8	71	85
L2 Level Trip	28	28	30
ADS Actuation	150	188	355
Core Dryout Initiation	330	280	535
L1 Level Trip	440	68	235
LPCS Actuation	516	435	685
PCT	540	530	697
Final Core Quench	546	554	725
LPCI Actuation	591	531	773
PCT Value (K)	646	801	637

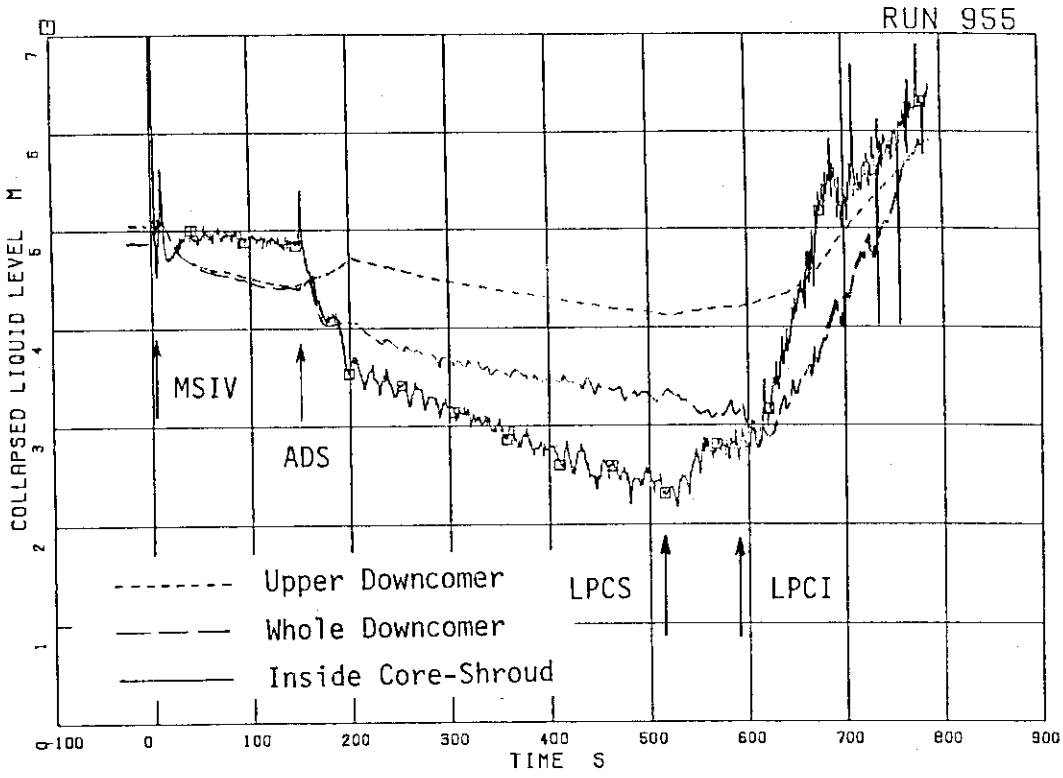

Fig. 6. 1 Collapsed watere levels inside core-shroud, in whole downcomer and upper downcomer in RUN 955

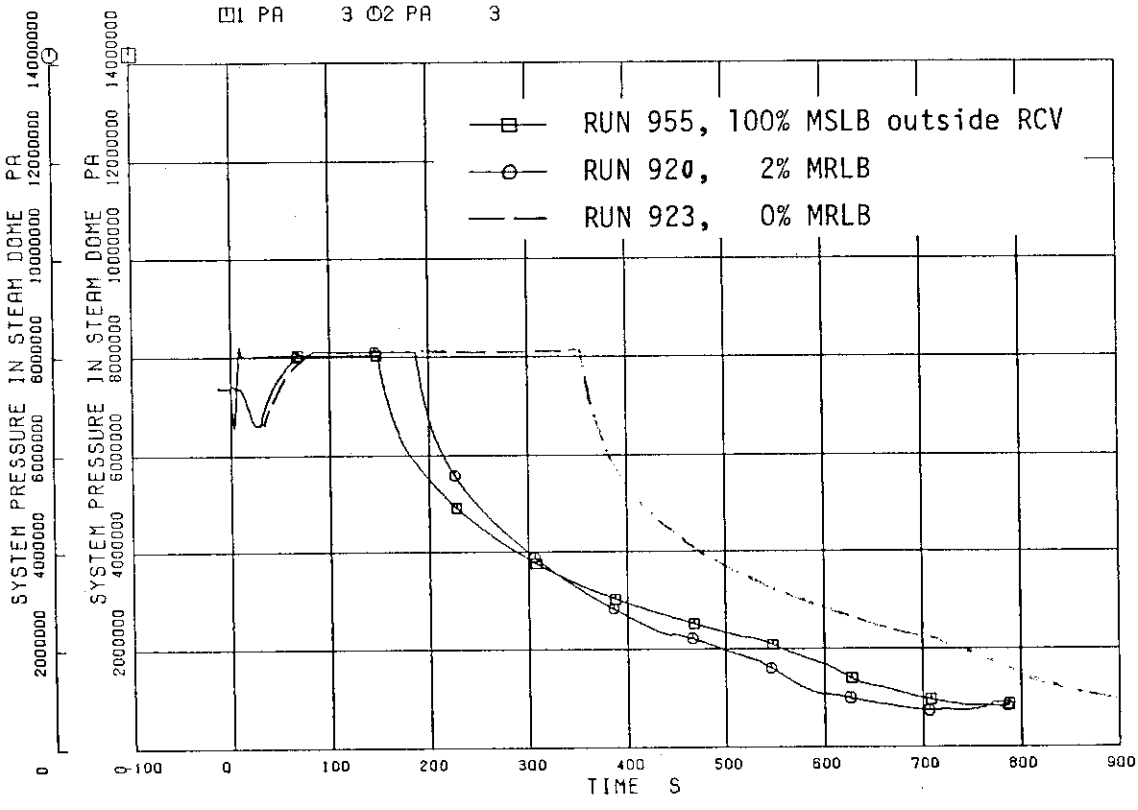

Fig. 6. 2 Comparison of pressure transient among three tests

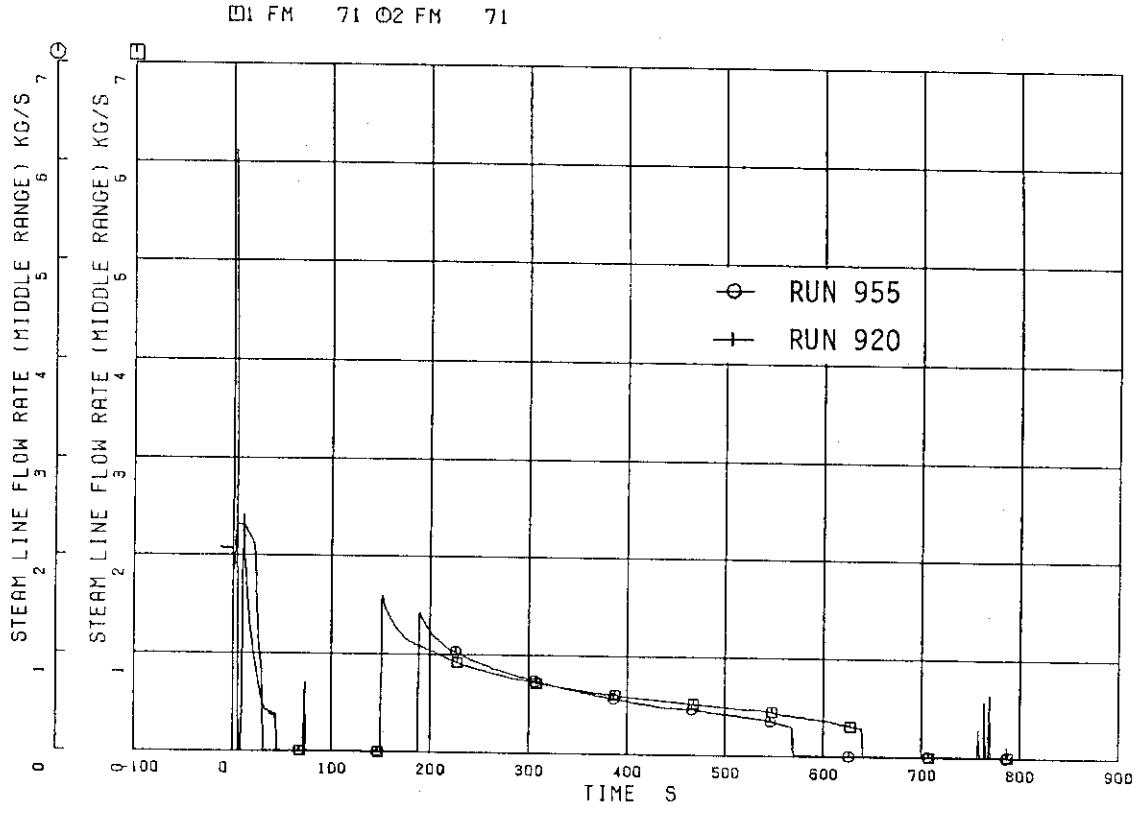

Fig. 6. 3 Comparison of steam line flow rates between RUNs 955 and 920

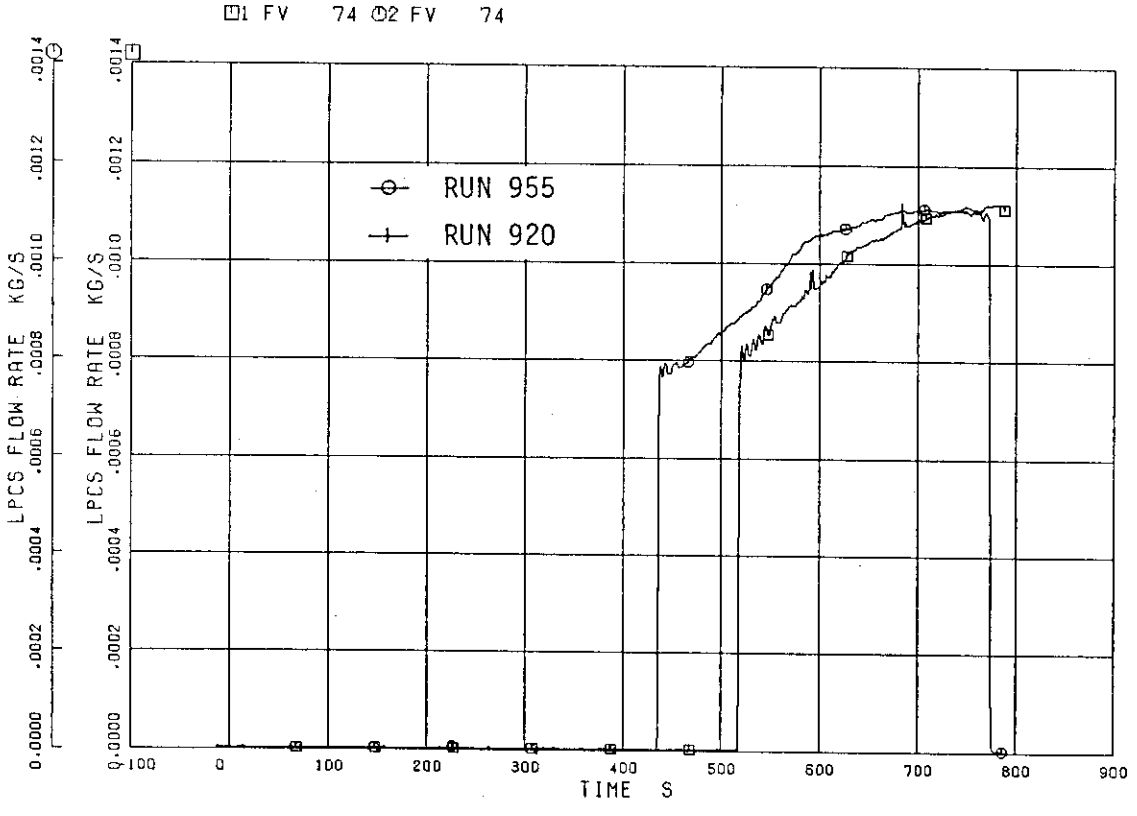

Fig. 6. 4 Comparison of LPCS flow rates between RUNs 955 and 920

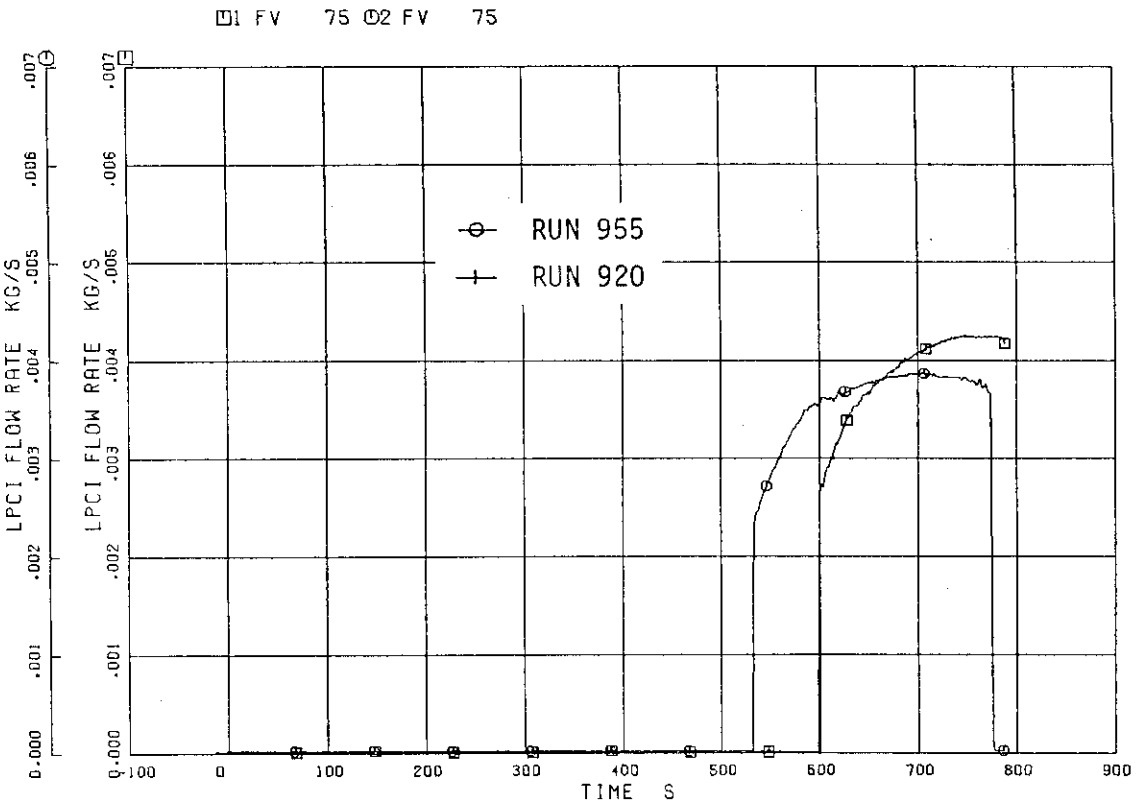

Fig. 6. 5 Comparison of LPCI flow rates between RUNs 955 and 920

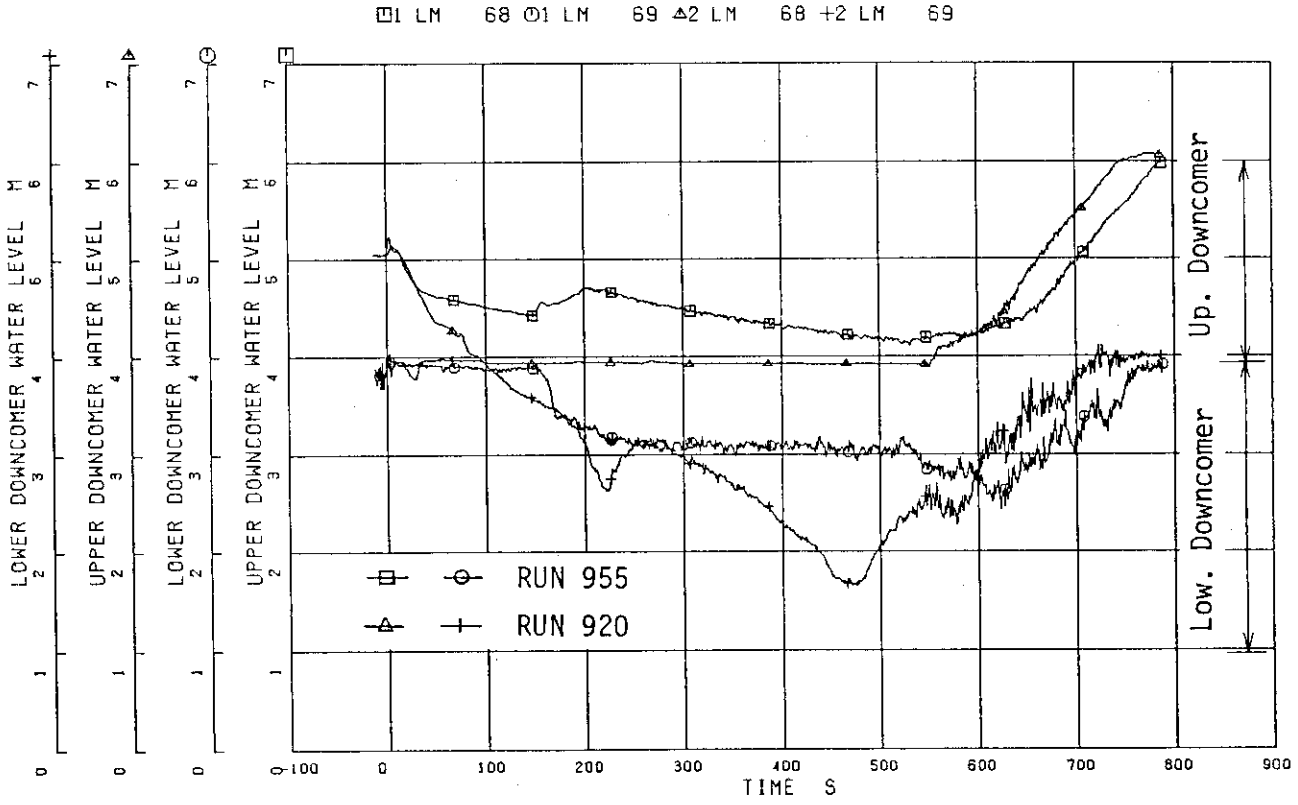

Fig. 6. 6 Comparison of water levels in both upper and lower downcomer

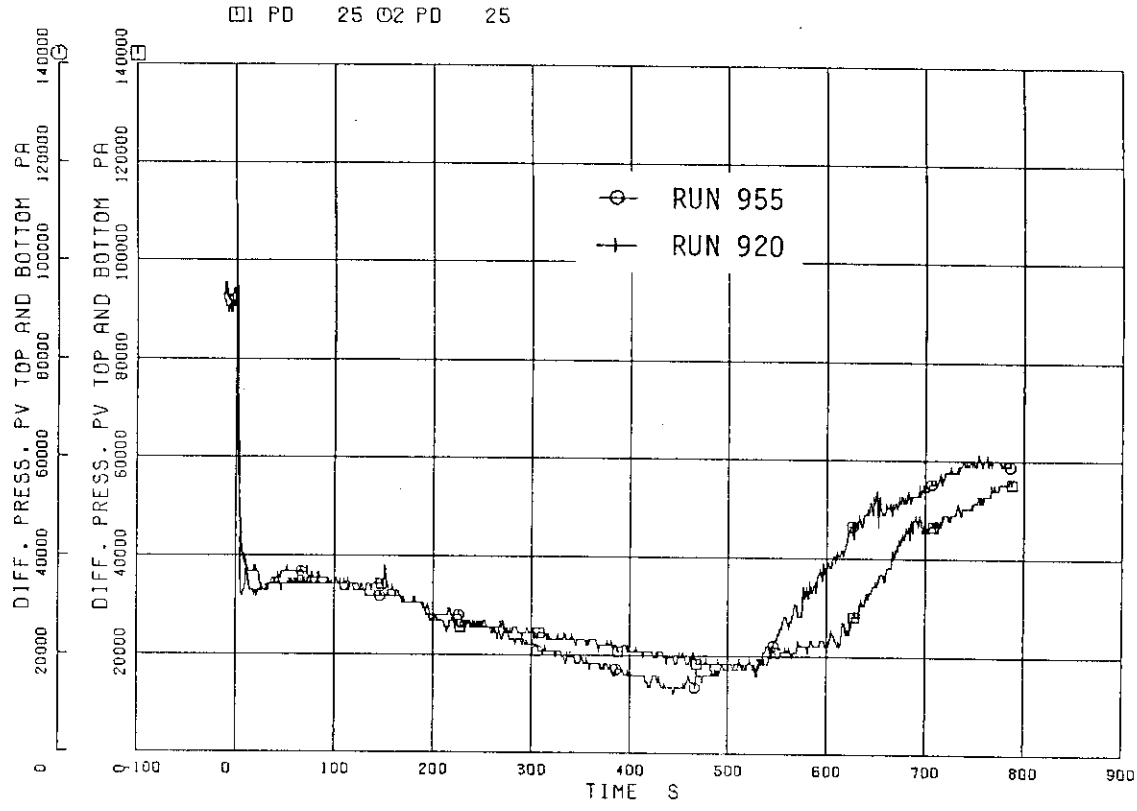

Fig. 6. 7 Comparison of differential pressure between PV top and bottom in RUNs 955 and 920

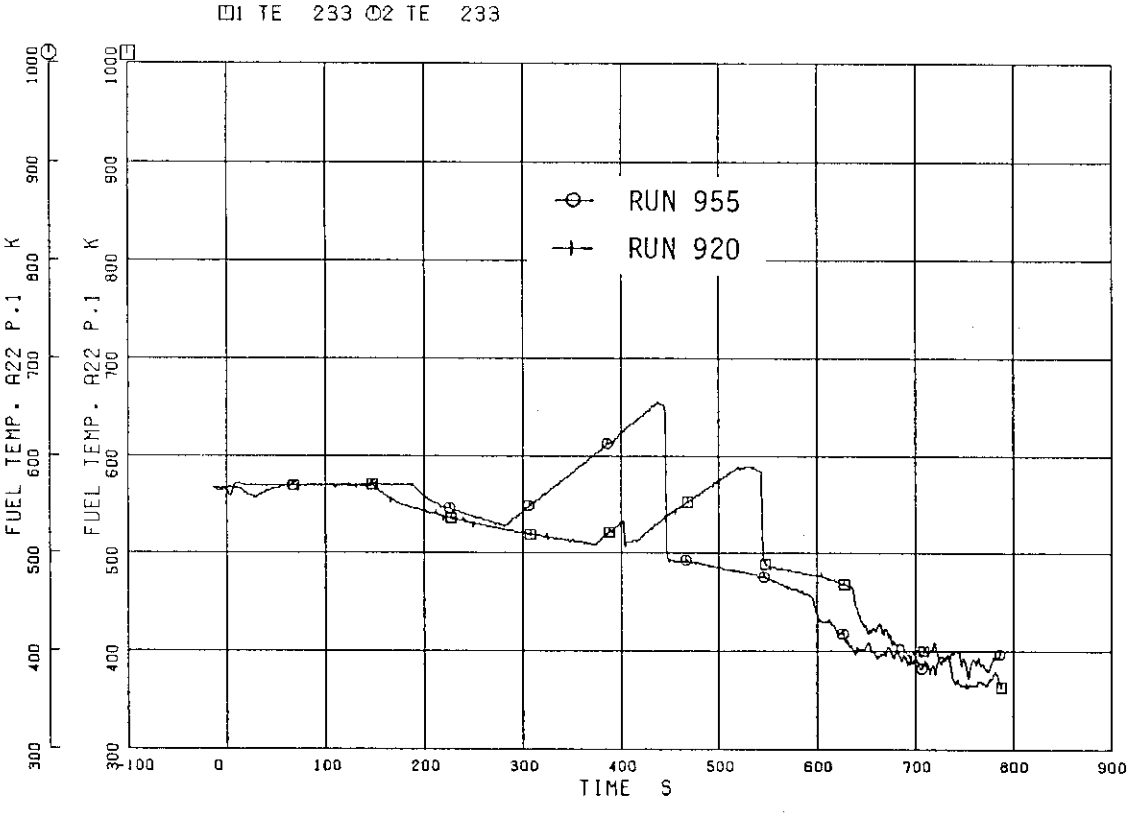

Fig. 6. 8 Comparison of fuel surface temperatures at position 1 (top) of average-power rod A22 between RUNs 955 and 920

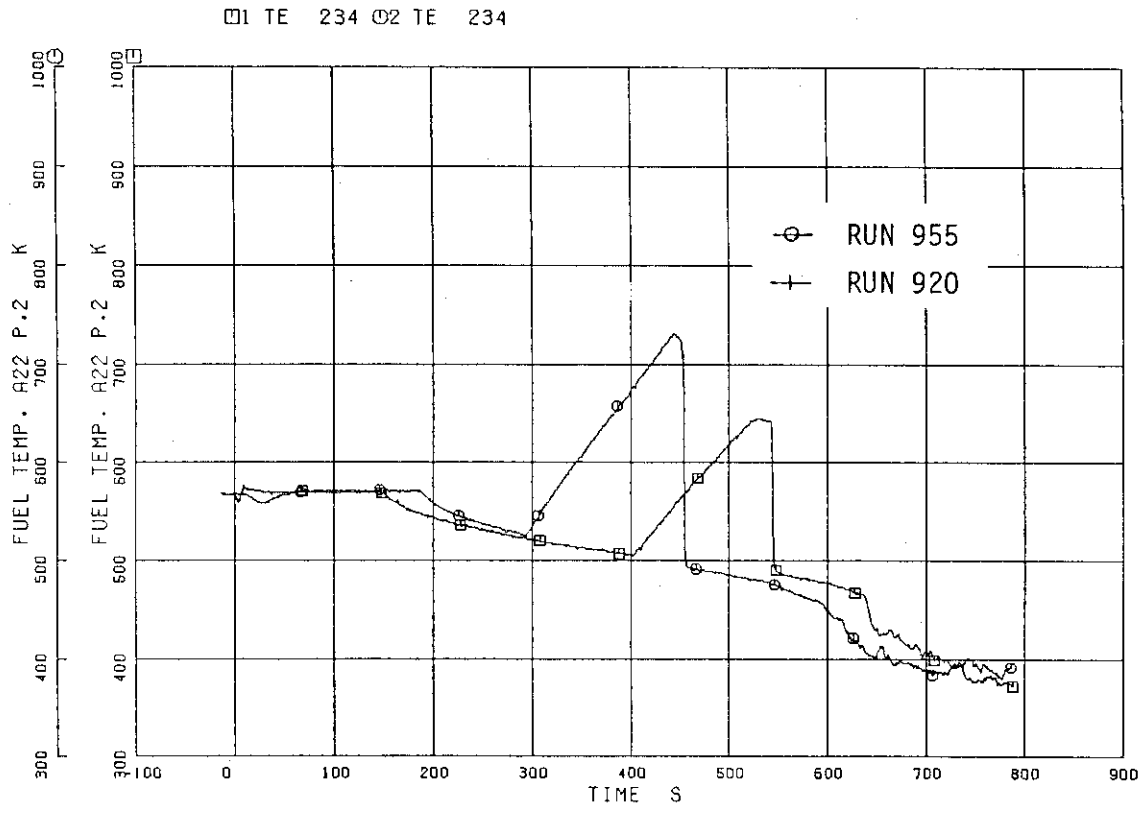

Fig. 6. 9 Comparison of fuel surface temperatures at position 2 of average-power rod A22 between RUNs 955 and 920

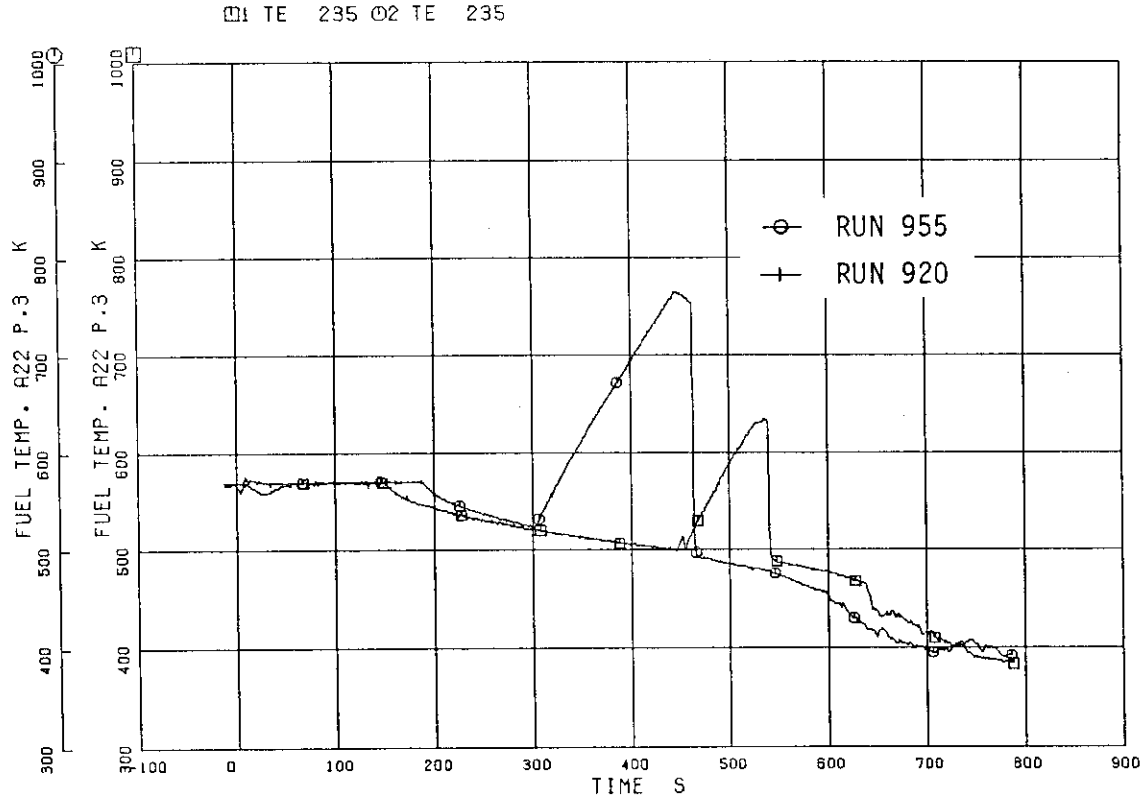

Fig. 6.10 Comparison of fuel surface temperatures at position 3 of average-power rod A22 between RUNs 955 and 920

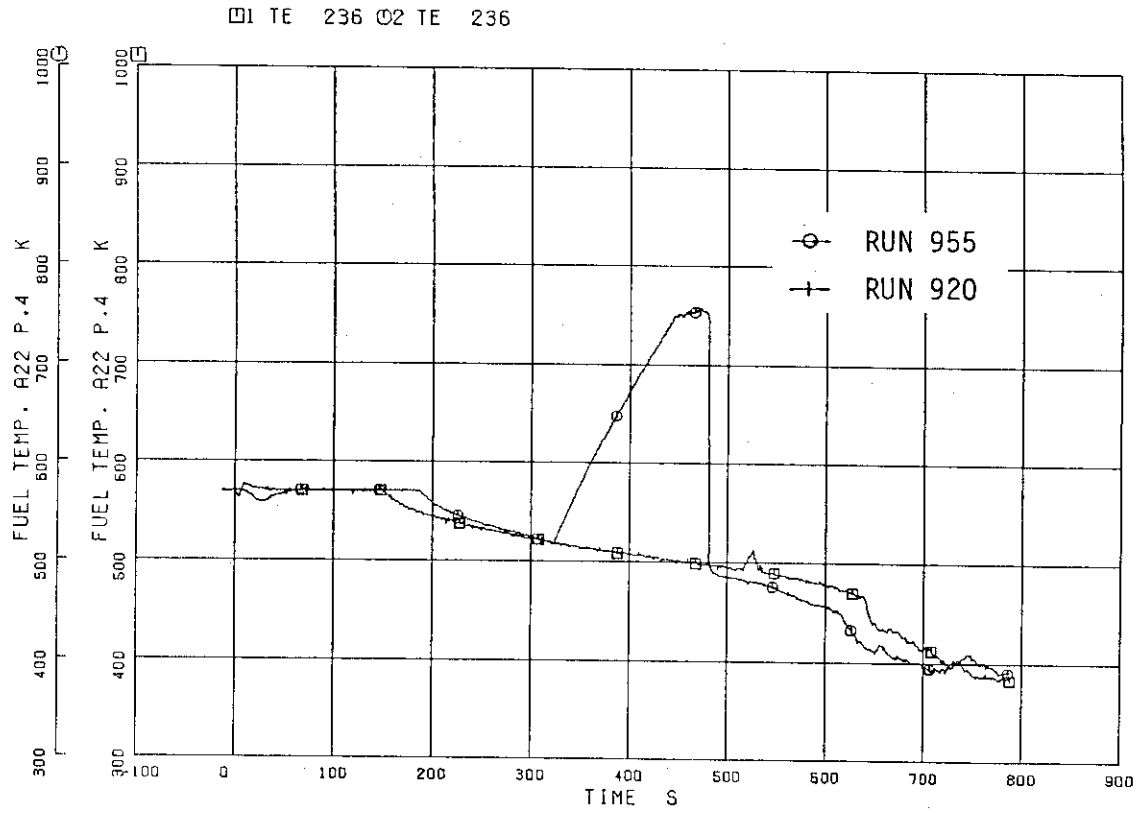

Fig. 6.11 Comparison of fuel surface temperatures at position 4 of average-power rod A22 between RUNs 955 and 920

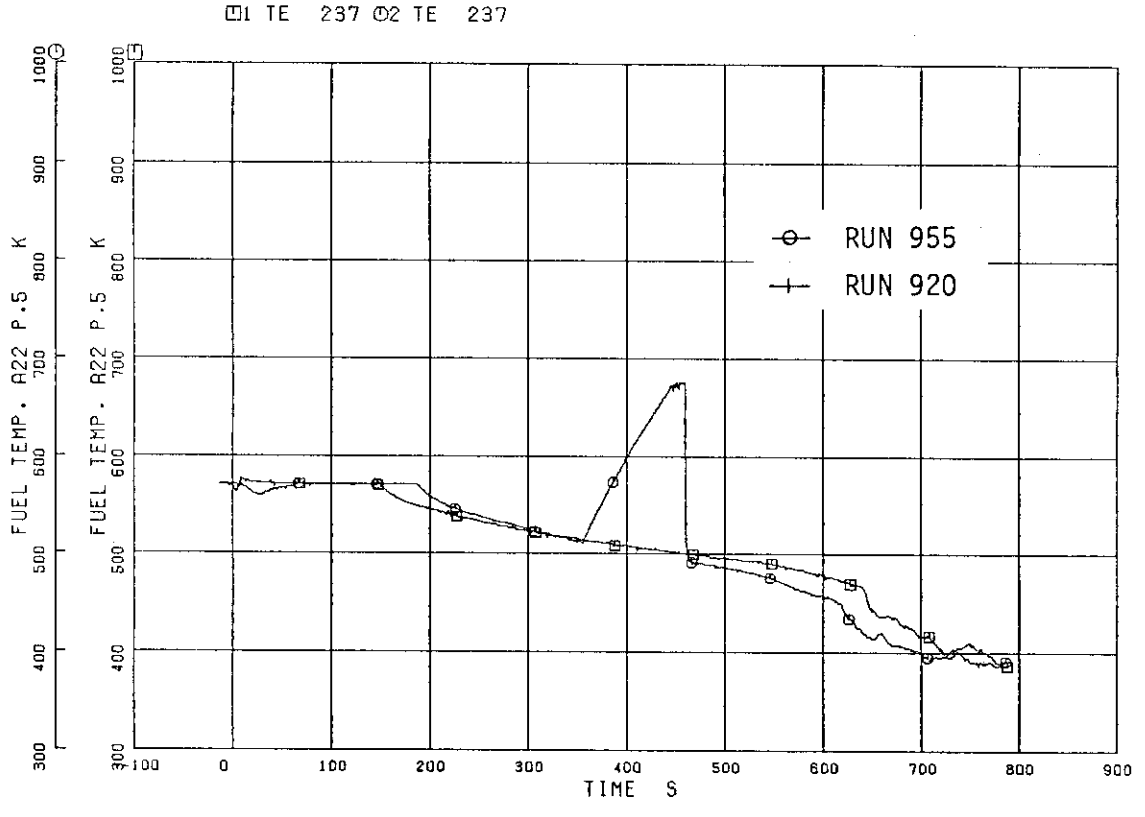

Fig. 6.12 Comparison of fuel surface temperatures at position 5 of average-power rod A22 between RUNs 955 and 920

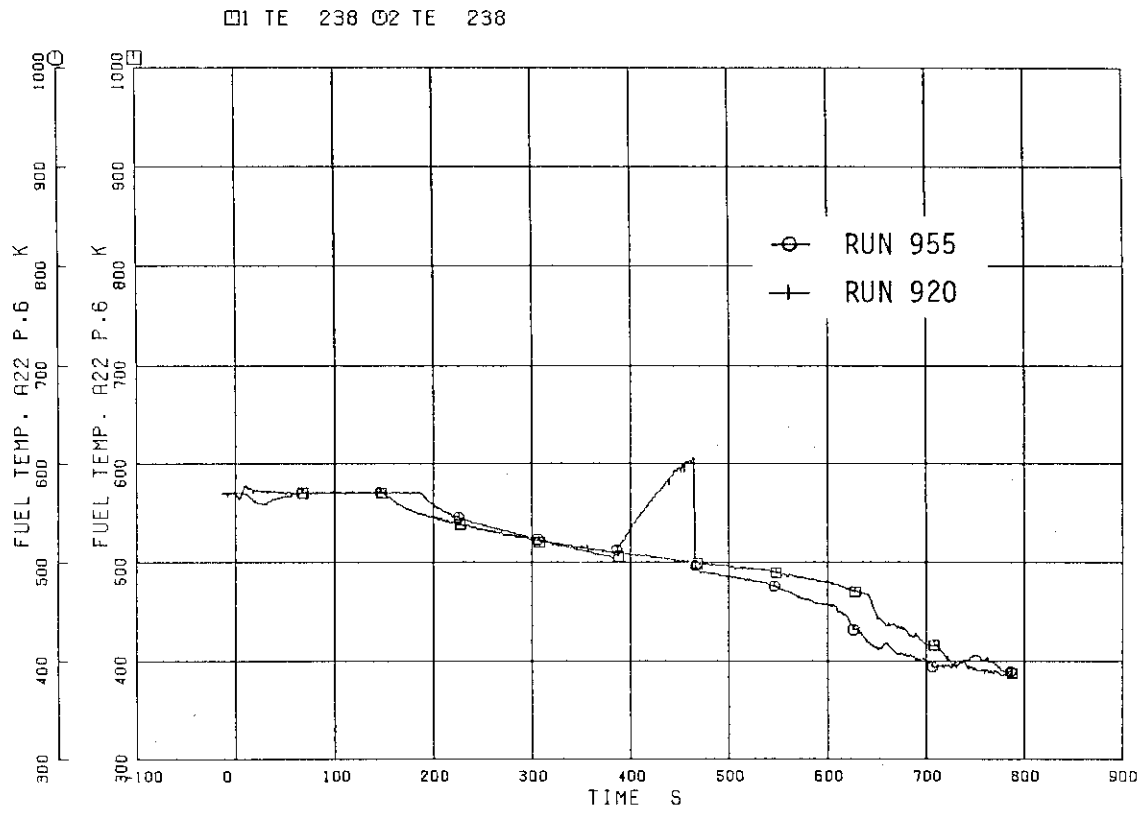

Fig. 6.13 Comparison of fuel surface temperatures at position 6 of average-power rod A22 between RUNs 955 and 920

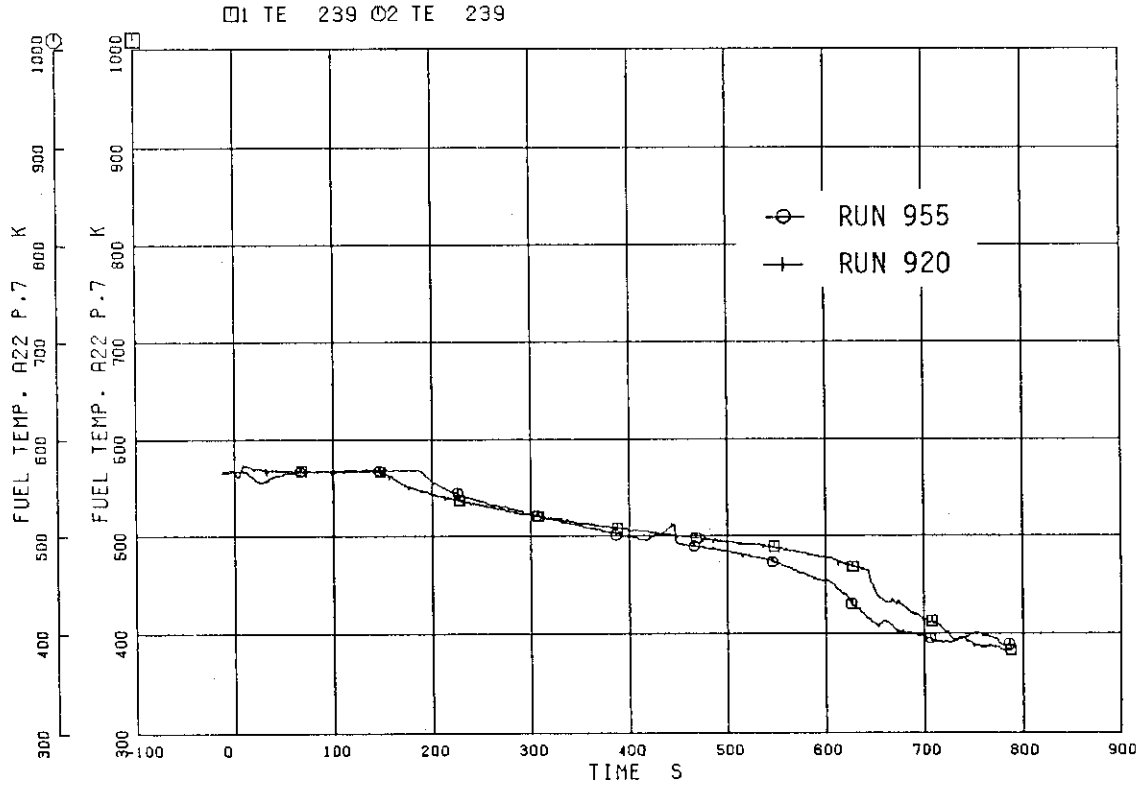

Fig. 6.14 Comparison of fuel surface temperatures at position 7 (bottom) of average-power rod A22 between RUNs 955 and 920

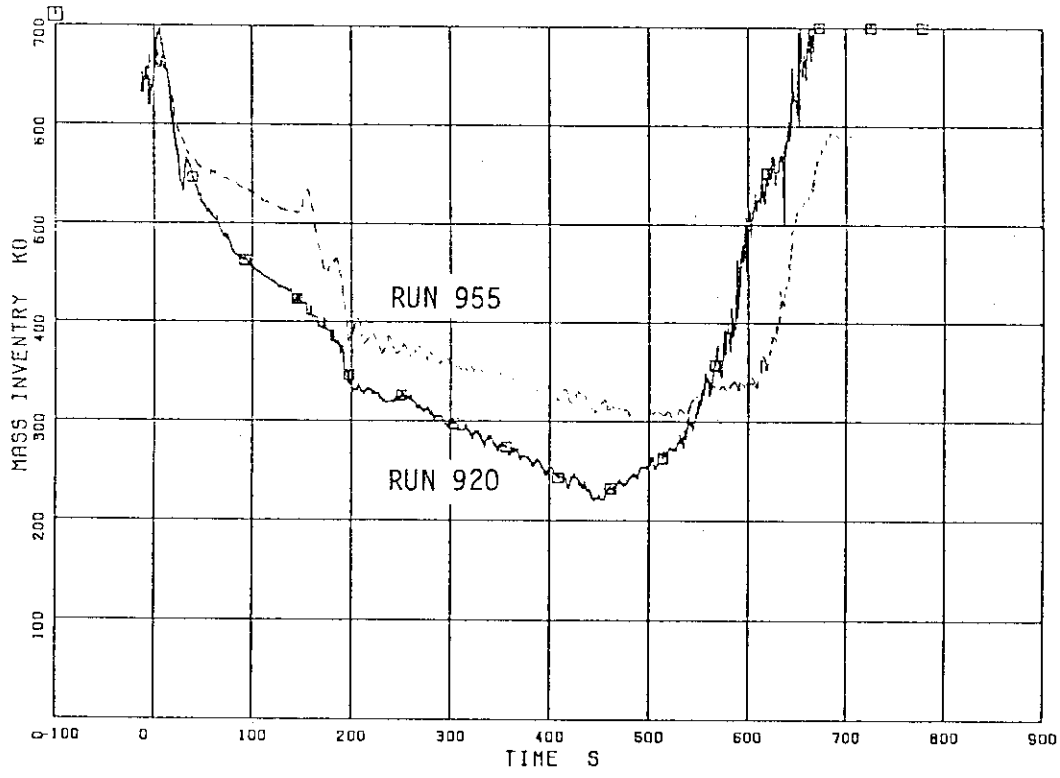

Fig. 6.15 Comparison of PV total mass inventory between RUNs 955 and 920

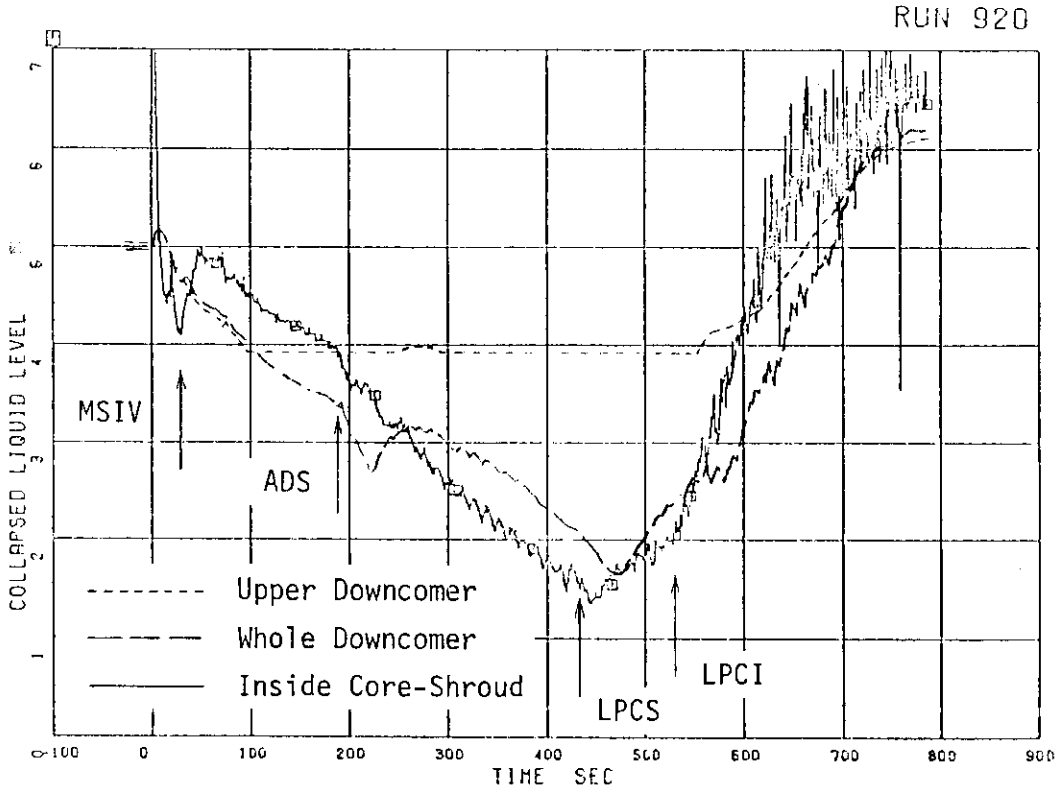

Fig. 6.16 Collapsed watere levels inside core-shroud, in whole downcomer and upper downcomer in RUN 920

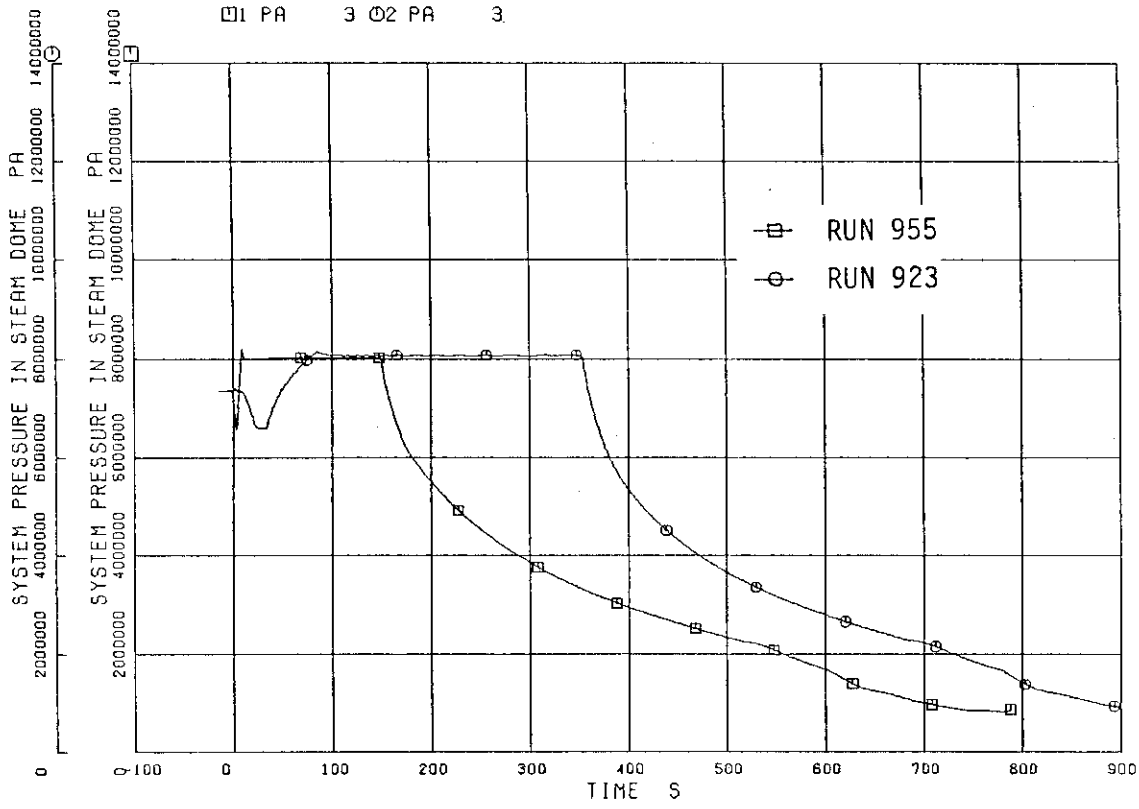

Fig. 6.17 Comparison of pressure transients between RUNs 955 and 923

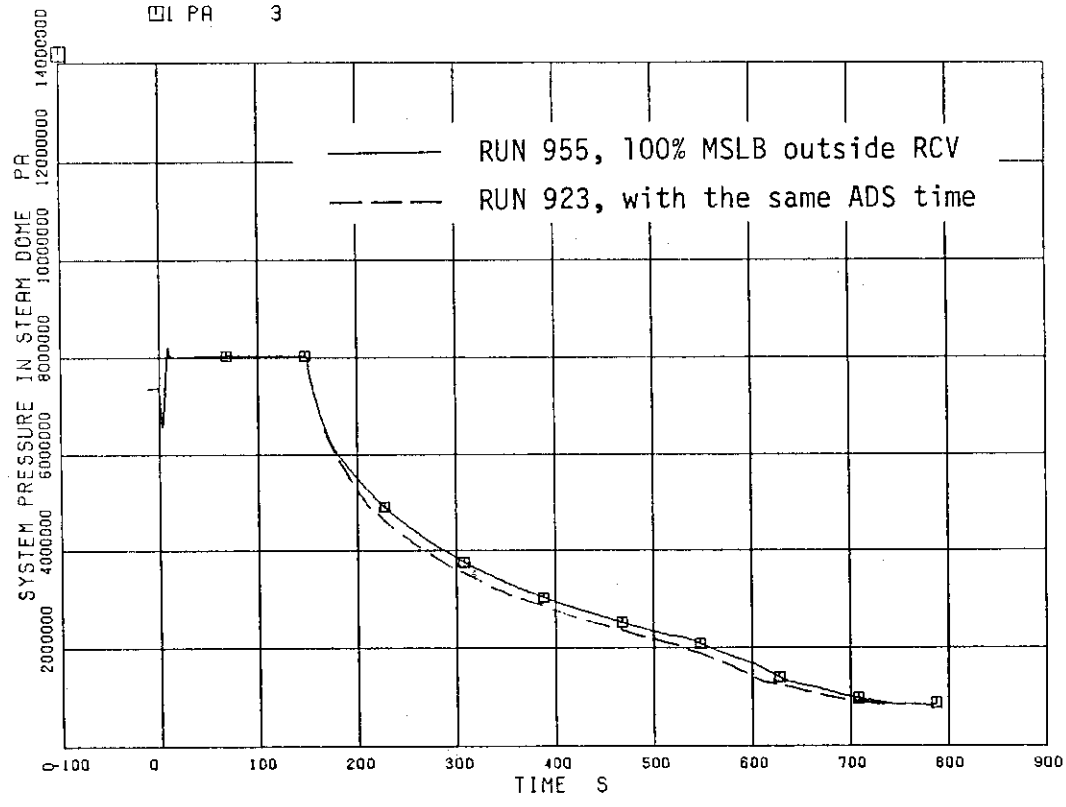

Fig. 6.18 Pressure transients of RUNs 955 and 923 with the same ADS actuation time at 150 s

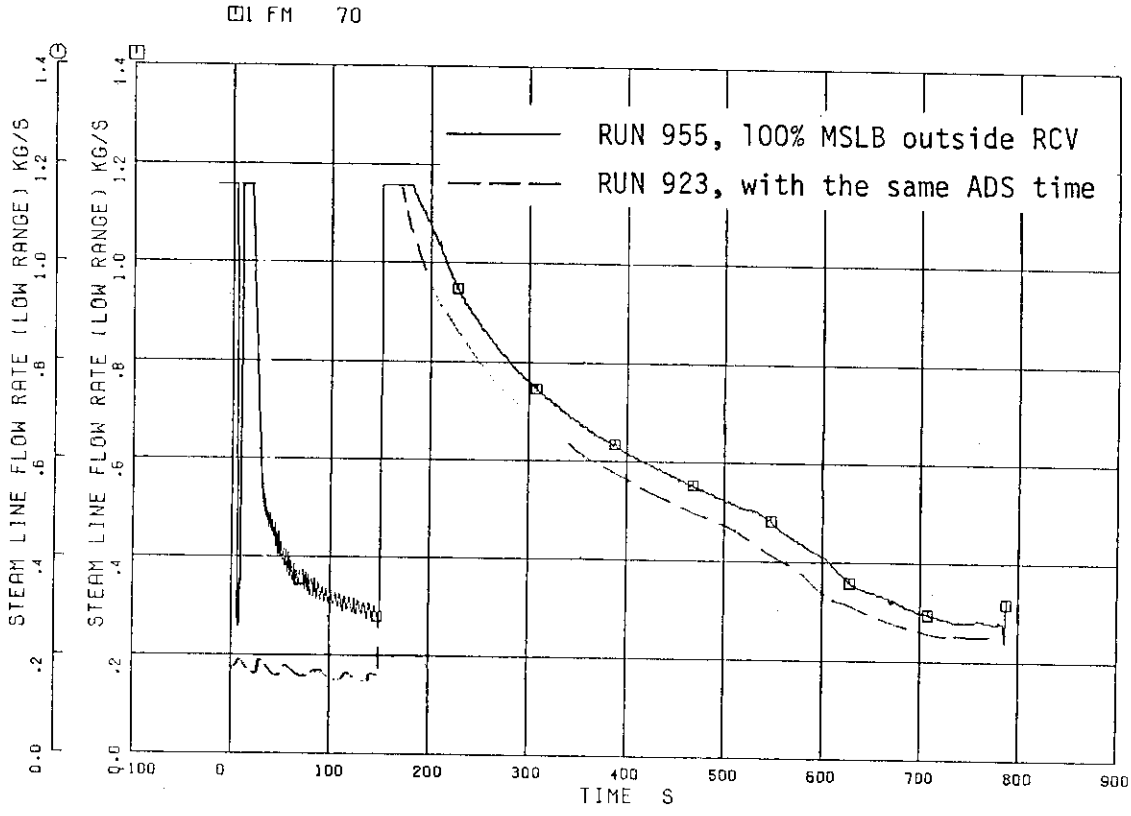

Fig. 6.19 Steam flow rates measured by a low-range flow meter in RUNs 955 and 923 with the same ADS actuation time

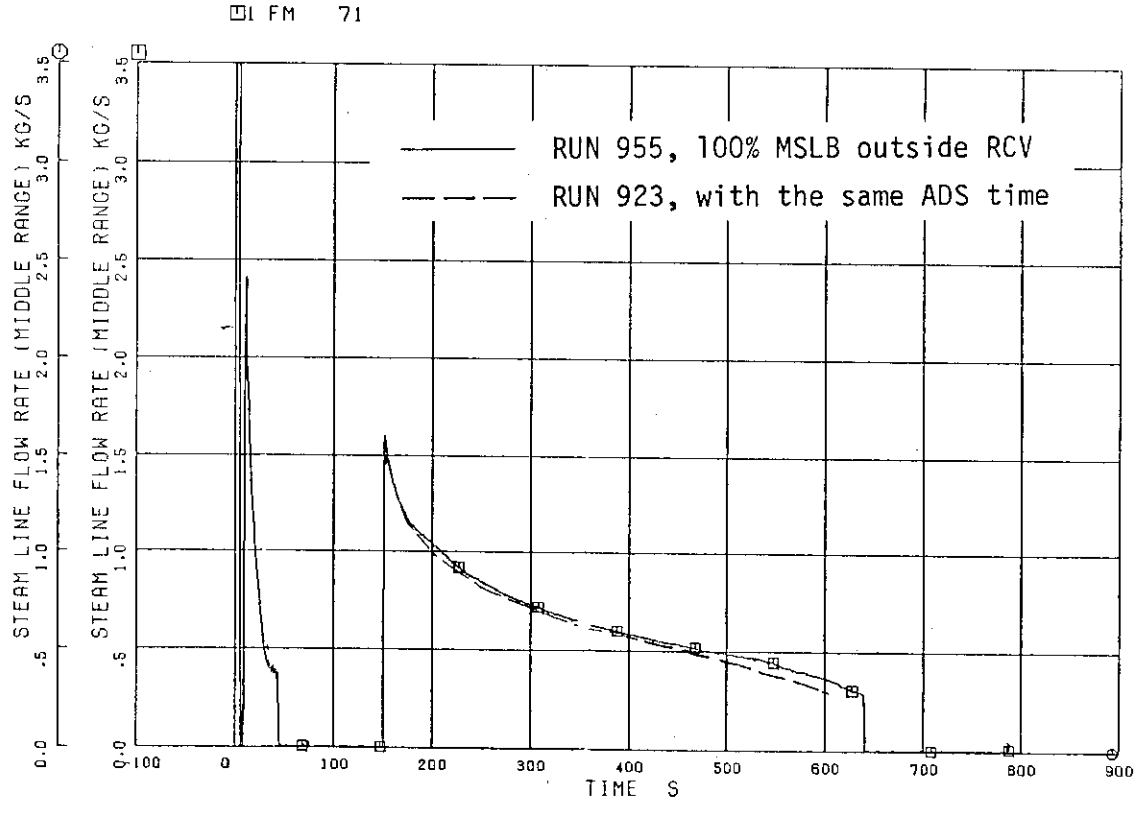

Fig. 6.20 Steam flow rates measured by a high-range flow meter in RUNs 955 and 923 with the same ADS actuation time

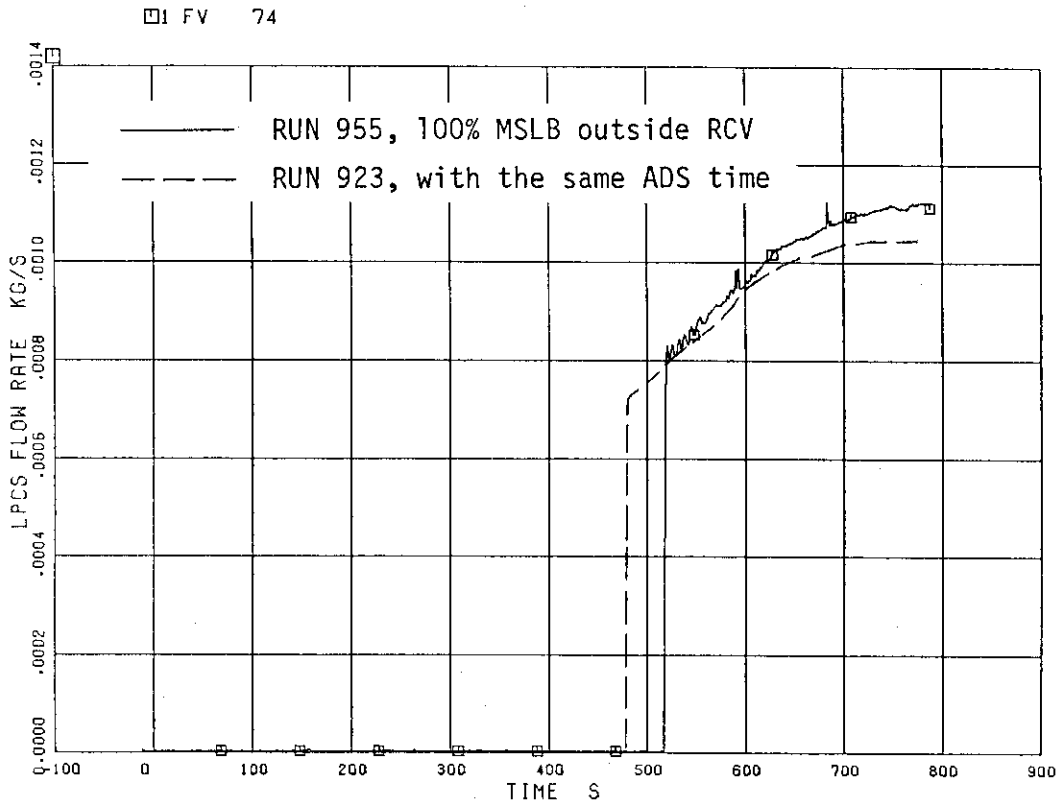

Fig. 6.21 LPCS injection flow rates of RUNs 955 and 923 with the same ADS actuation time

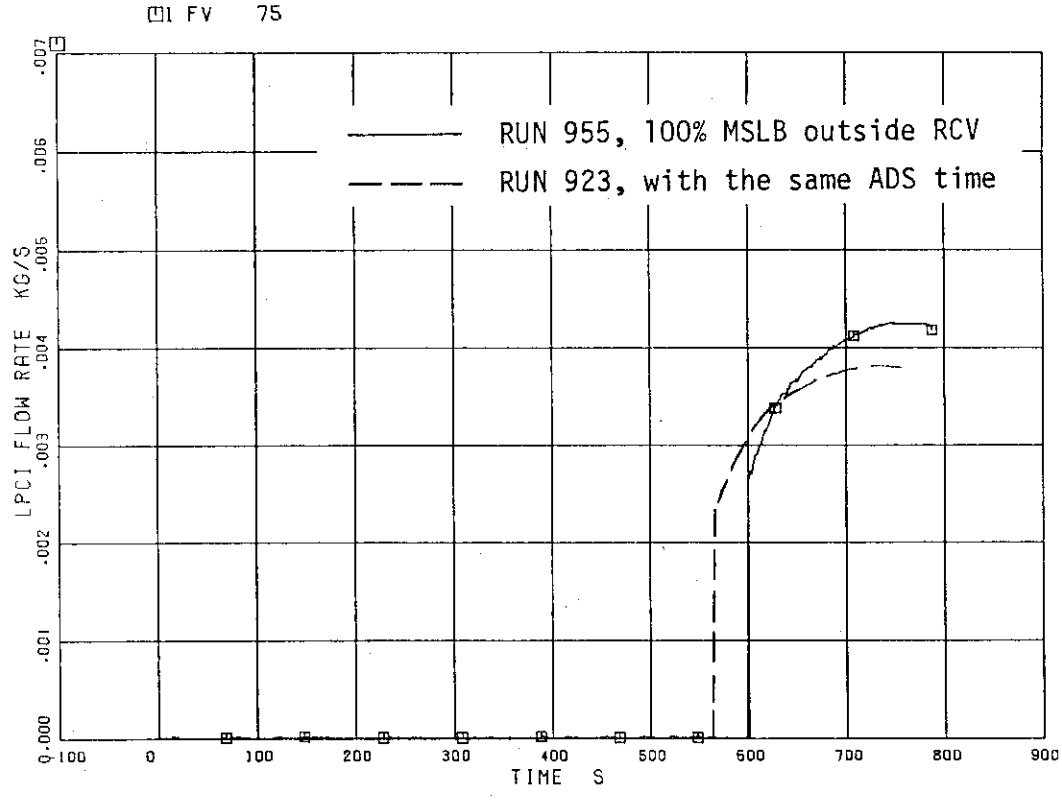

Fig. 6.22 LPCI injection flow rates of RUNs 955 and 923 with the same ADS actuation time

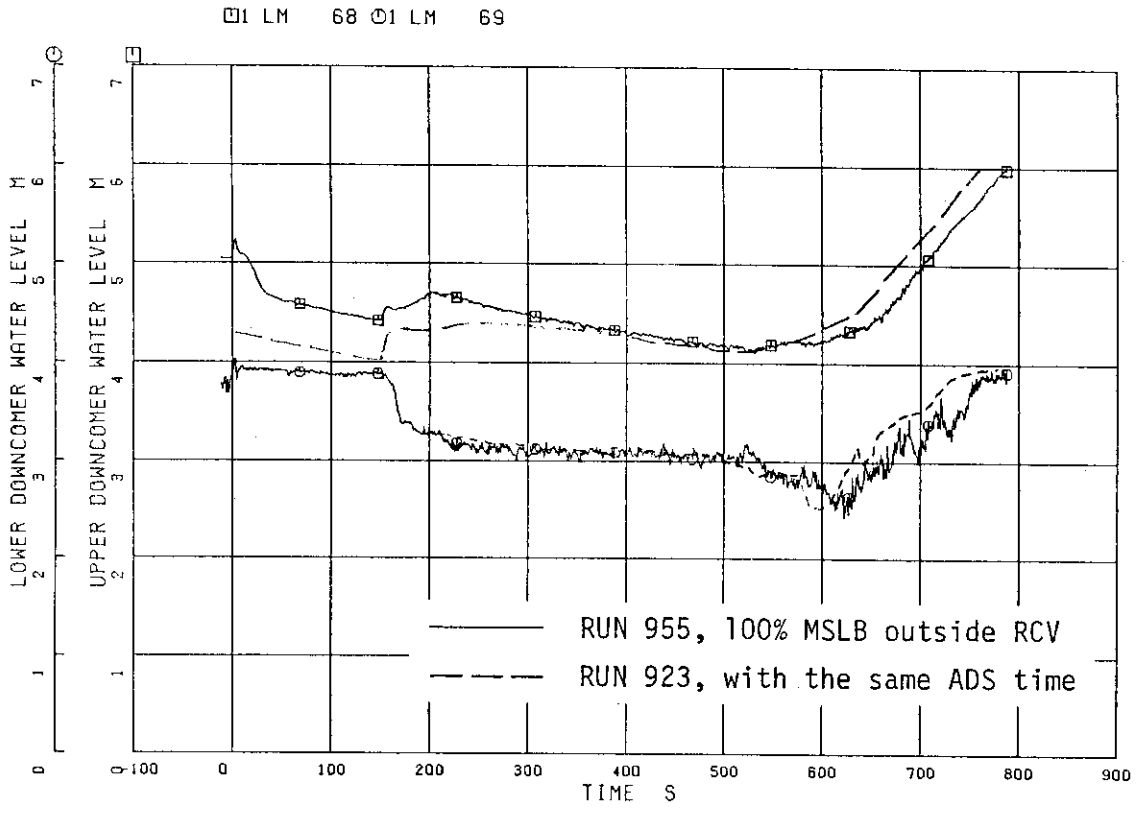

Fig. 6.23 Water levels in both upper and lower downcomers in RUNs 955 and 923 with the same ADS actuation time

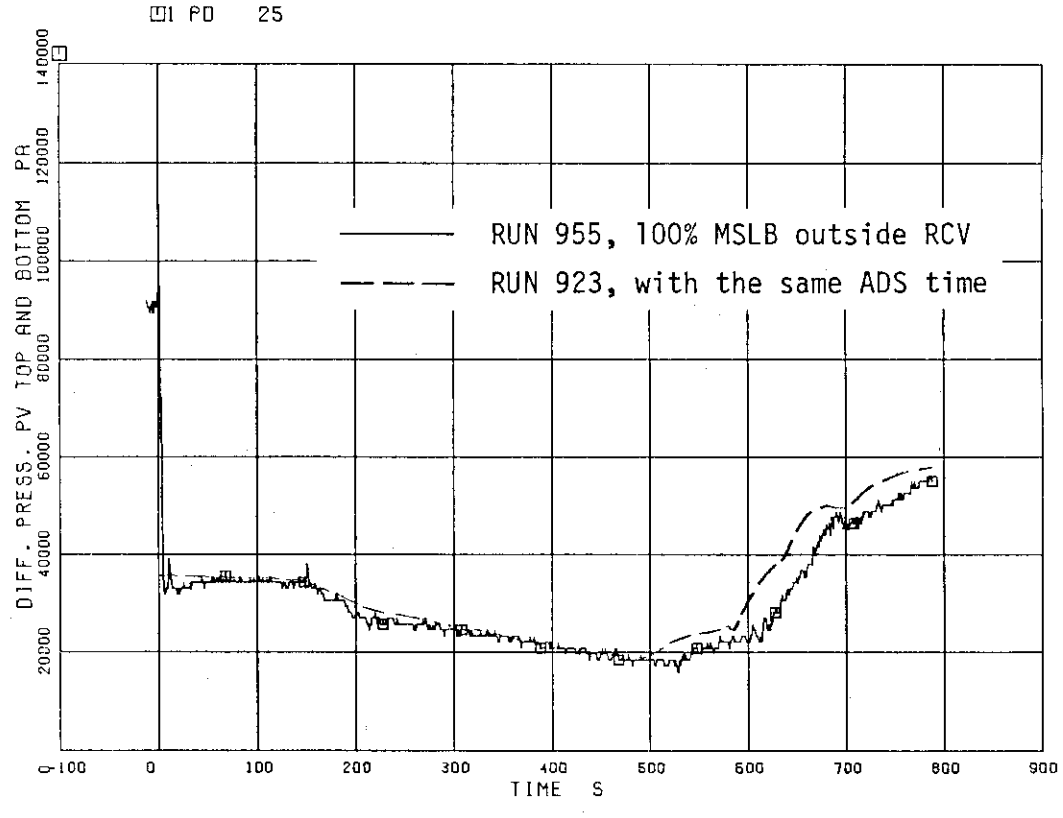

Fig. 6.24 Differential pressure between PV top and bottom in RUNs 955 and 923 with the same ADS actuation time

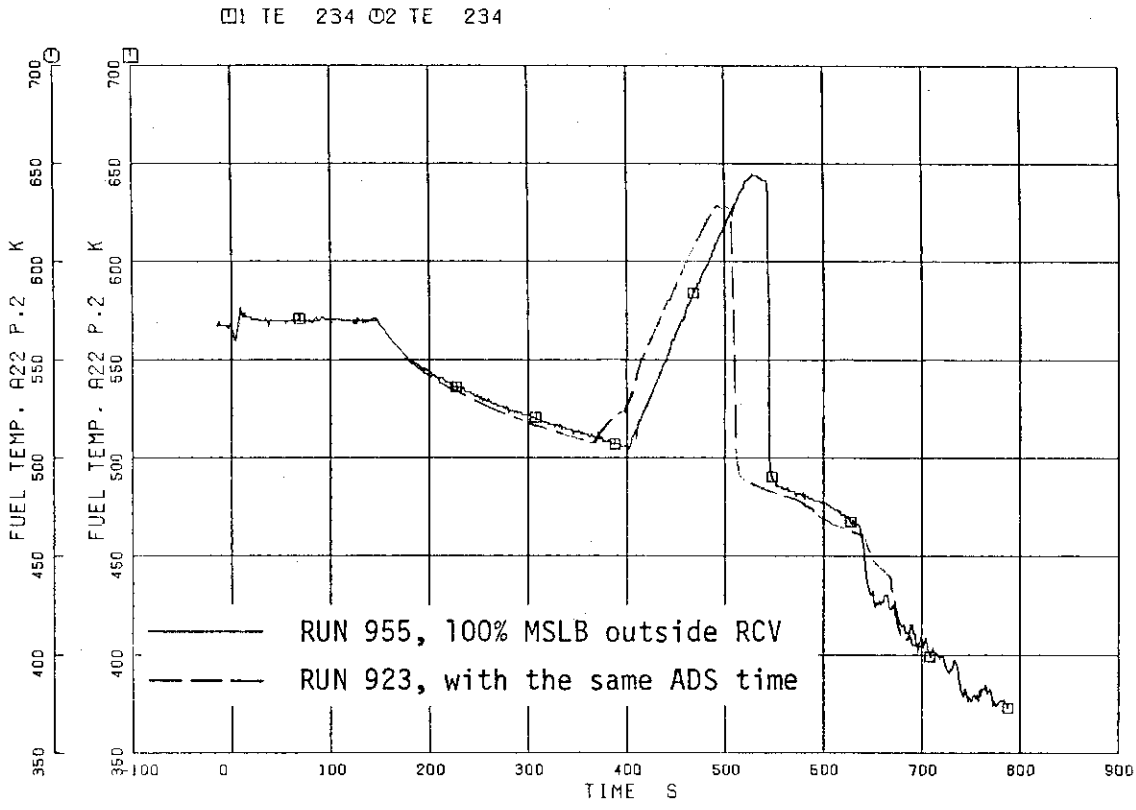

Fig. 6.25 Fuel surface temperature of at position 2 of A22 rod in RUNs 955 and 923 with the same ADS actuation time

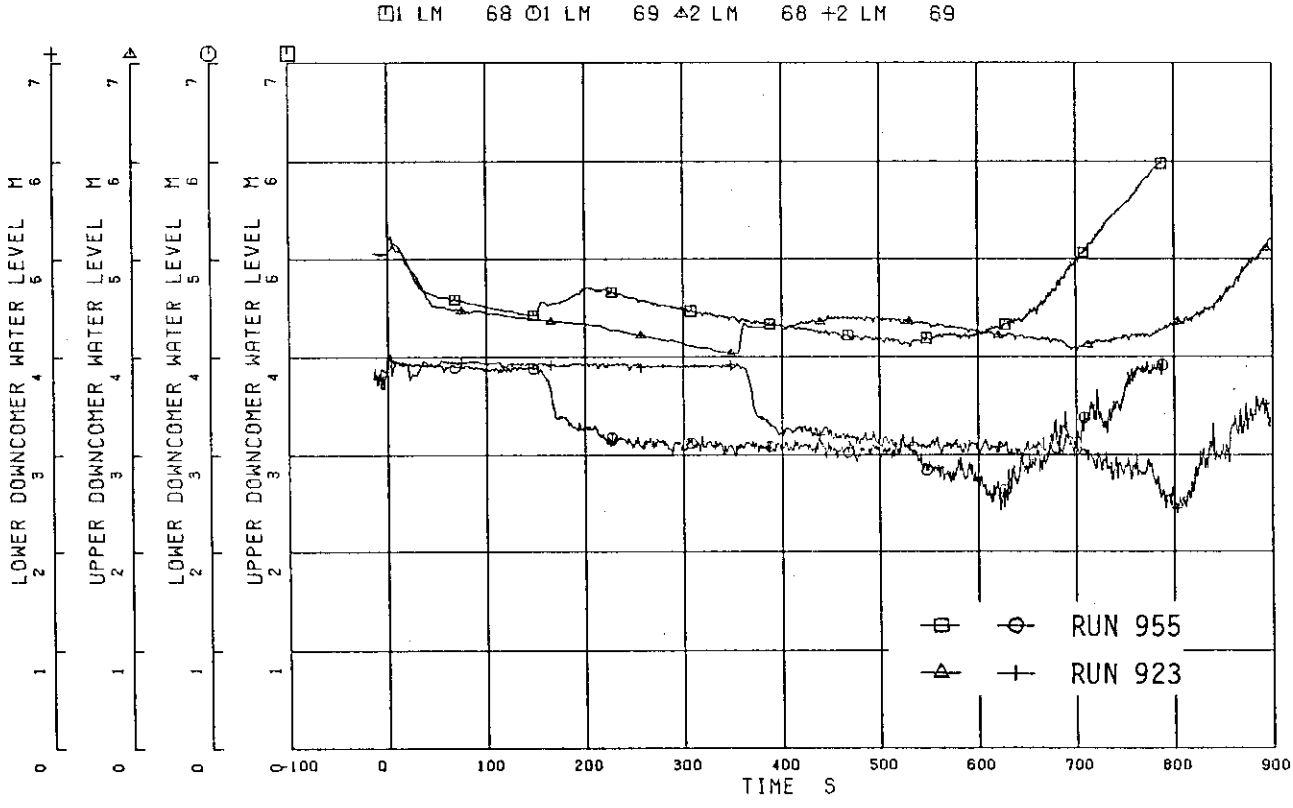

Fig. 6.26 Comparison of downcomer water levels between RUNs 955 and 923

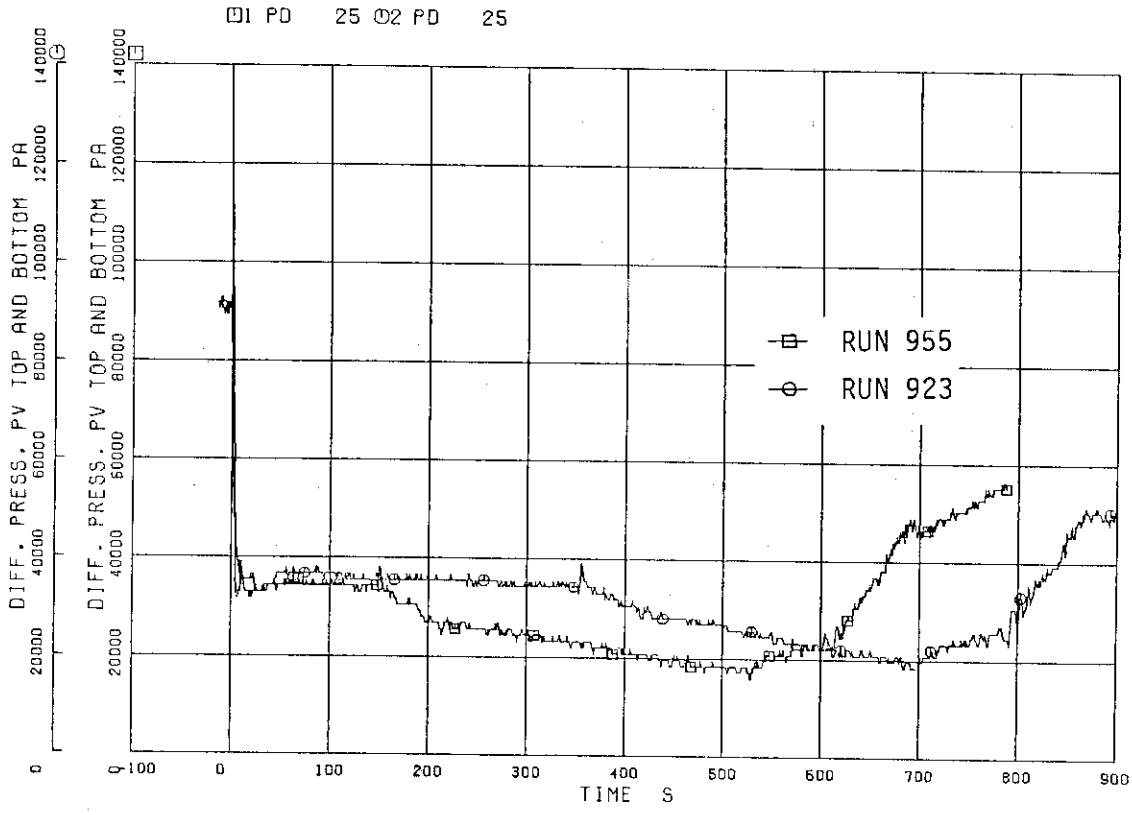

Fig. 6.27 Comparison of differential pressure between PV top and bottom in RUNs 955 and 923

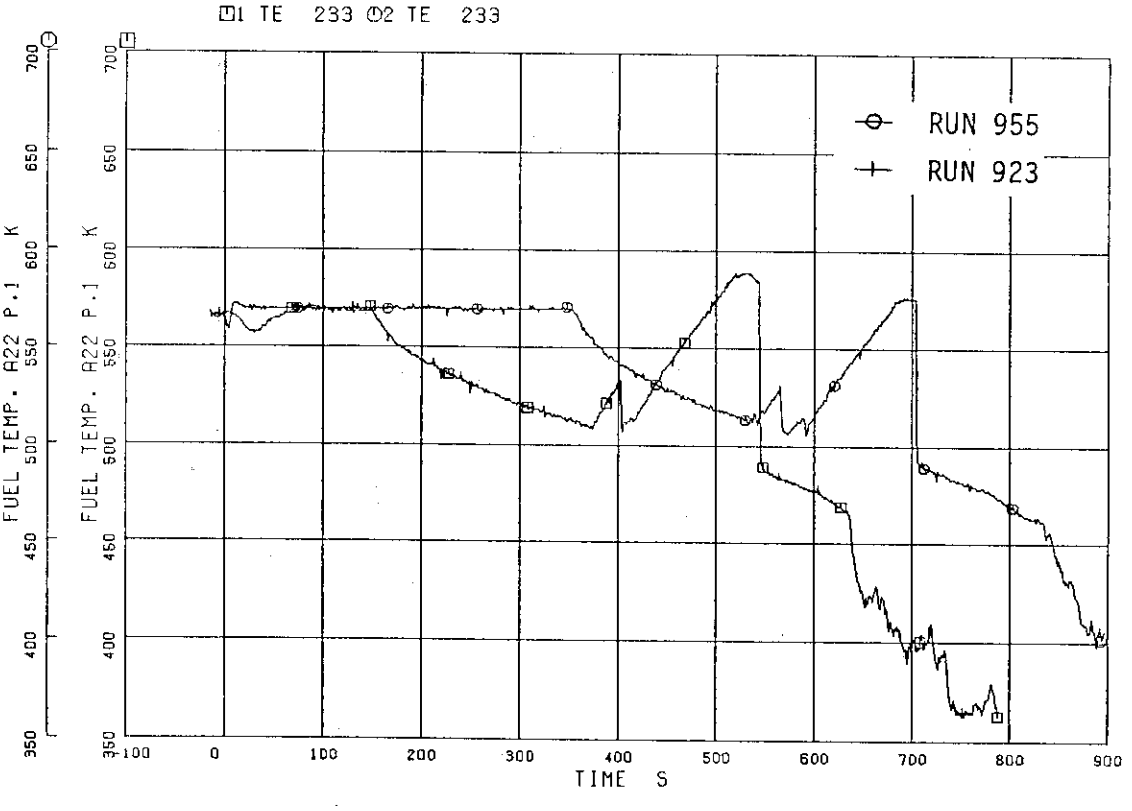

Fig. 6.28 Comparison of fuel surface temperatures at position 1 (top) of average-power rod A22 between RUNs 955 and 923

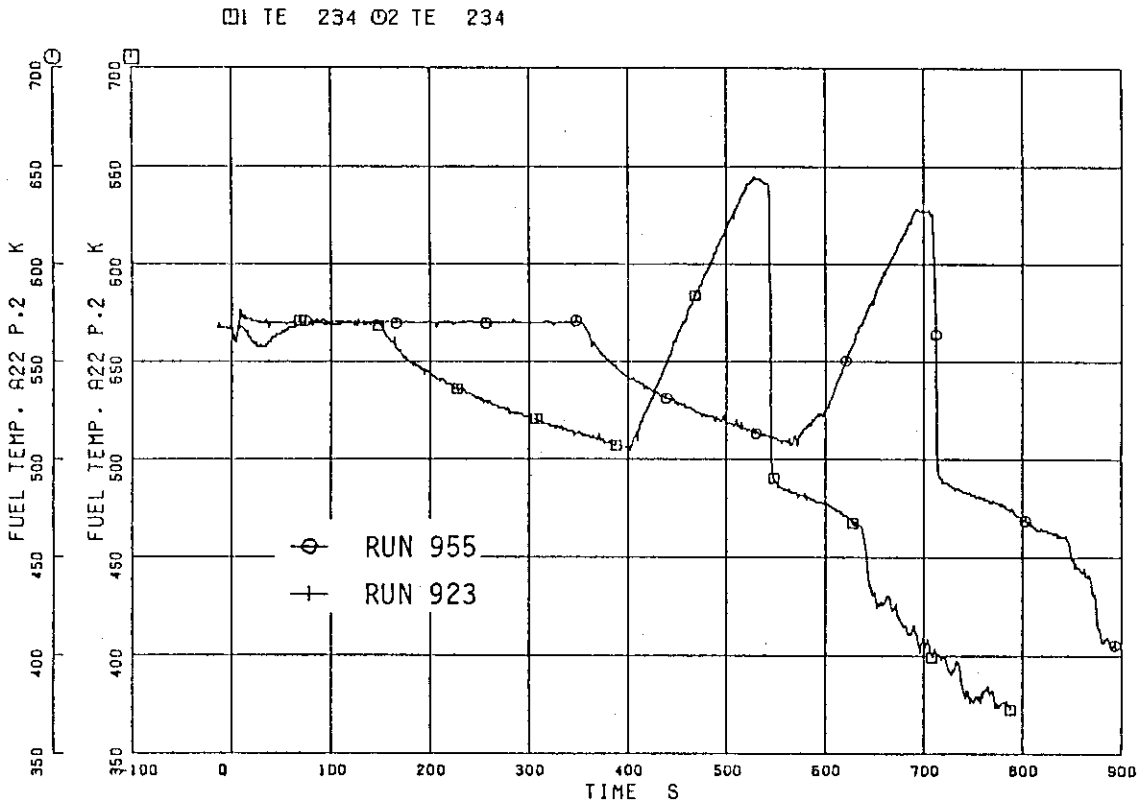

Fig. 6.29 Comparison of fuel surface temperatures at position 2 of average-power rod A22 between RUNs 955 and 923

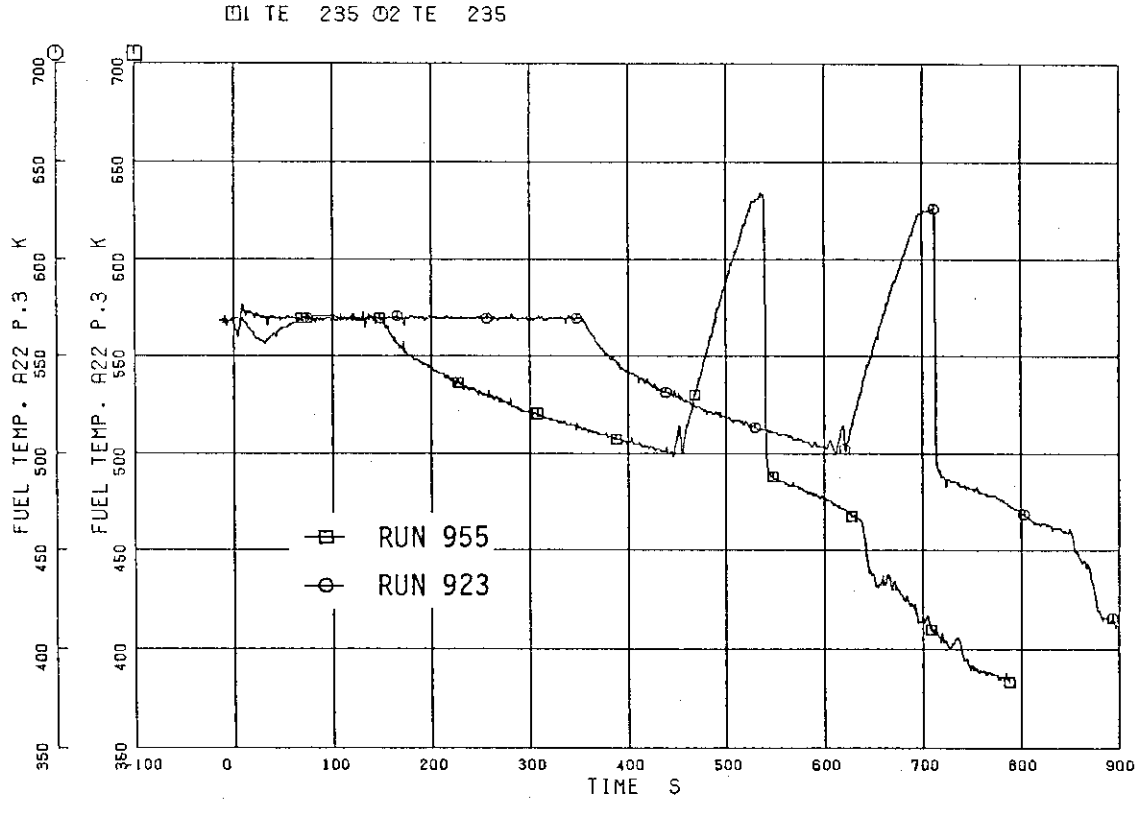

Fig. 6.30 Comparison of fuel surface temperatures at position 3 of average-power rod A22 between RUNs 955 and 923

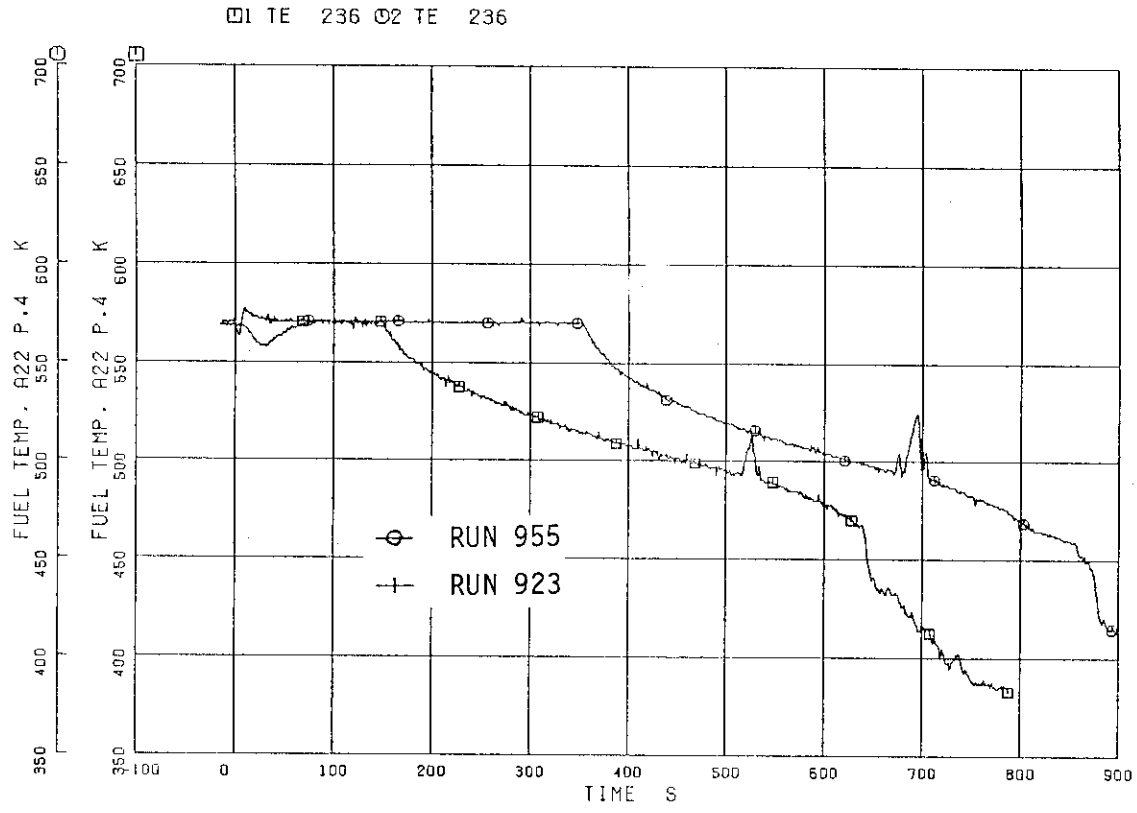

Fig. 6.31 Comparison of fuel surface temperatures at position 4 of average-power rod A22 between RUNs 955 and 923

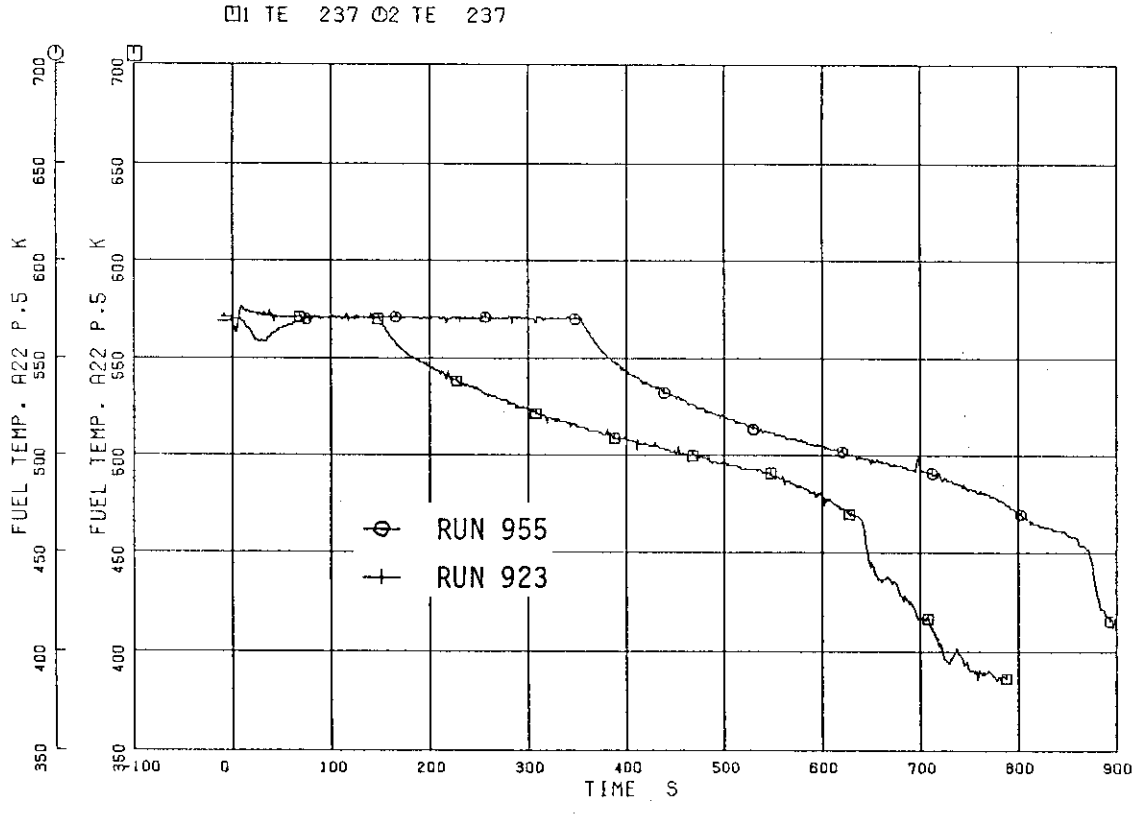

Fig. 6.32 Comparison of fuel surface temperatures at position 5 of average-power rod A22 between RUNs 955 and 923